

Advances

in Clinical and Experimental Medicine

MONTHLY ISSN 1899-5276 (PRINT) ISSN 2451-2680 (ONLINE)

www.advances.umed.wroc.pl

2019, Vol. 28, No. 10 (October)

Impact Factor (IF) – 1.227
Ministry of Science and Higher Education – 40 pts.
Index Copernicus (ICV) – 155.19 pts.



WROCLAW
MEDICAL UNIVERSITY

Advances
in Clinical and Experimental
Medicine



Advances in Clinical and Experimental Medicine

ISSN 1899-5276 (PRINT)

ISSN 2451-2680 (ONLINE)

www.advances.umed.wroc.pl

MONTHLY 2019
Vol. 28, No. 10
(October)

Advances in Clinical and Experimental Medicine is a peer-reviewed open access journal published by Wrocław Medical University. Its abbreviated title is Adv Clin Exp Med. Journal publishes original papers and reviews encompassing all aspects of medicine, including molecular biology, biochemistry, genetics, biotechnology, and other areas. It is published monthly, one volume per year.

Editorial Office

ul. Marcinkowskiego 2–6
50-368 Wrocław, Poland
Tel.: +48 71 784 11 36
E-mail: redakcja@umed.wroc.pl

Publisher

Wrocław Medical University
Wybrzeże L. Pasteura 1
50-367 Wrocław, Poland

© Copyright by Wrocław Medical University,
Wrocław 2019

Online edition is the original version of the journal

Editor-in-Chief

Maciej Bagłaż

Vice-Editor-in-Chief

Dorota Frydecka

Editorial Board

Piotr Dziągłiel
Marian Klinger
Halina Milnerowicz
Jerzy Mozrzyński

Thematic Editors

Marzenna Bartoszewicz (microbiology)
Marzena Dominiak (dentistry)
Paweł Domosławski (surgery)
Maria Ejma (neurology)
Jacek Gajek (cardiology)
Mariusz Kuształ
(nephrology and transplantology)
Rafał Matkowski (oncology)
Ewa Milnerowicz-Nabzdzyk (gynecology)
Katarzyna Neubauer (gastroenterology)
Marcin Ruciński (basic sciences)
Robert Śmigiel (pediatrics)
Paweł Tabakow (experimental medicine)
Anna Wiela-Hojeńska
(pharmaceutical sciences)
Dariusz Wołowicz (internal medicine)

International Advisory Board

Reinhard Berner (Germany)
Vladimir Bobek (Czech Republic)
Marcin Czyż (UK)
Buddhadeb Dawn (USA)
Kishore Kumar Jella (USA)

Secretary

Katarzyna Neubauer

Piotr Ponikowski
Marek Sąsiadek
Leszek Szenborn
Jacek Szepietowski

Statistical Editors

Dorota Diakowska
Leszek Noga
Lesław Rusiecki

Technical Editorship

Joanna Gudarowska
Paulina Kunicka
Marek Misiak

English Language Copy Editors

Eric Hilton
Sherill Howard Pocięcha
Jason Schock
Marcin Tereszewski

Pavel Kopel (Czech Republic)
Tomasz B. Owczarek (USA)
Ivan Rychlík (Czech Republic)
Anton Sculean (Switzerland)
Andriy B. Zimenkovsky (Ukraine)

Editorial Policy

Advances in Clinical and Experimental Medicine (Adv Clin Exp Med) is an independent multidisciplinary forum for exchange of scientific and clinical information, publishing original research and news encompassing all aspects of medicine, including molecular biology, biochemistry, genetics, biotechnology and other areas. During the review process, the Editorial Board conforms to the "Uniform Requirements for Manuscripts Submitted to Biomedical Journals: Writing and Editing for Biomedical Publication" approved by the International Committee of Medical Journal Editors (www.ICMJE.org/). The journal publishes (in English only) original papers and reviews. Short works considered original, novel and significant are given priority. Experimental studies must include a statement that the experimental protocol and informed consent procedure were in compliance with the Helsinki Convention and were approved by an ethics committee.

For all subscription-related queries please contact our Editorial Office:
redakcja@umed.wroc.pl

For more information visit the journal's website:
www.advances.umed.wroc.pl

Pursuant to the ordinance No. 134/XV R/2017 of the Rector of Wrocław Medical University (as of December 28, 2017) from January 1, 2018 authors are required to pay a fee amounting to 700 euros for each manuscript accepted for publication in the journal Advances in Clinical and Experimental Medicine.

„Podniesienie poziomu naukowego i poziomu umiędzynarodowienia wydawanych czasopism naukowych oraz upowszechniania informacji o wynikach badań naukowych lub prac rozwojowych – zadanie finansowane w ramach umowy 784/p-DUN/2017 ze środków Ministra Nauki i Szkolnictwa Wyższego przeznaczonych na działalność upowszechniającą naukę”.



Indexed in: MEDLINE, Science Citation Index Expanded, Journal Citation Reports/Science Edition, Scopus, EMBASE/Excerpta Medica, Ulrich's™ International Periodicals Directory, Index Copernicus

Typographic design: Monika Kołęda, Piotr Gil
DTP: Wydawnictwo UMW
Cover: Monika Kołęda
Printing and binding: EXDRUK

Contents

Original papers

- 1285 Dongcheng Lu, Qinyi Qin, Rongle Lei, Bangli Hu, Shanyu Qin
Targeted blockade of interleukin 9 inhibits tumor growth in murine model of pancreatic cancer
- 1293 Fuwen Zhang, Kun Cao, Gongwen Du, Qi Zhang, Zongsheng Yin
miR-29a promotes osteoblast proliferation by downregulating DKK-1 expression and activating Wnt/ β -catenin signaling pathway
- 1301 Małgorzata Krzystek-Korpacka, Krzysztof Kędzior, Leszek Masłowski, Magdalena Mierzchała, Iwona Bednarz-Misa, Agnieszka Bronowicka-Szydełko, Joanna Kubiak, Małgorzata Gacka, Sylwia Płaczkowska, Andrzej Gamian
Impact of chronic wounds of various etiology on systemic profiles of key inflammatory cytokines, chemokines and growth factors, and their interplay
- 1311 Hubert Gołąbek, Krzysztof Mariusz Borys, Meetu Ralli Kohli, Katarzyna Brus-Sawczuk, Izabela Strużycka
Chemical aspect of sodium hypochlorite activation in obtaining favorable outcomes of endodontic treatment: An in-vitro study
- 1321 Agnieszka Gala-Błądzińska, Jolanta Czarnota, Rafał Kaczorowski, Marcin Braun, Krzysztof Gargas, Halina Bartosik-Psujek
Mild hyponatremia discovered within the first 24 hours of ischemic stroke is a risk factor for early post stroke mortality
- 1329 Kajetan Juszcak, Adam Ostrowski, Jan Adamowicz, Piotr Maciukiewicz, Tomasz Drewa
Urinary bladder hypertrophy and overactive bladder determine urinary continence after radical prostatectomy
- 1339 Wojciech Homola, Mariusz Zimmer
Do lifestyle factors influence the rate of complications after amniocentesis?
- 1345 Dorota Sikorska, Krzysztof Pawlaczek, Ewa Baum, Maria Wanic-Kossowska, Natasza Czepulis, Joanna Łuczak, Włodzimierz Samborski, Andrzej Oko
The association of serum soluble Klotho levels and residual diuresis and overhydration in peritoneal dialysis patients
- 1351 Adam Rafał Poliwczak, Janusz Śmigielski, Agnieszka Bała, Ewa Straburzyńska-Migaj, Agata Tymińska, Paweł Balsam, Krzysztof Ozierański, Agnieszka Kapłon-Cieślicka, Joanna Zaprutko, Jarosław Drożdż
Treatment of heart failure in the elderly in Poland. The results of the Polish part of EURObservational Research Programme: The Heart Failure Pilot Survey
- 1359 Dorota Jesionek-Kupnicka, Marcin Braun, Tadeusz Robak, Wojciech Kuncman, Radzisław Kordek
A large single-institution retrospective analysis of aggressive B-cell lymphomas according to the 2016/2017 WHO classification
- 1367 Marta Anna Szmigiel, Joanna Wiktoria Przeździecka-Dołyk, Jacek Olszewski, Henryk Kasprzak
Pupil autoregulation impairment as an early marker of glaucomatous damage
- 1377 Dominika Zielecka-Dębska, Jerzy Błaszczak, Dawid Błaszczak, Jolanta Szelachowska, Krystian Lichoń, Adam Maciejczyk, Rafał Matkowski
The effect of the population-based cervical cancer screening program on 5-year survival in cervical cancer patients in Lower Silesia
- 1385 Dariusz Walkowiak, Anna Bukowska-Posadzy, Łukasz Kałużny, Mariusz Ołtarzewski, Rafał Staszewski, Michał Musielak, Jarosław Walkowiak
Therapy compliance in children with phenylketonuria younger than 5 years: A cohort study
- 1393 Murat Olukman, Cenk Can, Deniz Coşkunsever, Yiğit Uyanıgil, Türker Çavuşoğlu, Eser Sözmen, Soner Duman, Fatma Gül Çelenk, Sibel Ülker
Urotensin receptor antagonist palosuran attenuates cyclosporine-a-induced nephrotoxicity in rats

- 1403 Meng Wang, Liang Zhao, Hao Liang, Chunyuan Zhang, Liying Guan, Minglong Li
A new measurement site for echocardiographic epicardial adipose tissue thickness and its value in predicting metabolic syndrome
- 1409 Tianbing Duan, Jinxia Zhang, Dingcheng Xiang, Rui Song, Ranran Kong, Dingli Xu
Effectiveness and safety of intracoronary papaverine, alprostadil, and high dosages of nicorandil and adenosine triphosphate for measurement of the index of coronary microcirculatory resistance in a pig model
- 1419 Tanja Hojs Fabjan, Meta Penko, Radovan Hojs
Anemia on admission and long-term mortality risk in patients with acute ischemic stroke
- 1425 Leszek Kozłowski, Klaudia Kozłowska, Jolanta Małyszko
Hypertension and chronic kidney disease is highly prevalent in elderly patients with colorectal cancer undergoing primary surgery
- 1429 Magdalini Mitroudi, Dimitra Psalla, Konstantina Kontopoulou, Konstantinos Theocharidis, Dimitrios Sfoungaris
Is intestinal stasis sufficient by itself in promoting enterocolitis in a non-genetic rat model of Hirschsprung's disease?

Targeted blockade of interleukin 9 inhibits tumor growth in murine model of pancreatic cancer

Dongcheng Lu^{B,F}, Qinyi Qin^{B,C}, Rongle Lei^{C,E,F}, Bangli Hu^{D,E}, Shanyu Qin^{A,D,F}

First Affiliated Hospital of Guangxi Medical University, Nanning, China

A – research concept and design; B – collection and/or assembly of data; C – data analysis and interpretation; D – writing the article; E – critical revision of the article; F – final approval of the article

Advances in Clinical and Experimental Medicine, ISSN 1899–5276 (print), ISSN 2451–2680 (online)

Adv Clin Exp Med. 2019;28(10):1285–1292

Address for correspondence

Shanyu Qin
E-mail: qsy0511@163.com

Funding sources

National Natural Science Foundation of China
(grant No. 31360221)

Conflict of interest

None declared

Received on July 3, 2018

Reviewed on September 20, 2018

Accepted on February 18, 2019

Published online on October 23, 2019

Abstract

Background. Interleukin 9 (IL-9) has been implicated in the pathogenesis of several tumor types, but the role of anti-IL-9 in pancreatic cancer remains unclear.

Objectives. We aimed to explore the mechanism and effects of blocking IL-9 in a pancreatic cancer mouse model.

Material and methods. Panc02 cells were injected subcutaneously into mice to establish a mouse model. The mice were randomly categorized into 3 groups – the control group, the immunoglobulin G (IgG) group and the anti-IL-9 group – corresponding to intravenous tail injection of phosphate-buffered saline (PBS), IgG isotype antibody and anti-IL-9 antibody, respectively. Then, the expression of IL-9, interleukin-9 receptor (IL-9r), Janus kinase 1 (Jak1), Jak3, and signal transducer and activator of transcription 3 (Stat3) mRNA was tested with quantitative reverse-transcription polymerase chain reaction (qRT-PCR). Interleukin 9 in the tumor tissue was detected using enzyme-linked immunosorbent assay (ELISA). Western blotting and immunocytochemistry were performed to detect STAT3 and phosphorylation signal transducers and activators of transcription-3 (pSTAT3). Matrix metalloproteinase 2 (MMP2), MMP9 and vascular endothelial growth factor (VEGF) levels were assessed using immunocytochemistry.

Results. Tumor weight in the anti-IL-9 group was significantly lower than in the other groups ($p < 0.05$). There was a remarkable survival benefit in the anti-IL-9 group compared to the other groups ($p < 0.05$). The concentration of IL-9 in tumor tissue was significantly downregulated in the anti-IL-9-treated mice ($p < 0.05$). The expression of Jak1 and Jak3 mRNA and pSTAT3, MMP2 and MMP9 proteins in the anti-IL-9 group was lower than that of the PBS or IgG groups ($p < 0.05$), but the STAT3 and VEGF protein levels showed no significant difference ($p < 0.05$).

Conclusions. Anti-IL-9 antibody could effectively restrain the growth of pancreatic cancer in mice, and this effect may partly occur by blocking the STAT3 pathway.

Key words: pancreatic cancer, JAK2/STAT3 pathway, IL-9 antibody

Cite as

Lu D, Qin Q, Lei R, Hu B, Qin S. Targeted blockade of interleukin 9 inhibits tumor growth in murine model of pancreatic cancer. *Adv Clin Exp Med.* 2019;28(10):1285–1292. doi:10.17219/acem/104543

DOI

10.17219/acem/104543

Copyright

© 2019 by Wrocław Medical University
This is an article distributed under the terms of the
Creative Commons Attribution Non-Commercial License
(<http://creativecommons.org/licenses/by-nc-nd/4.0/>)

Introduction

Pancreatic cancer is one of the most aggressive metastatic malignancies, with a median survival rate of 6 months and a 5-year survival rate of 5%, and it ranks 4th among cancer-related deaths in the USA.^{1,2} Surgery, chemotherapy and radiation therapy are the main treatment options for pancreatic cancer. However, the current treatment strategies are ineffective due to the fact that most of the patients are in advanced stages when they are first diagnosed. Therefore, finding novel therapeutic strategies is crucial to improve the effectiveness of treatment and to prolong the survival of pancreatic cancer patients.

Interleukin 9 (IL-9) is a multifunctional cytokine secreted by a host of pro-inflammatory immune cells, including Th2 cells, Th9 cells and Th17 cells.^{3,4} Interleukin 9 activates a heterodimeric receptor that comprises the IL-9 receptor α -chain (*IL-9ra*) and the γ -chain (*IL-9ry*), and promotes the cross-phosphorylation of Janus kinase 1 (*Jak1*) and Janus kinase 3 (*Jak3*), which in turn induce the downstream activation of signal transducer and activator of transcription 3 (*Stat3*).⁵ Interleukin 9 has contrasting roles depending on the type of cancer. Studies have reported that while IL-9 impaired tumor cell growth in B16 melanoma and CT26 colon adenocarcinoma-tumor-bearing mice,⁶ it could promote cancer growth and exhibit an anti-apoptotic function in various transformed cell lines.^{7,8} Thus, further research is needed in order to confirm the role of IL-9 in various cancers.

We have previously reported that IL-9 plays a tumor-promoting role in pancreatic cancer cell lines^{9,10} and therefore postulated that neutralizing IL-9 may exert a tumor-suppressing function in pancreatic cancer. In this study, we investigated the effect of the anti-IL-9 antibody on a subcutaneous Pan02 model and its potential mechanism. We report that anti-IL-9 antibody treatment can partly inhibit a pancreatic cancer tumor in vivo, which may provide an effective therapeutic strategy against pancreatic cancer. The study scheme is presented in Fig. 1.

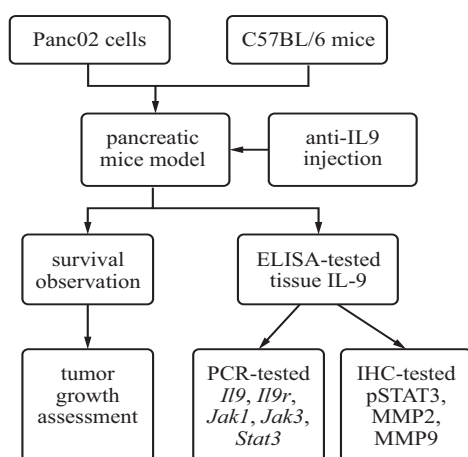


Fig. 1. The framework describing the idea of the study

Material and methods

Cell culture

Murine pancreatic adenocarcinoma cell line Panc02 was obtained from the American Type Culture Collection (ATCC) and cultured in Dulbecco's modified Eagle's medium (DMEM) (Gibco, Waltham, USA) supplemented with 100 mg/mL of streptomycin, 100 U/mL of penicillin and 10% fetal bovine serum (Gibco). The culture medium was replaced every 48 h unless otherwise described and the cells were incubated in 5% CO₂ and 95% air at 37°C.

Pancreatic cancer syngeneic model

Forty-eight SPF-grade C57BL/6 mice (20–24 g), 5–6 weeks of age, were purchased from Hunan SJA Laboratory Animal Co. Ltd. (Changsha, China) and housed in the Animal Center of Guangxi Medical University, Nanning, China, under humidity- and temperature-controlled conditions with a 12-hour light/dark cycle. All procedures for handling the animals were approved by the Animal Experiments Ethics Committee of Guangxi Medical University. The cells were trypsinized and washed with phosphate-buffered saline (PBS) (consisting of potassium dihydrogen phosphate, disodium hydrogen phosphate, sodium chloride, and potassium chloride) (Solarbio, Beijing, China). Panc02 cells (5×10^6) in 200 μ L of PBS were subcutaneously injected into the right flank. Once the tumors reached about 50 mm³, the tumor-bearing mice were tagged and divided into 3 groups (16 mice per group) and injected intravenously every 3 days for 18 days with sterile PBS, isotype control IgG (1 mg/kg) or anti-IL-9 antibody (1 mg/kg) (R&D Systems, Minneapolis, USA).

Tumor growth assessment

The tumor diameter was measured with a caliper every other day and the volume was calculated using the following formula:

$$(\text{short diameter})^2 \times (\text{long diameter}) \times 0.5^{11}$$

Eight mice from each group were sacrificed on the 5th day after the last treatment. Individual tumors from the mice were weighed and dissected for subsequent study. The inhibition rate was calculated using the following formula, in which A corresponds to the average tumor weight in the control group and B corresponds to tumor weight in the treated groups:

$$(\%) = [(A - B)/A] \times 100\%.$$

Survival observation

Surrogate endpoints for survival were used: either when the tumors reached an average diameter of 20 mm or when they became ulcerated.^{12,13} The survival time of the remaining mice (8 mice per group) was recorded at the end

of the observation period. The prolonged rate of survival time was calculated using the following formula, in which A corresponds to the average tumor weight in the control group and B corresponds to the average tumor weight in the treated groups:

$$(\%) = [(B - A)/A] \times 100\%.$$

During treatment with anti-IL-9 antibody, we also observed whether the mice displayed abnormal behavior, such as an altered mental state or weight loss.

RNA isolation and qRT-PCR

The total RNA was extracted from tumor tissues using an RNAiso plus Kit (TaKaRa, Beijing, China). cDNA synthesis was performed using a PrimeScript™ RT reagent Kit (TaKaRa). Real-time polymerase chain reaction (RT-PCR) was performed with PrimeScript™ RT PCR Master Mix according to the manufacturer's protocol. The forward and reverse primers used for PCR were as follows:

IL-9 forward 5'-ATG TTG GTG ACA TAC ATC CTT GC-3' and reverse 5'-TGA CGG TGG ATC ATC CTT CAG-3';
IL-9r forward 5'-GTA TTT ACA GGA TCG ACT GCC AC-3' and reverse 5'-CCC AGA AGG TGC ATT TGT GTT-3';
Jak1 forward 5'-GGAG GTA CTA CAC AGT CAA GGA CGA-3' and reverse 5'-AAA CAT TCC GGA GCG TAC C-3';
Jak3 forward 5'-CCA GAC CAG CAG AGG GAC TT-3' and reverse 5'-CCA AAG CGA ACA GCA GTA GGC-3';
Stat3 forward 5'-GTT CCT GGC ACC TTG GAT T-3' and reverse 5'-CAA CGT GGC ATG TGA CTC TT-3'.

The relative expression was normalized to GAPDH and gene expression was analyzed using the $2^{-\Delta\Delta CT}$ method.

Immunohistochemical analysis

The tumor tissues were formalin-fixed and paraffin-embedded, and specimen sections 4 μ m in thickness were prepared. The slides were treated in an autoclave oven for 5–10 min to unmask the heat-induced antigen and they were blocked with 5% goat serum in PBS for 1 h. The sections were incubated with primary antibodies against STAT3 (Cat# ab68153, 1:500, Abcam, Cambridge, UK), pSTAT3 (Cat# ab76315, 1:1000, Abcam), matrix metalloproteinases (MMPs) 2 and 9 (Cat# BM4098 and BM4075, 1:500, Boster Biological Technology, Pleasanton, USA), and vascular endothelial growth factor A (VEGF A) (Cat# M00045, 1:400, Boster Biological Technology) at 4°C overnight, followed by the secondary antibody (Cat# A-21074, Zymed, Waltham, USA) at room temperature for 30 min. Diaminobenzidine (DAB) was used to facilitate the locating of the antibody. Finally, the slides were rinsed in PBS and then counterstained with hematoxylin. The stained sections were captured using an Olympus DP72 microscope (Olympus Corporation, Shinjuku, Tokyo, Japan). The positively-labeled cells and negative cells in 5 randomly selected fields were counted at $\times 200$ magnification by 2

independent observers and the mean percentage of positive cells was calculated using Image-Pro Plus v. 6.0 (Media Cybernetics, Rockville, USA).

Western blot analysis

The proteins were collected from tumor tissues using RIPA lysis buffer (consisting of sodium chloride, tris(hydroxymethyl)aminomethane, sodium deoxycholate, and NP-40 lysis buffer) containing protease inhibitors and phosphatase inhibitors (Roche, Basel, Switzerland). The lysates were subjected to centrifugation at 12,000 rpm for 20 min at 4°C. The total protein was then measured with Pierce BCA assay (Solarbio). One part of 5 \times sample buffer and 4 parts of equal concentrations of protein were mixed and heated at 95°C for 10 min. Equal amounts of lysates were separated with 10% sodium dodecyl sulfate-polyacrylamide gel electrophoresis for 90 min and were blotted onto a polyvinylidene fluoride (PVDF) membrane (Merck Millipore, Burlington, USA). The membranes were blocked with 1 \times TBS containing 0.1% Tween 20 and 2% BSA at room temperature for 1 h and subsequently incubated with rabbit monoclonal anti-STAT3 (phospho-Y705; 1:2,000; Abcam) at 4°C overnight, followed by secondary fluorescent antibodies labeled with LI-COR IRDye 680 (LI-COR Biosciences, Lincoln, USA) at room temperature for 1 h. The signals were determined using Odyssey Infrared Imaging System and quantitated with LICOR imaging software (LI-COR Biosciences).

ELISA for IL-9

The tumor tissues were washed and homogenized in cold PBS before being stored at -20°C overnight. The tumor homogenates had undergone 2 freeze–thaw cycles and were subsequently centrifuged at 5,000 g for 5 min at 4°C. Interleukin 9 levels in the supernatant were determined using enzyme-linked immunosorbent assay (ELISA) Kits according to the manufacturer's instructions (Cusabio, Wuhan, China). The optical density was measured at 450 nm with a standard curve range of 15.6 pg/mL to 1,000 pg/mL.

Statistical analysis

The data is expressed as mean values \pm standard deviation (SD). All data was analyzed with SPSS v. 17.0 software (SPSS Inc., Chicago, USA). Comparisons between 2 groups were carried out using Student's t-test while comparisons among multiple groups were analyzed using the one-way analysis of variance (ANOVA) method followed by the least significant differences (LSD) post hoc test. The χ^2 test and Fisher's exact probability test were used to compare enumeration data. Survival analysis was performed using the Kaplan–Meier method and the log-rank test. Differences in means were considered statistically significant when $p < 0.05$.

Results

Blockading IL-9 slows in vivo pancreatic tumor growth

The tumors in the anti-IL-9 group showed significantly slower growth rates than those in the PBS and IgG groups ($p < 0.05$; Fig. 2A). Significant differences in tumor volume among the 3 groups were observed on day 17, whereas no significant differences between the PBS group and the IgG group were found. Additionally, tumor weight was significantly lower in the anti-IL-9 group than in both the PBS and IgG groups ($p < 0.05$; Fig. 2B). At the end of the experiment, the anti-IL-9 group achieved 24.2% tumor growth inhibition ($p < 0.05$ vs the control group). These results suggest that the anti-IL-9 antibody can inhibit tumor growth.

Neutralizing IL-9 extended survival time in a murine model

Measuring the time from Panc02 cell injection until the surrogate endpoint for survival, we found that administering anti-IL-9 significantly prolonged the survival of tumor-bearing mice compared to the PBS- or IgG-administered groups ($p < 0.05$; Fig. 3): the increase in survival time among the anti-IL-9 group was 16.8%. Additionally, exposure to anti-IL-9 treatment did not lead to abnormal behavior or dramatic changes in the body weight of these animals, implying its tolerability during a sustained period of administration.

Administering anti-IL-9 antibody decreased IL-9 concentration in tumor tissue

To determine whether the anti-IL-9 antibody treatment blocked IL-9 activity, the concentration of IL-9

in the tumor tissue was detected with ELISA. We observed a significant reduction in IL-9 activity in the anti-IL-9-treated mice compared to the PBS-treated and IgG-treated mice ($p < 0.05$; Fig. 4A). Similarly, quantitative reverse-transcription polymerase chain reaction (qRT-PCR) analysis suggests that the expression of *IL-9* mRNA was significantly lower after anti-IL-9 treatment ($p < 0.05$; Fig. 4B).

Treating with anti-IL-9 antibody alters the JAK-STAT pathway in tumor-bearing mice

Because IL-9-mediated signal transduction activated molecular members of the STAT3,⁵ MAPK and PI3K pathways¹⁴ – which were potentially involved in the activity of the IL-9–IL-9R axis – we postulated that the blockade of IL-9 may mediate the JAK/STAT pathway in pancreatic-tumor-bearing mice. As is shown in Fig. 5, the relative expression of *Jak1* and *Jak3* mRNA

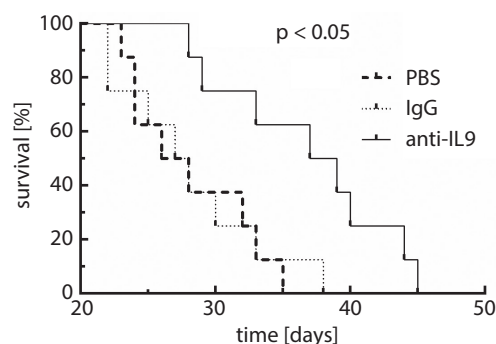


Fig. 3. Treatment with anti-IL-9 antibody extends the survival of mice. Tumor growth exceeding 20 mm or at signs of ulcerated was used as a surrogate for survival. Kaplan–Meier analysis demonstrates that the survival time ($n = 8$ /each) was significantly prolonged in anti-IL-9-treated mice compared to PBS- or IgG-treated mice ($p < 0.05$). Moreover, the mice experienced no apparent toxicity during the treatment

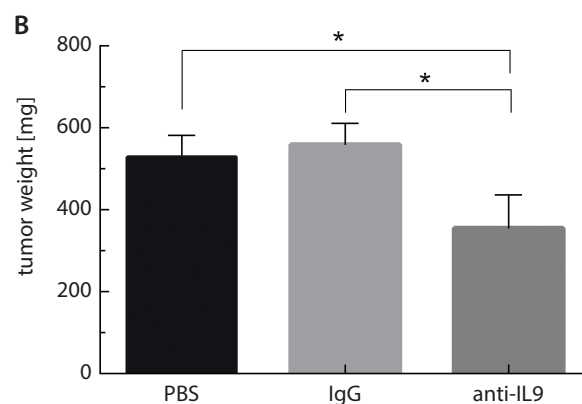
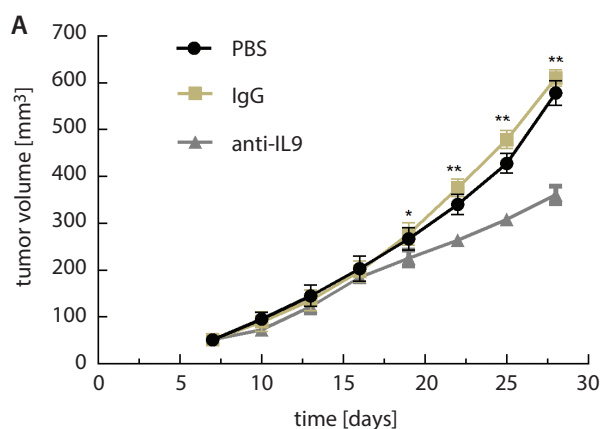


Fig. 2. Anti-IL-9 treatment results in slowed tumor growth in vivo. When tumors reached approx. 50 mm³, mice were randomly separated into 3 cohorts: PBS group, IgG group and anti-IL-9 group, and tumor growth was monitored. A – mice treated with anti-IL-9 antibody showed significant delay in tumor growth as compared to control groups ($p < 0.05$). Each data point represents average tumor volume ($n = 8$ /each) and error bars denote standard error; B – comparison of weight of tumor in different groups ($n = 8$ /each)

* $p < 0.05$ compared with PBS or IgG control group; data is shown as mean \pm SD.

in the anti-IL-9 group was markedly lower than that of the PBS or IgG groups ($p < 0.05$; Fig. 5B,C), whereas the mRNA levels of *IL-9r* and *Stat3* did not show any difference across all 3 groups ($p > 0.05$; Fig. 5A,D). Similarly, the western blot results showed that IL-9 inhibition failed to suppress STAT3 expression in the anti-IL-9 group ($p > 0.05$; Fig. 6A,B), but pSTAT3 expression was

effectively decreased in the tumor tissues from the anti-IL-9 group compared to those treated with PBS or IgG antibody ($p < 0.05$; Fig. 6A,C). Consistent with the above results, the immunohistochemistry results revealed that tumor tissues in the anti-IL-9 group expressed significantly less pSTAT3 protein when compared to the other groups ($p < 0.05$; Fig. 7).

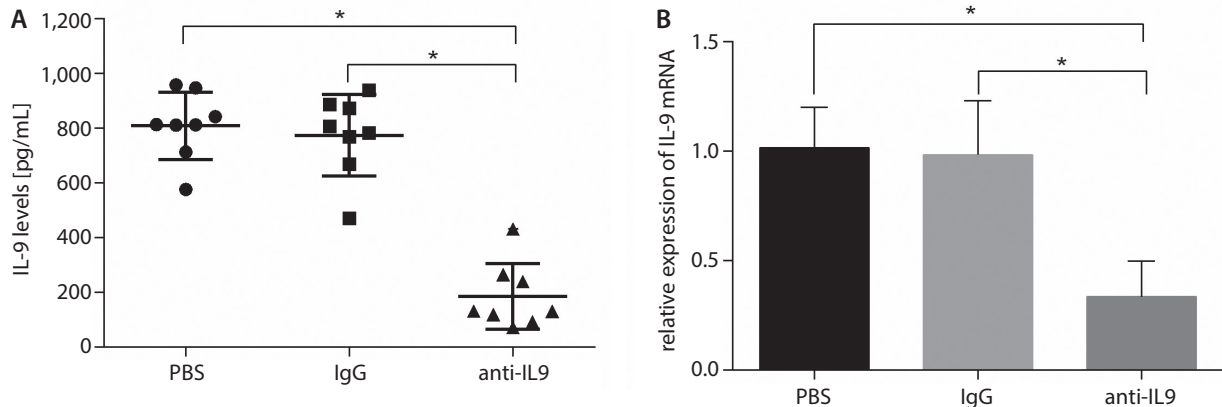


Fig. 4. Comparison of level of IL-9 in anti-IL-9 antibody, PBS and IgG-treated groups ($n = 8$ /each). The data confirmed antibody neutralization of IL-9 had a significant effect on the production of IL-9. A – concentration of IL-9 in tumor tissue was detected using ELISA; B – the expression of IL-9 mRNA was detected using qRT-PCR
* $p < 0.05$ compared with PBS or IgG control group; ns – $p > 0.05$ compared with PBS or IgG control group. Data is shown as mean \pm SD.

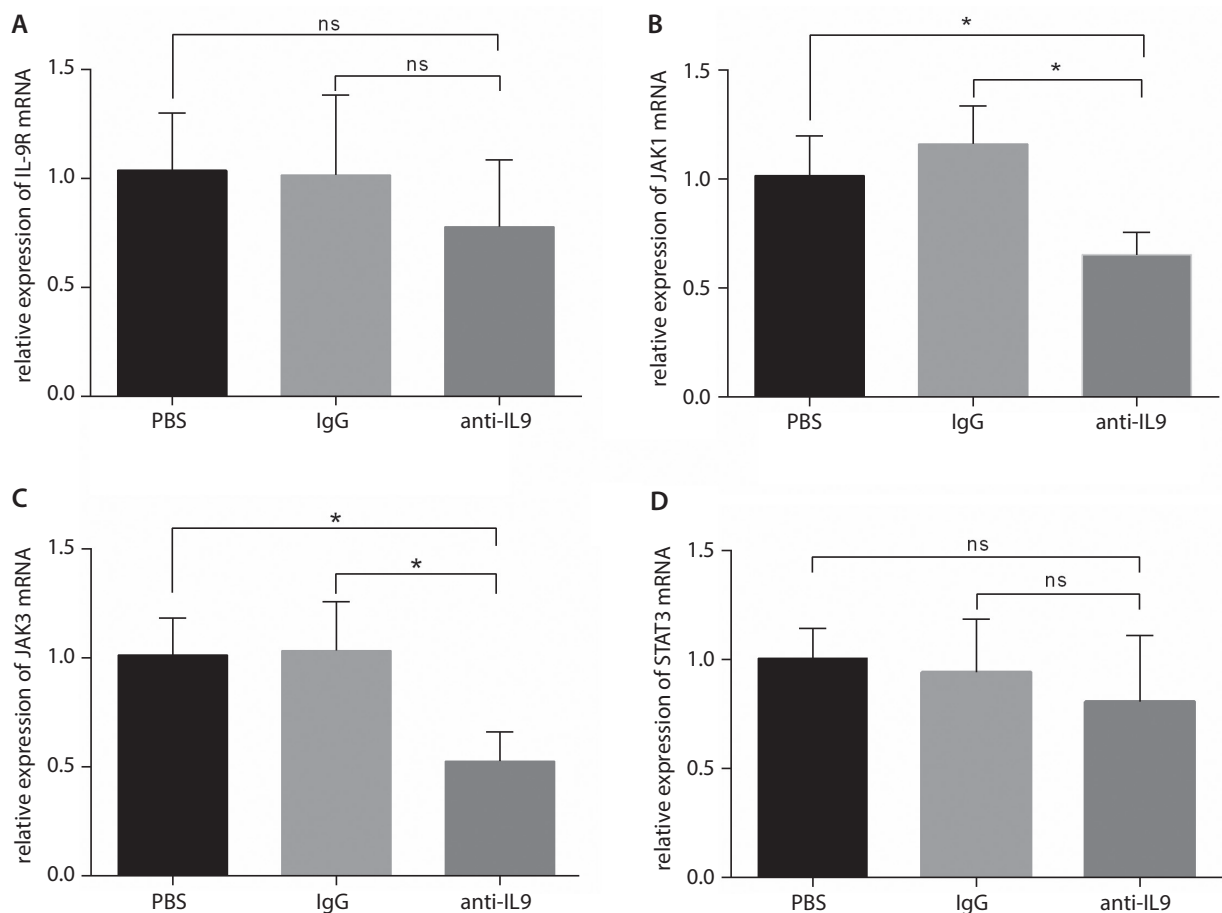


Fig. 5. The mRNA level of IL-9r, Jak1, Jak3, and Stat3 in mice with administration of PBS, IgG and anti-IL-9. A–D – relative expression of IL-9r, Jak1, Jak3, and Stat3 was detected using qRT-PCR.

* $p < 0.05$ compared with control PBS- or IgG-treated mice; ns – $p > 0.05$ compared with PBS or IgG control group. Data is presented as mean \pm SD.

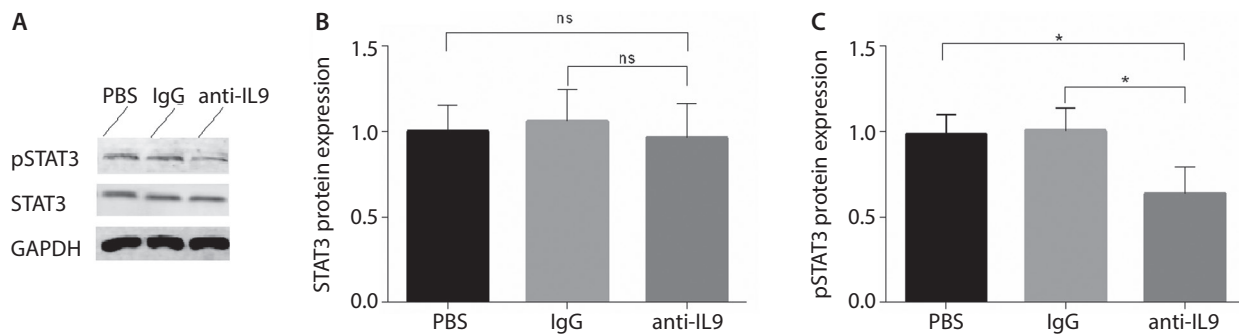


Fig. 6. Administration of anti-IL-9 antibody suppressed STAT3 phosphorylation in tumor tissue. A – expression of STAT3 and pSTAT3 was detected using western blot. B,C – western blot analysis indicated that the protein levels of pSTAT3 in anti-IL-9 group were significantly downregulated, but no significant changes in level of STAT3 protein was found

* $p < 0.05$ compared with PBS or IgG control group. Data is shown as mean \pm SD.

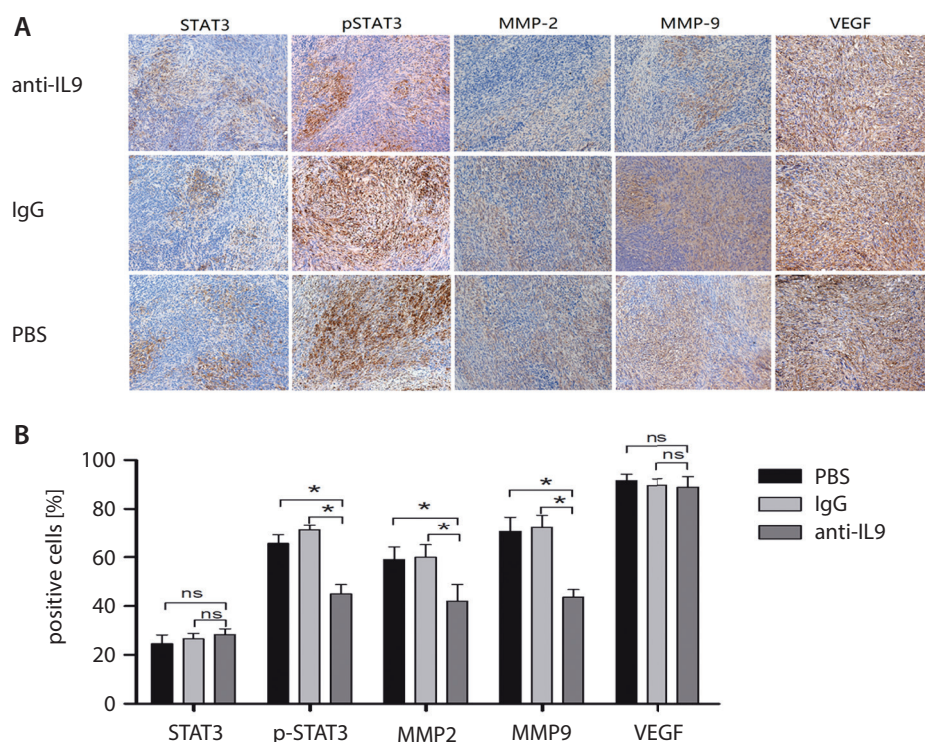


Fig. 7. The effect of anti-IL-9 antibody treatment on the expression of STAT3, pSTAT3, MMP2, MMP9, and VEGF in subcutaneous tumor. A – immunohistochemistry detected significantly less pSTAT3 (brown, nuclei), MMP2 (brown, cytoplasm) and MMP9 (brown, cytoplasm) in the tumors of anti-IL-9-treated mice than in those of PBS or IgG-treated mice. No significant changes was found in the levels of STAT3 (brown, cytoplasm) and VEGF (brown, cytoplasm) between groups; B – the semi-quantitative analysis of the above results

* $p < 0.05$ compared with PBS or IgG control group. All images are presented at $\times 200$ magnification.

Treating with anti-IL-9 antibody decreases STAT3-regulated downstream target products

Next, we determined whether suppressing pSTAT3 with the anti-IL-9 antibody could initiate the suppression of STAT3-regulated genes, MMP 2 and 9 and VEGF.¹⁵ As shown in Fig. 7, the tumor cells and stroma showed strong reactivity to the antibodies for STAT3, pSTAT3, MMP 2 and 9, and VEGF. Our immunohistochemistry results showed a significant reduction in pSTAT3-, MMP2- and MMP9-positive cells ($p < 0.05$; Fig. 7), whereas the number of STAT3- and VEGF-positive cells was not significantly different in the anti-IL-9 group compared to the PBS and IgG groups ($p > 0.05$; Fig. 7). We concluded

that anti-IL-9 antibody may inhibit pancreatic cancer growth by downregulating JAK/STAT3 signaling.

Discussion

Immune cells and the cytokines secreted by them are involved in a multitude of physiological and pathological processes.^{16,17} Interleukin 9, a pleiotropic cytokine secreted by a number of immune cells, is implicated in the pathogenesis of several diseases and conditions.^{5,6} Interleukin 9 facilitates an immunosuppressive environment to promote tumor growth or to restrain tumor progression based on tumor type.¹⁸ Interleukin 9 was shown to inhibit the growth of HTB-72 melanoma cells and it favors

the survival of CD4⁺CD8⁺ double-positive T cells; it also displays cytotoxic activity against melanoma cells.¹⁹ However, IL-9 also substantially contributes to the proliferation and migration of lung cancer cells while helping them escape apoptosis.²⁰ Similar biological functions of IL-9 were also observed in breast cancer,¹⁸ colon carcinoma¹⁸ and hematopoietic malignancies, such as diffuse large B-cell lymphoma (DLBCL).⁸ Moreover, IL-9 can protect DLBCL cell lines LY1 and LY8 from prednisolone and rituximab, whereas the effect of IL-9 on DLBCL cell lines could be impaired and reversed through the knock-down of IL-9R.⁸ Because IL-9 is strongly associated with tumor progression, blocking IL-9 may be an applicable strategy for tumor treatment. Smith et al. showed that the neutralization of IL-9 in conjunction with CpG-ODN injection could induce tumor rejection in BALB-neuT- and MUC-1-tolerant tumor models.²¹ Anti-IL-9 treatment inhibited tumor growth in WT mice with breast cancer cell line 4T1.¹⁸ In this setting, we investigated whether targeting IL-9 could influence pancreatic cancer progression.

A murine Panc02 model is widely used in pre-clinical study, and immunocompetent C57BL/6 mice provide a tumor microenvironment similar to a real immune environment.^{22,23} A significantly slower tumor growth rate and lower tumor weight were observed in the anti-IL-9 group compared to the PBS or IgG groups, indicating that the anti-IL-9 antibody could limit the growth of pancreatic cancer.

Next, we investigated the effect of anti-IL-9 treatment on survival. The results showed that neutralizing IL-9 significantly prolonged the survival time in Panc02-tumor-bearing mice. Notably, we observed that tumor growth occurred constantly in the survival period after the last administration of anti-IL-9, suggesting that the anti-IL-9 antibody could inhibit tumor growth only in a period of constitutive anti-IL-9 antibody injection, but failed to provide a long-term solution to inhibit tumor growth completely. In addition, the concentration of IL-9 in tumor tissue from the anti-IL-9 group was markedly reduced. Taken together, our results suggest that neutralizing IL-9 could inhibit the growth of pancreatic cancer in vivo by inhibiting IL-9.

The STAT3 signaling is involved in the regulation of the cell cycle, apoptosis, angiogenesis, metastasis, and immune evasion across a variety of tumor types, including pancreatic cancer.^{24–26} Notably, sustained activation of STAT3 at phosphorylated Tyr705 exists in 30–100% of human tumor specimens and in several pancreatic cancer cell lines.²⁷ Moreover, STAT3 was previously reported to be potentially involved in the IL-9–IL-9R axis, and IL-9-induced receptor activation promotes phosphorylation of JAK1 and JAK3, which leads to the downstream activation of the STAT3 pathway.^{5,14,28} Dysregulation of IL-9 in vitro could lead to autonomous cell growth and malignant transformation of lymphoid cells, which was strongly related to constitutive activation of the JAK/STAT pathway.²⁹ Thus, we postulate that an IL-9 blockade may affect

the STAT3 pathway. Consistent with this hypothesis, our results showed a dramatic reduction of JAK1, JAK3 and pSTAT3 in the tumor tissue from the mice injected with the anti-IL-9 antibody, so we concluded that the STAT3 pathway may be implicated in this process.

The activation of STAT3 has been reported to induce MMP9 expression³⁰ and to upregulate VEGF by directly binding to the VEGF promoter,³¹ thereby facilitating cell invasion. In this study, we further examined whether the alteration of STAT3 could influence the expression of MMP9 and VEGF. We observed that the expression of MMP2 and MMP9 was reduced after the administration of the anti-IL-9 antibody, but no significant change in the expression of VEGF was observed among the 3 groups, implying that the inhibition of the STAT3 pathway caused by anti-IL-9 could further suppress the expression of MMP2 and MMP9, but had no effect on VEGF expression.

Although our study elucidated the effect of anti-IL-9 in pancreatic cancer and its possible underlying mechanism, there were several limitations to this study. The pancreatic cancer mouse model was established using Panc02 cells; the effect and mechanism of IL-9 on pancreatic cancer should be verified in a mouse model established by the use of other pancreatic cancer cells. Although we showed an anti-IL-9-mediated STAT3 pathway inhibition in pancreatic cancer, a rescue experiment using STAT3 pathway inhibitors is needed to verify whether the pathway is truly involved in this process.

Conclusions

Our study demonstrated that treating pancreatic-tumor-bearing mice with the anti-IL-9 antibody can delay tumor growth, possibly via the inhibition of the STAT3 signaling pathway. Further experimentation using other pancreatic cancer mouse models is required to validate these results.

References

1. Siegel RL, Miller KD, Jemal A. Cancer statistics, 2017. *CA Cancer J Clin*. 2017;67(1):7–30.
2. Hidalgo M. Pancreatic cancer. *N Engl J Med*. 2010;362(17):1605–1617.
3. Stassen M, Schmitt E, Bopp T. From interleukin-9 to T helper 9 cells. *Ann NY Acad Sci*. 2012;1247:56–68.
4. Schmitt E, Klein M, Bopp T. Th9 cells, new players in adaptive immunity. *Trends Immunol*. 2014;35(2):61–68.
5. Noelle RJ, Nowak EC. Cellular sources and immune functions of interleukin-9. *Nat Rev Immunol*. 2010;10(10):683–687.
6. Rivera Vargas T, Humblin E, Vegran F, Ghiringhelli F, Apetoh L. TH9 cells in anti-tumor immunity. *Semin Immunopathol*. 2017;39(1):39–46.
7. Chen J, Petrus M, Bryant BR, et al. Autocrine/paracrine cytokine stimulation of leukemic cell proliferation in smoldering and chronic adult T-cell leukemia. *Blood*. 2010;116(26):5948–5956.
8. Lv X, Feng L, Ge X, Lu K, Wang X. Interleukin-9 promotes cell survival and drug resistance in diffuse large B-cell lymphoma. *J Exp Clin Cancer Res*. 2016;35(1):106.
9. Hu B, Qiu-Lan H, Lei RE, Shi C, Jiang HX, Qin SY. Interleukin-9 promotes pancreatic cancer cells proliferation and migration via the miR-200a/beta-catenin axis. *Biomed Res Int*. 2017;2017:2831056.

10. Huang Q, Lei R, Qin Q, Qin S, Jiang H, Hu B. Interleukin-9 promotes pancreatic cancer cell proliferation and migration via activation of STAT3 pathway [in Chinese]. *Xi Bao Yu Fen Zi Mian Yi Xue Za Zhi*. 2017; 33:1228–1233.
11. Back TA, Chouin N, Lindegren S, et al. Cure of human ovarian carcinoma solid xenografts by fractionated [211At] alpha-radioimmunotherapy: Influence of tumor absorbed dose and effect on long-term survival. *J Nucl Med*. 2017;58(4):598–604.
12. Kashiwagi H, McDunn JE, Goedegebuure PS, et al. TAT-Bim induces extensive apoptosis in cancer cells. *Ann Surg Oncol*. 2007;14(5): 1763–1771.
13. Hawkins WG, Gold JS, Dyllal R, et al. Immunization with DNA coding for gp100 results in CD4 T-cell independent antitumor immunity. *Surgery*. 2000;128(2):273–280.
14. Li HJ, Sun QM, Liu LZ, et al. High expression of IL-9R promotes the progression of human hepatocellular carcinoma and indicates a poor clinical outcome. *Oncol Rep*. 2015;34(2):795–802.
15. Banerjee K, Resat H. Constitutive activation of STAT3 in breast cancer cells: A review. *Int J Cancer*. 2016;138(11):2570–2578.
16. Makohon-Moore A, Iacobuzio-Donahue CA. Pancreatic cancer biology and genetics from an evolutionary perspective. *Nat Rev Cancer*. 2016;16(9):553–565.
17. Laheru D, Jaffee EM. Immunotherapy for pancreatic cancer: Science driving clinical progress. *Nat Rev Cancer*. 2005;5(6):459–467.
18. Hoelzinger DB, Dominguez AL, Cohen PA, Gendler SJ. Inhibition of adaptive immunity by IL9 can be disrupted to achieve rapid T-cell sensitization and rejection of progressive tumor challenges. *Cancer Res*. 2014;74(23):6845–6855.
19. Parrot T, Allard M, Oger R, et al. IL-9 promotes the survival and function of human melanoma-infiltrating CD4(+) CD8(+) double-positive T cells. *Eur J Immunol*. 2016;46(7):1770–1782.
20. Ye ZJ, Zhou Q, Yin W, et al. Differentiation and immune regulation of IL-9-producing CD4⁺ T cells in malignant pleural effusion. *Am J Respir Crit Care Med*. 2012;186(11):1168–1179.
21. Smith SE, Hoelzinger DB, Dominguez AL, Van Snick J, Lustgarten J. Signals through 4-1BB inhibit T regulatory cells by blocking IL-9 production enhancing antitumor responses. *Cancer Immunol Immunother*. 2011;60(12):1775–1787.
22. Partecke LI, Sendler M, Kaeding A, et al. A syngeneic orthotopic murine model of pancreatic adenocarcinoma in the C57/BL6 mouse using the Panc02 and 6606PDA cell lines. *Eur Surg Res*. 2011;47(2): 98–107.
23. Mace TA, Shakya R, Pitarresi JR, et al. IL-6 and PD-L1 antibody blockade combination therapy reduces tumour progression in murine models of pancreatic cancer. *Gut*. 2018;67(2):320–332.
24. Arpin CC, Mac S, Jiang Y, et al. Applying small molecule signal transducer and activator of transcription-3 (STAT3) protein inhibitors as pancreatic cancer therapeutics. *Mol Cancer Ther*. 2016;15(5):794–805.
25. Zimmers TA, Fishel ML, Bonetto A. STAT3 in the systemic inflammation of cancer cachexia. *Semin Cell Dev Biol*. 2016;54:28–41.
26. Yu H, Lee H, Herrmann A, Buettner R, Jove R. Revisiting STAT3 signaling in cancer: New and unexpected biological functions. *Nat Rev Cancer*. 2014;14(11):736–746.
27. Corcoran RB, Contino G, Deshpande V, et al. STAT3 plays a critical role in KRAS-induced pancreatic tumorigenesis. *Cancer Res*. 2011;71(14): 5020–5029.
28. Goswami R, Kaplan MH. A brief history of IL-9. *J Immunol*. 2011;186(6): 3283–3288.
29. Hornakova T, Staerk J, Royer Y, et al. Acute lymphoblastic leukemia-associated JAK1 mutants activate the Janus kinase/STAT pathway via interleukin-9 receptor alpha homodimers. *J Biol Chem*. 2009;284(11): 6773–6781.
30. Liu X, Lv Z, Zou J, et al. Elevated AEG-1 expression in macrophages promotes hypopharyngeal cancer invasion through the STAT3-MMP-9 signaling pathway. *Oncotarget*. 2016;7(47):77244–77256.
31. Middleton K, Jones J, Lwin Z, Coward JI. Interleukin-6: An angiogenic target in solid tumours. *Crit Rev Oncol Hematol*. 2014;89(1):129–139.

miR-29a promotes osteoblast proliferation by downregulating DKK-1 expression and activating Wnt/ β -catenin signaling pathway

Fuwen Zhang^{B-D,F}, Kun Cao^{B,F}, Gongwen Du^{C,D,F}, Qi Zhang^{C,D,F}, Zongsheng Yin^{A,C,E,F}

First Hospital Of Anhui Medical University, Hefei, China

A – research concept and design; B – collection and/or assembly of data; C – data analysis and interpretation; D – writing the article; E – critical revision of the article; F – final approval of the article

Advances in Clinical and Experimental Medicine, ISSN 1899–5276 (print), ISSN 2451–2680 (online)

Adv Clin Exp Med. 2019;28(10):1293–1300

Address for correspondence

Zongsheng Yin
E-mail: yinzongsheng730@163.com

Funding sources

None declared

Conflict of interest

None declared

Received on August 21, 2018
Reviewed on October 31, 2018
Accepted on February 18, 2019

Published online on September 16, 2019

Abstract

Background. MicroRNA (miRNA) is a kind of non-coding small RNA with a negative regulating function. Some miRNAs play a role in regulating the differentiation and function of osteoblasts, chondrocytes and osteoclasts.

Objectives. In this study, we analyzed the role of miR-29a and dickkopf-1 (DKK-1) in osteoblast differentiation.

Material and methods. Specimens were collected from the surgical resection of pathological ankylosing spondylitis (AS) tissue and some normal tissues. The expression of miR-29a, DKK-1 and β -catenin in normal and AS tissues were detected with real-time polymerase chain reaction (RT-PCR) and western blotting. Cell proliferation was detected with a Cell Counting Kit-8, cell migration and invasion were determined using a Transwell system and cell apoptosis was analyzed with flow cytometry. The luciferase reporter gene plasmid pGL3-DKK-1 and a point-mutation of the luciferase reporter gene plasmid mut-pGL3-DKK-1 were constructed.

Results. It was found that miR-29a could promote the proliferation of hFOB1.19 cells, while DKK-1 inhibited their proliferation. Also, miR-29a was able to inhibit the apoptosis of hFOB1.19 cells, while DKK-1 was able to promote the apoptosis of hFOB1.19 cells. When it comes to the invasion and migration of hFOB1.19 cells, miR-29a was found to promote it, while DKK-1 did not.

Conclusions. These findings will lead to a better understanding of the proliferation and differentiation of osteoblasts and will provide new insights for the treatment of this disease.

Key words: β -catenin, Dkk-1, miR-29a, si-RNA

Cite as

Zhang F, Cao K, Du G, Zhang Q, Yin Z. miR-29a promotes osteoblast proliferation by downregulating DKK-1 expression and activating Wnt/ β -catenin signaling pathway. *Adv Clin Exp Med.* 2019;28(10):1293–1300. doi:10.17219/acem/104533

DOI

10.17219/acem/104533

Copyright

© 2019 by Wrocław Medical University
This is an article distributed under the terms of the Creative Commons Attribution Non-Commercial License (<http://creativecommons.org/licenses/by-nc-nd/4.0/>)

Introduction

Osteoblasts and osteoclasts are the 2 major types of bone cells involved in the bone remodeling process. Bone mass is regulated both by the number of mature osteoblasts and by their bone-forming activity.¹ Osteoblasts come from mesenchymal stem cells (MSCs) which have multipotent differentiation potential. They can eventually become bone cells after cell proliferation, differentiation and mineralization, thus promoting bone formation and maintaining bone mass. Multiple signaling pathways have been found to be able to regulate osteoblast differentiation, i.e., BMP/Smads and Wnt/ β -catenin.²

MicroRNA (miRNA) is a class of noncoding single-strand RNA molecules encoded by endogenous genes, with a length of 19–25 nucleotides; it is highly conserved among species. The miRNA usually acts on 1 or more messenger RNAs (mRNA) and negatively regulates gene expression by degrading mRNA or inhibiting its translation level. Some miRNAs were reported to regulate stem cell differentiation into osteoblast and bone formation.^{3,4} MicroRNA-29 has been found to be the key regulator in bone formation, absorption, remodeling, and repair. Human miR-29 includes miR-29a-3p, miR-29b1, miR-29b2, and miR-29c. MicroRNA-29a signaling has been found to protect against glucocorticoid-induced disturbance of Wnt and DKK-1 activity and to improve osteoblast differentiation and mineral acquisition.^{5,6} MicroRNA-29b has been functionally characterized as a positive regulator of osteoblastogenesis.⁷ Previous studies have confirmed that in primary cultures of murine calvarial osteoblasts, expression of miR-29 family members did increase in osteoblastic differentiation progression.^{8,9} MicroRNA-29a could promote osteogenic differentiation of mesenchymal stem cells by targeting HDAC4.¹⁰

As a key signaling protein of the Wnt signaling pathway, β -catenin also plays an important role in postnatal bone development and bone maintenance in mice. The mutation of the β -catenin gene can induce bone loss and increase the number of osteoclasts in mice.¹¹ It can also induce ectopic chondrocyte formation and inhibit normal osteogenesis by selectively knocking out the β -catenin gene in the MSCs which are differentiated into osteoblast cell lines.¹² In addition, the related antagonists of the Wnt/ β -catenin signaling pathway – such as dickkopfs (DKKs), secretory curl-related proteins and bone sclerosis protein – can also act on the Wnt and LRP5/6 receptors, and can indirectly regulate bone mass and osteogenic differentiation.¹³ The Wnt/ β -catenin signaling pathway is composed of extracellular factor Wnt, transmembrane receptor, β -catenin, “degradation complex”, and transcription factor T cytokines. The transmembrane receptors are composed of 2 kinds of proteins: one is a member of the 7 transmembrane crimp protein receptor family and the other is LRP5/6, a member of the low-density-lipoprotein-receptor-related protein (LRP) family. Regular Wnt signals are

activated only when the curl protein and LRP are combined with Wnt. Therefore, restricting the expression of LRP or Wnt can block the Wnt/ β -catenin pathway, indicating that the expression level of dickkopf-1 (DKK-1) is related to the Wnt/catenin pathway, which contributes to the differentiation of osteoblasts.

In this study, we analyzed the role of miR-29a and DKK-1 in osteoblast differentiation. These findings will help to provide new insights for the treatment of this disease.

Material and methods

Subjects

Specimens were collected from the surgical resection of AS pathological tissue and some normal tissues from the Department of Spinal Surgery at the First Affiliated University Hospital of Anhui Medical University, Hefei, China, from June to December 2017. All subjects signed informed consent forms and the study was approved by the ethics committee of Anhui Medical University.

Cell culture

Human osteoblast cells from cell line hFOB1.19 were purchased from the American Type Culture Collection (ATCC; Manassas, USA). The cells were cultured with Dulbecco's modified Eagle medium (DMEM/F12) (HyClone; GE Healthcare Life Sciences, Logan City, USA) containing 10% fetal bovine serum (FBS) (HyClone; GE Healthcare Life Sciences), 0.03 mg/mL of G418, 100 U/mL of penicillin G, and 100 U/mL of treptomycin sulfate (Invitrogen, Carlsbad, USA). Nthyori 3-1 cells were cultured with HG RPMI1640 medium containing 10% FBS, 100 U/mL of penicillin G and 100 U/mL of treptomycin sulfate (Invitrogen) at 37°C in a humidified atmosphere with 5% CO₂.

RNA extraction and qRT-PCR

The total RNA was extracted using a Trizol reagent kit (Invitrogen) according to the manufacturer's protocol. RNA concentration and purity were measured using a Qubit Fluorometer (Thermo Fisher Scientific, Waltham, USA). A total of 1 μ g of RNA was subjected to reverse transcription using a MMLV Reverse Transcriptase Kit (Takara Bio China Inc., Dalian, China). Quantitative polymerase chain reaction (qPCR) was performed using a GenePharma Hairpin-itTM microRNA RT-PCR Quantitation Kit (Suzhou GenePharma Inc., Suzhou, China). The form of miRNA was mature, the primer was specific for 3p and the 2- $\Delta\Delta$ CT quantification method was used. The thermocycling conditions were as follows: pre-degeneration at 95°C for 10 min, followed by 40 cycles of 95°C for 12 s and 62°C for 40 s; *U6* and *GAPDH* genes were used as an internal control. The primers used in this study were as follows:

DKK-1 (accession number: NM_012242.3) forward: 5'-TG-GAACTCCCCTGTGATTGC-3' and reverse: 5'-AATAG-GCAGTGCAGCACCTT-3'; β -catenin (accession number: NM_957217.4) forward: 5'-GCGTTAACCTGCCTTT-GAGC-3' and reverse: 5'-CTGGGCTGGCATGTAAC-CA-3'; U6 forward: 5'-CTCGCTTCGGCAGCAC-3' and reverse: 5'-AACGCTTCACGAATTTGCGT-3'; *GAPDH* forward: 5'-ACCTGACCTGCCGTCTAGAA-3' and reverse: 5'-TCCACCACCCTGTTGCTGTA-3'.

Small interfering (si) RNA transfection

The cells were randomly divided into 4 groups: control, DKK-1 overexpression, DKK-1 siRNA, and miR-29a. MicroRNA-29a mimics, DKK-1 overexpression lysates and DKK-1 siRNAs were purchased from Hanbio Biotechnology Co., Ltd. (Shanghai, China). The mimic used in transfection was specific for 3p. They were transfected into the hFOB1.19 cells. All siRNA transfections were performed using Lipofectamine 2000 Reagent (Life Technologies, Carlsbad, USA), according to the manufacturer's recommendations.

Western blotting

The cells in the logarithmic growth period were harvested and lysed with Cell Lysis Solution (Sigma-Aldrich, St. Louis, USA); they were then centrifuged at 10,000 rpm at 4°C for 5 min. The nucleus and plasma proteins were extracted using a Nuclear and Cytoplasmic Protein Extraction Kit (Beyotime, Shanghai, China) according to manufacturer's instructions. The proteins were loaded on 10% sodium dodecyl sulfate (SDS)-polyacrylamide gels (50 μ g per lane) and transferred onto polyvinylidene fluoride membranes (PVDF; Amersham Biosciences, Piscataway, USA). The membranes were blocked for 2 h at 37°C with 5% non-fat milk in Tris-buffered saline with Tween 20 (TBST) and were incubated overnight at 4°C with primary antibodies, all sourced from Abcam (Cambridge, UK): 1:1000 DKK1; 1:1000 Wnt; 1:1000 β -catenin; 1:1000 p- β -catenin; 1:1000 caspase3; 1:1000 caspase 12; and 1:2000 *GAPDH*. Then, they were incubated with an HRP-conjugated secondary antibody (1:50,000, Abcam) for 1 h at 37°C. The membranes were coated with ECL luminescence reagent (Perkin-Elmer Inc., Waltham, USA) and, after the film was washed 3 times, they were observed using an Imagequant LAS4000 (GE Healthcare, Tokyo, Japan). *GAPDH* was used for normalization.

Cell proliferation detection

Cell proliferation was measured with a Cell Counting Kit-8 (CCK-8; Dojindo, Kumamoto, Japan) according to the manufacturer's protocol. The cells in the logarithmic growth phase were digested with trypsin and inoculated into 96-well plates (2,000 cells/well); they were then

cultured overnight. Into each well, 10 μ L of CCK-8 solution was added. The A450 values were determined with an Epoch Microplate Spectrophotometer (Bio Tek, Winooski, USA) every day after culturing for 1–5 days in order to evaluate the proliferation of cells.

Cell migration and invasion assay

Cell migration and invasion were determined using a Transwell system (Corning, Inc., Corning, USA). The cells were trypsinized and re-suspended in serum-free medium and 0.1 mL of cells (300,000/mL) were added to the upper chamber of the 24-well Transwell system. The invasion assay was performed using Matrigel matrix (BD Biosciences, San Jose, USA) as a barrier through which the cells had to pass. The migration assay did not use Matrigel. The lower chamber had 0.6 mL of a medium containing 10% FBS added to it. The cells were incubated at 37°C for 12 h for the migration test and they continued to culture at 37°C for 24 h for the invasion test. The cells were fixed and stained with 0.1% crystal violet dye (Richard-Allan Scientific, San Diego, USA). They were washed twice with PBS. The stained cells were observed under an inverted microscope.

Apoptosis analysis

Cell apoptosis was analyzed with flow cytometry (FAC-Scan; BD Biosciences) using an Annexin V-FITC Analysis Kit (Beyotime) according to manufacturer's instructions. The cells in each group were cultured for 48 h under the same conditions before being harvested and digested with trypsin. The digested cells were washed with the pre-cooled PBS 3 times, and were then lightly resuspended by adding 195 μ L of annexin V-FITC binding solution; 5 μ L of annexin V-FITC was added and the solution was gently mixed. The cells were incubated at room temperature (20–25°C), avoiding light, for 10–20 min after 10 μ L of propidium iodide staining solution was gently stirred in. They were detected using CELLQUEST software (BD Biosciences).

Double luciferase reporter gene analysis

The luciferase reporter gene plasmid pGL3-DKK-1 and a point-mutation of luciferase reporter gene, plasmid mut-pGL3-DKK-1, were constructed. The 293T cells were inoculated into 24-well plates and were cultured overnight; the luciferase reporter plasmid, Renilla luciferase and miR-29a-3p mimic or a control were transfected into the 293T cells simultaneously. The cells were split after culturing for 48 h using a Dual Luciferase Reporter Assay System (Promega, Madison, USA) according to manufacturer's instructions. The results were measured using a Panomics Luminometer (Affymetrix, Santa Clara, USA) after the luminescence reagent was added. Sea renin fluorescence was used as an internal reference.

Statistical analysis

Statistical analysis was performed using one-way analysis of variance (ANOVA) or Student's t-test with SPSS v. 17.0 software (SPSS Inc., Chicago, USA). The data are expressed as mean \pm standard deviation (SD). A p-value <0.05 was considered to be statistically significant.

Results

Changes of miR-29a, DKK-1 and β -catenin expression in normal and AS tissues

A total of 10 cases of pathological AS tissues and normal tissues were detected with real-time polymerase chain reaction (RT-PCR) and western blotting. We found that the expression level of DKK-1 was higher in AS tissues than in normal tissues ($p < 0.01$). However, the expression levels of β -catenin and miR-29a were lower in AS tissues than in normal tissues ($p < 0.01$, Fig. 1).

Upregulation of miR-29a or downregulation of DKK-1 expression promoted β -catenin expression in hFOB1.19 cells

The RT-PCR showed that miR-29a expression was upregulated in the miR-29a group; there were no obvious changes in the other groups. Compared with the control group, the expression of DKK was upregulated in the DKK overexpression group, and it was downregulated in the DKK/siRNA and miR-29a groups ($p < 0.01$). Western blotting showed that the expression of β -catenin, Cyt- β -catenin, Nuc- β -catenin, and Wnt in the DKK overexpression group was downregulated, while in the DKK/siRNA and miR-29a groups it was upregulated. The expression of p- β -catenin in the DKK overexpression group was upregulated, while it was downregulated in the DKK/siRNA and miR-29a groups ($p < 0.01$, Fig. 2).

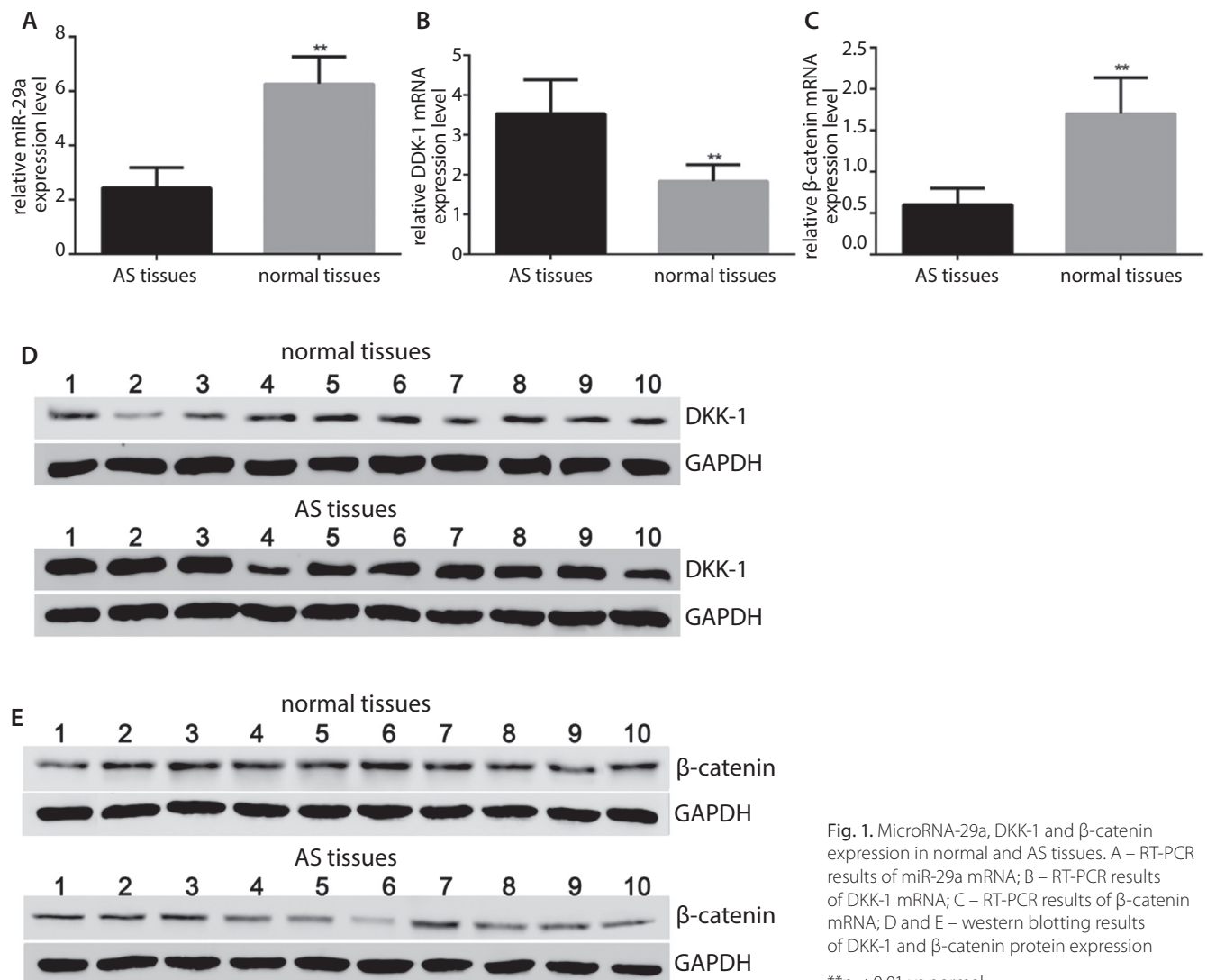


Fig. 1. MicroRNA-29a, DKK-1 and β -catenin expression in normal and AS tissues. A – RT-PCR results of miR-29a mRNA; B – RT-PCR results of DKK-1 mRNA; C – RT-PCR results of β -catenin mRNA; D and E – western blotting results of DKK-1 and β -catenin protein expression

** $p < 0.01$ vs normal.

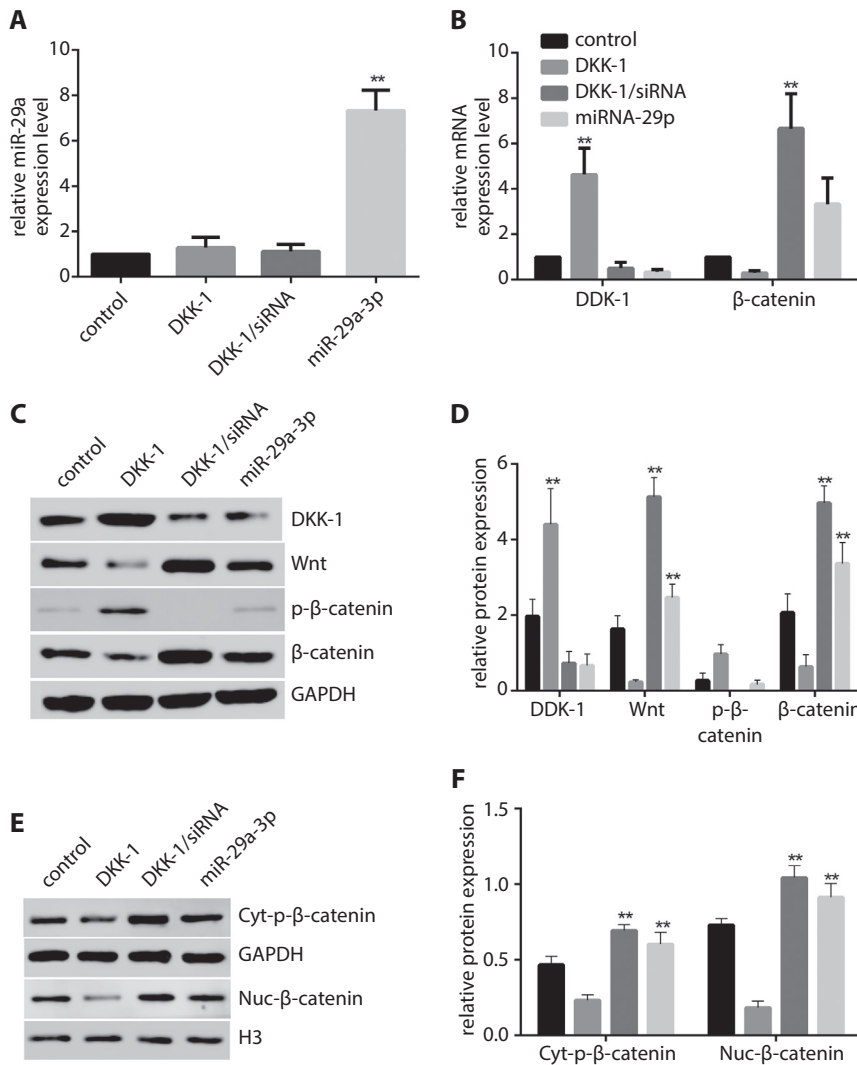


Fig. 2. Upregulation of miR-29a-3p or downregulation of DKK-1 expression promoted β-catenin expression in hFOB1.19 cells. A and B – RT-PCR results of miR-29a-3p, DKK-1 and β-catenin mRNA expression; C and D – western blotting results of DKK-1 Wnt, β-catenin and p-β-catenin protein expression; E and F – western blotting detection of β-catenin nuclear translocation
**p < 0.01 vs control.

MicroRNA-29a promoted the proliferation of hFOB1.19 cells, while DKK-1 inhibited their proliferation

Cell proliferation was detected using a CCK-8 kit. It was found that the upregulation of DKK-1 in hFOB1.19 cells inhibited the proliferation of hFOB1.19 cells, while the upregulation of miR-29a or downregulation of DKK-1 promoted the proliferation of hFOB1.19 cells (p < 0.05, Fig. 3).

MicroRNA-29a inhibited the apoptosis of hFOB1.19 cells, while DKK-1 promoted their apoptosis

Flow cytometry showed that the upregulation of miR-29a or the downregulation of DKK-1 in hFOB1.19 cells inhibited cell apoptosis, while the upregulation of DKK-1 in hFOB1.19 cells promoted cell apoptosis. Both the upregulation of miR-29a and the downregulation of DKK-1 at the same time inhibited the expression of apoptotic

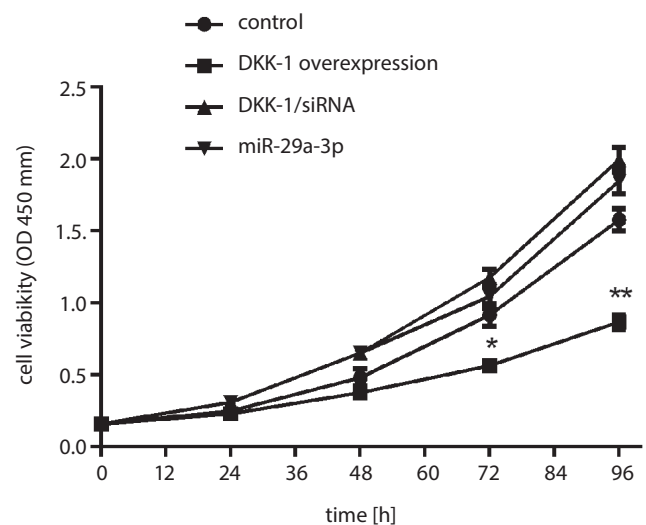


Fig. 3. MicroRNA-29a promoted the proliferation of hFOB1.19 cells, while DKK-1 inhibited the proliferation of hFOB1.19 cells
*p < 0.05 vs control, **p < 0.01 vs control.

proteins caspase-3 and caspase-12. The upregulation of DKK-1 promoted the expression of those 2 apoptotic proteins ($p < 0.01$, Fig. 4).

MicroRNA-29a promoted the invasion and migration of hFOB1.19 cells, while DKK-1 inhibited invasion and migration

The Transwell assays showed that the upregulation of miR-29a or the downregulation of DKK-1 in hFOB1.19 cells promoted the invasion and migration of hFOB1.19 cells, while the upregulation of DKK-1 inhibited the invasion and migration of hFOB1.19 cells ($p < 0.01$, Fig. 5).

MicroRNA-29a targeted 3'UTR of DKK-1 and inhibited its expression

The bioinformatics analysis predicted that miR-29a-3p can directly act on the 3'UTR of DKK-1. Analysis of the double luciferase reporter gene showed that miR-29a-3p could act on the 3'UTR of DKK-1 and could inhibit the expression of luciferase ($p < 0.01$). When the 3'UTR domain of DKK-1 was point-mutated, the inhibitory effect of miR-29a-3p disappeared (Fig. 6).

Discussion

A previous study reported that the overexpression of miR-29a significantly enhanced the differentiation of HMSCs into osteoblasts, while the inhibition of miR-29a markedly blocked the osteoblastic differentiation of HMSCs.¹⁰ In the current study, we found that miR-29a and DKK-1 played an important role in osteoblast differentiation. MicroRNA-29a promoted the proliferation of hFOB1.19 cells, while DKK-1 inhibited the proliferation of hFOB1.19 cells. MicroRNA-29a inhibited the apoptosis of hFOB1.19 cells, while DKK-1 promoted the apoptosis of hFOB1.19 cells. MicroRNA-29a promoted the invasion and migration of hFOB1.19 cells, while DKK-1 inhibited the invasion and migration of hFOB1.19 cells. Osteoblasts, as the main functional cells of bone formation, will gradually express specific markers, such as ALP, osteocalcin, serotype I procollagen C end peptide, etc., in the process of differentiation and maturation. At the same time, it is also regulated by a series of transcription factors, such as Runt-related transcription factor 2 (Runx2), Osterix/Sp7, β -catenin, transcription-activating factor 4, nuclear-factor-activating protein 1, SMADs, DKK-1, etc.¹⁴ They cooperate with each other to participate in the regulation

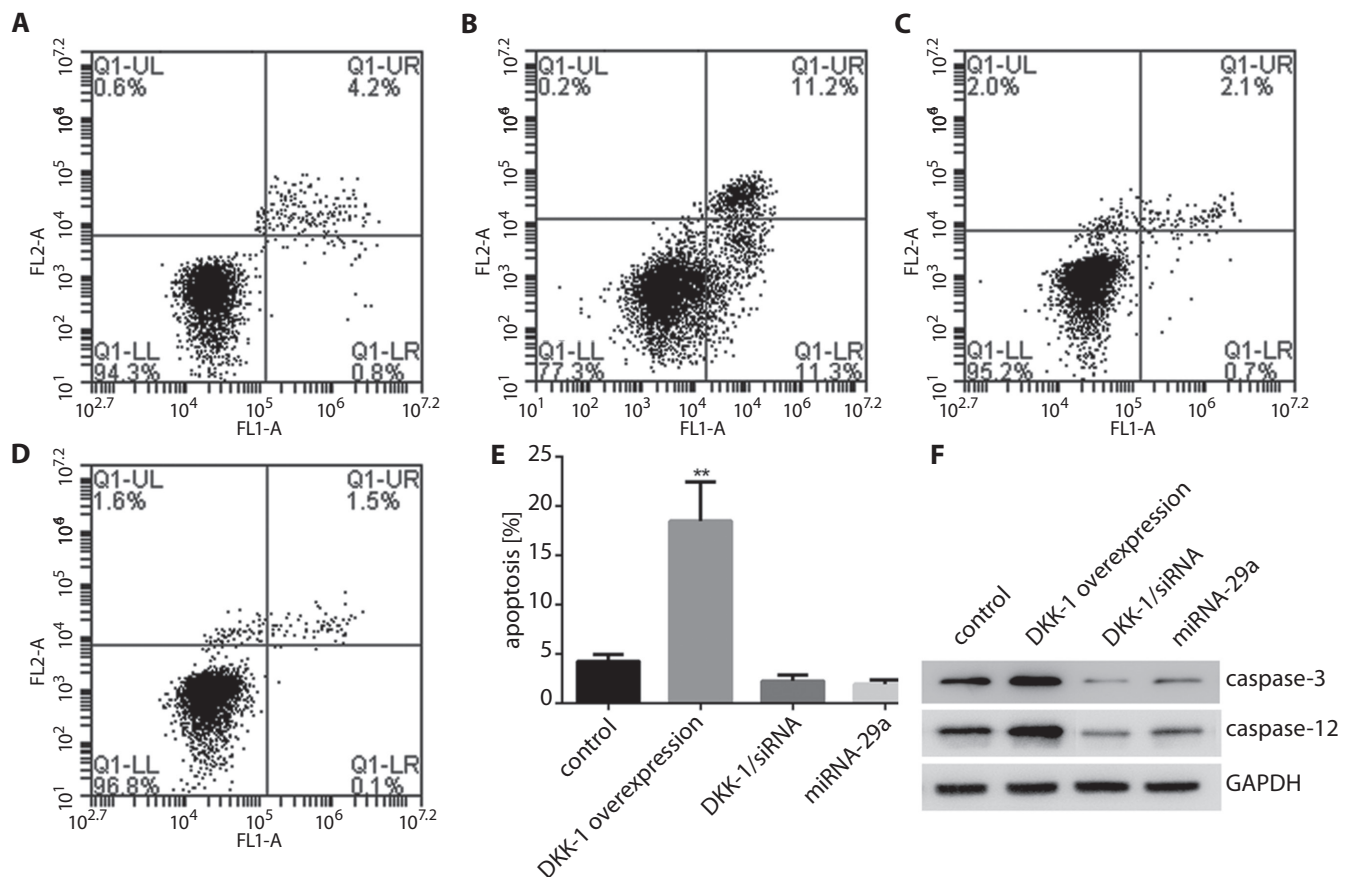


Fig. 4. MicroRNA-29a inhibited the apoptosis of hFOB1.19 cells, while DKK-1 promoted the apoptosis of hFOB1.19 cells. A – apoptosis detection in the control group; B – apoptosis detection in the DDK-1 overexpression group; C – apoptosis detection in the DKK/siRNA group; D – apoptosis detection in the miR-29a group; E – comparison of apoptosis ratio in different groups; F – western blotting results of caspase-3 and caspase-12 proteins expression

** $p < 0.01$ vs control.

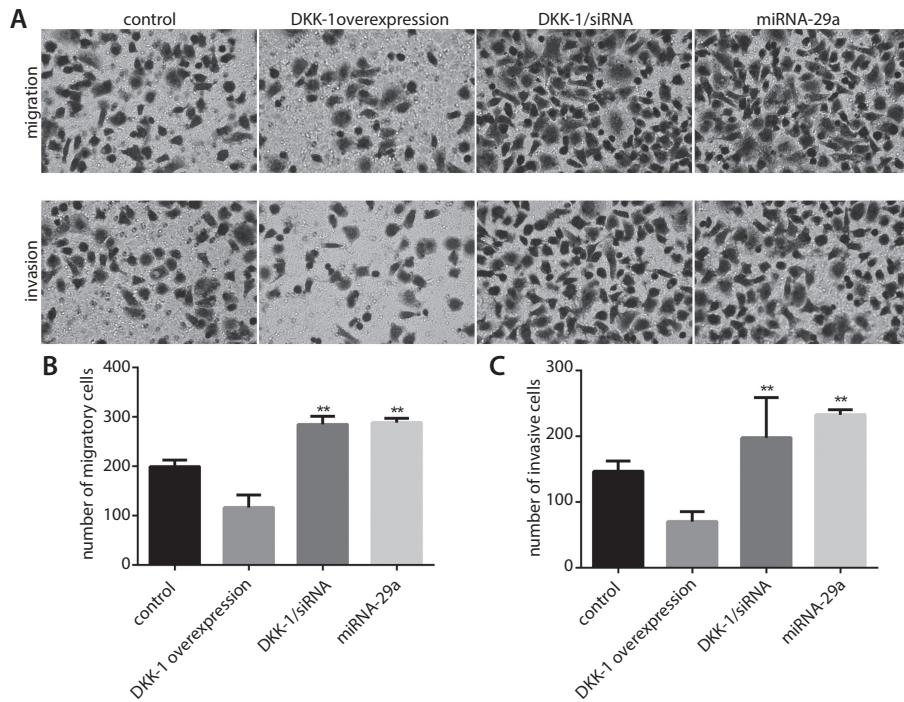


Fig. 5. MicroRNA-29a promoted the invasion and migration of hFOB1.19 cells, while DKK-1 inhibited invasion and migration. A – images of cell migration and invasion in different groups; B – comparison of cell migration in different groups; C – comparison of the cell invasion in different groups

**p < 0.01 vs control

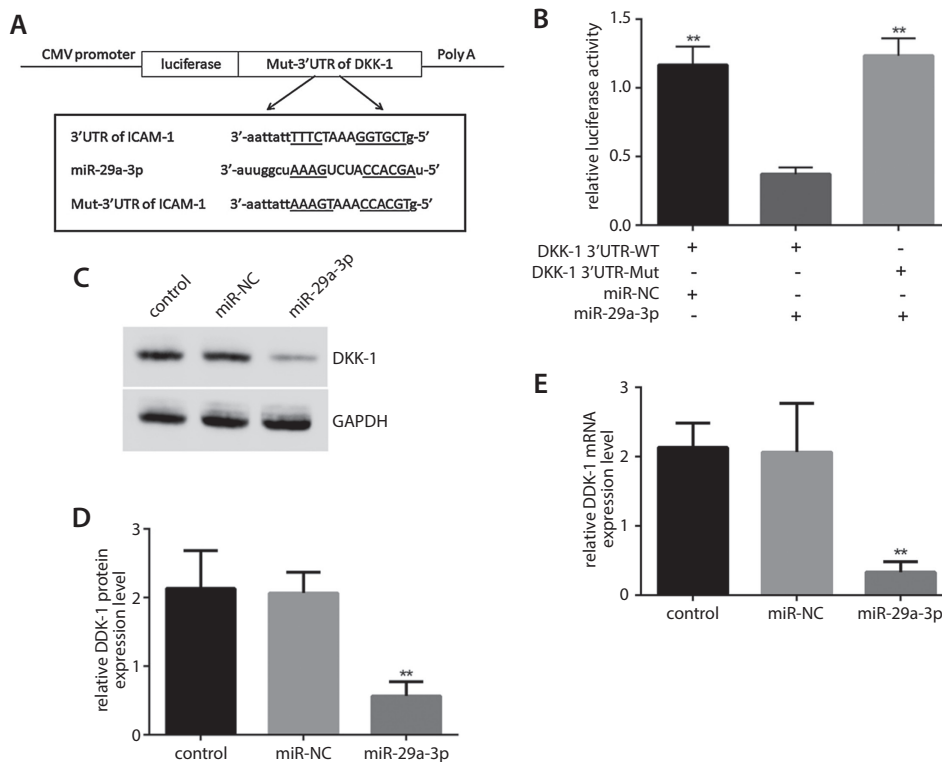


Fig. 6. MicroRNA-29a targeted 3'UTR of DKK-1 and inhibited its expression. A – construction of luciferase reporter gene vector containing wild type (WT) and mutated (Mut) DKK-1 3'UTR; B – miR-29a-3p targeted the 3'-UTR region of DKK-1; C and D – western blotting results showed that miR-29a-3p could downregulate DKK-1 protein expression; E – RT-PCR results showed that miR-29a-3p could downregulate DKK-1 mRNA expression

**p < 0.01 vs control.

of osteoblast differentiation and bone formation. In particular, all signaling pathways involved in the network directly or indirectly affect DKK-1, and ultimately regulate the expression of downstream target genes, thus they regulate osteoblast differentiation and bone formation.¹⁵ It has been found that DKK1 inhibits the expression of Wnt3a and indirectly inhibits the activity of β -catenin.¹⁶ In this study, we found that the expression level of DKK-1 was higher in AS tissues than in normal tissues. However,

the expression levels of β -catenin and miR-29a were lower in AS tissues than in normal tissues. The expression of DKK-1 could be downregulated by the overexpression of miR-29a. On the contrary, altered expression of DKK-1 does not affect the expression of miR-29a, which suggests that DKK-1 is the downstream responder of miR-29a.

In the classical Wnt signaling pathway, Wnt proteins (Wnt1, Wnt3a, Wnt8a, and Wnt10b) inhibit the activity of β -catenin-degrading complex after binding


to the transmembrane-specific receptor frizzled protein (Frz) and the low-density lipoprotein (LDL) receptor-related protein 5/6 (LRP5/6), so that the level of β -catenin in cells increases and the transcription of downstream target genes starts. Dickkopf-1 is an inhibitor of the classical Wnt signaling pathway; it can passivate LRP5/6 and weaken the binding of the Wnt protein to LRP5/6, thus inhibiting the activation of the classical Wnt signaling pathway.^{17,18} The Wnt signaling pathway is classified into classical and non-classical signaling pathways, based on whether or not β -catenin participates. The role of the classical Wnt signaling pathway (Wnt/ β -catenin pathway) in osteoblasts is an important topic in studies on bone growth and development and bone metabolism. MicroRNA-29a plays a key role in the process of osteogenic differentiation and is closely related to AS. Previous studies have indicated that miR29a is associated with bone formation. It suppressed osteonectin expression in osteoblasts by regulating the process of differentiation via the Wnt signaling pathway, and modulated osteoblast differentiation, playing an important role in skeletal remodeling and bone mass stability.^{19,20} It was found that when there was a lack of Wnt protein outside the cell, the β -catenin could be degraded, blocking the Wnt/ β -catenin signaling pathway and inhibiting the proliferation and differentiation of osteoblasts. Wnt/ β -catenin signaling plays a critical role in the achievement of peak bone mass, affecting the commitment of mesenchymal progenitors to the osteoblast lineage and determining the anabolic capacity of osteoblasts depositing bone matrix.^{21–23}

Conclusions


In brief, our results demonstrated that miR-29a could stimulate the proliferation, migration, invasion, and differentiation of osteoblasts by activating the Wnt/ β -catenin pathway in hFOB1.19 cells and reducing the expression of DKK-1.

ORCID iDs

Zongsheng Yin  <https://orcid.org/0000-0002-9886-2316>

Fuwen Zhang  <https://orcid.org/0000-0002-3923-386X>

Kun Cao  <https://orcid.org/0000-0001-9297-5240>

Gongwen Du  <https://orcid.org/0000-0002-7796-7629>

Qi Zhang  <https://orcid.org/0000-0003-0517-2031>

References

- Huang W, Yang S, Shao J, Li YP. Signaling and transcriptional regulation in osteoblast commitment and differentiation. *Front Biosci*. 2007;12:3068–3092.
- Liu DQ, Zhang J, Song HN, Zheng J, Wang XX. Expression of Smad4 and Smad7 of BMP signaling pathway in oral squamous cell carcinoma [in Chinese]. *Shanghai Kou Qiang Yi Xue*. 2013;22:492–497.
- Chen L, Holmstrom K, Qiu W, et al. MicroRNA-34a inhibits osteoblast differentiation and in vivo bone formation of human stromal stem cells. *Stem Cells*. 2014;32(4):902–912.
- Liu X, Xu H, Kou J, Wang Q, Zheng X, Yu T. MiR-9 promotes osteoblast differentiation of mesenchymal stem cells by inhibiting DKK1 gene expression. *Mol Biol Rep*. 2016;43(9):939–946.
- Wang FS, Chuang PC, Lin CL, et al. MicroRNA-29a protects against glucocorticoid-induced bone loss and fragility in rats by orchestrating bone acquisition and resorption. *Arthritis Rheum*. 2013;65(6):1530–1540.
- Ko JY, Chuang PC, Chen MW, et al. MicroRNA-29a ameliorates glucocorticoid-induced suppression of osteoblast differentiation by regulating beta-catenin acetylation. *Bone*. 2013;57(2):468–475.
- Li Z, Hassan MQ, Jafferji M, et al. Biological functions of miR-29b contribute to positive regulation of osteoblast differentiation. *J Biol Chem*. 2009;284(23):15676–15684.
- Kapinas K, Kessler C, Ricks T, Gronowicz G, Delany AM. MiR-29 modulates Wnt signaling in human osteoblasts through a positive feedback loop. *J Biol Chem*. 2010;285(33):25221–25231.
- Sudo R, Sato F, Azechi T, Wachi H. MiR-29-mediated elastin down-regulation contributes to inorganic phosphorus-induced osteoblastic differentiation in vascular smooth muscle cells. *Genes Cells*. 2015;20(12):1077–1087.
- Tan K, Peng YT, Guo P. MiR-29a promotes osteogenic differentiation of mesenchymal stem cells via targeting HDAC4. *Eur Rev Med Pharmacol Sci*. 2018;22(11):3318–3326.
- Wu S, Yu Q, Lai A, Tian J. Pulsed electromagnetic field induces Ca(2+)-dependent osteoblastogenesis in C3H10T1/2 mesenchymal cells through the Wnt-Ca(2+)/Wnt-beta-catenin signaling pathway. *Biochem Biophys Res Commun*. 2018;503(2):715–721.
- Mansouri R, Jouan Y, Hay E, et al. Osteoblastic heparan sulfate glycosaminoglycans control bone remodeling by regulating Wnt signaling and the crosstalk between bone surface and marrow cells. *Cell Death Dis*. 2017;8(6):e2902.
- Blitzer JT, Nusse R. A critical role for endocytosis in Wnt signaling. *BMC Cell Biol*. 2006;7:28.
- Delgado Cuenca P, Almaiman L, Schenk S, Kern M, Hooshmand S. Dried plum ingestion increases the osteoblastogenic capacity of human serum. *J Med Food*. 2017;20(7):653–658.
- John AA, Prakash R, Kureel J, Singh D. Identification of novel microRNA inhibiting actin cytoskeletal rearrangement thereby suppressing osteoblast differentiation. *J Mol Med (Berl)*. 2018;96(5):427–444.
- Tan J, Tong BD, Wu YJ, Xiong W. MicroRNA-29 mediates TGF β 1-induced extracellular matrix synthesis by targeting wnt/ β -catenin pathway in human orbital fibroblasts. *Int J Clin Exp Pathol*. 2014;7(11):7571–7577.
- Luyten FP, Tylzanowski P, Lories RJ. Wnt signaling and osteoarthritis. *Bone*. 2009;44(4):522–527.
- Clevers H, Nusse R. Wnt/beta-catenin signaling and disease. *Cell*. 2012;149(6):1192–1205.
- Weng LH, Wang CJ, Ko JY, Sun YC, Wang FS. Control of Dkk-1 ameliorates chondrocyte apoptosis, cartilage destruction and subchondral bone deterioration in osteoarthritic knees. *Arthritis Rheum*. 2010;62(5):1393–1402.
- Kapinas K, Kessler CB, Delany AM. MiR-29 suppression of osteonectin in osteoblasts: Regulation during differentiation and by canonical Wnt signaling. *J Cell Biochem*. 2009;108(1):216–224.
- Laine CM, Joeng KS, Campeau PM, et al. WNT1 mutations in early-onset osteoporosis and osteogenesis imperfecta. *N Engl J Med*. 2013;368(19):1809–1816.
- Moorer MC, Riddle RC. Regulation of osteoblast metabolism by Wnt signaling. *Endocrinol Metab (Seoul)*. 2018;33(3):318–330.
- Hill TP, Spater D, Taketo MM, Birchmeier W, Hartmann C. Canonical Wnt/beta-catenin signaling prevents osteoblasts from differentiating into chondrocytes. *Dev Cell*. 2005;8(5):727–738.

Impact of chronic wounds of various etiology on systemic profiles of key inflammatory cytokines, chemokines and growth factors, and their interplay

Małgorzata Krzystek-Korpaczka^{1,A–F}, Krzysztof Kędzior^{1,C,E,F}, Leszek Masłowski^{2,A,B,E,F},
Magdalena Mierzchała^{1,C–F}, Iwona Bednarz-Misa^{1,C,D,F}, Agnieszka Bronowicka-Szydełko^{1,B,E,F},
Joanna Kubiak^{2,B,E,F}, Małgorzata Gacka^{3,B,E,F}, Sylwia Płaczkowska^{4,C,E,F}, Andrzej Gamian^{1,A,E,F}

¹ Department of Medical Biochemistry, Faculty of Medicine, Wrocław Medical University, Poland

² Department of Angiology, Regional Specialist Hospital, Wrocław, Poland

³ Department of Angiology, Hypertension and Diabetes, Wrocław Medical University, Poland

⁴ Department of Professional Training in Clinical Chemistry, Wrocław Medical University, Poland

A – research concept and design; B – collection and/or assembly of data; C – data analysis and interpretation;

D – writing the article; E – critical revision of the article; F – final approval of the article

Advances in Clinical and Experimental Medicine, ISSN 1899–5276 (print), ISSN 2451–2680 (online)

Adv Clin Exp Med. 2019;28(10):1301–1309

Address for correspondence

Małgorzata Krzystek-Korpaczka

E-mail: malgorzata.krzystek-korpaczka@umed.wroc.pl

Funding sources

Statutory funding of Wrocław Medical University #ST-911.

Conflict of interest

None declared

Acknowledgements

The authors would like to thank the Foundation of Wrocław Medical University (FAM) and its Board Chairmen for financing a lease of the BioPlex 200 platform.

Received on July 28, 2018

Reviewed on September 15, 2018

Accepted on February 8, 2019

Published online on August 19, 2019

Cite as

Krzystek-Korpaczka M, Kędzior K, Masłowski L, et al. Impact of chronic wounds of various etiology on systemic profiles of key inflammatory cytokines, chemokines and growth factors, and their interplay. *Adv Clin Exp Med.* 2019;28(10):1301–1309. doi:10.17219/acem/103845

DOI

10.17219/acem/103845

Copyright

© 2019 by Wrocław Medical University

This is an article distributed under the terms of the Creative Commons Attribution Non-Commercial License (<http://creativecommons.org/licenses/by-nc-nd/4.0/>)

Abstract

Background. Non-healing wounds are becoming a growing concern for public health as a result of their increasing prevalence in progressively aging societies.

Objectives. The aim of this article is to evaluate the effects of wound etiology on a panel of circulating cytokines in patients with non-healing wounds of the lower extremities.

Material and methods. This prospective case-control study involved 104 individuals: healthy elderly people (n = 46) and patients with diabetes and/or cardiovascular disease (n = 58; among them 38 with chronic wounds of venous, ischemic or neurotrophic etiology). Selected serum cytokines – i.e. IL-1 β , IL-4, IL-6, IL-8, FGF-2, G-CSF, GM-CSF, MCP-1, MIP-1 α , TNF- α , VEGF-A, and PDGF-BB – were measured using the Luminex platform.

Results. Compared to healthy elderly people, presence of diabetes and/or cardiovascular disease was associated with elevated IL-6, IL-8, MCP-1 and G-CSF while non-healing wounds coexisted with the increase in the levels of all examined cytokines/growth factors except for G-CSF and GM-CSF. Among diseased elderly people, having wounds was associated with increased levels of IL-1 β , IL-4, IL-6, IL-8, FGF-2, MIP-1 α , PDGF-BB, and VEGF-A. Interleukin 1 β elevation was a sole independent predictor of chronic wounds with an odds ratio (OR) of 6.3. Cytokines in healthy seniors were loosely interrelated, while the levels of cytokines in diseased patients with wounds displayed a tight pattern of association. When stratified by their etiology, the association pattern for IL-6, IL-8, MCP-1, and VEGF-A was disrupted in neurotrophic wounds.

Conclusions. The results presented herein may improve our understanding of the pathomechanisms which lead to chronic wounds and of the effects they exert on a systemic level, as well as providing potential targets for more effective therapies.

Key words: diabetes, venous stasis, ischemic wounds, neurotrophic wounds, inflammation

Introduction

Conditions such as diabetes or atherosclerosis can disturb blood flow, damage blood vessels, and, if severe, result in ulcerations or gangrene, most often located in the lower limbs. Moreover, together with age and obesity, they are listed as key factors which adversely affect proper wound healing. Taking into account the prevalence of obesity, diabetes and cardiovascular disease among elderly people, chronic wounds of the lower extremities are becoming a growing socioeconomic problem for aging societies. Persistent, frequent and often infected, they reduce quality of life, rendering afflicted persons disabled and in need of repeated hospitalization.^{1,2} Non-healing wounds are a major cause of morbidity and mortality and are responsible for over 80% of diabetes-associated amputations.^{3,4} Chronic wounds are currently estimated to affect up to 2% of the general population but – because their prevalence is increasing – it is predicted that they will affect ¼ of elderly people by the year 2050.⁵

While the proper healing of an injury requires a sequence of events, tightly orchestrated in time and space by a plethora of humoral mediators, chronic wounds are believed to be locked in the initial inflammatory phase without resolution.⁴ A deregulated cytokine and growth factor network which promotes an inflammatory response but causes aberrations in immune cell recruitment, shifts in the proteolytic balance and impaired formation of blood vessels is implicated in the pathogenesis of chronic wounds.⁶ So far, most of the attention has been focused on profiling cytokines and growth factors in wound fluids and biopsies, as they are believed to reflect the microenvironment of non-healing wounds best, whereas the pathogenic significance of the accompanying systemic inflammation has received little attention.⁷ However, alterations in local cytokine and growth factor concentrations are unlikely to contribute to the systemic effects of chronic wounds, such as considerably higher mortality rates.^{8,9} Also, the collection and analysis of wound exudates pose some technical and interpretational problems.¹⁰ Even more importantly, high proteolytic activity – a hallmark of non-healing wounds⁴ – is likely to falsify any results.

Thus, the purpose of our study was to profile, on a systemic level, the key pro-inflammatory and pro-angiogenic cytokines and growth factors and their interplay in healthy elderly people compared with seniors burdened with chronic conditions like diabetes and cardiovascular disease, either without or with complications in the form of chronic wounds. Also, we aimed to compare the cytokine profiles and correlation patterns in patients with chronic wounds, stratified by wound type and etiology.

Material and methods

Study population

The study population consisted of 104 individuals: 48 apparently healthy seniors and 56 elderly patients with diabetes and/or cardiovascular disease – 38 of whom had chronic wounds of the lower extremities. Patients with chronic wounds were recruited from the Department of Angiology of the Regional Specialist Hospital in Wrocław, Poland. Only patients with chronic wounds in the course of cardiovascular disease or diabetes were included, while patients with non-healing wounds due to autoimmune diseases, malignancy, infections, or drugs were excluded. Wound etiology was determined by its characteristics (location and an appearance of the wound, its borders, and the surrounding skin, pain, and the presence of bleeding on manipulation) in conjunction with the patient's history and clinical assessment based on the ankle-brachial pressure index, ultrasound, angiography, and computed tomography (CT), among other things. The wound etiology was determined to be as follows: venous stasis ($n = 17$), ischemic (arterial) ($n = 13$) and neurotrophic ($n = 6$); in 2 cases, the dominant component was unclear (mixed ischemic/venous). Many of the patients ($n = 27$) exclusively had ulcerations, 5 had ulcerations and gangrene, and 6 had gangrene alone. Of the 11 patients with gangrene, 6 had wet gangrene and 5 had dry gangrene. Phlegmons were present in 5 patients. Data on hematological (hemoglobin, Hb; white blood cells, WBC; and platelets, PLT), coagulation (activated partial thromboplastin time, APTT) and biochemical (high-sensitive C-reactive protein, hsCRP; and fibrinogen) indices were prospectively collected and measured according to standard procedures.

Twenty age-matched patients with a similar chronic disease burden (type 2 diabetes associated with hypertension, hyperlipidemia, micro- and/or macroangiopathy, ischemic heart disease, or peripheral artery occlusive disease) but no limb ulcerations were recruited from the Department of Angiology, Hypertension, and Diabetes of the Wrocław Medical University as a reference. Age and sex-matched individuals with complaints of headaches and memory loss but without mild cognitive impairment or dementia and no other significant health history recruited from the Research, Science, and Educational Center of Dementia Diseases in Ścinawa, Poland served as an additional control group. The age distribution in these 3 groups was as follows: 68.3 ± 12.2 years, 65.7 ± 10.2 years and 64.4 ± 9.8 years ($p = 0.257$), respectively, while the female-to-male ratios were 17:21, 14:6 and 24:22 ($p = 0.185$), respectively.

The study conforms to the ethical principles outlined in the Declaration of Helsinki. The study design was approved by the Medical Ethics Committees of Wrocław Medical University and the Regional Specialist Hospital, and informed consent was obtained from the patients.

Analytical methods

Blood was drawn with venipuncture and was then clotted (30') and centrifuged (15', 720 × g). The resulting serum was frozen at –80°C until examination. Cytokine profiling was conducted in duplicate with flow cytometry-based method using magnetic microspheres conjugated with monoclonal antibodies using a BioPlex 200 (Bio-Rad, Hercules, USA), according to the manufacturer's instructions, incorporating Luminex xMAP® technology and validated custom plexes allowing for simultaneous measurement of interleukin (IL)-1β, IL-4, IL-6, IL-8, fibroblast growth factor (FGF)-2, granulocyte colony-stimulating factor (G-CSF), granulocyte-macrophage colony-stimulating factor (GM-CSF), monocyte chemoattractant protein (MCP)-1, macrophage inflammatory protein (MIP)-1α, tumor necrosis factor (TNF)-α, vascular endothelial growth factor (VEGF)-A, and platelet-derived growth factor (PDGF)-BB. Standard curves were drawn using 4- or 5-parameter logistic (PL) regression and the data was analyzed using BioPlex Manager v. 6.0 software (BioRad).

Statistical analysis

The data distribution was tested with the Kolmogorov–Smirnov test and equality of variances was tested using Levene's test. Intergroup differences were analyzed using one-way analysis of variance (ANOVA) and the t-test for independent samples with Welch correction, where appropriate, or the Kruskal–Wallis H test or Mann–Whitney U test. The data is presented as means or medians with a 95% confidence interval (95% CI). Frequency analysis was conducted using the χ² test. Patterns of univariate correlations were established using the Pearson's or Spearman's

tests. For limited data sets, the Spearman's test was applied, as it is less sensitive to outliers, and the results were additionally verified with the Kendall test. Logistic regression was conducted using the stepwise method with p = 0.05 and p = 0.1 as entrance and removal criteria. All calculated probabilities were two-tailed and p-values ≤0.05 were considered statistically significant. The analyses were performed using MedCalc® v. 14.10.2 (MedCalc Software, Mariakerke, Belgium) statistical software.

Results

Circulating cytokines in patients with chronic wounds and age-matched controls with or without comparable chronic disease burden

We compared the levels of circulating cytokines in patients with chronic wounds with those found in individuals with a comparable disease burden (cardiovascular disease or diabetes) but without chronic wounds, and with those of elderly people without significant medical history, who served as age-matched controls. Interleukin 6, IL-8, G-CSF, and MCP-1 were the only cytokines which were significantly higher in the patients without wounds than in the controls. In turn, compared to the healthy controls, the patients with chronic wounds had elevated levels of all cytokines apart from G-CSF and GM-CSF. The elevation of IL-1β, IL-4, IL-6, IL-8, FGF-2, MIP-1α, PDGF-BB, and VEGF-A was more accentuated in patients with chronic wounds than in patients with similar disease burden but no wounds (Table 1).

In a logistic regression analysis (stepwise method), an increase in IL-1β alone was an independent predictor

Table 1. Systemic levels of key inflammatory cytokines and growth factors in the study population

Cytokine/growth factor	Patients with chronic wounds (W)	Diseased seniors (D)	Controls (C)	p-value
IL-1β [ng/L]	6.5 (5.4–8.3) ^{D,C}	0 (0.0–0.4) ^U	0 (0.0–0.0) ^W	<0.001 ^K
IL-4 [ng/L]	5.9 (4.7–7.7) ^{D,C}	1.5 (1.2–1.9) ^U	1.3 (1.2–1.6) ^W	<0.001 ^K
IL-6 [ng/L]	23.3 (18.5–34.6) ^{D,C}	6.9 (5.3–10.1) ^{U,C}	4.6 (3.7–5.0) ^{W,D}	<0.001 ^K
IL-8 [ng/L]	139.6 (97.6–173.7) ^{D,C}	16.6 (11.4–24.1) ^{U,C}	10.7 (9.2–13.5) ^{W,D}	<0.001 ^K
FGF2 [ng/L]	32.1 (28.1–34.4) ^{D,C}	4.3 (0.2–6.3) ^U	4.1 (2.7–11.3) ^W	<0.001 ^K
G-CSF [ng/L]	24.3 (21.3–27.7)	32.7 (25.4–43.1) ^C	21.2 (17.8–25.3) ^D	0.009 ^A
GM-CSF [ng/L]	13.8 (11.0–18.4)	11.3 (7.0–22.7)	15.2 (11.7–19.4)	0.961 ^K
MCP-1 [ng/L]	70.2 (59.6–82.7) ^C	66.8 (53.4–83.6) ^C	38.5 (30.9–48.0) ^{W,D}	<0.001 ^A
MIP-1α [ng/L]	11.1 (9.7–13.6) ^{D,C}	1.4 (0.6–1.9) ^U	1.7 (1.1–2.4) ^W	<0.001 ^K
PDGF-BB [μg/L]	3.6 (2.8–4.5) ^{D,C}	2.1 (1.7–2.8) ^U	1.72 (1.4–2.1) ^W	<0.001 ^A
TNF-α [ng/L]	14.6 (11.0–18.6) ^C	12.9 (9.4–15.3)	10.6 (7.8–14.1) ^W	0.031 ^K
VEGF-A [ng/L]	328 (170.4–478.4) ^{D,C}	50.1 (26.2–88.2) ^U	46.6 (37.4–58.7) ^W	<0.001 ^K

Data is presented as means or medians with a 95% confidence interval (95% CI) and was analyzed with one-way ANOVA or the Kruskal–Wallis H test. D – significantly different from diseased seniors without chronic wounds; W – significantly different from patients with chronic wounds; C – significantly different from apparently healthy age-matched controls; K – Kruskal–Wallis H test; A – one-way ANOVA; IL - interleukin; FGF2 – fibroblast growth factor 2; G-CSF – granulocyte colony-stimulating factor; GM-CSF – granulocyte-macrophage colony-stimulating factor; MCP-1 – monocyte chemoattractant protein-1; MIP-1α – macrophage inflammatory protein-1α; PDGF-BB – platelet-derived growth factor BB; TNF-α – tumor necrosis factor α; VEGF-A – vascular endothelial growth factor A.

of the presence of chronic wounds ($b = 1.84$, const. -5.26 ; $p < 0.0001$) with an OR of 6.32 (95% CI = 2.6–15.6), correctly classifying 99% of cases with an area under the curve (AUC) = 0.995 (0.96–1.0).

Correlations of circulating cytokines and growth factors with laboratory parameters in patients with chronic wounds

Although there was no direct correlation with hemoglobin concentration, circulating IL-8 was significantly higher in the patients with hypochromia (137.6 pg/mL (107–168) vs 212.5 pg/mL (163–263), $p = 0.007$) and MIP-1 α (12.2 pg/mL (10.2–14.3) vs 15.1 pg/mL (12.7–17.4), $p = 0.061$), IL-6 (23.3 pg/mL (17.9–47.6) vs 42.2 pg/mL (26.5–133.2), $p = 0.071$), and VEGF-A (332 pg/mL (133–694) vs 614 pg/mL (326–1278), $p = 0.087$) tended to be

higher as well. MCP-1 ($r = -0.5$, $p = 0.036$) and PDGF-BB ($r = -0.48$, $p = 0.042$) were inversely correlated with activated partial thromboplastin time, an indicator of the efficacy of coagulation pathways, and a similar tendency was observed for IL-4 ($r = -0.46$, $p = 0.056$).

Apart from IL-6 ($r = 0.49$, $p = 0.009$, $n = 27$), none of the studied cytokines and growth factors correlated with CRP. However, there were significant positive correlations with fibrinogen: TNF- α ($r = 0.52$, $p = 0.012$), IL-1 β ($r = 0.48$, $p = 0.021$), IL-6 ($r = 0.45$, $p = 0.032$), GM-CSF ($r = 0.47$, $p = 0.023$), G-CSF ($r = 0.46$, $p = 0.029$), and FGF-2 ($r = 0.38$, $p = 0.073$). The same held true for WBC count: TNF- α ($r = 0.57$, $p = 0.002$), MIP-1 α ($r = 0.42$, $p = 0.031$), IL-4 ($r = 0.46$, $p = 0.016$), IL-1 β ($r = 0.54$, $p = 0.004$), IL-6 ($r = 0.38$, $p = 0.050$), IL-8 ($r = 0.47$, $p = 0.014$), GM-CSF ($r = 0.60$, $p < 0.001$), G-CSF ($r = 0.56$, $p = 0.002$), and FGF-2 ($r = 0.57$, $p = 0.002$). Likewise, positive correlations were

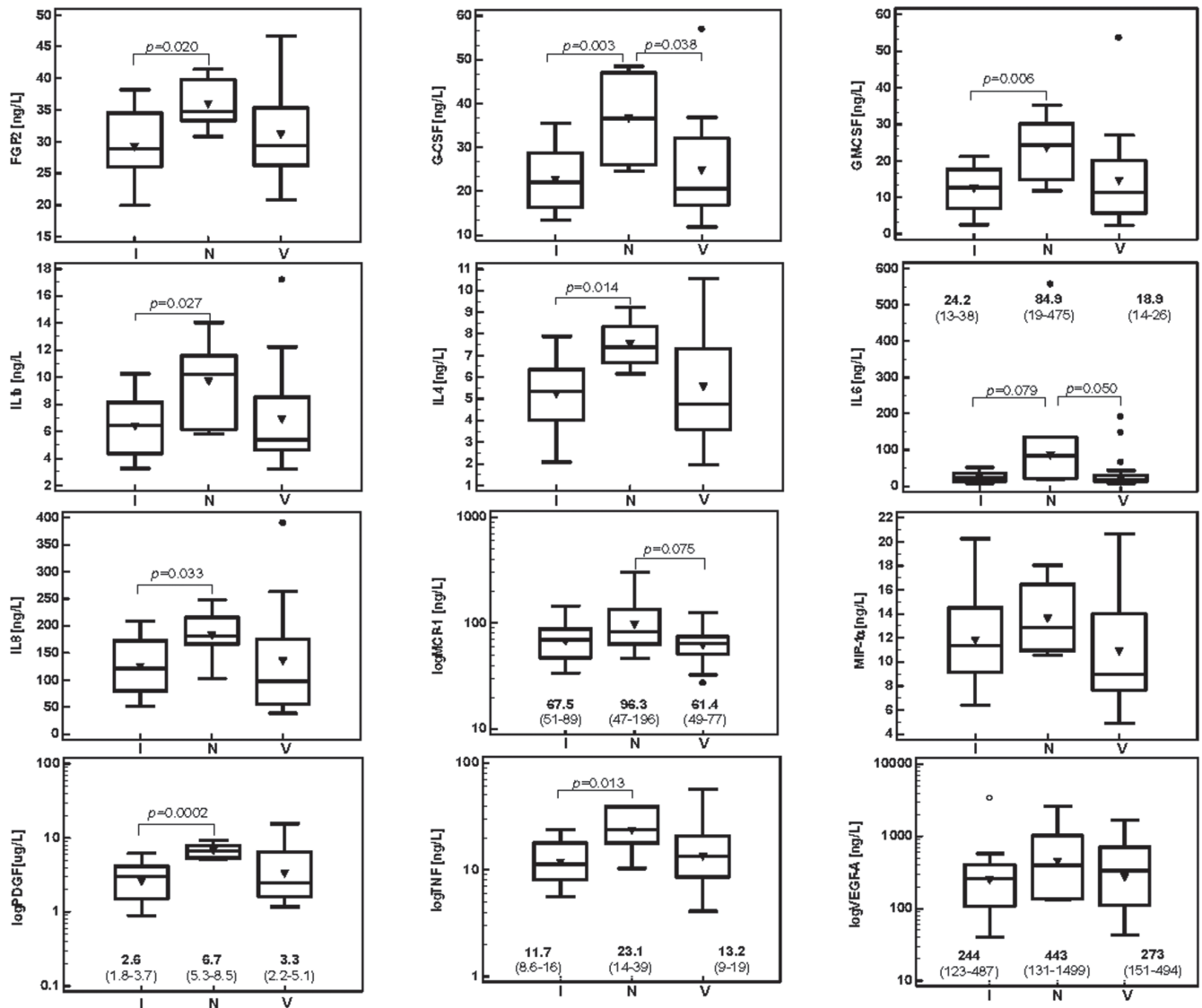


Fig. 1. Systemic levels of key inflammatory cytokines and growth factors in patients with chronic wounds stratified by wound etiology

I – patients with ischemic (arterial) wounds; N – patients with neurotrophic wounds; V – patients with vascular stasis wounds. Boxes represent interquartile range; bars inside boxes – medians; whiskers – 95% confidence intervals (95% CI); triangles – means.

found between fibrinogen and PLT count: TNF- α ($r = 0.44$, $p = 0.021$), MIP-1 α ($r = 0.52$, $p = 0.006$), IL-4 ($r = 0.38$, $p = 0.048$), IL-1 β ($r = 0.43$, $p = 0.025$), IL-8 ($r = 0.53$, $p = 0.004$), GM-CSF ($r = 0.45$, $p = 0.018$), and G-CSF ($r = 0.39$, $p = 0.044$).

Correlations of circulating cytokines and growth factors with wound type

There were tendencies towards more accentuated elevations of IL-6, IL-8, MIP-1 α , and VEGF-A levels ($p = 0.145$, $p = 0.186$, $p = 0.137$, and $p = 0.169$, respectively) in patients with both gangrene and ulcerations compared to those with ulcerations alone. There were no significant differences in circulating cytokines or growth factors in terms of the type of gangrene (wet vs dry) or the presence of phlegmon.

Correlations of circulating cytokines and growth factors with wound etiology

When stratified by wound etiology, there were significantly higher levels of IL-1 β , IL-4, IL8, FGF-2, G-CSF, GM-CSF, PDGF-BB, and TNF- α in patients with neurotrophic wounds than with ischemic ones. Interleukin 6 displayed a similar tendency. G-CSF and IL-6 were

significantly higher in neurotrophic wounds than venous ones as well (Fig. 1).

Moreover, G-CSF levels in patients with ischemic ($p = 0.015$) and venous ($p = 0.025$) wounds were significantly lower than in individuals with a similar burden of chronic diseases but no wounds. While IL-1 β , IL-4, IL-6, IL-8, FGF-2, MIP-1 α , and VEGF-A were significantly higher in patients with chronic wounds than in controls independent of their etiology, there were differences concerning PDGF-BB and TNF- α . The wound-associated elevation of PDGF-BB in these patients compared to ones with a similar disease burden was significant exclusively in neurotrophic wounds ($p < 0.001$; $p = 0.061$ for venous and $p = 0.384$ for ischemic). Compared to individuals without a significant medical history, there was no elevation of PDGF-BB in ischemic wounds ($p = 0.131$; $p = 0.0001$ for neurotrophic and $p = 0.003$ for venous). Tumor necrosis factor α was significantly higher in patients with neurotrophic wounds than in healthy controls ($p = 0.013$; $p = 0.179$ for ischemic and $p = 0.089$ for venous).

Cytokine interplay

The associations observed in the healthy elderly people were either nonexistent or less accentuated than those

Table 2. Cytokine correlation pattern in the study population

Cytokine/growth factor	FGF-2	G-CSF	GM-CSF	IL-1 β	IL-4	IL-6	IL-8	MCP-1	MIP-1 α	PDGF-BB	TNF- α	VEGF-A
FGF-2	–	ns 0.73 [#]	0.73 ^{S#} 0.47*	ns 0.50* ^S	0.51 ^{S#} 0.75 [#]	ns 0.74 ^{#S}	ns 0.70 ^{#S}	–0.29 ^{S*} ns	0.59 ^{S#} 0.70 ^{#S}	0.63 ^{S#} 0.63 [†]	0.39 ^{S†} 0.73 ^{#S}	ns 0.60 [†]
G-CSF	0.84 [#]	–	ns ns	0.49 ^{S#} 0.67 ^{†S}	0.52 [#] 0.80 [#]	0.63 ^{S#} 0.81 ^{#S}	0.58 [#] 0.76 ^{#S}	ns ns	0.32* 0.75 ^{#S}	ns 0.54*	0.60 [#] 0.84 ^{#S}	0.59 [#] 0.65 [†]
GM-CSF	0.89 [#]	0.92 [#]	–	ns 0.48* ^S	0.56 [#] 0.47* ^S	0.30 ^{S*} ns	ns ns	–0.35 ^{S*} ns	ns ns	0.55 [#] ns	0.39 [†] 0.46* ^S	ns ns
IL-1 β	0.83 [#]	0.97 [#]	0.93 [#]	–	0.39 ^{S†} 0.63 ^{S†}	0.58 ^{S#} 0.62 ^{S†}	ns 0.51* ^S	ns ns	ns ns	ns 0.47* ^S	0.48 ^{S#} 0.73 ^{#S}	0.44 ^{S†} 0.62 ^{#S}
IL-4	0.86 [#]	0.91 [#]	0.82 [#]	0.89 [#]	–	0.54 ^{S#} 0.56 ^{S†}	ns 0.62 ^{S†}	ns ns	0.36* 0.53* ^S	0.51 [#] 0.87 [#]	0.61 [#] 0.70 ^{#S}	0.32* 0.54*
IL-6	0.42 ^{S†}	0.68 ^{S#}	0.55 ^{S#}	0.62 ^{S#}	0.62 ^{S#}	–	0.37 ^{S*} 0.69 ^{#S}	ns ns	ns 0.54* ^S	ns ns	0.53 ^{S#} 0.66 ^{†S}	0.59 ^{S#} 0.74 ^{#S}
IL-8	0.58 [#]	0.75 [#]	0.61 [#]	0.71 [#]	0.76 [#]	0.80 ^{S#}	–	ns ns	ns 0.84 ^{#S}	ns ns	0.36* 0.57 ^{†S}	ns 0.61 [†]
MCP-1	0.39*	0.49 [†]	0.50 [†]	0.44 [†]	0.45 [†]	0.43 ^{S†}	0.44 [†]	–	ns ns	ns ns	ns ns	ns ns
MIP-1 α	0.68 [#]	0.78 [#]	0.69 [#]	0.77 [#]	0.84 [#]	0.69 ^{S#}	0.75 [#]	0.40*	–	0.37* ns	0.53 [#] 0.62 ^{†S}	ns 0.49* ^S
PDGF-BB	0.88 [#]	0.86 [#]	0.89 [#]	0.86 [#]	0.88 [#]	0.55 ^{S#}	0.63 [#]	0.47 [†]	0.72 [#]	–	0.31* 0.52* ^S	ns ns
TNF- α	0.76 [#]	0.85 [#]	0.85 [#]	0.86 [#]	0.75 [#]	0.55 ^{S#}	0.54 [#]	0.46 [†]	0.64 [#]	0.72 [#]	–	0.51 [#] 0.55* ^S
VEGF-A	0.55 [#]	0.69 [#]	0.57 [#]	0.64 [#]	0.65 [#]	0.77 ^{S#}	0.77 [#]	0.46 [†]	0.72 [#]	0.53 [#]	0.51 [†]	–

Unless otherwise indicated, data is presented as Pearson’s correlation coefficients. * – $p < 0.05$; † – $p < 0.01$; # – $p < 0.001$; S – Spearman’s correlation coefficient; ns – not statistically significant. Correlations for the chronic wound group are presented on the left of the table. Correlations for the healthy elders are presented on the right of the table in regular font. Correlations for the diseased seniors without chronic wounds are presented on the right of the table in italic font.

Table 3. Cytokine correlation pattern in patients with chronic wounds stratified by wound etiology

Cytokine/growth factor	FGF-2	G-CSF	GM-CSF	IL-1 β	IL-4	IL-6	IL-8	MCP-1	MIP-1 α	PDGF-BB	TNF- α	VEGF-A
FGF-2	–	ns 0.69 [†]	0.94 [†] 0.81 [#]	ns 0.71 [†]	0.83* 0.75 [†]	ns ns	ns ns	ns ns	ns ns	1.00 [#] 0.79 [#]	ns 0.65*	ns ns
G-CSF	0.78 [#]	–	ns 0.88 [#]	0.94 [†] 0.95 [#]	0.89* 0.88 [#]	ns ns	ns 0.86 [†]	ns ns	0.94 [†] 0.73 [†]	ns 0.56*	0.99 [#] 0.81 [#]	ns ns
GM-CSF	0.87 [#]	0.84 [#]	–	0.83* 0.90 [#]	0.94 [†] 0.80 [#]	ns ns	ns 0.67*	ns ns	0.83* 0.67*	0.94 [†] 0.62*	ns 0.89 [#]	ns ns
IL-1 β	0.76 [#]	0.95 [#]	0.90 [#]	–	0.94 [†] 0.87 [#]	ns ns	ns 0.82 [#]	ns ns	1.00 [#] 0.66*	ns 0.60*	0.93 [†] 0.85 [#]	ns 0.56*
IL-4	0.76 [#]	0.96 [#]	0.76 [#]	0.92 [#]	–	ns ns	ns 0.71 [†]	ns ns	0.94 [†] 0.78 [†]	0.83* 0.79 [†]	0.87* 0.75 [†]	ns ns
IL-6	0.53*	0.75 [#]	0.52*	0.64 [†]	0.66 [†]	–	ns 0.63*	ns ns	ns ns	ns ns	ns ns	ns 0.80 [#]
IL-8	0.60*	0.89 [#]	0.60*	0.79 [#]	0.86 [#]	0.92 [#]	–	ns ns	ns 0.76 [†]	ns ns	ns 0.68*	ns 0.85 [#]
MCP-1	0.49*	0.55*	0.51*	0.50*	0.48*	0.67 [†]	0.58*	–	ns ns	ns ns	ns ns	ns ns
MIP-1 α	0.71 [#]	0.92 [#]	0.73 [#]	0.91 [#]	0.94 [#]	0.69 [†]	0.84 [#]	ns	–	ns 0.64*	0.93 [#] 0.58*	ns 0.68 [†]
PDGF-BB	0.87 [#]	0.94 [#]	0.86 [#]	0.92 [#]	0.94 [#]	0.63 [†]	0.80 [#]	0.49*	0.88 [#]	–	ns ns	ns ns
TNF- α	0.69 [†]	0.80 [#]	0.88 [#]	0.90 [#]	0.76 [#]	ns	0.59*	0.55*	0.73 [#]	0.79 [#]	–	ns ns
VEGF-A	0.65 [†]	0.81 [#]	0.57 [†]	0.69 [†]	0.81 [#]	0.85 [#]	0.88 [#]	0.64 [†]	0.81 [#]	0.71 [#]	ns	–

* – <0.05; † – <0.01; # – <0.001; ns – not statistically significant. Data is presented as Spearman's rank correlation coefficients. Correlations for venous etiology are presented on the left of the table. Correlations calculated for neurotrophic etiology (in regular font) and for ischemic etiology (in italic font) are presented on the right of the table.

in patients burdened with chronic diseases. Compared to patients with chronic wounds, there were no interrelationships for MCP-1 and only a few for IL-8, MIP-1 α , PDGF-BB, and VEGF-A. In patients with chronic wounds, all cytokines were correlated and the statistical power of most of the observed associations was high (Table 2).

The analysis of patterns of cytokine correlation in patients with wounds stratified by wound etiology revealed a pattern of tight associations for venous wounds, while in ischemic wounds the associations were looser, even more so in neurotrophic wounds. The disruption of cytokine interrelationships in neurotrophic wounds was particularly evident for IL-6, IL-8, MCP-1, and VEGF-A – whose levels did not correlate with any other cytokine – and, to a lesser extent, for PDGF-BB and FGF-2 (Table 3).

Discussion

While there are number of studies which have profiled mediators of inflammation, angiogenesis and matrix remodeling in wound exudates, we focused on the levels of these mediators in circulation. The investigation of wound fluids is compelling, as it may potentially provide insight into what happens directly at the site of inflammation. However, due to the extremely high proteolytic activity which may falsely increase or decrease the availability of antigen epitopes for

antibody-based assays or may cause artificial mass shifts in proteomic analyses, the examination of exudates may be equally misleading. It may account for reported increases in the levels of some cytokines with collection time and for a diminished ability of exudate to stimulate human dermal fibroblasts despite an elevated cytokine concentrations.¹¹ Consequently, the results of such analyses are often contradictory, as exemplified by calcium-binding proteins S100A8 and A9, the deficiency¹² and overexpression¹³ of which have both been named a hallmark of non-healing wounds. Moreover, circulating mediators can both regulate local processes in a wound and exert an effect systemically. As such, profiling them may help to reveal the mechanisms responsible for systemic events contributing to the considerably higher mortality rates of diabetics with ulcerations than those without wounds ($R = 1.49$)⁸ or of seniors with chronic wounds of various etiology compared to the age-matched general population (28 vs 4%).⁹

Corroborating previous reports,^{7,14–17} all of our patients with diabetes and/or cardiovascular disease, regardless their wound status, had elevated levels of the cytokines characteristic of vascular inflammation and inflammatory milieu in diabetes: MCP-1, IL-6 and IL-8. MCP-1 is a key monocyte-attracting chemokine released from vascular endothelial cells (ECs) and smooth muscle cells (SMCs) during the initial phases of atherosclerosis. It facilitates trans-endothelial migration of adherent monocytes¹⁸

and induces EC and SMC migration as well as SMC proliferation.¹⁹

Circulating MCP-1 is believed to be a reliable marker of atherosclerotic plaque burden.²⁰ As such, the equally high levels of MCP-1 in our diseased patients with and without chronic wounds confirms that both study groups were well-matched with respect to the degree of their affliction. Elevated MCP-1 in the serum of diabetic patients who developed foot ulcers has been predictive of healing failure.²¹

Interleukin 8, primarily a neutrophil-attracting chemokine, is involved in the induction of monocyte adhesion to the endothelium, the stimulation of SMC proliferation and migration, and – in later stages – in the enhancement of plaque angiogenesis.¹⁸ Interleukin 6, in turn, is one of the key leukocyte-derived pro-inflammatory cytokines which stimulates MCP-1 synthesis in macrophages and CRP expression in hepatocytes, as well as inducing SMC proliferation.²² However, inflammation is associated not only with the initiation of atherosclerosis, but also with its progression and the induction of plaque rupture.²³ In this respect, it is interesting that the elevation of IL-6 and IL-8 levels was more accentuated in diseased seniors with wounds than in those without wounds (3.4-fold and 8.4-fold, respectively) and in diseased patients without wounds than in their healthy peers (1.5-fold). Interleukin 6, as well as IL-6-induced expression of CRP and MCP-1 in plaque macrophages, causes an overexpression of tissue factor (TF) and hence activates the pro-coagulant pathway. Accordingly, there was an adverse correlation between MCP-1 and APTT which, if shortened, might be indicative of an increased risk of thromboembolism. Also, IL-6 enhances the expression of matrix metalloproteinases (MMPs), facilitating the disintegration of fibrous caps, and thus destabilizing plaques.^{19,22} Similarly, IL-8 induces the endothelial expression of MMP-2 and MMP-9²⁴ and inhibits the expression of their inhibitor, TIMP-1.²⁵ As such, a more pronounced systemic elevation of these MMPs in combination with non-healing wounds promotes and sustains inflammatory milieu within blood vessels and may translate into the progression of atherosclerosis, plaque disruption and thrombosis. Accordingly, an elevation in circulating IL-8¹⁸ or IL-6 level^{16,19} is an independent predictor of cardiovascular events in various clinical settings. Locally, such a substantial upregulation of circulating IL-6 and IL-8 may contribute to enhanced proteolytic activity and a degradation of growth factors within wounds, further disturbing their proper healing.

In addition to IL-6 and IL-8, IL-1 β and MIP-1 α were also more markedly upregulated in patients with chronic wounds. Interleukin 1 β released from keratinocytes signals skin disruption, initiating and orchestrating the inflammatory response to injury.²⁶ Accordingly, IL-1 β alone was capable of correctly predicting the presence of wounds with 99% accuracy. Moreover, we observed a close correlation between IL-1 β and all other evaluated cytokines and growth factors, which were either less accentuated or absent

in individuals without chronic wounds. On the other hand, IL-1 β is a pivotal activator of endothelial pro-coagulant activity and a suppressor of anticoagulant mechanisms, thereby contributing to microvascular thrombosis.²² Moreover, since lipid overload is one of the key factors contributing to plaque instability,²³ the persistent upregulation of circulating IL-1 β , an inhibitor of cholesterol efflux regulatory protein (CERP),²⁷ may facilitate atheroma rupture as well. Increased plaque infiltration with T cells and macrophages is yet another indicator of plaque instability.²³ In this respect, only in patients with diabetes/cardiovascular disease and chronic wounds, an 8-fold upregulation of circulating MIP-1 α translates into accelerated migration of Th1 cells and cytotoxic CD8⁺ T lymphocytes into the inflamed vessels,²⁸ the destabilization of existing atheromas, and – locally – the perpetuation and acceleration of inflammation within the wound. Indeed, an elevation in circulating MIP-1 α has been associated with short-term mortality in patients with acute coronary syndrome.²⁹

Several studies have shown lower levels of growth factors within chronic wounds than acute ones.²⁶ However, notwithstanding reservations concerning the reliability of wound examinations, it has been suggested that chronic wounds might not necessarily be deficient in growth factors but that the growth factors might be inefficient, being trapped within the fibrin cuffs surrounding the capillaries.³⁰ Undoubtedly, the high activity of wound proteases is likely to degrade both endogenous and exogenous growth factors, rendering them ineffective as well. Moreover, the deregulation of downstream events has been demonstrated and is likely to contribute.²⁶ Accordingly, in our patients with chronic wounds, the levels of key circulating growth factors necessary for proper wound healing were significantly higher: FGF-2 (7-fold), PDGF-BB (1.7-fold) and VEGF-A (8-fold). Corroborating our observations, an elevation in FGF-2 and PDGF-AA but not VEGF-A was associated with a failure for diabetic foot ulcers to heal.²¹ As with pro-inflammatory cytokines, the persistent systemic upregulation of growth factors might be detrimental. In fact, FGF-2, through the upregulation of MMP-2 and MMP-9 expression and activity, contributes to the thinning of the fibrous cap of an atheroma.³¹ VEGF-A has been shown to prompt apoptosis in macrophages,³² a phenomenon which is critical for resolving inflammation in normal wound healing but which contributes to atheroma rupture if it affects plaque macrophages. Moreover, VEGF-A induces tissue factor expression in the endothelium, whereas PDGF-BB is responsible for vascular smooth muscle cells, monocytes and macrophages. This, in turn, initiates clotting cascade and thrombus formation on the one hand, and the proliferation and migration of vascular SMCs leading to plaque progression, destabilization and rupture on the other hand.³³

Apart from creating a pro-coagulant environment which promotes arterial and venous thrombosis, persistently elevated levels of pro-inflammatory cytokines may

also contribute to the pathogenesis of anemia of chronic disease. Interleukin 6 plays a pivotal role in regulating levels of hepcidin, a major regulator of iron homeostasis. Additionally, pro-inflammatory cytokines directly affect erythropoiesis by inhibiting the synthesis of erythropoietin by or interfering with its signaling pathways.³⁴ Accordingly, circulating IL-8 was significantly higher in patients with hypochromia, while IL-6, MIP-1 α and VEGF-A displayed a similar tendency.

Data concerning an association of IL-4 with wound healing are scarce. Animal models show the involvement of IL-4 in normal wound healing, where it activates fibroblasts and stimulates the synthesis of extracellular matrix.³⁵ Interleukin 4 is involved in the activation of macrophages into a wound-healing phenotype as well. However, IL-4 has also been demonstrated to hamper the pro-angiogenic capacity of macrophages by downregulating hypoxia-inducible factor (HIF)-1 α translation.³⁶ In vitro, stimulation with IL-4 reduced the migration of lung epithelial cells and hindered sinonasal epithelial wound closure.³⁷ Corroborating the notion that IL-4 contributes to prolonged healing, circulating IL-4 was significantly upregulated in patients with non-healing wounds. While other Th2 cytokines display an anti-atherogenic effect, the role of IL-4 remains ambiguous but there are suggestions that it is a promoter of plaque progression.²⁷ Supporting this concept, IL-4 in our patients positively correlated with WBC and PLT counts and inversely with APTT.

Contrary to other cytokines, the systemic levels of G-CSF and GM-CSF were not elevated in our patients. In fact, G-CSF levels in patients with wounds of ischemic or venous etiology were significantly lower. G-CSF is a hematopoietic cytokine which plays a crucial role in the host response to infection. It is responsible for increasing the number of neutrophils in circulation by stimulating the proliferation, survival and differentiation of their precursors as well as their release from blood marrow. It is also believed to display immunomodulatory and antibiotic-enhancing activities; exogenous G-CSF application has been found to be beneficial as well.³ Locally, insufficient levels of G-CSF in patients with chronic wounds may contribute to the ineffectiveness of neutrophils infiltrating the wound in fighting infection. Decreased systemic G-CSF concentrations may render patients with infected chronic wounds more susceptible to severe complications in a form of bacterial infection of the surrounding skin and bones – or even sepsis, if the infection spreads to the circulatory system. GM-CSF promotes healing through many mechanisms, e.g., by increasing VEGF expression in the ulcer bed³⁸ and an increased healing of chronic leg ulcers treated with GM-CSF has been shown.³⁹ Beidler et al.⁴⁰ demonstrated that higher systemic levels of GM-CSF at presentation were predictive of faster healing venous ulcers following multi-layer compression therapy.

As pointed out by Trøstrup et al.,¹¹ the current knowledge on the differences or similarities between chronic

wounds of various etiologies is insufficient, yet necessary to optimize treatment. To shed some light on the subject, we compared the profiles of circulating cytokines in patients stratified by wound etiology. Reflecting the prevalence in the general population, chronic wounds of venous etiology were the most common, whereas there were only a few cases of neurotrophic wounds in our study group. Nevertheless, neurotrophic wounds were associated with significantly higher levels of circulating IL-1 β , IL-4, IL-8, FGF-2, G-CSF, GM-CSF, PDGF-BB, and TNF- α than ischemic wounds and higher levels of IL-6 and G-CSF than venous wounds.

Various cells involved in the tissue response to injury communicate through the cytokine network to orchestrate the event from inflammation induction to resolution and wound closure, making the proper interplay of cytokines critical.⁶ In addition to the differences in the systemic levels with respect to wound etiology, we observed a disruption of cytokine interrelationships in neurotrophic wounds. This was particularly evident for key inflammatory cytokines and chemokines – IL-6, IL-8 and MCP-1 – whose levels did not correlate with any other cytokine. The correlation pattern was also disrupted in the case of pro-angiogenic factors VEGF-A, PDGF-BB and FGF-2, supporting the notion that deregulation of their signaling and cross-talk plays a role in wound healing failure.

In conclusion, cytoprofilng revealed a pro-inflammatory state in patients with chronic wounds which might translate into enhanced pro-coagulant, pro-thrombotic and proteolytic activities that would locally contribute to prolonged healing or healing failure and – on a systemic level – may increase the risk of cardiovascular events and/or anemia of chronic disease. We also demonstrated that wound etiology affects the profile of circulating cytokines and growth factors as well as their interplay, altered particularly in patients with wounds of neurotrophic origin. Our findings may improve our understanding of the pathomechanisms leading to chronic wounds and the effects they exert on a systemic level, as well as providing potential targets for more effective therapies.


ORCID iDs

Małgorzata Krzystek-Korpacka  <https://orcid.org/0000-0002-2753-8092>


Krzysztof Kędzior  <https://orcid.org/0000-0001-7206-8600>

Leszek Masłowski: brak

Magdalena Mierzchała-Pasierb  <https://orcid.org/0000-0003-0674-429X>


Iwona Bednarz-Misa  <https://orcid.org/0000-0001-7244-2017>


Agnieszka Bronowicka-Szydelko

 <https://orcid.org/0000-0001-9967-036X>

Joanna Kubiak: brak

Małgorzata Gacka  <https://orcid.org/0000-0001-5760-1534>

Sylwia Płaczkowska  <https://orcid.org/0000-0002-1466-3820>

Andrzej Gamian  <https://orcid.org/0000-0002-2206-6591>

References

1. Rayner R, Carville K, Keaton J, Prentice J, Santamaria N. Leg ulcers: Atypical presentations and associated comorbidities. *Wound Practice and Research*. 2009;17:168–185.

2. Green J, Jester R, McKinley R, Pooler A. The impact of chronic venous leg ulcers: A systematic review. *J Wound Care*. 2014;23(12):601–612.
3. de Lalla F, Pellizzer G, Strazzabosco M, et al. Randomized prospective controlled trial of recombinant granulocyte colony-stimulating factor as adjunctive therapy for limb-threatening diabetic foot infection. *Antimicrob Agents Chemother*. 2001;45(4):1094–1098.
4. Guo S, DiPietro LA. Factors affecting wound healing. *J Dent Res*. 2010;89(3):219–229.
5. Mustoe TA, O'Shaughnessy K, Kloeters O. Chronic wound pathogenesis and current treatment strategies: A unifying hypothesis. *Plast Reconstr Surg*. 2006;117(7 Suppl):355–415.
6. Wong VW, Crawford JD. Vasculogenic cytokines in wound healing. *Biomed Res Int*. 2013;2013:190486.
7. Tuttolomondo A, La Placa S, Di Raimondo D, et al. Adiponectin, resistin and IL-6 plasma levels in subjects with diabetic foot and possible correlations with clinical variables and cardiovascular co-morbidity. *Cardiovasc Diabetol*. 2010;9:50.
8. Iversen MM, Tell GS, Riise T, et al. History of foot ulcer increases mortality among individuals with diabetes: Ten-year follow-up of the Nord-Trøndelag Health Study, Norway. *Diabetes Care*. 2009;32(12):2193–2199.
9. Escandon J, Vivas AC, Tang J, Rowland KJ, Kirsner RS. High mortality in patients with chronic wounds. *Wound Rep Reg*. 2011;19(4):526–528.
10. Zillmer R, Trøstrup H, Karlsmark T, Ifversen P, Agren MS. Duration of wound fluid secretion from chronic venous leg ulcers is critical for interleukin-1a, interleukin-1b, interleukin-8 levels and fibroblast activation. *Arch Dermatol Res*. 2011;303(8):601–606.
11. Trøstrup H, Bjarnsholt T, Kirketerp-Møller K, Høiby N, Moser C. What is new in the understanding of non-healing wounds epidemiology, pathophysiology, and therapies. *Ulcers*. 2013;2013:625934.
12. Trøstrup H, Lundquist R, Christensen LH, et al. S100A8/A9 deficiency in nonhealing venous leg ulcers uncovered by multiplexed antibody microarray profiling. *Br J Dermatol*. 2011;165(2):292–301.
13. Eming SA, Koch M, Krieger A, et al. Differential proteomic analysis distinguishes tissue repair biomarker signatures in wound exudates obtained from normal healing and chronic wounds. *J Proteome Res*. 2010;9(9):4758–4766.
14. Panee J. Monocyte chemoattractant protein 1 (MCP-1) in obesity and diabetes. *Cytokine*. 2012;60(1):1–12.
15. Kim CS, Park HS, Kawada T, et al. Circulating levels of MCP-1 and IL-8 are elevated in human obese subjects and associated with obesity-related parameters. *Int J Obes (Lond)*. 2006;30(9):1347–1355.
16. Su D, Li Z, Li X, et al. Association between serum interleukin-6 concentration and mortality in patients with coronary artery disease. *Mediators Inflamm*. 2013;2013:726178.
17. Souza JR, Oliveira RT, Blotta MH, Coelho OR. Serum levels of interleukin-6 (IL-6), interleukin-18 (IL-18) and C-reactive protein (CRP) in patients with type-2 diabetes and acute coronary syndrome without ST-segment elevation. *Arq Bras Cardiol*. 2008;90(2):86–90.
18. Apostolakis S, Vogiatzi K, Amanatidou V, Spandidos DA. Interleukin 8 and cardiovascular disease. *Cardiovasc Res*. 2009;84(3):353–360.
19. Koenig W, Khuseyinova N. Biomarkers of atherosclerotic plaque instability and rupture. *Arterioscler Thromb Vasc Biol*. 2007;27(1):15–26.
20. Amasyali B, Kose S, Kursaklioglu H, Barcina C, Kilicb A. Monocyte chemoattractant protein-1 in acute coronary syndromes: Complex vicious interaction. *Int J Cardiol*. 2009;136(3):356–357.
21. Dinh T, Tecilazich F, Kafanas A, et al. Mechanisms involved in the development and healing of diabetic foot ulceration. *Diabetes*. 2012;61(11):2937–2947.
22. Levi M, van der Poll T, Büller HR. Bidirectional relation between inflammation and coagulation. *Circulation*. 2004;109(22):2698–2704.
23. van der Wal AC, Becker AE. Atherosclerotic plaque rupture: Pathologic basis of plaque stability and instability. *Cardiovasc Res*. 1999;41(2):334–344.
24. Li A, Dubey S, Varney ML, Dave BJ, Singh RK. IL-8 directly enhanced endothelial cell survival, proliferation, and matrix metalloproteinases production and regulated angiogenesis. *J Immunol*. 2003;170(6):3369–3376.
25. Moreau M, Brocheriou I, Petit L, Ninio E, Chapman MJ, Rouis M. Interleukin-8 mediates downregulation of tissue inhibitor of metalloproteinase-1 expression in cholesterol-loaded human macrophages: Relevance to stability of atherosclerotic plaque. *Circulation*. 1999;99(3):420–426.
26. Barrientos S, Stojadinovic O, Golinko MS, Brem H, Tomic-Canic M. Growth factors and cytokines in wound healing. *Wound Repair Regen*. 2008;16(5):585–601.
27. Ait-Oufella H, Taleb S, Mallat Z, Tedgui A. Recent advances on the role of cytokines in atherosclerosis. *Arterioscler Thromb Vasc Biol*. 2011;31(5):969–979.
28. Bromley SK, Mempel TR, Luster AD. Orchestrating the orchestrators: Chemokines in control of T cell traffic. *Nat Immunol*. 2008;9(9):970–980.
29. de Jager SC, Bongaerts BW, Weber M, et al. Chemokines CCL3/MIP1a, CCL5/RANTES and CCL18/PARC are independent risk predictors of short-term mortality in patients with acute coronary syndromes. *PLoS One*. 2012;7(9):e45804.
30. Robson MC. The role of growth factors in the healing of chronic wounds. *Wound Rep Reg*. 1997;5(1):512–517.
31. Sapienza P, di Marzo L, Borrelli V, et al. Basic fibroblast growth factor mediates carotid plaque instability through metalloproteinase-2 and -9 expression. *Eur J Vasc Endovasc Surg*. 2004;28:89–97.
32. Petreaca ML, Yao M, Ware C, Martins-Green MM. Vascular endothelial growth factor promotes macrophage apoptosis through stimulation of tumor necrosis factor superfamily member 14 (TNFSF14/LIGHT). *Wound Repair Regen*. 2008;16(5):602–614.
33. Steffel J, Lüscher TF, Tanner FC. Tissue factor in cardiovascular diseases: Molecular mechanisms and clinical implications. *Circulation*. 2006;113(5):722–731.
34. Morceau F, Dicato M, Diederich M. Pro-inflammatory cytokine-mediated anemia: Regarding molecular mechanisms of erythropoiesis. *Mediators Inflamm*. 2009;2009:405016.
35. Salmon-Ehr V, Ramont L, Godeau G, et al. Implication of interleukin-4 in wound healing. *Lab Invest*. 2000;80(8):1337–1343.
36. Dehne N, Tausendschön M, Essler S, Geis T, Schmid T, Brüne B. IL-4 reduces the proangiogenic capacity of macrophages by down-regulating HIF-1a translation. *J Leukoc Biol*. 2014;95(1):129–137.
37. Ahdieh M, Vandenbos T, Youakim A. Lung epithelial barrier function and wound healing are decreased by IL-4 and IL-13 and enhanced by IFN-g. *Am J Physiol Cell Physiol*. 2001;281(6):C2029–2038.
38. Cianfarani F, Tommasi R, Failla CM, et al. Granulocyte/macrophage colony-stimulating factor treatment of human chronic ulcers promotes angiogenesis associated with de novo vascular endothelial growth factor transcription in the ulcer bed. *Br J Dermatol*. 2006;154(1):34–41.
39. Dogra S, Sarangal R. Summary of recommendations for leg ulcers. *Indian Dermatol Online J*. 2014;5(3):400–407.
40. Beidler SK, Douillet CD, Berndt DF, Keagy BA, Rich PB, Marston WA. Inflammatory cytokine levels in chronic venous insufficiency ulcer tissue before and after compression therapy. *J Vasc Surg*. 2009;49(4):1013–1020.

Chemical aspect of sodium hypochlorite activation in obtaining favorable outcomes of endodontic treatment: An in-vitro study

*Hubert Gołabek^{1,A-E}, *Krzysztof Mariusz Borys^{2,A-E}, Meetu Ralli Kohli^{3,C-E}, Katarzyna Brus-Sawczuk^{1,C,E}, Izabela Strużycka^{1,C,E,F}

¹ Department of Comprehensive Dental Care, Medical University of Warsaw, Poland

² Faculty of Chemistry, Warsaw University of Technology, Poland

³ Department of Endodontics, University of Pennsylvania School of Dental Medicine, Philadelphia, USA

A – research concept and design; B – collection and/or assembly of data; C – data analysis and interpretation;

D – writing the article; E – critical revision of the article; F – final approval of the article

Advances in Clinical and Experimental Medicine, ISSN 1899–5276 (print), ISSN 2451–2680 (online)

Adv Clin Exp Med. 2019;28(10):1311–1319

Address for correspondence

Hubert Gołabek

E-mail: hubert58@vp.pl

Funding sources

Krzysztof M. Borys acknowledges the Warsaw University of Technology for financial support.

Conflict of interest

None declared

Acknowledgements

The authors acknowledge the assistance of Andrzej Giniewicz, PhD Eng, from the Faculty of Pure and Applied Mathematics, Wrocław University of Science and Technology, Poland, in the statistical analysis of the results.

* These authors contributed equally to this work.

Received on November 30, 2018

Reviewed on December 15, 2018

Accepted on February 18, 2019

Published online on August 29, 2019

Cite as

Gołabek H, Borys KM, Kohli MR, Brus-Sawczuk K, Strużycka I. Chemical aspect of sodium hypochlorite activation in obtaining favorable outcomes of endodontic treatment: An in-vitro study. *Adv Clin Exp Med.* 2019;28(10):1311–1319. doi:10.17219/acem/104523

DOI

10.17219/acem/104523

Copyright

© 2019 by Wrocław Medical University

This is an article distributed under the terms of the Creative Commons Attribution Non-Commercial License (<http://creativecommons.org/licenses/by-nc-nd/4.0/>)

Abstract

Background. Endodontic treatment is one of the most widely performed procedures in a dental office. New techniques for enhancing the effectiveness of irrigants are being introduced into the dental market. It is crucial to choose a proper method to obtain the highest possible long-term success of performed endodontic treatment. Sodium hypochlorite (NaOCl) appears to be one of the most common and profitable solutions for root canal irrigation. The activation of a solution may be analyzed in 2 fields, physical – turbulence of flow, and chemical – disintegration of irrigant molecules into very active radicals that improve its activity. While the physical alternations of irrigant flow with different techniques are widely studied, there are not many attempts to approach the subject in chemical terms.

Objectives. The aim of the study was to compare the chemical effectiveness of 2 methods of NaOCl activation: ultrasonics vs the Self-Adjusting File system (SAF) as an adjunct to increase the efficacy of the irrigant.

Material and methods. The level of activation was evaluated via a reaction of the activated NaOCl samples, with 9-fluorenonol as the starting organic material. The model reaction is based on the oxidation of 9-fluorenonol to 9-fluorenon. The evaluation was performed using ¹H nuclear magnetic resonance (NMR) spectroscopy, comparing the spectra obtained for the examined mixtures.

Results. Nuclear magnetic resonance studies show that the use of ultrasonics resulted in increased chemical degradation of NaOCl as compared to the SAF system and non-agitated samples. The prevalence of chemical activation in the ultrasonic group over the SAF group was almost 3 times higher, 3.11 to 1.20, respectively. The Kruskal–Wallis rank sum test revealed there is a statistically significant difference in distributions between the groups.

Conclusions. Both SAF and ultrasonics activate NaOCl. Ultrasonic agitation provided higher chemical activation of NaOCl solution than the SAF. The use of ultrasonic agitation of NaOCl in endodontic treatment will allow us to obtain better long-term clinical results.

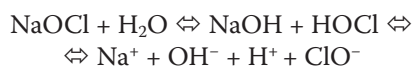
Key words: NMR, sodium hypochlorite, endodontics, Self-Adjusting File, ultrasonics

Introduction

Sodium hypochlorite (NaOCl) is the most commonly used irrigant in endodontic treatment. Coolidge introduced it as early as in 1919.¹ It is an inorganic compound with the chemical formula NaOCl. Commonly referred to as bleach, it is actually a diluted aqueous solution of NaOCl. It has numerous applications ranging from an oxidizing and chlorinating agent in organic synthesis (used in the chemical industry) to water treatment, bleaching and disinfection.

In dentistry, NaOCl is used in the form of dilute aqueous solutions with concentrations varying from 0.1% to 6.0%. Being a highly oxidizing compound, it shows suitable properties for dissolving remnants of dental pulp as well as acting as an antimicrobial agent.² These features prompted the use of aqueous NaOCl in endodontics.

Pécora et al. reported that NaOCl exhibits a dynamic equilibrium in an aqueous solution, according to the equation³:



As an ionic compound, NaOCl dissociates in water to sodium cation (Na^+) and hypochlorite anion (ClO^-), which is in equilibrium with its protonated form (HOCl). Both hypochlorous acid and the hypochlorite anion are strong oxidizing agents. HClO and ClO^- have been reported to react with proteins, amino acids, peptides, and lipids. Estrela suggests NaOCl acts as a dissolving agent for organic matter, e.g., fats.⁴

An ultrasonic wave is an acoustic wave which transmits energy of a vibrating file to the irrigating agent. Waves in the 20,000–25,000 Hz frequency range, which cause several physical and biological effects, are used in endodontics. The increase of energy in the system treated with ultrasonics results in heating of the surrounding fluid, which subsequently results in a better bactericidal effect.⁵ The presence of cavitation and microstreaming effects is equally significant. The emerging waves disrupt bacterial cells and eliminate necrotic remnants. This mixing of the fluid and its turbulent flow has a significant influence on the efficacy of root canal irrigation.^{6,7}

The Self-Adjusting File (SAF) is a rotary system for mechanical instrumentation. It is also the only system that enables instrumentation and irrigation at the same time.⁸ This is a hollow cylinder, made of Ni-Ti alloy with fusiform holes along the entire length.⁹ The file can compress and decompress according to the topography and morphology of the treated canal. Two sizes, 1.5 mm and 2 mm in diameter, are available.¹⁰ Action of the SAF is based on back and forth sliding motions in the vertical axis. The RDT3 head connected to an endodontic motor with the speed set to 3,000–5,000 rpm is used for the SAF.^{10,11} The file is connected to a VATEA (ReDent Nova, Ra'anana, Israel) pump with a silicon tube, which delivers the irrigant along

the entire length of the root canal during continuous instrumentation with a speed adjustable in the 1–10 mL/min range.^{12–14} It is recommended to fill the pump with NaOCl or ethylenediaminetetraacetic acid (EDTA) solution.^{10,12} The efficacy of NaOCl and EDTA in removing the smear layer and dentin using SAF has been proved and is not dependent on the concentration of the agent, even in the apical 1/3 of the canal.^{12,15} It is advised to work with SAF in the canal about 4 min – 2 cycles of 2 min for 1 root canal with a short pause for recapitulation.^{16–18} In our study, Endostation (ReDent Nova, Israel) was used. It combines an endodontic motor with the VATEA pump in one device.

According to Tiong and Price, during ultrasonic agitation, hypochlorous acid undergoes homolysis with formation of a hydroxyl radical and a chlorine radical.¹⁹ The homolytic processes occur when energy is delivered to HOCl molecules. This can be achieved in many different ways, e.g., under UV irradiation as reported by Zeng et al.²⁰ The resulting radicals are a species highly reactive towards a wide range of biochemical compounds – proteins and glycolipids – leading to the degradation of biological matter.²¹ The chemical equation of homolytic degradation is presented below:



One of the first investigations to quantify the action of NaOCl was described by Austin and Taylor in 1918.²² The authors measured the amount of chlorine remaining in the solution when exposed to normal vs necrotic tissue. The amount of remaining chlorine directly corresponded to its tissue-dissolving capacity. As NaOCl dissolved the tissue, chlorine levels decreased. The amount of chlorine remaining in the solution was measured indirectly on the basis of the amount of sodium thiosulfate used to reduce chlorine in the solution.

Activation of NaOCl can be considered 2-fold: physical activation wherein the turbulence of the flow is enhanced, and chemical activation based on HOCl degradation to highly reactive radical species. The rationale for the current experiment is that a quantitative evaluation of an oxidized product will help measure the oxidative potential of NaOCl at a given time. Selective oxidation of an organic compound with NaOCl may serve as a useful method to estimate its oxidation potential. Hence, the aim of this experiment was to evaluate the chemical activation of NaOCl quantitatively by measuring the capacity of the irrigant to oxidize 9-fluorenone as a model organic compound.

Material and methods

Experimental setup

All chemicals used in this study were obtained from commercial sources and used as such, without further purification. The following chemicals were used (name, purity,

additives if present, source): NaOCl, 5.25 wt% aqueous solution (Cerkamed, Stalowa Wola, Poland); 9-fluorenol, 96% (Sigma-Aldrich, St. Louis, USA); ethyl acetate, >98% (POCH S.A., Gliwice, Poland); tetra-*n*-butylammonium bromide, 99% (Sigma-Aldrich); chloroform- d_3 ($CDCl_3$), 99.8 atom% D, with 0.5 wt% silver foil as stabilizer and 0.03% (v/v) tetramethylsilane (TMS) (Sigma-Aldrich).

1H NMR spectra were recorded on a Varian VNMRs 500 MHz NMR spectrometer (Varian, Atlanta, USA) in $CDCl_3$, using TMS as an internal standard for chemical shift calibration. All chemical shifts are reported in ppm. Armar Chemicals 5 mm NMR Tubes (5HP type) (Armar Chemicals, Döttingen, Switzerland) were used. Concentration under reduced pressure was carried out with a Heidolph rotary evaporator (Heidolph, Schwabach, Germany).

Due to the comparative character of the study, all possible measures were taken to ensure that all procedures were carried out as similarly as possible while evaluating both NaOCl activation methods. Each reading was done in triplicate and each result given as an average, along with standard deviation (SD) from the 3 readings.

Sodium hypochlorite activation

A 12 mL glass vial with a plastic cap was used to fill 10 mL samples of 5.25% (w/w) aqueous solution of NaOCl. For each activation method, 2 samples of the NaOCl stock solution were prepared as mentioned above. Activation was carried out by submerging the respective system in the sample for a 4-minute period. The SAF system – a 1.5 mm diameter and 25 mm length file – was used at a speed of 5,000 rpm, with the RDT3 head connected to a handpiece on the Endostation (ReDent Nova) with an adjustable rotary speed setting, according to the manufacturer's instructions. Constant irrigant flow was not supplied to SAF during the study. For ultrasonic activation, an ISO 20 K-file (Woodpecker, China) connected to an endodontic adapter (Endochuck 120°, Woodpecker, China) and a handpiece on an ultrasound device (Woodpecker UDS-P LED) with the endodontic function turned on (only the 'E' light was on and the power was at first grade, according to the user's manual).

Reaction between sodium hypochlorite and 9-fluorenol

Each reaction was carried out in a 12 mL glass vial equipped with a plastic cap and a magnetic stirring bar. Following a procedure modified from Mirafzal et al.,²³ 9-fluorenol (185 mg, 1.02 mmol) was dissolved in ethyl acetate (1.5 mL). Next, tetra-*n*-butylammonium bromide (30 mg, 0.0931 mmol, 9 mol%) was added as a solid in one portion. The tested sample of NaOCl solution (1.5 mL) was added to the resulting solution in one portion. The reaction mixture was stirred for 30 min. Using a syringe, a portion of the organic layer (1 mL) was transferred from the vial

to a 10 mL glass round-bottom flask. The solution was concentrated under reduced pressure to dryness, using a rotary evaporator. $CDCl_3$ (0.7 mL) was added to the so-obtained residue, resulting in the formation of a clear solution. The absolute concentration of the NMR sample, given with respect to the organic compound used, was equal to 1.45 mol/dm.³ To prepare for 1H NMR analysis, the solution was then transferred to an NMR tube using a plastic syringe, and the tube was closed with a plastic cap.

Statistical analysis

The statistical analysis was made using an open source statistical environment R v. 3.5.1.²⁴ (<https://www.R-project.org/>). The Kruskal–Wallis rank sum test was available as `kruskal.test` function from R package, including test statistics, p-value and number of degrees of freedom (df), follows in implementation the theoretical results from Hollander and Wolfe.²⁵

Results

Model for the study

The reaction under assessment is the phase-transfer-catalyzed oxidation of 9-fluorenol with NaOCl (Fig. 1).^{23,26} The rationale behind picking it as a model reaction is given in the Discussion section. The experiment was performed on 3 samples: commercially available non-activated NaOCl solution, NaOCl solution subjected to ultrasonic activation and NaOCl solution activated with the SAF system.

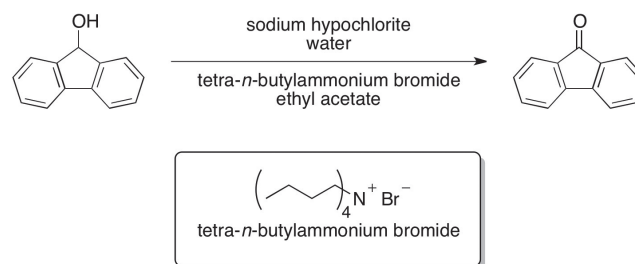


Fig. 1. Equation of the model reaction used in this study: oxidation of 9-fluorenol with sodium hypochlorite and tetra-*n*-butylammonium bromide as a phase-transfer catalyst

1H NMR spectroscopy

1H NMR spectra were recorded in $CDCl_3$ at 298 K (25°C) and 499.93 MHz. A standard proton pulse sequence (s2pul) was used, with relaxation delay at 1.000 s, pulse at 45.0°, acquisition time at 2.045 s and 8,012.8 Hz spectral width. Acquisition of each spectrum comprised 16 scans.

The spectra were processed using iNMR Reader software (Mestrelab Research, Santiago de Compostela, Spain). The raw NMR files (FIDs) were subjected to automatic Fourier transform (FT) with FT size equal to 64k. Automatic

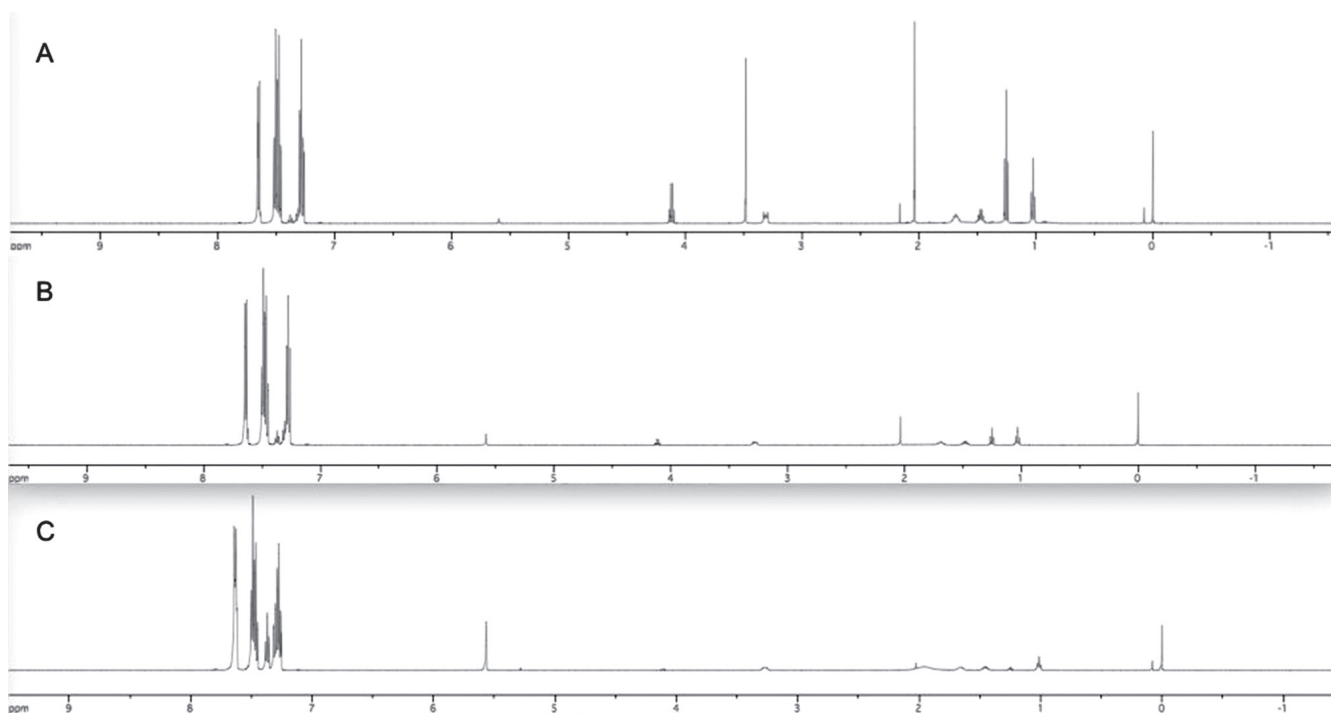


Fig. 2. Comparison of whole ^1H NMR spectra obtained from the evaluation experiments carried out on: (A) non-activated NaOCl; (B) NaOCl activated with the SAF system; (C) NaOCl activated with ultrasonics

baseline correction for a 1D spectrum, implemented in the iNMR Reader software, was applied to each spectrum, setting the baseline intensity to 0 and thus allowing to reliably integrate the peaks. Full view of the obtained ^1H NMR spectra, 1 for each kind of samples examined, is presented in Fig. 2. The spectra are shown in the range between 9.0 ppm and 0.0 ppm, with TMS signal at 0.0 ppm.

The analytically useful peaks are in the 7.8 ppm to 7.0 ppm (aromatic region) and 5.6 ppm to 5.5 ppm (benzylic protons) range. The signals of chemical shifts below 5.0 ppm include peaks derived from hydrogen atoms in: ethyl acetate (solvent in the reaction), tetra-*n*-butylammonium bromide (catalyst), water and TMS (NMR chemical shift standard). The peaks in the region below 5.0 ppm were not relevant for the study and have been omitted in Fig. 3 for clarity. Both aromatic and benzylic signals were integrated, providing the relative ratio of the total areas of the peaks. The comparative spectroscopic analyses of reactions mixtures obtained from respective solutions are showed in Fig. 3.

Chemical concept of the study

The chemical concept applied here is that aromatic protons can serve as an internal reference to evaluate the extent of oxidation and therefore the effectiveness of NaOCl activation. The interpretation of the changes occurring in the mixture upon oxidation is straightforward, as both the 9-fluorenol and 9-fluorenone have aromatic protons, while only the 9-fluorenol has a benzylic proton (Fig. 4). Upon oxidation, the number of aromatic protons (and

thus the integration of the aromatic region) is equal both in the starting material and the product and is unchanged during the oxidation.^{27,28} The variable here is the benzylic signal, which decreases in its intensity (and integration) upon oxidation.

The ratio of integration values of signals derived from benzylic protons to aromatic protons may be correlated with the efficiency of 9-fluorenol oxidation and establishes the basis for evaluating the NaOCl activation method. The higher benzylic-to-aromatic signal ratio, the less efficient was the oxidation of 9-fluorenol to 9-fluorenone. Less efficient oxidation of the starting material means that a smaller amount of hypochlorite was left in the solution after its activation, which points to a higher extent of the decomposition of hypochlorite upon activation. This is an indication of better efficacy of NaOCl and hence a more effective method to activate the irrigant. To convey the idea more clearly, the logical sequence behind it is summarized graphically in Fig. 5.

Numerical results of the study

The numerical results of the analyses are presented in Table 1. As each experiment was done 3-fold, 3 entries for each activation mode are provided. As aforementioned, the number of aromatic protons remain unaffected upon oxidation, so the integration of their signals can serve as an internal standard for determining the integration ratio.²⁹ The integration of the aromatic region was then set by default to 1.00. As all further discussion is based on the integration ratios, setting the aromatic region

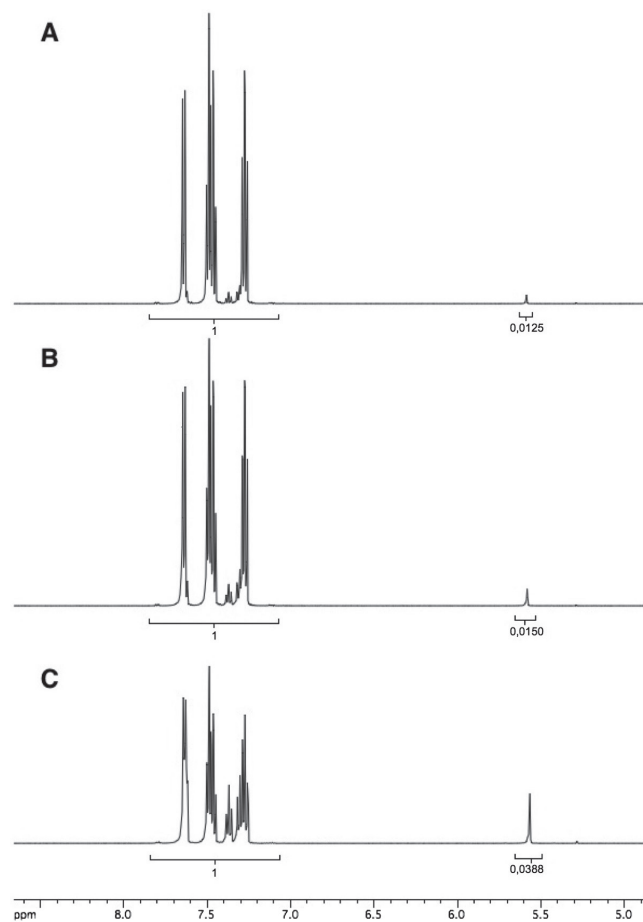


Fig. 3. Comparison of ^1H NMR spectra obtained from the evaluation experiments carried out on: (A) non-activated NaOCl; (B) NaOCl activated with the SAF system; (C) NaOCl activated with ultrasonics. The peak in the 5.60–5.50 region corresponds to the benzylic hydrogen atom in the structure of 9-fluorenol. The region below 5.0 ppm was omitted for clarity. Each integration value given below the peak is an average determined from 3 experiments conducted on every sample

integration to 1.00 makes it easier to evaluate and discuss the results.

With this in mind, there is no need to reference the integration of signals against the internal standard used, i.e., TMS. The additive of TMS in the commercial deuterated solvent was used only for calibrating the chemical shift of the observed signals, with TMS having the chemical

Table 1. Results of the spectroscopic studies

Activation mode	Benzylic-to-aromatic signals integration ratio	Average	Standard deviation (SD)	Recalculated integration ratio ¹
No activation	0.0127 : 1.00 0.0122 : 1.00 0.0125 : 1.00	0.0125	0.0003	1.00
SAF	0.0154 : 1.00 0.0152 : 1.00 0.0143 : 1.00	0.0150	0.0006	1.20
Ultrasonics	0.0386 : 1.00 0.0382 : 1.00 0.0396 : 1.00	0.0388	0.0007	3.11

¹ The benzylic-to-aromatic signals integration ratio, recalculated with respect to the value of the “no activation” ratio equal to 1.00.

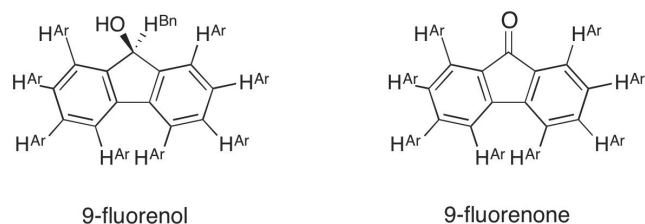


Fig. 4. Chemical structures of 9-fluorenol and 9-fluorenone, with hydrogen (H) atoms described (Ar = aromatic, Bn = benzylic)

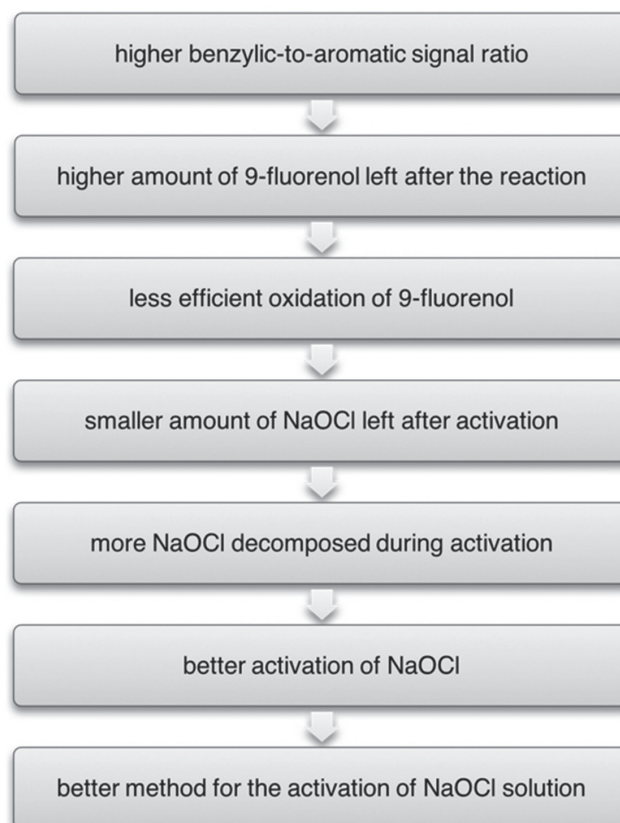


Fig. 5. Summary of the chemical concept behind the proposed evaluation

shift of 0.00 ppm. Tetramethylsilane would not have been a reliable reference for the integration due its volatility³⁰ and hence tendency to change its concentration over time, making it an invalid reference for any quantitative studies.

The use of another chemical shift standard widely used in molecular medicine studies, namely 3-(trimethylsilyl)-2,2,3,3-tetradeuteropropionic acid (TSP), would not be possible due to the fact that TSP is insoluble in deuterated chloroform which was the deuterated solvent used in this study. Deuterated chloroform was picked as a deuterated solvent of choice due to its capability to dissolve the organic compounds well, both the substrate (9-fluorenol) and the product

(9-fluorenone) as well as any amount of the catalyst left in the organic phase during the extraction.^{27,28,31} Moreover, the use of TSP could lead to misleading results as TSP tends to be unstable in the presence of oxidative agents. If any traces of NaOCl had been left after the extraction process (which is unlikely but cannot be excluded), TSP would have got oxidized, hence making its use as a standard invalid.

In all experiments, the benzylic-to-aromatic ratios were found to be between 0.0122:1.00 and 0.0396:1.00. That observation was expected, as the integration should have fallen within the 0.1250 for 9-fluorenone (equal to 1:8 ratio, with 1 benzylic proton and 8 aromatic protons) and 0 for 9-fluorenone (0:8 ratio, with no benzylic protons and 8 aromatic protons) bracket. Importantly, none of the ratios were equal to 0, as that would mean 9-fluorenone was oxidized completely which would preclude any qualitative or quantitative conclusions being drawn.

For each activation mode, an average ratio was determined from 3 experiments, along with its SD. The integration ratios were then recalculated with respect to the “no activation” ratio set to 1.00. The ratio values for the SAF and ultrasonic activation modes were found to be 1.20 and 3.11, respectively.

Differences in the results between the examined groups of samples are clearly visible in Fig. 6. The obtained integration ratios of all results in the SAF and ultrasonics groups are higher than the values for a non-activated group.

Statistical analysis results

Taking into account the means and SDs of benzylic-to-aromatic signals integration ratio between groups, our hypothesis states that their distribution is not equal. Due to the fact that there is no way to reliably test for normality when we have 3 observations per group, a non-parametric approach is used. The null hypothesis that the cumulative distribution function in all 3 groups is equal is tested against the alternative hypothesis that at least 2 out of 3 cumulative distribution functions in the groups are different. The hypotheses are tested using ANOVA on ranks, i.e., using the Kruskal–Wallis rank-sum test. The value of the test statistics, which under the null hypothesis has a χ^2 distribution with 2 df, is 7.2. It follows that the p-value in this test is equal to 0.02732372, which is lower than the 0.05 significance level. The null hypothesis is rejected, thus at the 0.05 significance level there is a statistically significant difference in distributions between the groups.

It is important to note, that in this case the usual interpretation of Kruskal–Wallis rank sum test using medians is not possible. For the test to be interpreted in terms of medians, we should verify first that all 3 distributions come from the same family of location-scale distributions. This is not possible with the available data, due to the small number of observations. For the same reason, it is also impossible to perform a non-parametric post-hoc analysis using the Wilcoxon rank sum test.

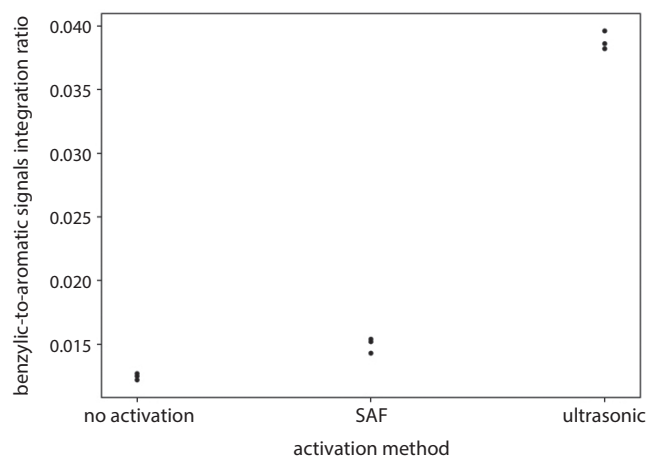


Fig. 6. A graph presenting data points from the spectroscopic study. The results both in the SAF and ultrasonics groups clearly predominate over the control group (no activation). The results in the ultrasonics group are more than 3-fold higher in comparison to these in the SAF group

By looking at the data points in Fig. 6 and knowing that the continuous distribution functions are different, we can postulate that they do differ in mean.

Discussion

Stojicic et al. suggested several methods for improving efficacy of NaOCl. Changes in concentration, temperature, agitation, increase of pH, and prolonged contact time are some of them.³² Moorer and Wesselink stressed the impact of mechanical agitation to be the most significant mode of NaOCl activation. They claim fluid flow is the key for effective tissue dissolution and disinfection as well as emphasize that ultrasounds ensure the best quality of turbulent flow.³³ An increase in flow and more turbulence enables the solution to reach hardly accessible areas and therefore improve efficacy. Sáinz-Pardo et al. also provide evidence that ultrasonic agitation ensures proper fluid flow throughout the working length of a root canal.³⁴ Besides fluid dynamics, the exact mechanism responsible for the improved efficacy is not clear.³⁵ This is the first investigation of its kind to evaluate whether a chemical activation of NaOCl also occurs during agitation.

To evaluate the methods for hypochlorite activation, we searched the chemical literature for reactions which use NaOCl solutions as a reagent. We preferred a reaction that did not take long to carry out in order to shorten the evaluation as much as possible. Other criteria that needed to be met included the following: easy reaction set-up (ideally no specialized glassware or equipment), mild conditions (preferably room temperature, atmospheric pressure, no need for the use of inert gases like argon or nitrogen), inexpensive and easily commercially available chemicals (including the starting materials, solvents and optionally catalysts) as well as the possibility to carry out the evaluation using an analytical method yielding readily interpretable

and unequivocal results. After a detailed literature survey, we picked the phase-transfer-catalyzed oxidation of 9-fluorenone with NaOCl as the model reaction.

The role of NaOCl solution is to provide hypochlorite anions (ClO^-), which serve as an oxidant towards benzylic alcohol. Importantly for the evaluation of oxidation potential, hypochlorite reacts with 9-fluorenone selectively, affording solely the oxidation product – 9-fluorenone. 9-fluorenone is not prone to spontaneous oxidation neither in pure oxygen nor in the air, even upon prolonged storage. These properties made the quantitative evaluation of oxidation product exclusive to NaOCl, and hence valid. Moreover, it facilitates handling of 9-fluorenone, as no specialized chemical skills or sophisticated equipment is required.

Among the many variants of 9-fluorenone oxidations, the one chosen by us is preferable also because it does not require the presence of expensive, metal-based catalysts, elevated temperature or irradiation. For an effective execution of 9-fluorenone oxidation with hypochlorite, it is sufficient to make use of inexpensive and easily applicable phase-transfer catalysis (PTC).³¹ The method, originally developed in the 1960s, is particularly useful for reactions occurring in 2-phase systems, i.e., in reaction mixtures containing 2 immiscible (or miscible to a limited extent) layers. For example, such layers may be made up of a reagent aqueous solution (in our case: aqueous solution of NaOCl) and a solution of the starting organic material (here: 9-fluorenone) in an organic solvent immiscible with water (e.g., ethyl acetate). The reaction between the organic substrate and the inorganic reagent (hypochlorite anion) takes place at the interphase between those 2 layers. For the oxidation to proceed efficiently, both the substrate and the oxidant must come together in the interphase at the same time. Here a phase-transfer catalyst comes in useful. The PTC catalysts usually contain a heteroatom (particularly nitrogen), in the form of a cationic ammonium species with a general formula of R_4N^+ , where R is an organic group, most commonly an aliphatic chain. Such a structure has a dual nature in terms of polarity: the cationic nitrogen atom serves as the polar (hydrophilic) center, while the aliphatic hydrocarbon chains are highly non-polar (hydrophobic, but with high affinity to the organic layer). This duality makes it possible for the cation of the catalyst to be transported to both the organic and aqueous layers, efficiently delivering the hypochlorite anion from the aqueous layer to the interphase with the organic layer. In this study, tetra-*n*-butylammonium bromide was used as the phase-transfer catalyst.

Having an appropriate model reaction at hand, we embarked on the search for a method for both a qualitative and a quantitative analysis of the reaction mixture composition, i.e., the identity and content of the substrate and product. We chose nuclear magnetic resonance (NMR) spectroscopy for this purpose. The NMR spectroscopy is one of the most important research techniques used to investigate the structure, content and interactions

of organic compounds. The method is basically based on the phenomenon of energy transitions occurring within the nuclei of atoms when an external magnetic field is applied. By investigating the electromagnetic signals in this process and working them out mathematically, a so-called NMR spectrum can be obtained. The NMR method we decided to use was proton NMR (^1H NMR), as it allows one to obtain qualitative and quantitative information on protons (hydrogen nuclei) in the organic compounds structure present in the analyzed mixture.

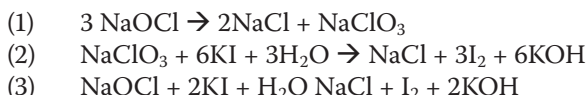
Only a few reports on the use of spectroscopic methods in endodontic research have been published, all of them being relatively recent. A study by Sireesha et al. on the comparison of micro and nano substances used as temporary intracanal dressings was based on infrared spectroscopy (Fourier-transform infrared spectroscopy – FTIR) to analyze the interactions between nanoparticles.³⁶ The conclusion from the study was that the tested nano-calcium hydroxide and nano-chitosan compounds are superior to ordinary calcium hydroxide and chitosan both in terms of better penetration of dentinal tubules and lower susceptibility to root fracture. One can find an example of the use of mass spectrometry (MS) in a study by Chávez de Paz et al.³⁷ An evaluation of the coexistence of *Enterococcus faecalis* bacteria strains with other bacteria within the root canal system has showed that in this case bacteria can interact synergistically as well as antagonistically. X-ray spectroscopy is another example of spectroscopy used in endodontic research, and in particular wavelength-dispersive X-ray spectroscopy (WDXS or WDS) used in the Han study to assess the calcium and silicon uptake by dentin from Biodentine and MTA.³⁸ The study shows that the dentin adjacent to a given material exhibited greater influence of calcium and silicon from the Biodentine material.

By using the concept of spectroscopic data analysis described in the Results section, we were able to qualitatively and quantitatively compare the activation methods. Based on the ^1H NMR integration ratios recalculated with reference to the ratio obtained for non-activated NaOCl, the occurrence of chemical activation of hypochlorite by both the SAF and ultrasonics was confirmed. Quantitatively, the ultrasonic activation was over 2 times more effective compared to the SAF activation (1.2-fold activation for SAF compared to 3.1-fold activation for ultrasonics).

All the results obtained in the SAF and ultrasonic groups predominated these in the non-activated group. What is more, all results in the ultrasonic group were higher than those measured in the SAF group. The consequence and reproducibility in each group with a low SD value lays a basis for the use of this method in other NaOCl-related studies and analyses in the future. Similar experiments on other NaOCl agitation methods would have a worthwhile contribution in understanding their clinical efficacy.

It is worth noticing that another dentistry-related study on NaOCl capacity for oxidation can be found

in literature.³⁹ However, it used a non-spectroscopic method for NaOCl analysis, namely a redox titration called iodometry. Zehnder assessed the buffered and unbuffered solution of NaOCl for tissue dissolution.³⁹ However, the disadvantage of that approach was that potassium iodide (KI; used as a titrating solution) is known to be reactive not only towards NaOCl, but also other oxidants present in the solution. This appears even more perspicuous when the equations of NaOCl comproportionation (Equation 1) as well as non-selectivity of potassium iodide oxidation (Equations 2 and 3) are taken into account.



Sodium hypochlorite (NaOCl) is known to comproportionate into sodium chlorate (NaClO₃) and sodium chloride while in aqueous solutions, especially over prolonged storage. Importantly, both NaOCl and NaClO₃ are able to oxidize potassium iodide. The titration result may then be false due to lack of selectivity.

The reactions used in our study display specificity towards NaOCl, with 9-fluorenone being selectively oxidized by it. Despite a great number of works on chlorine-based oxidants, NaClO₃ has never been found to oxidize any secondary alcohols like 9-fluorenone.

In conclusion, a spectroscopy-based protocol for a quantitative evaluation of activation of NaOCl was proposed and successfully implemented. The comparative ¹H NMR data, derived from the experiments on the irrigant capacity to oxidize 9-fluorenone, unequivocally showed that both SAF and ultrasonics activate NaOCl. In addition, it was shown that ultrasonic agitation provided better chemical activation of the NaOCl solution than the SAF.

From a medical perspective, it is worthwhile to point out that any contact between an ultrasonic file with canal walls diminishes the activation effect.⁴⁰ This is the main impediment to achieving proper ultrasonic activation on the whole working length in severely curved canals.

On another concluding note, we believe that such an interdisciplinary approach towards solving challenges on the border of medicine and science will soon become an important area for research and such results may quickly become clinically relevant. In this case, the significance of the study lies in providing a dental practitioner with specific information on choosing the best way for NaOCl activation, making canal disinfection as thorough as possible and increasing the efficiency as well as the long-term results of endodontic treatment in the clinic.

A molecular approach in exploring the dental field may give extraordinary opportunities in future scientific projects in this area of medicine. Nowadays, microbiological and clinical studies underlie the majority of new techniques and devices being introduced into the market and, in consequence, the dental practice. However, it is molecular medicine and experimental approach that explain

the fundamental aspects of biological and chemical mechanisms behind these developments and boosts the understanding of everyday activities undertaken by physicians and dentists. The described influence of the SAF motion and ultrasonic wave on changes in the molecular composition of NaOCl solution should make one aware that any step taken during a clinical procedure may hinder or improve the overall outcome. Advantageous properties of NaOCl for endodontics that are strengthened by additional activation methods like ultrasonics can be correctly understood only by means of a thorough experimental analysis. The mechanisms behind the observed macroscopic phenomena in the clinical environment are often comprehensively understandable only at the molecular level.

ORCID iDs

Hubert Gołabek  <https://orcid.org/0000-0003-0840-2752>
 Krzysztof Mariusz Borys  <https://orcid.org/0000-0002-6131-4236>
 Meetu Ralli Kohli  <https://orcid.org/0000-0003-2788-8903>
 Katarzyna Brus-Sawczuk  <https://orcid.org/0000-0003-3139-0112>
 Izabela Strużycka  <https://orcid.org/0000-0002-7058-3614>

References

- Coolidge ED. The diagnosis and treatment of conditions resulting from diseased dental pulps. *J Am Dent Assoc.* 1996;6(4):337–349.
- Senia ES, Marshal FJ, Rosen S. The solvent action of sodium hypochlorite on pulp tissue of extracted teeth. *Oral Surg Oral Med Oral Pathol.* 1971;31(1):96–103.
- Pécora JD, Sousa-Neto MD, Estrela C. Soluções irrigadoras auxiliares do preparo do canal radicular. In: Estrela C, Figueiredo JAP, eds. *Endodontia – Princípios biológicos e mecânicos.* São Paulo, Brazil: Artes Médicas; 1999:552–569.
- Estrela C, Estrela CR, Barbin EL, Spanó JC, Marchesan MA, Pécora JD. Mechanism of action of sodium hypochlorite. *Braz Dent J.* 2002;13(2): 113–117.
- Gołabek H, Duszkiewicz P, Szutowska A, Mielko E, Strużycka I. Review of techniques and current possibilities of root canal irrigation. *Dental Forum.* 2015;43:85–92.
- Baker NA, Eleazer PD, Averbach RE, Seltzer S. Scanning electron microscopic study of the efficacy of various irrigating solutions. *J Endod.* 1975;1(4):127–135.
- Beer R, Baumann MA, Kielbassa AM. *Ilustrowane kompendium endodoncji.* Lublin, Poland: Czelej; 2009.
- Gołabek H, Brus-Sawczuk K, Strużycka I. The Self Adjusting File – a review. New system, a new look into the root canal space? *Dental Forum.* 2014;42:89–94.
- Solomonov M. Eight months of clinical experience with the Self-Adjusting File System. *J Endod.* 2011;37(6):881–887.
- De-Deus G, Souza EM, Barino B, Maia J, Zamolyi RQ, Reis C, Kfir A. The Self-Adjusting File optimizes debridement quality in oval-shaped root canals. *J Endod.* 2011;37(5):701–705.
- Hof R, Perevalov V, Eltanani M, Zary R, Metzger Z. The Self-Adjusting File (SAF). Part 2: Mechanical analysis. *J Endod.* 2010;36(4):691–696.
- Kaya S, Yiğit-Özer S, Adigüzel Ö. Evaluation of radicular dentin erosion and smear layer removal capacity of Self-Adjusting File using different concentrations of sodium hypochlorite as an initial irrigant. *Oral Surg Oral Med Oral Pathol Oral Radiol Endod.* 2011;112(4):524–530.
- Cohen S, Levin MD, Berman LH. The SAF EndoSystem: Adaptive 3-D cleaning, shaping, and disinfection. *Endod Prac.* 2011;4(2):34–38.
- Block R, Supan P, Bushell A. The Self Adjusting File (SAF) System: Perspectives on a new endodontic technique. *The Communicator.* 2012; Winter:24–28.
- Metzger Z, Teperovich E, Cohen R, Zary R, Paqué F, Hülsmann M. The Self-Adjusting File (SAF). Part 3: Removal of debris and smear layer: A scanning electron microscope study. *J Endod.* 2010;36(4): 697–702.

16. Özer SY, Adigüzel O, Kaya S. Removal of debris and smear layer in curved root canals using Self-Adjusting File with different operation times: A scanning electron microscope study. *Int Dent Res*. 2011; 1(1):1–6.
17. Metzger Z, Teperovich E, Zary R, Cohen R, Hof R. The Self-Adjusting File (SAF). Part 1: Respecting the root canal anatomy – a new concept of endodontic files and its implementation. *J Endod*. 2010;36(4): 679–690.
18. Alves FRF, Almeida BM, Neves MA, Rôças IN, Siqueira JR Jr. Time-dependent antibacterial effects of the Self-Adjusting File used with two sodium hypochlorite concentrations. *J Endod*. 2011;37(10):1451–1455.
19. Tiong TJ, Price GJ. Ultrasound promoted reaction of Rhodamine B with sodium hypochlorite using sonochemical and dental ultrasonic instruments. *Ultrason Sonochem*. 2012;19(2):358–364.
20. Zeng Q, Fu J, Shi YT, Zhu HL. Degradation of C.I. Disperse Blue 56 by ultraviolet radiation/sodium hypochlorite. *Ozone Sci Eng*. 2009; 31(1):37–44.
21. Krumova K, Cosa G. *Overview of Reactive Oxygen Species. Singlet Oxygen: Applications in Biosciences and Nanosciences*. Vol. 1. Cambridge, UK: The Royal Society of Chemistry; 2016.
22. Austin JH, Taylor HD. Behavior of hypochlorite and of chloramine-T solutions in contact with necrotic and normal tissues in vivo. *J Exp Med*. 1918;27(5):627–633.
23. Mirafzal GA, Lozeva AM. Phase transfer catalyzed oxidation of alcohols with sodium hypochlorite. *Tetrahedron Lett*. 1998;39(40):7263–7266.
24. R Core Team. R: A language and environment for statistical computing. R Foundation for Statistical Computing, Vienna, Austria, 2018: URL <https://www.R-project.org/>.
25. Hollander M, Wolfe DA. *Nonparametric Statistical Methods*. New York, USA: John Wiley & Sons; 1973:115–120.
26. Jones CS, Albizati K. Sodium hypochlorite oxidation of 9-fluorenonol to 9-fluorenone: A reaction monitored by thin layer chromatography. *J Chem Educ*. 1994;71:A271–A272.
27. Laudadio G, Govaerts S, Wang Y, et al. Selective C(sp³)-H aerobic oxidation enabled by Decatungstate photocatalysis in flow. *Angew Chem Int Ed Engl*. 2018;57(15):4078–4082.
28. Xuan Q, Zhao C, Song Q. Umpolung of protons from H₂O: Q metal-free chemoselective reduction of carbonyl compounds via B₂pin₂/H₂O systems. *Org Biomol Chem*. 2017;15(24):5140–5144.
29. Kato R, Yoshimasa K, Egashira T, Oya T, Oyaizu K, Nishide H. A ketone/ alcohol polymer for cycle of electrolytic hydrogen-fixing with water and releasing under mild conditions. *Nat Commun*. 2016;7:13032.
30. Ho HA, Manna K, Sadow AD. Acceptorless photocatalytic dehydrogenation for alcohol decarbonylation and imine synthesis. *Angew Chem Int Ed Engl*. 2012;51(34):8607–8610.
31. Yamanaka M, Shivanyuk A, Rebek J Jr. Kinetics and thermodynamics of hexameric capsule formation. *J Am Chem Soc*. 2004;126(9): 2939–2943.
32. Stojicic S, Zivkovic S, Qian W, Zhang H, Haapasalo M. Tissue dissolution by sodium hypochlorite: Effect of concentration, temperature, agitation, and surfactant. *J Endod*. 2010;36(9):1558–1562.
33. Moorer WR, Wesselink PR. Factors promoting the tissue dissolving capability of sodium hypochlorite. *Int Endod J*. 1982;15(4):187–196.
34. Sáinz-Pardo M, Estevez R, De Pablo Óv, Rossi-Fedele G, Cisneros R. Root canal penetration of a sodium hypochlorite mixture using sonic or ultrasonic activation. *Braz Dent J*. 2014;25(6):489–493.
35. Zehnder M. Root canal irrigants. *J Endod*. 2006;32(5):389–398.
36. Sireesha A, Jayasree R, Vidhya S, Mahalaxmi S, Sujatha V, Kumar TSS. Comparative evaluation of micron- and nano-sized intracanal medicaments on penetration and fracture resistance of root dentin: An in vitro study. *Int J Biol Macromol*. 2017;104(Pt B):1866–1873.
37. Chávez de Paz LE, Davies JR, Bergenholtz G, Svensäter G. Strains of *Enterococcus faecalis* differ in their ability to coexist in biofilms with other root canal bacteria. *Int Endod J*. 2015;48(10):916–925.
38. Han L, Okiji T. Uptake of calcium and silicon released from calcium silicate-based endodontic materials into root canal dentine. *Int Endod J*. 2011;44(12):1081–1087.
39. Zehnder M, Kosicki D, Luder H, Sener B, Waltimo T. Tissue-dissolving capacity and antibacterial effect of buffered and unbuffered hypochlorite solutions. *Oral Surg Oral Med Oral Pathol Oral Radiol Endod*. 2002;94(6):756–762.
40. Sabins RA, Johnson JD, Hellstein JW. A comparison of the cleaning efficacy of short-term sonic and ultrasonic passive irrigation after hand instrumentation in molar root canals. *J Endod*. 2003;29(10): 674–678.

Mild hyponatremia discovered within the first 24 hours of ischemic stroke is a risk factor for early post stroke mortality

Agnieszka Gala-Błądzińska^{1,2,A–E}, Jolanta Czarnota^{3,B–D}, Rafał Kaczorowski^{3,B,C,E},
Marcin Braun^{4,5,C,D}, Krzysztof Gargas^{1,C,D}, Halina Bartosik-Psujek^{1,3,A,C,E,F}

¹ Faculty of Medicine, University of Rzeszów, Poland

² Dialysis Center, St. Queen Jadwiga Clinical District Hospital No. 2, Rzeszów, Poland

³ Department of Neurology, St. Queen Jadwiga Clinical District Hospital No. 2, Rzeszów, Poland

⁴ Department of Pathology, Chair of Oncology, Medical University of Lodz, Poland

⁵ Postgraduate School of Molecular Medicine, Warsaw Medical University, Poland

A – research concept and design; B – collection and/or assembly of data; C – data analysis and interpretation;
D – writing the article; E – critical revision of the article; F – final approval of the article

Advances in Clinical and Experimental Medicine, ISSN 1899–5276 (print), ISSN 2451–2680 (online)

Adv Clin Exp Med. 2019;28(10):1321–1327

Address for correspondence

Agnieszka Gala-Błądzińska
E-mail: agala.edu@gmail.com

Funding sources

None declared

Conflict of interest

None declared

Received on March 29, 2018

Reviewed on November 3, 2018

Accepted on January 21, 2019

Published online on September 13, 2019

Cite as

Gala-Błądzińska A, Czarnota J, Kaczorowski R, Braun M, Gargas K, Bartosik-Psujek H. Mild hyponatremia discovered within the first 24 hours of ischemic stroke is a risk factor for early post stroke mortality. *Adv Clin Exp Med.* 2019;28(10):1321–1327. doi:10.17219/acem/103070

DOI

10.17219/acem/103070

Copyright

© 2019 by Wrocław Medical University

This is an article distributed under the terms of the Creative Commons Attribution Non-Commercial License (<http://creativecommons.org/licenses/by-nc-nd/4.0/>)

Abstract

Background. Comorbidities, complications and laboratory abnormalities are common in stroke patients. One of the common problems is hyponatremia (serum sodium (Na) level <135 mmol/L), but the relationship between hyponatremia and the prognosis in patients with stroke is not well understood.

Objectives. The aim of this study was to investigate the prevalence and severity of hyponatremia, as well as its impact on prognosis in stroke patients on admission to hospital.

Material and methods. The study involved the analysis of the first measurement of the Na level after the admission and its correlations with comorbidities, the scale of clinical assessment of stroke severity (NIHSS), the size and location of the stroke, and mortality. A retrospective study was conducted on 502 patients (among them 263 women) admitted to the hospital on stroke onset (440 ischemic stroke (IS) and 62 hemorrhagic stroke (HS) patients). The post-stroke mortality was defined as early if death occurred within 30 days.

Results. Hyponatremia was found in 18.4% of patients with IS and 25.8% of patients with HS, irrespective of age and gender. Hyponatremia is an independent prognostic factor of mortality in people with IS ($p = 0.003$). Na levels were lower in IS patients who died than in those who remained alive (134.8 ± 4.99 mmol/L vs 136.6 ± 3.01 mmol/L; $p = 0.02$). Higher mortality rate was observed among IS patients under 75 years of age and Na level ≤ 132 mmol/L. In patients with IS, hyponatremia correlates with NIHSS ($p = 0.005$) and the size and location of the stroke ($p = 0.002$).

Conclusions. Hyponatremia is more frequently observed in patients with HS than IS. Mild hyponatremia is already known to be an independent prognostic factor in the mortality of people with IS and it may also have value as a prognostic factor in the mortality of the IS population. In a patient with a suspected stroke, there is a need to control electrolyte levels at the onset of the stroke, especially in patients with comorbidities, irrespective of age.

Key words: stroke, hyponatremia, hospital mortality

Introduction

Hyponatremia is defined as a decrease in the serum sodium (Na) concentration below 135 mmol/L.^{1–3} It is a common electrolytic disorder diagnosed in patients hospitalized due to different neurological diseases, such as subarachnoid hemorrhage, brain injury and meningitis.⁴ Cardiovascular disorders, including strokes, constitute the cause of half of the deaths of Europeans⁵ and Americans.⁶ In stroke patients, different comorbidities and complications are very common, and there are studies evaluating their impact on neurological condition during the acute phase of stroke, on disability, and on early mortality.⁷

Natremia can be both the cause and the effect of brain damage. As a result of damage to the brain due to a stroke, cerebral salt-wasting syndrome (CSWS) or inadequate secretion of vasopressin (SIADH) may result, resulting in hyponatremia. At the same time, in acute hyponatremia, as a result of the sudden loss of Na from intravascular fluid and a decrease in the osmolality of the serum, brain cells can swell as a consequence of the passage of water from the vascular bed to the nerve cells because of the higher osmolality of the intracellular fluid. However, if corrected too quickly, chronic hyponatremia may cause osmotic demyelination syndrome and irreversible brain damage. In addition, and as a result of brain damage in the course of a stroke, central diabetes insipidus can occur, resulting in a loss of clean water and hypernatremia. At the same time, we often observe hypernatremia in those stroke patients with accompanying unconsciousness that prevents them from drinking fluids.^{8,9}

When examining a patient with a newly diagnosed stroke, the differential diagnosis of hyponatremia should also consider any co-morbidities or pharmacotherapies that may influence or be associated with hyponatremia.¹ Patients, especially those with ischemic stroke (IS), also often suffer from metabolic syndrome, whose components, such as hyperglycemia, hyperlipidemia and hypertension, can generate hyponatremia per se; this syndrome can also be a result of the patient's pharmacotherapy. In addition, hyponatremia is often associated with other diseases of affluence, such as heart failure or chronic kidney disease. Hyponatremia may also be the result of liver failure, hypothyroidism and adrenal insufficiency, vomiting

or diarrhea.^{4,6} The drugs that can often cause hyponatremia include diuretics (in particular thiazides), antidepressants, anticonvulsants (carbamazepine), some cytostatics, and non-steroidal anti-inflammatory drugs.^{1,9}

Hyponatremia has been evaluated in only a few studies so far, and a relationship between hyponatremia during the first day of stroke and 30-day mortality has been found.^{7,10,11} However, the cut-off value for natremia below which the mortality increases significantly has not been determined in any previous study. Therefore, we evaluated the correlation between the value of natremia and demographic data, length of hospitalization, and the patient's clinical status on the day of hospital discharge.

The aim of the study was to investigate the prevalence and severity of hyponatremia on the first day of stroke, as well as the relationship between hyponatremia and the consequences of stroke. Special attention was paid to the impact of hyponatremia on mortality.

Material and methods

A retrospective study involved patients admitted to the Neurology Department of the St. Queen Jadwiga Clinical District Hospital No. 2 in Rzeszów (Poland) from January 1, 2015 to December 30, 2015. The study included 501 stroke patients (263 women and 239 men) admitted to the hospital on the first day of the stroke. On the basis of clinical symptoms and computed tomography (CT) or magnetic resonance imaging (MRI) scans, 440 patients were diagnosed with IS and 62 with hemorrhagic stroke (HS) (Table 1). Patients with hemorrhage related to anticoagulation, trauma, tumor and arteriovenous malformations, or after acute thrombolysis or coagulopathy were excluded. We used the National Institutes of Health Stroke Scale (NIHSS) to assess the severity of stroke symptoms at the time of admission and of discharge.¹⁰ Also, we used the Paciaroni et al. scale to assess the distribution and size of the IS (Table 3), and the results are presented in Table 4.

On admission to the hospital, all patients underwent laboratory tests including serum electrolyte concentrations. Serum natremia was determined in blood samples collected on a clot, with the indirect potentiometric method with ion selective electrodes using the Beckman Coulter® AU 680

Table 1. Characteristics of stroke patients

Variable	Ischemic stroke			Hemorrhagic stroke		
	total	alive	deaths	total	alive	deaths
n [%]	440	396 (90.0)	44 (10.0)	62	41 (67.2)	21 (33.8)
men, n [%]	205	189 (92.2)	16 (7.8)	34	22 (64.7)	12 (35.3)
women, n [%]	235	207 (88.1)	28 (11.9)	28	19 (67.9)	9 (32.1)
Age [years]						
median	73.0	72.3	81.3	75.4	73.8	78.3
mean (±SD)	76 ±13.9	75 ±14.0	83 ±9.5	77 ±13.5	74 ±13.8	82 ±12.5
range (min–max)	24–96	24–96	48–99	24–95	24–95	48–94

SD – standard deviation.

Table 2. Participation of patients with IS and HS depending on the value of natremia

Variable	Normonatremia n [%]	Mild hyponatremia n [%]	Moderate hyponatremia n [%]	Severe hyponatremia n [%]
Hemorrhagic stroke (n = 62)	46 (74.3)	13 (20.9)	2 (3.2)	1 (1.6)
Ischemic stroke (n = 440)	359 (81.6)	66 (15.0)	12 (2.7)	3 (0.7)

biochemical analyzer (Beckman Coulter, Brea, USA). Hyponatremia was diagnosed if the serum Na concentration was below 135 mmol/L. For evaluation of the effects of serum hyponatremia on early post-stroke mortality and functional outcome, the first measurements of natremia obtained in the emergency room before any diagnostic or therapeutic intervention were analyzed. Patients diagnosed with hyponatremia were treated according to the etiology, gravity and duration of hyponatremia. The period of 30 days between stroke and death was assumed as a definition of early post-stroke mortality. All patients were clinically assessed using the Rankin scale on the day of discharge from the hospital or on day 30 of hospitalization.

Statistical analysis

The statistical analysis was performed on the basis of paper and electronic medical records. Categorical data was reported as numbers of patients (percentage of the appropriate group). Median (lower–upper quartile) or mean \pm standard deviation (SD) were reported for continuous variables. The analysis was started by checking the normal distribution (Shapiro–Wilk test) and variance homogeneity (Levene’s test). A non-parametric Mann–Whitney U test was performed. For categorical data, the χ^2 test was used. Differences were considered significant at the level of $p < 0.05$. For the receiver operating characteristic (ROC) curve analysis, cut-off values optimizing the Youden index were calculated. To determine better predictability of death based on Na level, a Kaplan–Meier probability of survival was estimated. A multivariate analysis of survival and hyponatremia was performed using Cox’s proportional hazard regression model. Statistical calculations were performed using the STATISTICA v. 12 software package (StatSoft Inc., Tulsa, USA).

Results

The mean Na level was 136.5 ± 3.26 (median = 137, min = 116, max = 147) in IS and 135.9 ± 3.94 (median = 136, min = 118, max = 144) in HS. The differences were statistically nonsignificant. There was no correlation between the age of patients and serum Na concentrations in both the whole population and after distinction between the HS and IS groups. There were no differences in serum Na concentrations between men and women (Mann–Whitney U test $p = 0.3$ and $p = 0.2$, respectively). The average length of hospitalization of patients with IS was 17 ± 23.4 days

Table 3. Distribution and size of ischemic stroke according to the Paciaroni et al. scale¹⁴

Type of stroke	The size of the stroke	Range of vascularization
1	small	change in front or posterior vascularization <1.5 cm
2	average	change including cortical branches of MCA change including deep MCA branches change on the border between the 2 territories change including cortical PCA branches change including deep PCA branches change including cortical ACA branches
3	large – front	change covering the entire range of MCA, PCA and ACA change including 2 cortical MCA branches change includes cortical and deep MCA branches change covering more than 1 arterial range
4	large – rear	change involving the brain stem or cerebellum >1.5 cm

MCA – middle cerebral artery; PCA – posterior cerebral artery; ACA – anterior cerebral artery.

(median = 10.5, min = 1, max = 120) and with HS was 7.3 ± 7.0 days (median = 5, min = 1, max = 30). Serum Na level below 135 mmol/L was found in 97 (19.3%) patients with stroke. Hyponatremia was found in 81 patients (18.4%) with IS and 16 patients (25.8%) with HS.

On the basis of serum Na concentrations, hyponatremia was divided into mild (130–135 mmol/L), moderate (125–129 mmol/L) and severe (<125 mmol/L). The participation of patients depending on the value of natremia in patients with IS and HS is presented in Table 2. Among patients with IS and normo-natremia, mortality was 9% (n = 31), whereas in the group of patients with hyponatremia, mortality was 16% (n = 13).

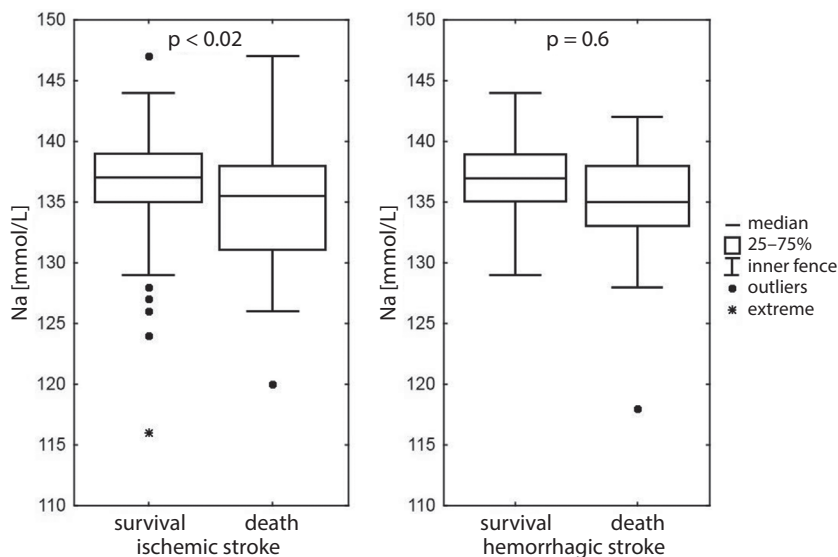
Our univariate analyses of patients with IS showed that hyponatremia as well as neurological deficits (estimated using NIHSS), the size and location of the stroke (estimated using the Paciaroni et al. scale¹⁴), patients’ ages and comorbidities (such as arterial hypertension, chronic kidney disease, heart failure, and hyperlipidemia) were independent predisposing factors in the early deaths of study group members (Table 4).

Moreover, higher mortality was observed in younger, i.e., under 75 years of age, patients with IS and hyponatremia. In the group of patients under 75 years of age with normo-natremia, mortality was 8.6% whereas among the same age group with hyponatremia, mortality was 16.0%. The differences were statistically significant

Table 4. Influence of clinical factors and results of laboratory tests in relation to mortality in patients with IS in single and multivariate analyses

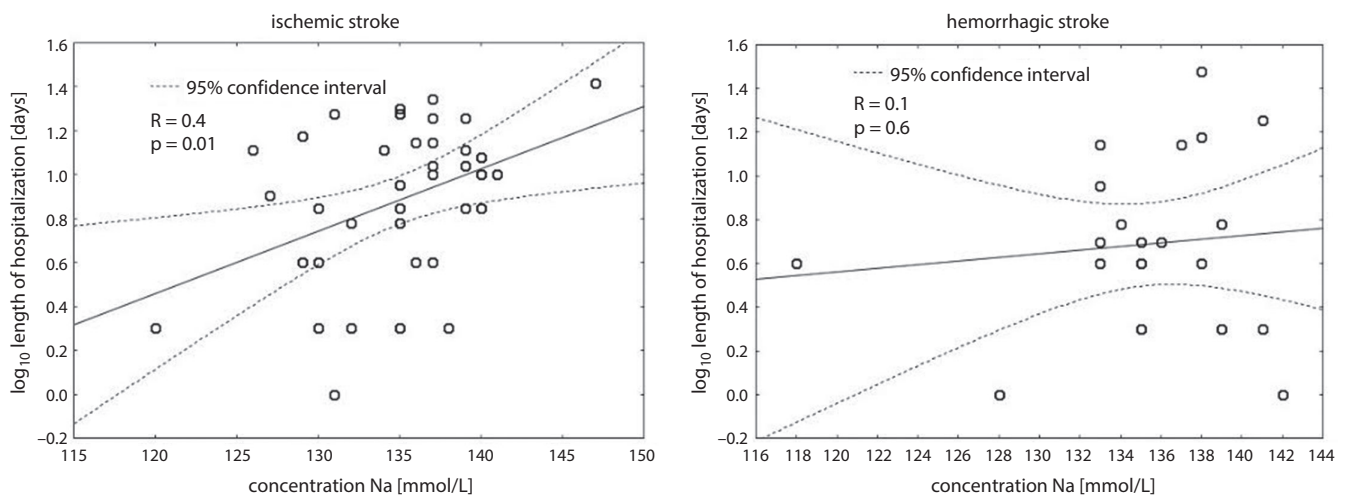
Variable	p-value from univariate analysis (log-rank)	p-value from multivariate analysis (Cox)	Hazard ratio	Confidence interval (95% CI)	Type of the effect
NIHSS at admission [points]	<0.0001	<0.0001	1.15	1.09–1.21	higher – poor prognosis
Age [years]	0.0003	0.0046	1.05	1.01–1.08	older – poor prognosis
Arterial hypertension [1/0]	0.0042	0.4416	1.33	0.64–2.74	YES – better prognosis
Chronic kidney disease [1/0]	0.0325	0.5088	0.73	0.29–1.83	YES – poor prognosis
Heart failure [1/0]	0.0025	0.4992	0.79	0.39–1.58	YES – poor prognosis
Hyperlipidemia [1/0]	0.0313	0.3342	1.51	0.65–3.52	YES – poor prognosis
Type of stroke [1/0]*	<0.0001	0.0666	0.45	0.19–1.08	higher – poor prognosis
Hyponatremia [1/0]	0.0034	0.8637	0.94	0.48–1.85	YES – poor prognosis
NIHSS at dismissal [points]	0.9985	NS	NS	NS	NS
Sex [male/female]	0.0593	NS	NS	NS	NS
Obesity [1/0]	0.5665	NS	NS	NS	NS
Hypothyroidism [1/0]	0.0897	NS	NS	NS	NS
Atrial fibrillation [1/0]	0.3417	NS	NS	NS	NS
Diabetes mellitus type 2 [1/0]	0.3461	NS	NS	NS	NS

NS – nonsignificant variables; NIHSS – National Institutes of Health Stroke Scale; * type of stroke as defined in Table 3.

**Fig. 1.** Effect of natremia on mortality in patients with IS and HS

(χ^2 with Yates's correction = 4.01; degrees of freedom (df) = 1; $p = 0.04$). Sodium levels were significantly lower in those IS patients who died (134.8 ± 4.99 ; median = 135) than in those who remained alive (136.6 ± 3.01 ; median = 137; $p = 0.02$; Mann-Whitney U test with correction for continuity) (Fig. 1).

Sodium levels were lower in patients with HS who died (135.3 ± 5.18 ; median = 135) than in those who remained alive (136.3 ± 3.15 ; median = 137) but

**Fig. 2.** Relationship between the value of natremia and the survival of IS and HS patients

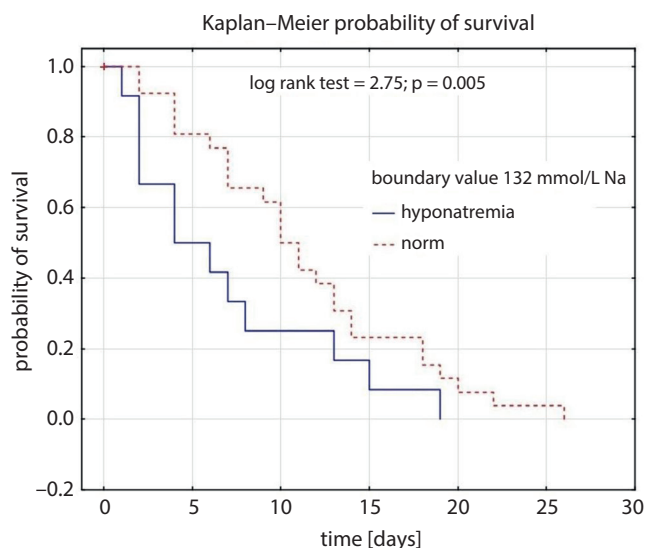


Fig. 3. Survival curve of patients with IS related to the value of natremia

the differences were nonsignificant. Fourteen (30.4%) patients with HS and normo-natremia died during hospitalization. In the group with HS and hyponatremia (n = 16), 7 (43.7%) patients died, whereas 9 (56.3%) were discharged home. However, the relationship was statistically nonsignificant.

Among patients who died in the course of an IS, we showed a statistically significant negative correlation between the length of hospitalization and natremia (p = 0.01). No such correlation was found for HS and hyponatremia (Fig. 2).

On the basis of the single and multifactorial analysis, it was found that in patients with HS there is no statistically significant correlation between their mortality and the co-existence of any of the following: type 2 diabetes, atrial fibrillation, hypertension, heart failure, chronic kidney

disease, hypothyroidism, obesity, hyperlipidemia, or hyponatremia. In addition, in patients with HS, mortality is not affected by their age or gender. However, patients with HS did have a worse prognosis if they had a higher NIHSS score than other stroke patients when admitted to the hospital (p = 0.004, 95% confidence interval (95% CI) = 1.07–1.28). No significant relationship was found between the Rankin scale assessed on discharge from hospital and natremia for all HS population (χ^2 NW = 3.66; df = 5; p = 0.59) and all IS population (χ^2 NW = 4.16; df = 5; p = 0.52).

The ROC curve for Na concentration in the IS group was calculated as area under curve (AUC) = 0.616 (95% CI = 0.508–0.724) Z = 2.107; p < 0.03. Next, the cut-off point that best discriminated the group in terms of death was determined (132 mmol/L). This new parameter was used to recalculate survival curves. At a value of Na concentration \leq 132 mmol/L, there is a statistically significant difference between the survival probability curves for patients with IS who died within 30 days of hospitalization (log-rank = 2.75; p = 0.005) (Fig. 3).

As a result of the multivariate analysis, we found that there was a significant relationship between hyponatremia observed on the first day of IS and the clinical status of the patients when evaluated using the NIHSS scale (Fig. 4), assessment of the size and location of the stroke assessed using the Paciaroni et al. scale¹⁴ (p = 0.002) and the observed co-occurrence of atrial fibrillation (p = 0.04). These dependencies were not found in HS.

Discussion

Our observation indicates that stroke frequently coexists with hyponatremia, i.e., in over 18% and 25% of cases of IS and HS, respectively. In the study by Gray et al., hyponatremia was observed in 24% of patients with IS during the entire hospitalization period,² whereas in the study by Kuramatsu et al., the percentage of patients with IS and concurrent hyponatremia was 15.3%.³ In our study, the rate of patients with IS and hyponatremia diagnosed on hospital admission was 18.4%, which is a slightly higher value than presented in the works mentioned above. One reason for this observation may be the fact that the patient population in our study was considerably older (76 \pm 13.9 years) compared to the populations studied by Gray et al. and Kuramatsu et al. (69.8 \pm 13.6 years and 59.4 \pm 12.1 years, respectively).^{2,3} An increase in the severity of hyponatremia

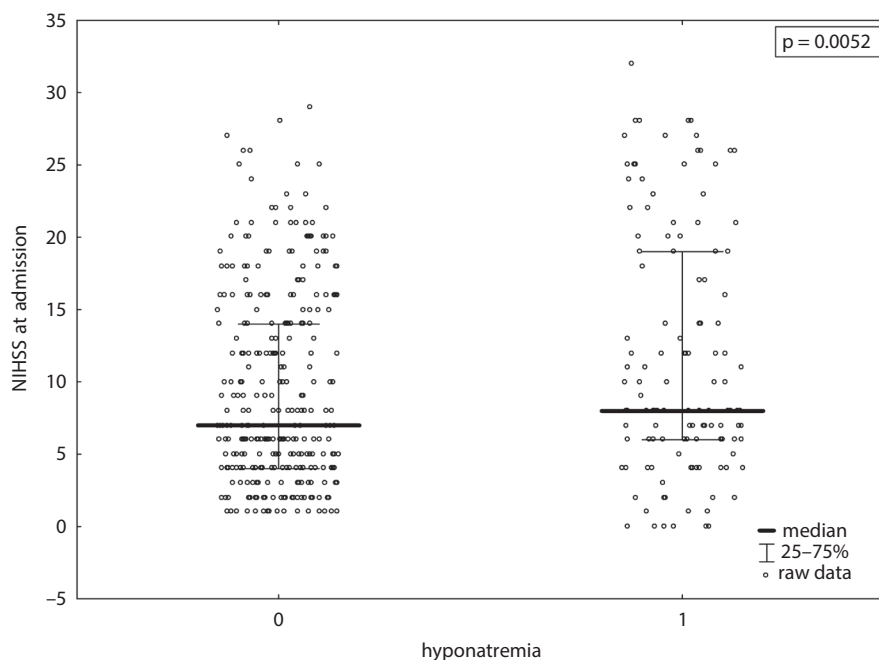


Fig. 4. Correlation of hyponatremia and IS in patients' NIHSS clinical scores on admission

along with patient's age is observed in clinical practice and may be associated with higher comorbidity and polypragmasia.¹⁴ Moreover, in the population studied, the mean hospitalization time of patients with IS was longer by approx. 10 days. Therefore, it may be concluded that the health status and prognosis in the population of IS patients were worse.

In our study, when we assessed patients with IS who were in a worse clinical condition than other patients using the NIHSS scale at admission, hyponatremia was more often observed. These observations are consistent with the results of Rodrigues et al.¹⁵ The presence of a positive correlation between the patient's NIHSS assessment which is based solely on physical examination, with a natremia laboratory test result, provides useful information for the clinician wishing to make a prognosis. At the same time, we proved that the location and size of the stroke site, as shown using the Paciaroni et al. scale, also has a significant influence on the emergence of hyponatremia in patients with IS. In our study, in the group of patients with IS the mortality rate in individuals with hyponatremia was 1.8 times higher than in those with normo-natremia. This correlation is statistically significant. We also observed a trend to increase the 30-days mortality in patients with HS and hyponatremia, but it was statistically non-significant. These trends are consistent with the research by Kuramatsu et al.³

In patients with IS, we found they had a higher risk of death in the following situations: if their clinical status on the NIHSS scale was worse than other patients; if they were older than others; if they had chronic kidney disease, heart failure or hyperlipidemia; or if they received a higher score on the Paciaroni et al. scale.¹³ The unfavorable influence of these clinical factors and abnormalities in laboratory tests on the prognosis of patients with IS is widely known.^{11,16} Some other studies also indicate that the concurrence of hyponatremia and IS at the onset of the disease extend the time of hospitalization.² However, in our population of those IS patients with hyponatremia who died, no correlation with the length of hospital stay was observed, which may be due to the relatively small size of the group studied. In this study, in the IS population, a significant, over 2-fold, increase in mortality was observed in the group of patients with hyponatremia found at hospital admission compared to the patients with normo-natremia. Our study has confirmed that the mortality of patients with IS and hyponatremia is significantly higher than in patients with normal natremia ($p = 0.02$). Similar observations were made by other authors.^{4,10,11,15} Moreover, we noticed that the severity of hyponatremia found at hospital admission determined the length of survival in patients with IS.

Additionally, we observed that Na concentration ≤ 132 mmol/L diagnosed on the first day of IS is a risk factor for mortality within 30 days of stroke onset. This finding is the first in the literature available, and it appears

to be important for clinicians. Therefore, if a patient with natremia of 132 mmol/L or lower is admitted to the neurology department due to IS, particularly careful monitoring should be applied due to the increased risk of early stroke-related mortality. Moreover, in a study conducted by Soiza et al. in patients hospitalized due to IS or HS, hyponatremia in acute stroke admissions is independently associated with higher mortality in patients below 75 years of age.¹⁰ Our study confirms this unexpected finding regarding increased mortality in the group of younger patients. It has been established that high blood pressure, high cholesterol, smoking, obesity, and diabetes are the leading causes of stroke. In the 21st century, these disorders significantly affect the condition of blood vessels, leading consequently to mortality due to cardiovascular problems.⁶ Increased mortality due to IS in the younger population requires a detailed analysis of the causes of the observed epidemiology in future studies. Special attention should be paid to comorbidities, as they can significantly worsen the prognosis in this group of patients. In our study, the coexistence of heart failure and IS has proved to be a significant and independent risk factor in the emergence of hyponatremia. However, in a study by Huang et al., among the risk factors for stroke, diabetes and renal failure were found to be significantly higher among patients with hyponatremia.¹¹

Nevertheless, our study has several shortcomings. First, its retrospective single-center design did not allow us to answer the question why hyponatremia showed increased in-hospital mortality. Second, this is a preliminary study and it evaluates only the relationship between hyponatremia and the clinical condition of patients. Few prospective studies regarding the effect of hyponatremia on prognosis in stroke are available. One of them was conducted by Saleem et al., but its results are difficult to assess since hyponatremia was defined as serum Na concentration below 130 mmol/L, and the time of the assessment of natremia relative to the onset of the disease was not provided.¹³ A prospective, well-designed and preferably multicenter study should be performed on the relationship between hyponatremia and its comorbidities, as well as laboratory parameters. This would allow identification of the causes of pathophysiological changes leading to hyponatremia and prognosis in patients after stroke.

Conclusions


Hyponatremia is more frequently observed in patients with HS than IS. Mild hyponatremia is already an independent prognostic factor in the mortality of people with IS and Na concentrations in blood serum may be a predictor of mortality in IS. In addition, and importantly for the clinician, hyponatremia correlates with the clinical condition of the patient and with the size and location of the stroke in patients with IS. Hence, in a patient with

a suspected stroke, there is a need to control electrolyte levels at the onset of the stroke, especially in patients with comorbidities, irrespective of age.

ORCID iDs

Agnieszka Gala-Błądzińska  <https://orcid.org/0000-0001-6617-0852>

Rafał Kaczorowski  <https://orcid.org/0000-0002-8377-7960>

Marcin Braun  <https://orcid.org/0000-0003-3804-7042>

Krzysztof Gargas  <https://orcid.org/0000-0002-0863-2630>

Halina Bartosik-Psujek  <https://orcid.org/0000-0002-2860-6456>

References

- Kim DK, Joo KW. Hyponatremia in patients with neurologic disorders. *Electrolyte Blood Press.* 2009;7(2):51–57.
- Gray JR, Morbitzer KA, Liu-De Ryke X, Parker D, Zimmerman LH, Rhoney DH. Hyponatremia in patients with spontaneous intracerebral hemorrhage. *J Clin Med.* 2014;3(4):1322–1332.
- Kuramatsu JB, Bobinger T, Volbers B, et al. Hyponatremia is an independent predictor of in-hospital mortality in spontaneous intracerebral hemorrhage. *Stroke.* 2014;45(5):1285–1291.
- Lasek-Bal A, Holecki M, Kret B, Hawrot-Kawecka A, Duława J. Evaluation of influence of chronic kidney disease and sodium disturbances on clinical course of acute and sub-acute stage first-ever ischemic stroke. *Med Sci Monit.* 2014;20:1389–1394.
- The Global Status Report on Noncommunicable Diseases 2011. Editors: World Health Organization; 2011.
- Benjamin EJ, Blaha MJ, Chiuve SE et al. American Heart Association Statistics Committee and Stroke Statistics Subcommittee. Heart disease and stroke statistics 2017 update: A report from the American Heart Association. *Circulation.* 2017;135(10):e229–e445.
- Karlinski MA, Bembenek JP, Baranowska A, Kurkowska-Jastrzebska I, Czlonkowska A. Noninfectious complications of acute stroke and their impact on hospital mortality in patients admitted to a stroke unit in Warsaw from 1995 to 2015. *Neurol Neurochir Pol.* 2018;52(2):168–173.
- Cuesta M, Hannon MJ, Thompson CJ. Diagnosis and treatment of hyponatremia in neurosurgical patients. *Endocrinol Nutr.* 2016;63(5):230–238.
- Podestà MA, Faravelli I, Cucchiari D, et al. Neurological counterparts of hyponatremia: Pathological mechanisms and clinical manifestations. *Curr Neurol Neurosci Rep.* 2015;15(4):18.
- Soiza RL, Cumming K, Clark AB, et al. Hyponatremia predicts mortality after stroke. *Int J Stroke.* 2015;10(Suppl A):100:50–55.
- Saleem S, Yousuf I, Gul A, Gupta S, Verma S. Hyponatremia in stroke. *Ann Indian Acad Neurol.* 2014;17(1):55–57.
- Brott T, Adams HP Jr, Olinger CP, et al. Measurements of acute cerebral infarction: A clinical examination scale. *Stroke.* 1989;20(7):864–870.
- Paciaroni M, Angeli G, Corea F, et al. Early hemorrhagic transformation of brain infarction: Rate, predictive factors, and influence on clinical outcome. *Stroke.* 2008;39(8):2249–2256.
- Rodrigues B, Staff I, Fortunato G, McCullough LD. Hyponatremia in the prognosis of acute ischemic stroke. *J Stroke Cerebrovasc Dis.* 2014;23(5):850–854.
- Huang WY, Weng WC, Peng TI, et al. Association of hyponatremia in acute stroke stage with three-year mortality in patients with first-ever ischemic stroke. *Cerebrovasc Dis.* 2012;34:55–62.
- Félix-Redondo FJ, Consuegra-Sánchez L, Ramírez-Moreno JM, Lozano L, Escudero V, Fernández-Bergés D. Ischemic stroke mortality tendency (2000–2009) and prognostic factors. ICTUS Study-Extremadura (Spain). *Rev Clin Esp (Barc).* 2013;213(4):177–185.

Urinary bladder hypertrophy and overactive bladder determine urinary continence after radical prostatectomy

Kajetan Juszcak^{1,2,A–F}, Adam Ostrowski^{2,C,F}, Jan Adamowicz^{2,C,F}, Piotr Maciukiewicz^{1,E,F}, Tomasz Drewa^{2,3,A,E,F}

¹ Department of Urology, Ludwik Rydygier Memorial Specialized Hospital, Kraków, Poland

² Department of General and Oncologic Urology, Nicolaus Copernicus University, Bydgoszcz, Poland

³ Department of General and Oncologic Urology, Nicolaus Copernicus Hospital, Toruń, Poland

A – research concept and design; B – collection and/or assembly of data; C – data analysis and interpretation;

D – writing the article; E – critical revision of the article; F – final approval of the article

Advances in Clinical and Experimental Medicine, ISSN 1899–5276 (print), ISSN 2451–2680 (online)

Adv Clin Exp Med. 2019;28(10):1329–1337

Address for correspondence

Kajetan Juszcak

E-mail: kaj.juszcak@gmail.com

Funding sources

None declared

Conflict of interest

None declared

Received on October 30, 2018

Reviewed on November 19, 2018

Accepted on February 18, 2019

Published online on March 14, 2019

Abstract

Background. Several clinical and biological factors exacerbate urinary incontinence (UI) and reduce the patient's quality of life after radical prostatectomy (RP).

Objectives. The purpose of this study was to evaluate the effects of urinary bladder hypertrophy and overactive bladder (OAB) on UI in patients after RP.

Material and methods. Seventy patients were enrolled in the study and were divided into 2 groups: patients with bladder outlet obstruction (BOO) but without OAB (group I; n = 20) and patients with BOO and OAB (group II; n = 50). Before the RP procedure, all patients were administered IPSS and OAB symptom questionnaires and ultrasonography and uroflowmetry were performed. The follow-up visits were scheduled for 1, 3, 6, 9, and 12 months after the operation to evaluate postoperative continence.

Results. The results show that patients with BOO and concurrent OAB experienced urinary bladder hypertrophy. Patients with OAB presented a normal desire to void with less urinary bladder capacity. The coexistence of OAB before RP resulted in more extensive UI, as measured with the ICIQ-UI-SF scores and postoperative daily pad usage. A gradual improvement in urinary continence was observed. Urinary incontinence was significantly less severe in successive check-ups (3, 6, 9, and 12 months after RP). Urgency was responsible for 1–15% or 16–29% of episodes of urinary leakage in 20% and 16% of cases, respectively.

Conclusions. Patients with preoperative OAB are at a higher risk of developing more severe UI after RP, and the restoration of pre-surgery urinary continence is limited.

Key words: radical prostatectomy, urinary incontinence, bladder wall thickness, urinary bladder hypertrophy, overactive bladder

Cite as

Juszcak K, Ostrowski A, Adamowicz J, Maciukiewicz P, Drewa T. Urinary bladder hypertrophy and overactive bladder determine urinary continence after radical prostatectomy. *Adv Clin Exp Med.* 2019;28(10):1329–1337. doi:10.17219/acem/104532

DOI

10.17219/acem/104532

Copyright

© 2019 by Wrocław Medical University

This is an article distributed under the terms of the Creative Commons Attribution Non-Commercial License (<http://creativecommons.org/licenses/by-nc-nd/4.0/>)

Introduction

Prostate cancer is one of the most common neoplasms among elderly males in Europe.¹ High-risk prostate cancer accounts for 26–39% of all cancers and most of the patients with organ-confined prostate cancer undergo radical prostatectomy (RP).² The most common postoperative complications are erectile dysfunction and urinary incontinence (UI). In general, patients who have undergone RP mainly report stress urinary incontinence.³ However, stress with coexisting urge UI (mixed type) is also observed in a smaller percentage of patients after RP. The etiopathogenesis of UI after RP is multifactorial.⁴ Our observations indicate that a certain group of patients who undergo open retropubic radical prostatectomy is characterized by more intense UI, because of overactive bladder (OAB) and other reasons. Overactive bladder develops due to secondary changes within the urinary bladder wall caused by long-term obstruction of urine flow at the enlarged prostate. Prostate cancer always coexists with benign prostatic hyperplasia, which is responsible for benign prostatic enlargement (BPE). Benign prostatic enlargement leads to urinary bladder outlet obstruction, which causes structural changes to the bladder (e.g., hypertrophy). Urinary bladder hypertrophy may lead to detrusor muscle overactivity, according to the myogenic theory of this disease's development. Overactive bladder can increase stress UI and significantly reduce patients' quality of life after RP. Ultrasonographic measurement of bladder wall thickness is useful in OAB diagnosis. Increased thickness of the urinary bladder remains a valuable positive predictor of detrusor overactivity development in patients diagnosed with OAB.⁵ Several predictive factors for UI after RP have been defined: the patient's age, body mass index (BMI), lower urinary tract symptom score, prostate volume, and comorbidity index. Moreover, detrusor overactivity correlates with continence status following RP.^{4,6} Based on clinical observations and a number of factors affecting urinary continence after surgery, the issue of post-prostatectomy UI is demanding. In general, the severity of UI after RP is unpredictable; it also varies in each patient depending on other factors affecting the patient's continence (especially bladder hypertrophy).⁷ Therefore, the purpose of the study was to evaluate the effect of urinary bladder structural changes due to bladder outlet obstruction (BOO) and OAB on UI in patients with prostate cancer undergoing open retropubic RP.

Methods

Patients

The study included 90 patients with prostate cancer who qualified for open retropubic RP, and was conducted from 2016 to 2018. All patients presented with organ-confined

prostate cancer (cT1c-T2c) confirmed by magnetic resonance imaging. Seventy patients were enrolled for further analysis. The remaining 20 patients were excluded from the study for incomplete follow-up due to the need for adjuvant therapy (radiotherapy) or for failure to report for follow-up visits after surgery.

Study protocol

All 70 patients with prostate cancer selected for further analysis presented with BOO, based on the average urine flow rates (Q_{avg}) obtained from uroflowmetry. The cut-off value of Q_{avg} was set at <10 mL/s. All patients were divided into two groups: patients with BOO but without OAB (group I) and patients with BOO and concurrent OAB (group II). The two groups were necessary due to the diversity of lower urinary tract symptoms (LUTS) observed in the patients due to OAB. All patients presented voiding LUTS due to BOO, and the majority of patients also presented storage LUTS due to OAB. At the initial assessment, all patients with prostate cancer who qualified for open retropubic RP were given the International Prostate Symptom Score (IPSS) questionnaire. The IPSS questionnaire assesses LUTS and consists of 7 questions about symptoms related to benign prostatic hyperplasia and its enlargement, as well as 1 question about quality of life of the patients. The scoring range is from 0 to 35 points. The scores 0, 1–7, 8–19, and 20–35 points are defined as asymptomatic patient, mild LUTS, moderate LUTS, and severe LUTS, respectively. Overactive bladder symptoms were estimated using 2 different OAB symptom scores (OABSS), designed by Blaivas et al. and Homma et al.^{8–10} Blaivas's OABSS scale is focused on LUTS due to OAB, as well as urinary bladder self-control. It consists of 7 questions and the scoring range is from 0 to 28 points. The higher the overall score, the greater the severity of OAB symptoms. Homma's OABSS scale is a questionnaire consisting of 4 questions about the number of LUTS due to OAB. The total score is the sum of all 4 scores related to each OAB symptom and the scoring range is from 0 to 15 points. The highest score indicates extremely severe OAB symptoms.¹¹ An OABSS total score of >3 points on the Homma questionnaire and/or >4 points on the Blaivas questionnaire were set as the inclusion criterion for group II (patients with OAB).

Additionally, we performed an ultrasonographic evaluation of the urinary bladder and prostate and a uroflowmetry test for each patient (see below). The follow-ups were scheduled for 1, 3, 6, 9, and 12 months after open retropubic RP in order to evaluate the functional outcomes and the severity of UI. At the follow-ups, postoperative continence was assessed and each patient was asked to complete an ICIQ-UI-SF questionnaire (International Consultation on Incontinence Questionnaire Urinary Incontinence – Short Form). The validated ICIQ-UI-SF questionnaire evaluates 3 issues of urine leakage: “frequency,” “quantity,” and “impact on everyday life.” The total score is the sum

of points connected with these 3 issues and it ranges from 0 to 21 points. The ICIQ-UI-SF questionnaire contains 8 additional questions concerned with the occurrence of urine leakage which are not included in the total ICIQ-UI-SF questionnaire score.¹² Stress UI was also estimated, based on measurements of pad usage per day. A daily pad usage of 0 pads and/or an ICIQ-UI-SF score of 0 points indicated that the patient was continent; all patients with a daily pad usage of 1 were defined as socially continent. These criteria for determining continence status were based on the study by Grabbert et al.¹³ In addition, we created a new scale (the VAS-UI: Visual Analogue Scale – Urinary Incontinence) to assess the contribution of urgency to UI after open retropubic RP. The VAS-UI consists of a straight line whose endpoints represent “0% urge UI and 100% stress UI” and “100% urge UI.” The patients were asked after surgery to indicate between the 2 endpoints the proportion of their incontinence that is urge UI. The study was approved by the Local Ethical Committee.

Ultrasonographic evaluation

At the initial consultation (before RP), each patient underwent a transabdominal ultrasonographic evaluation (USG) of the structure of the prostate and urinary bladder. Three-dimensional ultrasonography was used to assess the prostate volume [mL]. In each patient, the USG was performed when urinary bladder filling was related to a normal desire to void. This was done in order to reproduce the physiological (functional) filling of the urinary bladder and the bladder and detrusor wall thickness (BWT and DWT) for each patient. Functional urinary bladder wall thickness (fBWT) (in mm) and functional detrusor muscle thickness (fDWT) (in mm) were measured along the sagittal plane in the anterior bladder wall. The means of 3 measurements of fBWT and fDWT were calculated. Moreover, we recorded the surface area (SA) (in cm²), which covers the bladder capacity and illustrates the degree to which the bladder is filled. In addition, we defined a new parameter called the adjusted-BWT index (aBWTi). The aBWT index is calculated from the functional urinary bladder wall thickness (fBWT), the surface area (SA), and the prostate volume (V_{prostate}) using the following formula: $\text{aBWTi} = \text{fBWT} \times \text{SA} \times 0.1/V_{\text{prostate}}$. It is known that the BWT depends on the degree to which the urinary bladder is full. In addition, the prostate volume determines the extent of the bladder outlet obstruction. A bladder outlet obstruction which is increased due to an enlarged prostate affects the urinary bladder structure and the thickening of the urinary bladder wall. Therefore, in our cohort we measured the functional bladder wall thickness (fBWT), which is affected by the degree of bladder filling. The main goal in defining this new parameter was an attempt to homogenize the study group, but we also tried to define a simple parameter to determine the severity of UI after open retropubic RP for urologists conducting

preoperative evaluations of patients with prostate cancer who qualified for radical treatment. The aBWT index, thanks to its simplicity and straightforward calculation (based only on USG measurements of the urinary bladder and prostate), can become a useful tool in the preoperative assessment of RP and in determining the predictive factor of UI after RP.

Uroflowmetry

Uroflowmetry was performed in each patient at the initial assessment (before RP). Uroflowmetry was initiated when the patient reported a normal desire to void. We recorded the following parameters: 1) the maximum urine flow rate (Q_{max}) (in mL/s), 2) the average urine flow rate (Q_{avg}) (in mL/s), and 3) the urine flow time (FT) (in seconds). After the patient voided, we measured the post-void residual urine (PVR) (in mL) using three-dimensional transabdominal ultrasonography. In addition, we introduced a new parameter to evaluate the area under the uroflowmetric curve: the UFM_{AUC} . The UFM_{AUC} is the absolute value obtained by multiplying the average urine flow (Q_{avg}) by the urine flow time (FT). The UFM_{AUC} seems to more accurately describe the function of the lower urinary tract than single parameters, such as Q_{max} and Q_{avg} , which depend on how full the bladder is. Considering the fact that uroflowmetry is dependent on bladder fullness, the creation of the UFM_{AUC} provides for a more unified study group and links urine flow rate to bladder fullness and the efficacy of bladder voiding (functional activity), which is indirectly expressed by the FT during uroflowmetry. The main goal in defining the UFM_{AUC} was to unify the study group despite the different bladder volumes producing a normal desire to void.

Exclusion criteria

The exclusion criteria were as follows: 1) neoadjuvant (any time before) or adjuvant radiotherapy or brachytherapy (within the 12-month follow-up period); 2) macroscopic infiltration of the urinary bladder (pT4); 3) neurological deficiencies (e.g., stroke, spinal cord injury, multiple sclerosis, Parkinson's disease, etc.) which would cause an inability to control the urinary bladder; 4) urethral strictures; 5) previous surgery – such as transurethral resection of the prostate (TURP) or adenectomy – performed up to 12 months prior to the RP; and 6) any form of constant catheterization (indwelling catheter or clean intermittent catheterization).

Statistical analysis

All of the results are presented as medians (along with 25th–75th percentiles). The normality of the data was determined by the Kolmogorov–Smirnov test. As the data did not fulfil the criteria of normality, a nonparametric

Friedman test was performed – followed, where necessary, by a Wilcoxon test with Bonferroni correction – to compare the differences between dependent groups (repeated measurements). The Mann–Whitney test was used to compare the differences between independent groups (group I vs. group II). Intragroup measurements of all analyzed preoperative and postoperative parameters were tested using Spearman's correlation due to the “non-normal” distribution of the data. The data was considered statistically significant when $p < 0.05$. The statistical analyses were conducted using SPSS v. 24.0 software (IMB Corp., Armonk, USA).

Results

Preoperative assessment

The mean age of the patients in groups I and II were 66.5 and 68.0 years, respectively. The preoperative lower urinary tract symptom evaluations, USG characteristics, and uroflowmetric parameters are summarized in Table 1. All patients included in the study presented BOO and moderate or severe lower urinary tract symptoms (LUTS), based on their IPSS score and uroflowmetry. In comparison with group I (BOO without OAB), more patients in group II reported LUTS due to OAB on the Blaivas and Homma OABSS questionnaires (1 vs 12, $p < 0.05$; and 1 vs 6, $p < 0.05$, respectively). Patients with BOO and concurrent

OAB experienced more urinary bladder hypertrophy than patients with only BOO. Urinary bladder hypertrophy was identified during USG as an increased functional bladder wall thickness (fBWT) and functional detrusor wall thickness (fDWT) (2.7 vs 2.3 mm, $p < 0.05$; and 1.3 vs. 1.0 mm, $p < 0.05$, respectively). Moreover, patients with OAB experienced a normal desire to void when their bladders were less full, which was reflected in the reduced surface area under ultrasound (37.0 vs 53.0 cm², $p < 0.05$); consequently, the median values of voided urine volume were correspondingly smaller (194 vs 340 mL, $p < 0.05$). Compared to patients with BOO, the adjusted-BWT index in patients with BOO and OAB was lower, though not statistically significantly lower. The UFM_{AUC} was significantly higher in patients with BOO than in patients with coexisting OAB (346 vs 195, $p < 0.05$).

Postoperative assessment

The postoperative ICIQ-UI-SF scores were analyzed in all 70 patients during the 12 months of follow-up. Of the patients with BOO but not OAB (group I), 50% achieved complete urinary continence within 12 months of RP (ICIQ-UI-SF score = 0 points), whereas only 30% of patients with BOO and concurrent OAB (group II) did so. All of the patients with BOO and OAB suffered moderate to severe UI according to their ICIQ-UI-SF scores (6–10 and >11 points, respectively) in the 3 months after RP. Patients with BOO but not OAB mostly reported mild UI in the 3 months after surgery in 75% of the cases. Six months after the surgery, none of the patients reported UI (ICIQ-UI-SF score >11 points). The Friedman test revealed that the ICIQ-UI-SF questionnaire differed with time in both group I ($\chi^2(4) = 72.903$, $p = 0.000$) and group II ($\chi^2(4) = 197.204$, $p = 0.000$). Postoperative ICIQ-UI-SF questionnaire scores in the 12-month period are summarized in Table 2.

Table 1. Preoperative lower urinary tract symptom evaluation, ultrasonography characteristics, and uroflowmetry parameters in patients with prostate cancer who qualified for radical prostatectomy

Questionnaire evaluation			
Questionnaire	Group I	Group II	p-value
OABSS (Blaivas et al.)	1 (1–2)	12 (7–14)	$p < 0.05$
OABSS (Homma et al.)	1 (1–2)	6 (3–8)	$p < 0.05$
IPSS	12 (5–16)	13 (10–17)	ns
Ultrasonography			
Parameter	Group I	Group II	p-value
Prostate volume [mL]	40 (35–48)	40 (35–51)	ns
fBWT [mm]	2.3 (2.1–2.6)	2.7 (2.3–3.1)	$p < 0.05$
fDWT [mm]	1.0 (0.9–1.1)	1.3 (1.1–1.7)	$p < 0.05$
SA [cm ²]	53.0 (44.4–60.8)	37.2 (30.3–48.5)	$p < 0.05$
aBWT _I index [1]	0.26 (0.23–0.35)	0.24 (0.18–0.34)	ns
Uroflowmetry			
Parameter	Group I	Group II	p-value
Q _{max} [mL/s]	13 (10–16)	10 (7–11)	$p < 0.05$
Q _{avg} [mL/s]	8 (7–9)	6 (4–8)	$p < 0.05$
Flow time [s]	42 (33–49)	35 (29–44)	$p < 0.05$
V _{void} [mL]	340 (302–379)	194 (159–263)	$p < 0.05$
PVR [mL]	20 (0–40)	30 (0–55)	ns
UFM _{AUC} [1]	346 (262–381)	195 (150–261)	$p < 0.05$

Table 2. Postoperative ICIQ-UI-SF questionnaire scores

Follow-up	Group	Score							
		0 points		1–5 points		6–10 points		over 11 points	
		n	[%]	n	[%]	n	[%]	n	[%]
1 month	I	0	0	0	0	8	40	12	60
	II	0	0	0	0	1	2	49	98
3 months	I	0	0	15	75	4	20	1	5
	II	0	0	0	0	37	74	13	26
6 months	I	0	0	19	95	0	0	0	0
	II	0	0	26	52	24	48	0	0
9 months	I	4	20	16	80	0	0	0	0
	II	1	2	49	98	0	0	0	0
12 months	I	10	50	10	50	0	0	0	0
	II	15	30	35	70	0	0	0	0

In our cohort, we observed a gradual improvement in urinary continence (groups I and II). The reduction in the severity of UI was statistically significant in the successive follow-ups (3, 6, 9, and 12 months after RP) (Table 3).

In comparison with patients with BOO alone, the severity of postoperative UI was significantly higher in patients with BOO and OAB symptoms at the 9-month follow-up. After 12 months, we recorded no statistically significant difference in UI (Table 4).

We found statistically significant positive correlations between the Blaivas et al. OABSS score and the severity of UI, according to the ICIQ-UI-SF questionnaires (1, 3, 6, and 9 months after RP, $p < 0.01$ for each). Moreover, Homma OABSS scores positively correlated with the severity of UI, according to the ICIQ-UI-SF questionnaire 3 months after surgery ($p < 0.01$) (Fig. 1).

Table 3. Comparison of postoperative evaluations in successive follow-ups in groups I and II

Group	Follow-up				
	1 month	3 months	6 months	9 months	12 months
ICIQ-UI-SF questionnaire					
I	12 (9–13)	5 (3–6)*	3 (3–3)*,&	1 (1–3)*,&,#	0.5 (0–1)*,&,#,¶
II	14 (13–16)	9 (7–11)*	5 (4–6)*,&	3 (3–3)*,&,#	1 (0–3)*,&,#,¶
Daily pad usage					
I	2 (1–2)	2 (1–2)	1 (1–1)*,&	0 (0–1)*,&,#	0 (0–0)*,&,#
II	3 (3–4)	2 (2–3)*	1 (1–2)*,&	1 (0–1)*,&,#	0 (0–1)*,&,#,¶
Percentage attendance of urge urinary incontinence					
I	0 (0–20)	0 (0–20)	0 (0–0)	0 (0–0)	0 (0–0)
II	13 (0–26)	13 (0–26)	10 (0–20)*,&	0 (0–15)*,&,#	0 (0–15)*,&,#

* $p < 0.005$ vs 1 month; & $p < 0.005$ vs 3 months; # $p < 0.005$ vs 6 months; ¶ $p < 0.005$ vs 9 months.

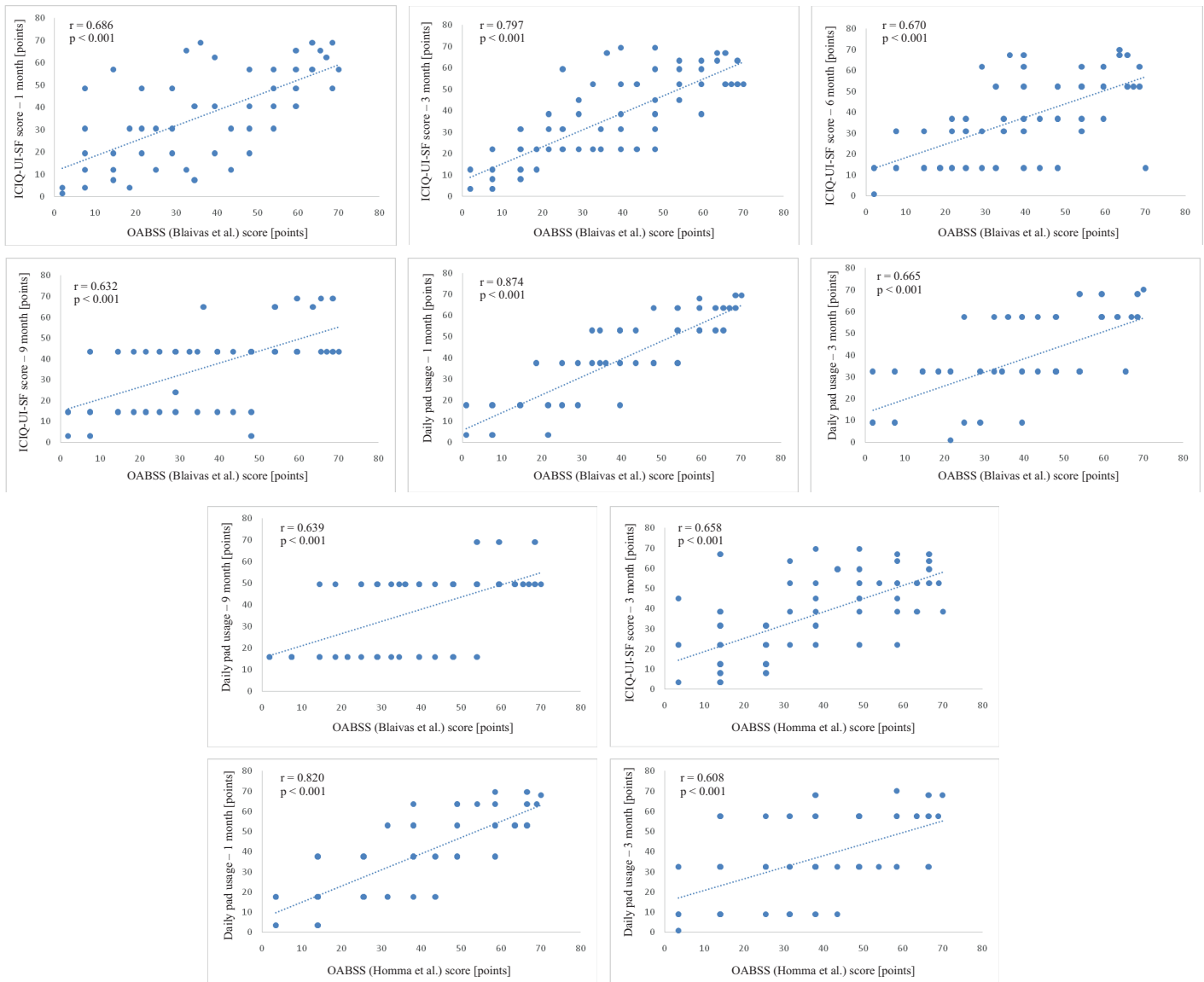


Fig. 1. Correlations between OABSS questionnaire scores and ICIQ-UI-SF questionnaire scores or daily pad usage after radical prostatectomy

Table 4. Comparison of postoperative evaluations of groups I and II

Postoperative evaluation	Follow-up	Group I	Group II	p-value
ICIQ-UI-SF questionnaire	1 month	12 (9–13)	14 (13–16)	p < 0.05
	3 months	5 (3–6)	9 (7–11)	p < 0.05
	6 months	3 (3–3)	5 (4–6)	p < 0.05
	9 months	1 (1–3)	3 (3–3)	p < 0.05
	12 months	0.5 (0–1)	1 (0–3)	ns
Pad usage	1 month	2 (1–2)	3 (3–4)	p < 0.05
	3 months	2 (1–2)	2 (2–3)	p < 0.05
	6 months	1 (1–1)	1 (1–2)	p < 0.05
	9 months	0 (0–1)	1 (0–1)	p < 0.05
	12 months	0 (0–0)	0 (0–1)	ns
Percentage attendance of urge urinary incontinence	1 month	0 (0–20)	13 (0–26)	ns
	3 months	0 (0–20)	13 (0–26)	ns
	6 months	0 (0–0)	10 (0–20)	p < 0.05
	9 months	0 (0–0)	0 (0–15)	p < 0.05
	12 months	0 (0–0)	0 (0–10)	p < 0.05

Table 5. Postoperative daily pad usage

Follow-up	Group	Number of pads per day					
		0 pad		1 pad		> 1 pad	
		n	[%]	n	[%]	n	[%]
1 month	I	0	0	5	25	15	75
	II	0	0	1	2	49	98
3 months	I	0	0	8	40	12	60
	II	1	2	7	14	42	84
6 months	I	3	15	17	85	0	0
	II	4	8	30	60	16	32
9 months	I	15	75	5	25	0	0
	II	16	32	31	62	3	6
12 months	I	17	85	3	15	0	0
	II	31	62	19	38	0	0

Regarding daily pad usage in our cohort, we observed that most of the patients with only BOO (group I) reported full urinary continence in terms of pad usage (85%). Concurrent OAB symptoms (group II) influenced the everyday use of pads. In this group of patients, full urinary continence (0 pads per day) and social continence (1 pad per day) were reported in 62% and 38% of cases, respectively. None of the patients from our cohort were using more than 1 pad per day by the 12-month follow-up examination. In the first 3 months post-op, most of the patients experienced UI requiring the use of at least 1 pad per day (60% for patients without OAB and 84% for patients with OAB). The Friedman test showed that daily pad usage differed with time in both group I ($\chi^2(4) = 71.150$, $p = 0.000$) and group II ($\chi^2(4) = 183.361$, $p = 0.000$). Postoperative daily pad usage over the 12-month period is summarized in Table 5.

According to these results, urinary continence improved with time after RP. We also observed a reduction in postoperative daily pad usage over time (Table 3). As compared to the patients with BOO alone, the patients with OAB symptoms and BOO required more pads per day in the first 9 months following RP. At the 12-month follow-up, we recorded no statistically significant differences in daily pad usage (Table 4).

A statistically significant positive correlation was found between the Blaivas OABSS score and daily pad usage (1, 3, and 9 months after RP, $p < 0.01$ for each). Also, the Homma OABSS score positively correlated with daily pad usage at the 1-month and 3-month follow-up examinations ($p < 0.01$) (Fig. 1).

In our cohort, at least 50% of patients reported stress UI (urine leakage not triggered by urgency). We observed that 36% of the patients with BOO and OAB still experienced mixed UI 12 months after RP; the mixed UI was mainly of the stress type. In 20% of the patients with BOO and OAB, urgency was the cause of urinary leakage in 1–15% of episodes of UI, while in 16% of patients it contributed to 16–29% of UI episodes. The Friedman test revealed that the proportion of urge UI differed with time only in group II ($\chi^2(4) = 32.680$, $p = 0.000$) — not in group I. The postoperative proportion of urge UI 12 months after RP is summarized in Table 6.

Discussion

Development of OAB after RP accounts for 15.2 to 37.8% of cases.¹⁴ Several underlying mechanisms in the pathogenesis of post-prostatectomy OAB have been proposed. The impact that surgery has on the anatomical relationships of the lower urinary tract and its innervation seems indisputable if we consider the context of UI. A number of preoperative factors also have a negative impact on a patient's continence after RP (e.g., the patient's age, preexisting LUTS, body weight, functional urinary bladder changes, etc.).⁴ Preoperative functional changes of the bladder (hypertrophy of the bladder wall) are caused by bladder outlet obstruction due to benign enlargement of the prostate. In our cohort, patients with OAB symptoms had hypertrophy of the bladder wall and detrusor muscle. It is worth mentioning that increased thickness of the bladder is a predictor of detrusor overactivity in patients with OAB.^{7,15}

The main goal of our study was to carry out a functional assessment and analysis of the physiological conditions for each patient during ultrasound of the urinary bladder. Patients with prostate cancer who qualify for RP belong to a very heterogeneous group due to the varying severity of bladder outlet obstruction and associated voiding issues and/or storage LUTS. In our cohort, the patients with OAB symptoms were characterized by less urinary bladder capacity, so this dependence could affect the absolute

Table 6. Postoperative percentage attendance of urge urinary incontinence in urinary incontinence after radical prostatectomy

Follow-up	Group	Percentage attendance of urge urinary incontinence							
		0%		1–15%		16–29%		above 30%	
		n	[%]	n	[%]	n	[%]	n	[%]
1 month	I	11	55	0	0	7	35	1	5
	II	23	46	3	6	13	26	11	22
3 months	I	11	55	2	10	6	30	1	5
	II	24	48	3	6	11	22	12	24
6 months	I	16	80	3	15	1	5	0	0
	II	24	48	9	18	12	24	5	10
9 months	I	20	100	0	0	0	0	0	0
	II	28	56	12	24	9	18	1	2
12 months	I	20	100	0	0	0	0	0	0
	II	32	64	10	20	8	16	0	0

value (non-physiological) of BWT and DWT. It seems reasonable to measure BWT and DWT at a constant bladder volume in further experiments. We observed no statistically significant differences of adjusted-BWT index in either group. The lack of differences in aBWTi could be explained by the fact that there is no simple correlation between increasing prostate volume and more severe LUTS as a result of bladder outlet obstruction. Smaller prostates often cause more severe bladder outlet obstruction. The creation of the UFM_{AUC} seems to be justified, as it contains two variables which are dependent on how full the urinary bladder is: flow time and average urine flow. In our cohort, patients with OAB symptoms had a lower value of UFM_{AUC}. Thus, this parameter may be useful in the preoperative evaluation of patients with prostate cancer who qualified for RP — along with other data (e.g., OABSS questionnaire scores, fBWT, fDWT, etc.) — for predicting the degree of UI after surgery.

Our results revealed that the coexistence of OAB in patients before RP results in more extensive UI after surgery, as measured by the ICIQ-UI-SF score. Sebesta et al. reported that approximately one-third of patients' urgency or urge UI was the primary cause of UI following RP.¹⁶ Most patients after RP regain continence comparable to their presurgical continence within the first 12 months post-op. However, during the subsequent 12 months, a modest improvement in continence has also been observed.^{4,17} In our cohort, patients with OAB were characterized by a slower improvement in urinary continence at the 12-month follow-up than patients with only bladder outlet obstruction. Only 30% of OAB patients were fully continent according to their ICIQ-UI-SF scores (0 points) after RP. Urodynamic evaluations of patients after RP revealed detrusor overactivity in about 3–63% of cases.³ In their study, Hosier et al. showed that OAB and storage LUTS frequently occur in patients who have undergone RP;¹⁸ Song et al. reported that more than half of their patients developed detrusor overactivity within

3 years of RP.¹⁹ Similarly, in our cohort, 36% of the patients still experienced urge UI 12 months after surgery. The severity of this type of incontinence ranged from 1–15% (20% of patients) to 16–19% (16% of patients).

Moreover, we observed increased daily pad usage following RP in patients with OAB. In our cohort, patients with no OAB symptoms reported full or social continence in the 12-month postoperative period in 85% and 15% of cases, respectively, while patients with concurrent OAB achieved full continence in 62% of cases and social continence in 38% of cases. In their long-term functional analysis of patients after RP, Grabbert et al. found full and social continence in terms of pad usage in 36% and 27% of patients after 3 months, in 53% and 24% after 12 months, in 56% and 22% after 24 months, and in 63% and 17% of cases after 36 months.¹³ Sebesta et al. reported that 31.7% of their RP cohort were fully continent.¹⁶ Urine leakage at least once a day occurred in 16.8% and 9.2% of patients, respectively.

Regarding the occurrence of urgency in the post-prostatectomy period, all patients without OAB prior to surgery reported UI due to urgency. Conversely, patients with LUTS caused by OAB before RP still reported urge UI in 36% of cases after 12 months. The urgency was responsible for 1–15% or 16–29% of episodes of urinary leakage in 20% and 16% of cases, respectively. In most cases, it is difficult to indicate whether urine leakage is caused by urgency. Urgency may exacerbate the existing stress UI. In contrast, episodes of urgency may result from the activation of the reflex arc connecting the proximal urethra to the detrusor muscle. Stress UI is always present to varying degrees in patients after RP. It should also be mentioned that stress UI may intensify urge UI. Based on an animal model, it can be postulated that this phenomenon is likely associated with the stimulation of the afferent nerves of the proximal part of the urethra by urine (due to sphincter insufficiency after RP), leading to detrusor muscle contraction (inducing or exacerbating

existing detrusor overactivity).²⁰ The Visual Analogue Scale – Urinary Incontinence (VAS-UI) that we use seems to be very helpful in patients with prostate cancer who qualify for RP. In the case of a patient with coexisting OAB, a heavier course of UI should be expected. The VAS-UI scale is a simple diagnostic tool that provides a quick and easy indication of whether a given patient actually has urgency after surgery. This information seems crucial for more precisely managing patients who present with OAB symptoms following RP as well as for administering drugs which affect urinary bladder function (e.g., anticholinergic drugs, β 3-adrenergic agonists, etc.), and thus for reducing the severity of OAB and post-prostatectomy UI.

In our analysis, we found a statistically significant positive correlation between Blaivas OABSS score and post-operative UI according to ICIQ-UI-SF score (9 months after surgery) and daily pad usage (1, 3, and 9 months after surgery). The Homma OABSS score was characterized by fewer statistically significant positive correlations with UI as assessed in the postoperative course. The scores from this questionnaire correlated with daily pad usage during the first 3 months after surgery, as well as with the ICIQ-UI-SF score 3 months after RP. Our data indicates that the OABSS questionnaire designed by Blaivas et al. is a precise diagnostic tool for OAB as it assesses the degree of overlap of OAB symptoms and it can indicate the probability of an unfavorable course of recovery after RP (more severe and longer lasting UI), especially during the first 9 months after a procedure.

Considering the above-mentioned data, urinary bladder wall hypertrophy and functional disorder of the urinary bladder (e.g., OAB) are important factors affecting urinary continence after RP. Overactive bladder may develop because of long-term bladder outlet obstruction and benign prostatic enlargement, which coexist in most patients diagnosed with prostate cancer. Furthermore, RP may intensify preoperative OAB. In many cases, RP affects the innervation of lower urinary tracts and leads to functional changes in the bladder, such as detrusor overactivity and/or decreased bladder compliance. Patients with preoperative OAB are at higher risk of developing more severe UI after RP, the return to urinary continence will be slower, and the continence regained after 12 months will be slightly worse than for patients without OAB. The improvement in postoperative urinary continence should be multidirectional, especially during the first 2 years after RP. Pelvic floor muscle physiotherapy can reduce the degree of stress UI, which is also responsible for urinary bladder dysfunction (especially OAB). On the other hand, patients with OAB should receive targeted therapy to reduce the severity of OAB. This treatment should include pharmacotherapy, e.g., antimuscarinic drugs and/or β 3-adrenergic agonists (first-line treatment). In cases where the patient does not respond to pharmacotherapy, intravesical botulinum toxin type A injections should be considered as a second-line treatment after RP. Perhaps

in the future, patients with severe OAB who are at a higher risk of unfavorable post-prostatectomy UI outcomes will undergo intravesical botulinum toxin type A injections at the same time as their RP. However, further research is necessary in this area.

Conclusions

In summary, our study showed that patients with bladder outlet obstruction and concurrent OAB are characterized by urinary bladder hypertrophy. The coexistence of OAB in patients before RP results in more severe UI after the surgery, as measured by ICIQ-UI-SF score and daily pad usage; the restoration of pre-surgery urinary continence is also limited. The OABSS questionnaire designed by Blaivas et al. is a precise diagnostic tool for OAB and should be widely implemented in urological practice in the preoperative assessment of patients with prostate cancer who qualify for RP.

References

1. Arnold M, Karim-Kos HE, Coebergh JW, et al. Recent trends in incidence of five common cancers in 26 European countries since 1988: Analysis of the European Cancer Observatory. *Eur J Cancer*. 2015;51:1164–1187.
2. Kliment J, Elias B, Baluchova K, Kliment J. The long-term outcomes of radical prostatectomy for very high-risk prostate cancer pT3b-T4 NO-1 on definitive histopathology. *Cent Eur J Urol*. 2017;70(1):13–19.
3. Pastore AL, Palleschi G, Illiano E, Zucchi A, Carbone A, Costantini E. The role of detrusor overactivity in urinary incontinence after radical prostatectomy: a systemic review. *Minerva Urol Nefrol*. 2017;69(3):234–241.
4. Heesakkers J, Farag F, Bauer RM, Sandhu J, De Ridder D, Stenzl A. Pathophysiology and contributing factors in postprostatectomy incontinence: A review. *Eur Urol*. 2017;71(6):936–944.
5. Kuo HC. Measurement of detrusor wall thickness in women with overactive bladder by transvaginal and transabdominal sonography. *Int Urogynecol J Pelvic Floor Dysfunct*. 2009;20:1293–1299.
6. Ficarra V, Novara G, Rosen RC, et al. Systematic review and meta-analysis of studies reporting urinary continence recovery after robotic-assisted radical prostatectomy. *Eur Urol*. 2012;62:405–417.
7. Juszczak K, Ostrowski A, Bryczkowski M, Adamczyk P, Drewa T. A hypothesis for the mechanism of urine incontinence in patients after radical prostatectomy due to urinary bladder hypertrophy. *Adv Clin Exp Med*. 2018 Aug 29. doi:10.17219/acem/79935.
8. Lin YT, Chou ECL. Assessment of overactive bladder (OAB) – symptom scores. *Incont Pelvic Floor Dysfunct*. 2009; 3(Suppl 1):9–14.
9. Blaivas JG, Panagopoulos G, Weiss JP, Somaroo C. Validation of the overactive bladder symptom score. *J Urol*. 2007;178:543–547.
10. Homma Y, Yoshida M, Seki N, et al. Symptom assessment tool for overactive bladder syndrome – overactive bladder symptom score. *Urology*. 2006;68(2):318–323.
11. Juszczak K, Adamczyk P, Maciukiewicz P, Drewa T. Clinical outcomes of intravesical injections of botulinum toxin type A in patients with refractory idiopathic overactive bladder. *Pharmacol Rep*. 2018;70(6):1133–1138.
12. Espuna-Pons M, Dilla T, Castro D, Carbonell C, Casariego J, Puig-Closta M. Analysis of the value of the ICIQ-UI SF questionnaire and stress test in the differential diagnosis of the type of urinary incontinence. *Neurourol Urodyn*. 2007;26(6):836–841.
13. Grabbert M, Buchner A, Butler-Ransohoff C, Kretschmer A, Stief CG, Bauer RM. Long-term functional outcome analysis in a large cohort of patients after radical prostatectomy. *Neurourol Urodyn*. 2018;37(7):2263–2270.

14. Peyronnet B, Brucker BM. Management of overactive bladder symptoms after radical prostatectomy. *Curr Urol Rep*. 2018;19(12):95.
15. Kuo HC. Measurement of detrusor wall thickness in women with overactive bladder by transvaginal and transabdominal sonography. *Int Urogynecol J Pelvic Floor Dysfunct*. 2009;20:1293–1299.
16. Sebesta M, Cespedes RD, Luhman E, Optenberg S, Thompsom IM. Questionnaire-based outcomes of urinary incontinence and satisfaction rates after radical prostatectomy in a national study population. *Urology*. 2002;60(6):1055–1058.
17. Lepor H, Kaci L, Xue X. Continence following radical retropubic prostatectomy using self-reporting instruments. *J Urol*. 2004;71:1212–1215.
18. Hosier GW, Tennankore KK, Himmelman JG, Gajewski J, Cox AR. Overactive bladder and storage lower urinary tract symptoms following radical prostatectomy. *Urology*. 2016;94:193–197.
19. Song C, Lee J, Hong JH, Choo MS, Kim CS, Ahn H. Urodynamic interpretation of changing bladder function and voiding pattern after radical prostatectomy: A long-term follow-up. *BJU Int*. 2010;106:681–686.
20. Jung SY, Fraser MO, Ozawa H, et al. Urethral afferent nerve activity affects the micturition reflex; implication for the relationship between stress incontinence and detrusor instability. *J Urol*. 1999;162(1):204–212.

Do lifestyle factors influence the rate of complications after amniocentesis?

Wojciech Homola^{A–D,F}, Mariusz Zimmer^{A,C,E,F}

2nd Department of Gynecology and Obstetrics, Wrocław Medical University, Poland

A – research concept and design; B – collection and/or assembly of data; C – data analysis and interpretation; D – writing the article; E – critical revision of the article; F – final approval of the article

Advances in Clinical and Experimental Medicine, ISSN 1899–5276 (print), ISSN 2451–2680 (online)

Adv Clin Exp Med. 2019;28(10):1339–1344

Address for correspondence

Wojciech Homola
E-mail: wojtek.homola@gmail.com

Funding sources

None declared

Conflict of interest

None declared

Received on August 24, 2018
Reviewed on October 1, 2018
Accepted on November 27, 2018

Published online on June 18, 2019

Abstract

Background. The impact of lifestyle factors including health-promoting physical activity on complication rate following amniocentesis is unclear.

Objectives. To examine the further course of pregnancy in patients undergoing amniocentesis in relation to selected risk factors including the level of health-promoting activity and occupational work on the complication rate after genetic amniocentesis.

Material and methods. Medical records from 317 diagnostic amniocenteses were analyzed and 230 procedures carried out on 219 pregnant women were included in the study.

Results. The mean maternal age was 34.50 ± 5 years (range: 22–47 years). In the patients studied, amniocentesis was performed at 12–24 gestational weeks with a median at 16 gestational weeks (mean: 16.13 ± 2.02 weeks). Overall, 174 amniocenteses (75.6%) did not reveal any genetic disorder while 56 (24.4%) confirmed a genetic disorder. One hundred procedures (43.5%) were followed by at least 1 complication, while 130 procedures (56.5%) were uneventful. The following complications were observed: general pain – 37 (16%), fever – 5 (2.2%), dizziness – 7 (3%), amniotic fluid leakage – 5 (2.2%), vaginal bleeding – 3 (1.3%), and fetal death – 11 (4.8%). The following lifestyle factors were reported: use of stimulants – 12 (5.2%), occupational work – 158 (68.7%), commuting – 137 (59.6%), and physical activity – 62 (27%). Abdominal pain/uterine contractions were significantly more frequent with generalized pain, fever, vaginal bleeding, and physical activity. The presence of dizziness correlated with generalized pain in women who were working and commuting. Working occupationally when pregnant correlated positively with practicing sport. Better newborn condition was significantly correlated with older gestational age and longer sick leave.

Conclusions. Physical activity performed by pregnant women after amniocentesis increases the risk of post-procedural complications such as abdominal pain, uterine contractions, dizziness, and syncope. Reducing physical effort 2 weeks after the procedure is recommended. Further studies are warranted.

Key words: amniocentesis, lifestyle factors, occupational work, prenatal care, adverse events

Cite as

Homola W, Mariusz Zimmer M. Do lifestyle factors influence the rate of complications after amniocentesis? *Adv Clin Exp Med.* 2019;28(10):1339–1344. doi:10.17219/acem/100360

DOI

10.17219/acem/100360

Copyright

© 2019 by Wrocław Medical University
This is an article distributed under the terms of the
Creative Commons Attribution Non-Commercial License
(<http://creativecommons.org/licenses/by-nc-nd/4.0/>)

Introduction

Congenital defects and genetic abnormalities of the fetus may appear both in high-risk and healthy pregnant women, hence the necessity to conduct prenatal tests in all pregnant women.¹ It has been estimated that approx. 2–3% of children are born with a congenital malformation. Out of these, 65–70% of cases are of unknown etiology, 20% have genetic disorders, 3–5% chromosomal aberrations, 2–3% disorders as a consequence of infection, and 2–3% disorders caused by a teratogenic factor.² Chromosomal aberrations alone occur in approx. 50% of aborted embryos, in 2% of fetuses at 16–18 weeks of pregnancy and in 1 in 160 cases of live births.³

Proper prenatal diagnosis reduces perinatal mortality. The detection of abnormalities in fetal development makes it possible to start targeted monitoring during pregnancy, introduce indirect treatment through the mother, correct defects using intrauterine procedures, prepare the fetus for an earlier delivery, and properly arrange the conditions and medical staff to carry out medical intervention immediately after delivery. Information about serious chromosome aberration allows for earlier termination of a pregnancy that would end in spontaneous abortion or death during or after delivery in most cases.^{4,5}

Invasive prenatal testing poses a risk of complications to healthy fetuses, therefore their use is only advised when screening suggests abnormalities or a family history of fetal abnormalities exists.^{1,6} Prenatal tests are conducted according to evidence-based medicine using reliable and up-to-date methods for assessment of the condition of the fetus.^{7,8} Invasive examinations, including amniocentesis, provide practically 100% accuracy in the detection of chromosomal aberrations. During amniocentesis, amniotic fluid is sampled which may be associated with the occurrence of potential complications.⁹ As early as in 1986, Tabor et al. found that amniocentesis is associated with an increased rate of miscarriage.¹⁰ The prevalence of such consequences dropped from 2.1% to 1.4% after the introduction of ultrasound control during amniotic fluid collection. An analysis of 68,000 amniocenteses showed that the rate of pregnancy loss equals approx. 0.33%. Other possible complications include injuries of the fetus caused by the needle, such as scars visible on the skin of the newborn, eye injuries and subdural hematoma. Additionally, an increased risk of the development of respiratory distress syndrome and pneumonia has been reported.¹⁰ Obstetric complications such as bleeding and amniotic fluid leakage appear so rarely that it is difficult to estimate the risk of their occurrence.¹¹ The percentage of miscarriages after amniocentesis correlates positively with the age of women at the intervention, the number of punctures, the presence of myomas, and obesity of the pregnant woman but are negatively correlated with the operator's experience.^{1,12–14} Lifestyle factors have not been discussed in the literature although patients often ask healthcare providers

whether they should change their daily activity directly after the amniocentesis and later in the course of their pregnancy.

Taking into account the constant development of prenatal testing and the lack of studies on the impact of lifestyle factors on the prevalence of complications after amniocentesis, the aim of the study was to examine the further course of pregnancy in patients undergoing amniocentesis in relation to selected risk factors including the level of health-promoting activity and occupational work on the complication rate after genetic amniocentesis.

Material and methods

Medical records from 317 diagnostic amniocenteses conducted in our institution were used. Every patient was invited to participate in the study and to answer a questionnaire. We failed to contact 16 patients (5%) due to a lack of response or changes in contact information. Another 70 patients (22.2%) refused to participate in the study. Ultimately, the study group included 230 procedures carried out on 219 pregnant women. Clinical data was retrieved retrospectively from patient medical records. Data on daily living activities and lifestyle factors were retrieved from a postnatal survey. The study was conducted after obtaining approval from the Commission of Bioethics at Wrocław Medical University, Poland. All subjects gave a written informed consent for participation in the study.

The demographic and clinical data collected, as well as the answers provided by the patients in the survey, were statistically analyzed using the STATISTICA software package v. 10 (StatSoft, Tulsa, USA). The data was presented as means (standard deviation – SD) and percentages. Comparisons between groups were conducted with χ^2 test or Fisher exact test and Mann–Whitney U test. Spearman's correlation rank was used to determine correlations between variables. Differences were considered statistically significant at $p < 0.05$.

Results

In the study group, 216 amniocenteses (93.9%) were performed on singleton pregnancies (including 6 amniocenteses performed as repeated procedures), while 14 amniocenteses (6.1%) were performed on twin pregnancies. The mean maternal age was 34.50 ± 5 years (range: 22–47 years). In the patients studied, amniocentesis was performed at 12–24 gestational weeks with a median at 16 gestational weeks (mean: 16.13 ± 2.02 weeks). Patients referred for amniocentesis were mainly primigravidae ($n = 92$; 40%), secundigravidae ($n = 79$; 35%) and tertigravidae ($n = 44$; 19%), while quadri- and quintigravidae ($n = 12$; 5% and $n = 3$; 1%) constituted a small percentage of the study group. Overall, 208 (94.43%) of 230 amniocenteses were performed in naturally conceived

pregnancies, while 22 (9.57%) were in pregnancies conceived with assisted reproductive technology (ART).

The studied amniocenteses were divided into 2 groups; group A in which the result did not reveal any genetic disorder (n = 174; 75.6%) and group B in which genetic disorder was confirmed (n = 56; 24.4%). The most common defect (n = 22) was Down syndrome (trisomy 21). It was concomitant with a congenital heart defect in 2 cases, and in 1 case with Klinefelter syndrome, an exceptionally rare comorbidity of Down syndrome. Multiple fetal anomalies were found in 2 cases, Edwards syndrome in 5 and Turner

syndrome in 6. The remaining cases comprised rare genetic disorders.

In the study group, a total of 100 procedures (43.5%) were followed by at least 1 complication, while 130 procedures (56.5%) were uneventful. The most common complications included abdominal pain and contractions as well as generalized pain. Table 1 presents complications after amniocentesis by the result of the procedure.

In the present study, several lifestyles factors and their association with complications following amniocentesis were examined. Factors analyzed included the use of stimulants

during pregnancy, occupational work and the necessity to commute, duration of sick leave, and health-promoting physical activity. Stimulants were used in 12 (5.2%) of the 230 procedures; genetic disorder was diagnosed in 1 baby. Of the stimulant users, 4 women were smoking (3–10 cigarettes a day) and 3 were consuming alcohol – mainly wine. Overall, 72 procedures were performed on women who did not work during pregnancy and 158 on those who did. The mean distance traveled to work for working women was 56.3 km. Only 20 women did not have to commute. Sixteen working women were not on sick leave at all, while 132 were on sick leave with an average number of sick weeks of 13.9 (range: 1–38 weeks). Some women were engaged in various forms of health-promoting physical activity: 62 procedures were performed on physically active women while 68 on physically inactive ones. The following types of physical activity were reported: swimming, walking, mountain hiking, jogging, prenatal exercise classes, gymnastics, and dancing classes. The presence of selected lifestyle factors is summarized in Table 2.

Correlation analysis showed clinically interesting associations. Abdominal pain/uterine contractions were significantly more frequent as concomitant with generalized pain, fever, vaginal bleeding, and physical activity in the course of pregnancy. The presence of dizziness correlated with generalized pain in women who were working and commuting. Fetal death was positively correlated with genetic disorders. Additionally, working occupationally when pregnant correlated positively with practicing sports.

The condition of the newborn as measured with Apgar score was significantly positively correlated with the duration of pregnancy (the longer pregnancy, the better the condition of the newborn)

Table 1. Comparison of complication rate following amniocentesis by result of genetic testing

Complication	Group A (n = 174) normal karyotype	Group B (n = 56) genetic disorder	p-value
Abdominal pain/uterine contractions *	3.39 (1.48)	2.95 (1.29)	0.8794
Generalized pain **			0.4009
no	144 (82.76%)	49 (87.50%)	
yes	30 (17.24%)	7 (12.5%)	
Fever ***			0.0604
no	172 (98.85%)	53 (94.64%)	
yes	2 (1.15%)	3 (5.36%)	
Dizziness/syncope ***			0.8795
no	167 (96.17%)	54 (93.43%)	
yes	7 (3.83%)	2 (3.57%)	
Amniotic fluid leakage ***			0.0604
no	172 (98.85%)	53 (94.64%)	
yes	2 (1.15%)	3 (5.36%)	
Vaginal bleeding ***			0.7151
no	172 (98.85%)	55 (97.78%)	
yes	2 (1.15%)	1 (2.22%)	
Fetal death ***			0.0017
no	170 (97.7%)	49 (87.50%)	
yes	4 (2.30%)	7 (12.50%)	

Results presented as number (%) or mean (standard deviation – SD). Bold denotes statistical significance. * Mann–Whitney U test; ** χ^2 test; *** Fisher exact test.

Table 2. Comparison of lifestyle factors following amniocentesis by result of genetic testing

Lifestyle factor	Group A (n = 174) Normal karyotype	Group B (n = 56) Genetic disorder	p-value
Stimulants *			<0.001
no	163 (99.39%)	55 (83.33%)	
yes	1 (0.61%)	11 (16.67%)	
Occupational work **			0.861
no	55 (30.61%)	17 (30.36%)	
yes	119 (68.39%)	39 (69.64%)	
Commuting **			0.84
no	71 (40.81%)	22 (39.29%)	
yes	103 (59.19%)	34 (60.71%)	
Sick leave [weeks] ***	19 (11.75–27.25)	7.0 (3.25–12)	<0.001
Physical activity *			0.943
no	125 (71.84%)	43 (76.79%)	
yes – sporadic	31 (17.82%)	9 (16.07%)	
yes – 2–5 times a week	8 (4.60%)	2 (3.57%)	
yes – every day	10 (5.75%)	2 (3.57%)	
Distance from work [km]	10.0 (6.0–22.0)	12.5 (8.5–23.0)	0.4239

Results presented as numbers (%) or median (interquartile range). Bold denotes statistical significance. * Fisher exact test; ** χ^2 test; *** Mann–Whitney U test.

Table 3. Correlations between study parameters described by Spearman's correlation rank coefficients

Factor	Gestational age at amniocentesis	Gestational age at amniocentesis	Apgar at 1 min	Parity	Abdominal pain/uterine contractions	Generalized pain	Fever	Dizziness/syncope	Amniotic fluid leakage	Vaginal bleeding	Fetal death	Genetic disorder	Stimulants	Occupational work	Commuting	Physical activity	Sick leave
Gestational age at amniocentesis	–	0.00	0.08	–0.10	–0.10	–0.10	–0.15	–0.03	–0.09	–0.09	–0.04	–0.05	0.01	0.15	0.11	0.01	–0.23
Apgar at 1 min	0.00	–	0.09	–0.06	–0.02	–0.06	–0.15	–0.02	–0.11	–0.02	–0.33	–0.71	0.06	–0.05	0.04	0.08	0.37
Parity	0.08	0.09	–	–0.02	–0.02	–0.04	–0.05	–0.09	–0.09	0.02	0.02	–0.01	0.04	0.01	0.02	–0.01	0.00
Abdominal pain/uterine contractions	–0.10	–0.02	–0.02	–	–	0.58	0.14	0.17	0.07	0.18	0.05	–0.04	–0.05	–0.02	0.05	0.15	0.07
Generalized pain	–0.10	–0.06	–0.04	–	0.58	–	0.02	0.22	0.02	0.16	0.01	–0.06	–0.05	–0.01	–0.02	0.09	0.10
Fever	–0.15	–0.15	–0.05	0.02	0.02	0.02	–	–0.03	0.39	–0.02	0.11	0.12	–0.03	0.10	0.11	0.05	–0.13
Dizziness/syncope	–0.03	–0.02	–0.09	0.17	0.17	0.22	–0.03	–	0.12	–0.02	–0.05	–0.01	0.05	0.14	0.18	0.15	–0.06
Amniotic fluid leakage	–0.09	–0.02	–0.09	0.07	0.07	0.02	0.39	0.12	–	–0.02	–0.03	0.12	–0.03	0.10	0.10	0.05	–0.03
Vaginal bleeding	–0.09	–0.02	0.02	0.18	0.18	0.16	–0.02	–0.02	–0.02	–	–0.03	0.02	–0.03	–0.09	–0.10	–0.07	0.02
Fetal death	–0.04	–0.33	–	0.16	0.16	0.16	–0.02	–0.03	–0.03	–	–	0.21	–0.05	0.11	0.10	–0.09	–0.01
Genetic disorder	–0.05	–0.71	–0.01	0.21	0.21	0.16	0.11	–0.05	–0.03	–0.03	–	–	–0.09	0.01	–0.08	–0.05	–0.52
Stimulants	0.01	0.06	0.04	–0.03	–0.03	–0.03	0.12	0.05	–0.03	–0.03	–0.05	–0.09	–	–0.01	0.04	0.07	0.07
Occupational work	0.15	–0.05	0.01	–0.02	–0.02	–0.01	0.10	0.14	0.10	–0.09	0.11	0.01	–0.01	–	0.71	0.22	–0.45
Commuting	0.11	0.04	0.02	–0.02	0.05	–0.02	0.11	0.18	0.10	–0.10	0.10	0.04	0.04	0.71	–	0.22	–0.23
Physical activity	0.01	0.08	–0.01	0.09	0.15	0.09	0.05	0.15	0.05	–0.07	–0.09	–0.05	0.07	0.22	0.22	–	–0.13
Sick leave	–0.23	0.37	0.00	0.10	0.07	0.10	–0.13	–0.06	–0.03	0.02	–0.01	–0.52	0.07	–0.45	–0.23	–0.13	–

Bold denotes statistical significance.

and being on sick leave (newborns of mothers who were on sick leave had higher Apgar scores). Table 3 shows correlations between the parameters studied.

Discussion

Taking into account lifestyle factors, our study showed that women who received an amniocentesis result indicating genetic disorder used stimulants more often and had a lower number of sick leave weeks in comparison to women in whom amniocentesis yielded normal results. Of the amniocentesis complications, only fetal death occurred significantly more often in the group with genetic disorders than in the groups with normal karyotype. Occupational work during pregnancy and commuting to work significantly correlated with the occurrence of dizziness and physical activity. Health-promoting physical activity was associated with more frequent abdominal pain and contractions as well as dizziness and syncope. Being on sick leave correlated with better newborn status as measured with Apgar score.

The health benefits of physical activity have been well documented. According to the American College of Obstetricians and Gynecologists (ACOG), physical activity during pregnancy has minimal risks for the fetus and the mother. The ACOG also recommends moderate-intensity exercise for at least 20–30 min per day on most or all days of the week, noting however that further research is needed to study the effects of exercise on pregnancy-specific outcomes.¹⁵ Many women attend prenatal exercise classes, but there are no criteria that would help qualify women for such physical activity. Most of them decided to participate on their own, while some discuss the possibility of practicing sports with their physician, who can advise based on his/her experience and individual assessment of health status. Women also report barriers that reduce their physical activity during pregnancy such as health problems (80%) and the feeling of being tired (46%). Another barrier is lack of time (34%), which affects pregnant women who already have children to a greater degree (47%) than primiparae (14%).¹⁶ Pre-pregnancy habits are transferred to the period of pregnancy.

Women who had been physically inactive before becoming pregnant notice more barriers in accessing physical activity and fewer benefits than those who had previously practiced sports.¹⁷

Only a few papers address practicing sports during uncomplicated pregnancy in low-risk pregnant women. Those studies are usually conducted on small groups of patients and have a high rate of withdrawal. A wide variety of forms of physical activity, as well as diversified duration and intensity of physical effort, is another source of heterogeneity. Nevertheless, the meta-analysis conducted by Perales et al. did not identify any study which reported a negative effect of health-promoting physical activity on the health of the mother and the fetus in the low-risk group. The greatest benefits were obtained from the combination of aerobic and endurance exercises compared to only 1 type of exercise. The greatest benefit of the exercises was the improvement of cardiorespiratory fitness, which worsens as pregnancy advances.¹⁸

In the literature, few reports on the impact of physical activity on the risk of eclampsia in pregnant women have been published. Spracklen et al. compared the following groups of patients: 258 pregnant women with preeclampsia, 221 pregnant women with hypertension and 174 healthy pregnant women (control group). The results of this study showed the positive impact of the health-promoting physical activity on blood pressure. A significant drop in the risk of preeclampsia and hypertension was observed for every 10-minute increase per week; however, this risk increased significantly when women performed heavy household chores for longer than 180 min per week.¹⁹ Sauder et al. found that physical activity was the only modifiable risk factor which can reduce the risk of glycemic disorders.²⁰ A meta-analysis of pooled data from 10 studies including 3,401 participants revealed a slight protective effect against the development of gestational diabetes mellitus.²¹ The study by Szegda et al. conducted among Latina women aimed to reveal an association between physical activity and the development of depression. The authors did not observe any significant associations between health-promoting physical activity and the presence of depressive symptoms, although they assumed that physical activity might have a potential protective mechanism against depressive symptoms.²²

The best of our knowledge, no studies on the effect of physical activity on well-being were previously performed among pregnant women undergoing amniocentesis. In our study, only 26% of women referred for amniocentesis practiced sport or participated in exercise classes such as swimming, walking, mountain hiking, jogging, prenatal exercise classes, gymnastics, and dancing classes. Moreover, only 12 of the active women (6%) were practicing every day. Taking into account complications following amniocentesis, a significant correlation was found between physical activity and the occurrence of pain; therefore, a recommendation to patients

undergoing amniocentesis to abandon physical activity for at least the period of increased risk of complications should be considered. On the other hand, a significant positive correlation between the intensity of physical effort and gestational weeks at birth suggests that physical activity may reduce the effect of other risk factors of premature delivery. Interestingly, the significant correlation between physical activity and occupational work indicates that physically active women are more active in general because a higher level of physical activity was not associated with less family burden; the correlation between physical activity and parity was insignificant. This topic is interesting and worth future research.

Occupational work may be associated with heavy physical effort or the need to maintain an unnatural position for a longer period of time. Spracklen et al. confirmed the impact of occupational work on preeclampsia risk. They found that this risk decreased only in women who worked in a standing position. A 1-hour increase in the time spent on feet decreased the risk of preeclampsia; however, an increase in standing in one place at work increased the risk of hypertension. Women who spend more than 40 h per week at work were at greater risk than those who worked less than 36 h per week.¹⁹

In the present study on women subjected to amniocentesis, 115 women (69%) worked during pregnancy and most of them commuted to work. Both occupational work and the need to commute were significantly correlated with dizziness following amniocentesis. Correlations were also examined for women on sick leave and revealed that a greater number of sick leave weeks was significantly correlated with older gestational age and better health condition of the newborn as measured with Apgar score. These relationships may indicate that women on sick leave had more time to rest and use healthcare resources.

Stimulants have a well-documented negative impact on the course of pregnancy. Cigarette smoke is particularly harmful and contributes to the development of such pathologies as a low birth weight of the fetus, intrauterine growth restriction, preterm delivery, oligohydramnios, disorders of placental circulation, abnormal placental location, premature detachment of the placenta, and premature rupture of the amniotic membranes.^{23,24} Despite this, approx. 25% of Polish women smoke, and half of them continue to smoke during pregnancy.²⁵ Smoking may increase the risk of consequences after amniocentesis because it is an invasive procedure which is associated with puncture of maternal abdominal tissues and fetal membranes as well as in some cases even the placenta. The negative impact of smoking on wound healing after surgery has been thoroughly examined. Smoking alters tissue micro-environment. It changes inflammatory and regenerative response on a cellular level, leading to a delay in wound healing and increase in complication rate.^{26–29} The most common addiction reported by women in the study group was smoking. However, the percentage of smokers was

very low compared to the average in the Polish population and amounted to 2%. Four smokers disclosed their habit and reported smoking 3–10 cigarettes a day. There was no association between smoking and any of the complications following amniocentesis. This may be due to the low number of smokers in the study group. On the other hand, a low percentage of smokers confirms high awareness and high compliance with medical recommendations.

In the framework of the current study, apart from answering closed-ended questions about their pregnancy, the amniocentesis procedure and further course of the pregnancy from the procedure to the delivery, patients could add personal comments and suggestions, and describe subjective feelings associated with amniocentesis. After the analysis of those comments, we conclude that most of the women experienced high-intensity anxiety before the procedure due to the uncertainty of the test result, worries about the further course of pregnancy and the lack of knowledge about amniocentesis itself. The women highlighted that good interpersonal contact with the staff performing the procedure, calm and honest conversation before amniocentesis, and discussing the procedure and possible complications in a comprehensible way play a key role in eliminating the described anxiety. In the opinion of patients, such conduct of the amniocentesis significantly alleviated the psychological tension and anxiety that appeared at qualification for amniocentesis and the decision to undergo the procedure. Reports from the literature are in line with our findings. They confirm that pregnant women experience anxiety both before amniocentesis and after receiving a positive result.³⁰

Conclusions

Physical activity performed by pregnant women after amniocentesis increases the risk of post-procedural complications such as abdominal pain and uterine contractions as well as dizziness and syncope. To increase the safety of amniocentesis, it seems reasonable to limit the physical activity of the woman within 2 weeks directly after the procedure. The impact of lifestyle factors on the frequency of complications turned out to be an interesting aspect of the safety analysis of invasive procedures; therefore, it is worth studying this topic in the future, especially in the scope of prenatal testing.

References

- PTG. Polish Gynaecological Society guideline on prenatal diagnosis [in Polish]. *Ginekol Pol.* 2009;80(5):390–393.
- Finnell RH. Teratology: General considerations and principles. *J Allergy Clin Immunol.* 1999;103(2 Pt 2):S337–S342.
- Hassold TJ, Jacobs PA. Trisomy in man. *Annu Rev Genet.* 1984;18:69–97.
- van der Pal-de Bruin KM, Graafmans W, Biermans MC, et al. The influence of prenatal screening and termination of pregnancy on perinatal mortality rates. *Prenat Diagn.* 2002;22(11):966–972.
- Postoev VA, Grijbovski AM, Nieboer E, Odland JO. Changes in detection of birth defects and perinatal mortality after introduction of prenatal ultrasound screening in the Kola Peninsula (North-West Russia): Combination of two birth registries. *BMC Pregnancy Childbirth.* 2015;15:308.
- Kancelaria Sejmu. Ustawa z dnia 7 stycznia 1993 r. o planowaniu rodziny, ochronie płodu ludzkiego i warunkach dopuszczalności przerywania ciąży. 1993. Dz.U. 1993 nr 17 poz. 78.
- Greenberg M, Druzin M, Gabbe S. Przedporodowa diagnostyka stanu płodu. In: Oszukowski P, Dębski R, eds. *Położnictwo – ciąża prawidłowa i powikłana*, 6 ed. Wrocław, Poland: Elsevier Urban & Partner; 2014:267–295.
- Collins SL, Impey L. Prenatal diagnosis: Types and techniques. *Early Hum Dev.* 2012;88(1):3–8.
- Breckwoldt, Fabel G, Martius G, Martius J, Pfliegerer A, Schneider H. *Ginekologia i położnictwo*. Wrocław, Poland: Wydawnictwo Medyczne Urban & Partner; 1997.
- Tabor A, Philip J, Madsen M, Bang J, Obel EB, Norgaard-Pedersen B. Randomised controlled trial of genetic amniocentesis in 4606 low-risk women. *Lancet.* 1986;1(8493):1287–1293.
- Seeds JW. Diagnostic mid trimester amniocentesis: How safe? *Am J Obstet Gynecol.* 2004;191(2):607–615.
- Harper LM, Cahill AG, Smith K, Macones GA, Odibo AO. Effect of maternal obesity on the risk of fetal loss after amniocentesis and chorionic villus sampling. *Obstet Gynecol.* 2012;119(4):745–751.
- Tabor A, Alfirevic Z. Update on procedure-related risks for prenatal diagnosis techniques. *Fetal Diagn Ther.* 2010;27(1):1–7.
- Mujezinovic F, Alfirevic Z. Technique modifications for reducing the risks from amniocentesis or chorionic villus sampling. *Cochrane Database Syst Rev.* 2012;8:CD008678.
- ACOG Committee Opinion No. 650: Physical activity and exercise during pregnancy and the postpartum period. *Obstet Gynecol.* 2015; 126(6):e135–e142.
- Jelsma JG, van Leeuwen KM, Oostdam N, et al. Beliefs, barriers, and preferences of European overweight women to adopt a healthier lifestyle in pregnancy to minimize risk of developing gestational diabetes mellitus: An explorative study. *J Pregnancy.* 2016;2016:3435791.
- Da CD, Ireland K. Perceived benefits and barriers to leisure-time physical activity during pregnancy in previously inactive and active women. *Women Health.* 2013;53(2):185–202.
- Perales M, Santos-Lozano A, Ruiz JR, Lucia A, Barakat R. Benefits of aerobic or resistance training during pregnancy on maternal health and perinatal outcomes: A systematic review. *Early Hum Dev.* 2016;94:43–48.
- Spracklen CN, Ryckman KK, Triche EW, Saftlas AF. Physical activity during pregnancy and subsequent risk of preeclampsia and gestational hypertension: A case control study. *Matern Child Health J.* 2016; 20(6):1193–1202.
- Sauder KA, Starling AP, Shapiro AL, et al. Diet, physical activity and mental health status are associated with dysglycaemia in pregnancy: The Healthy Start Study. *Diabet Med.* 2016;33(5):663–667.
- Russo LM, Nobles C, Ertel KA, Chasan-Taber L, Whitcomb BW. Physical activity interventions in pregnancy and risk of gestational diabetes mellitus: A systematic review and meta-analysis. *Obstet Gynecol.* 2015;125(3):576–582.
- Szegda K, Bertone-Johnson ER, Pekow P, et al. Physical activity and depressive symptoms during pregnancy among Latina women: A prospective cohort study. *BMC Pregnancy Childbirth.* 2018;18(1):252.
- Rogers JM. Tobacco and pregnancy: Overview of exposures and effects. *Birth Defects Res C Embryo Today.* 2008;84(1):1–15.
- Longo LD. Some health consequences of maternal smoking: Issues without answers. *Birth Defects Orig Artic Ser.* 1982;18(3 Pt A):13–31.
- Piekoszewski W, Florek E. Tobacco in statistics at the turn of the new century [in Polish]. *Przegl Lek.* 2006;63(10):823–826.
- Rinker B. The evils of nicotine: An evidence-based guide to smoking and plastic surgery. *Ann Plast Surg.* 2013;70(5):599–605.
- Sorensen LT, Nielsen HB, Kharazmi A, Gottrup F. Effect of smoking and abstention on oxidative burst and reactivity of neutrophils and monocytes. *Surgery.* 2004;136(5):1047–1053.
- Sorensen LT, Zillmer R, Agren M, Ladelund S, Karlsmark T, Gottrup F. Effect of smoking, abstention, and nicotine patch on epidermal healing and collagenase in skin transudate. *Wound Repair Regen.* 2009; 17(3):347–353.
- Sorensen LT, Toft BG, Rygaard J, et al. Effect of smoking, smoking cessation, and nicotine patch on wound dimension, vitamin C, and systemic markers of collagen metabolism. *Surgery.* 2010;148(5):982–990.
- Mousavi S, Hantoushzadeh S, Sheikh M, Shariat M. Maternal anxiety and the second-trimester prenatal screening: A prospective cohort study. *Fetal Diagn Ther.* 2015;38(4):269–275.

The association of serum soluble Klotho levels and residual diuresis and overhydration in peritoneal dialysis patients

Dorota Sikorska^{1,A–F}, Krzysztof Pawlaczyk^{2,A,F}, Ewa Baum^{3,E,F}, Maria Wanic-Kossowska^{2,B,F}, Natasza Czepulis^{4,B,F}, Joanna Łuczak^{2,B,F}, Włodzimierz Samborski^{1,E,F}, Andrzej Oko^{2,A,E,F}

¹ Department of Rheumatology and Rehabilitation, Poznan University of Medical Sciences, Poland

² Department of Nephrology, Transplantology and Internal Medicine, Poznan University of Medical Sciences, Poland

³ Department of Philosophy and Bioethics, Poznan University of Medical Sciences, Poland

⁴ Department of Pathophysiology, Poznan University of Medical Sciences, Poland

A – research concept and design; B – collection and/or assembly of data; C – data analysis and interpretation;

D – writing the article; E – critical revision of the article; F – final approval of the article

Advances in Clinical and Experimental Medicine, ISSN 1899–5276 (print), ISSN 2451–2680 (online)

Adv Clin Exp Med. 2019;28(10):1345–1349

Address for correspondence

Dorota Sikorska

E-mail: dorotasikorska@ump.edu.pl

Funding sources

The study was supported with a Poznan University of Medical Sciences Grant for Young Researchers (No. 502-14-02225363-99663).

Conflict of interest

None declared

Acknowledgements

We would like to thank Janusz Witowski for comments that greatly improved the manuscript.

Received on February 25, 2018

Reviewed on May 21, 2018

Accepted on February 18, 2019

Published online on March 11, 2019

Abstract

Background. Klotho, originally identified as an anti-aging factor, is a transmembrane protein expressed in the kidney. It has been reported that Klotho deficiency could be associated with a loss of residual renal function and cardiovascular complications in peritoneal dialysis (PD) patients.

Objectives. The main aim of the study was to evaluate whether serum levels of Klotho correlate with residual diuresis and hydration status in PD patients.

Material and methods. The cross-sectional study involved 57 PD patients ≥ 18 years of age who had been on PD ≥ 3 months. Serum Klotho was measured using high-sensitivity enzyme-linked immunosorbent assay (ELISA). Hydration status was assessed with bioimpedance analysis (BIA).

Results. Serum levels of soluble Klotho ranged from 100 pg/mL to 700 pg/mL. The patients were divided into 2 subgroups, with Klotho levels below and above the median (260 pg/mL). The data revealed a tendency for lower residual diuresis (1.3 ± 1.0 L vs 1.8 ± 0.8 L; $p = 0.055$) in patients with lower levels of Klotho in serum. Serum Klotho correlated negatively with overhydration according to BIA ($r = -0.27$; $p = 0.044$) and positively with residual diuresis ($r = 0.26$; $p = 0.045$).

Conclusions. Soluble Klotho correlates inversely with hydration status in BIA. Residual urine output, but not dialysis parameters, could be associated with the levels of serum soluble Klotho in PD patients.

Key words: peritoneal dialysis, Klotho, overhydration

Cite as

Sikorska D, Pawlaczyk K, Baum E, et al. The association of serum soluble Klotho levels and residual diuresis and overhydration in peritoneal dialysis patients. *Adv Clin Exp Med.* 2019;28(10):1345–1349. doi:10.17219/acem/104552

DOI

10.17219/acem/104552

Copyright

© 2019 by Wrocław Medical University

This is an article distributed under the terms of the Creative Commons Attribution Non-Commercial License (<http://creativecommons.org/licenses/by-nc-nd/4.0/>)

Klotho was first identified in mice as an anti-aging factor.¹ Full-length alpha-Klotho is a single-pass transmembrane protein that exists in 2 forms, membrane and secreted Klotho, which have different functions.² The membrane form acts as a co-receptor for fibroblast growth factor-23 (FGF-23) and plays an important role in calcium-phosphate metabolism.^{2,3} Soluble Klotho (called α -Klotho, with molecular mass 130-kDa) seems to function as a humoral factor with various biological effects, and it works independently of FGF-23 signaling.⁴ Among the pleiotropic actions that soluble Klotho is responsible for are tissue protection from oxidative stress, fibrosis and apoptotic stimuli; regulation of blood phosphate and vitamin D3 levels; and the activity of multiple cell surface calcium and potassium ion channels.^{2,3,5} There are data suggesting that secreted Klotho exerts phosphaturic effects independently of FGF-23.³ Soluble Klotho has also been associated with protective effects against vascular calcification.⁶ Furthermore, soluble Klotho could be a potential biomarker for predicting adverse renal outcomes in patients with advanced chronic kidney disease (CKD).^{7–9} However, the exact diagnostic and therapeutic role of Klotho in humans is not fully known yet.³

Klotho is expressed in several organs, including the parathyroid glands, the choroid plexus of the brain and, predominantly, in the distal tubular epithelial cells of the kidney.¹⁰ The kidney is the major source of Klotho in humans, and this organ is involved in Klotho homeostasis, responsible for producing and releasing Klotho into the circulation.¹¹ Patients with CKD display decreased Klotho gene expression in several tissues, including the kidney. This results in reduced levels of circulating Klotho. Serum soluble Klotho is decreased in all stages of CKD, especially in dialysis patients.^{8,11} It is likely that serum soluble Klotho protein concentration is related to residual renal function.⁸ However, the relationship between the soluble form of Klotho and residual renal function in chronic peritoneal dialysis (PD) patients remains poorly understood.^{7,9}

The aim of this study was to assess whether serum soluble Klotho levels could be associated with residual renal function and hydration status in PD patients. To the best of our knowledge, this is the first study evaluating the relationship between serum Klotho and hydration status as assessed with bioimpedance analysis (BIA) in patients on PD.

Material and methods

Patients

This investigator-initiated cross-sectional study involved 57 Caucasian patients undergoing PD in 3 regional dialysis centers. The inclusion criteria were: age ≥ 18 years, time on PD ≥ 3 months, and informed consent. The exclusion criteria were: any acute inflammatory disease within 12 weeks prior to enrolment, amputated limbs and cardiac pacemakers or implantable cardioverter defibrillators. The study was

approved by the Poznan University of Medical Sciences Bioethics Committee (No. 424/13) and informed consent was obtained from all the participants included in the study.

Volume status

A peritoneal equilibration test (PET) using a 4-hour dwell of 2.27%-glucose dialysate was used to assess peritoneal membrane transport.¹²

Hydration status was assessed with bioimpedance spectroscopy using the Body Composition Monitor (BCM) (Fresenius Medical Care GmbH, St. Wendel, Germany).¹³ The measurements were performed in the supine position under standardized conditions. Values below -1.1 L and above $+1.1$ L corresponded to hypovolemia and hypervolemia, respectively.¹³ Clinical assessments of hydration status were based on blood pressure measurements and on the symptoms of overhydration: the presence of dyspnea, peripheral edema and jugular vein distension.

Laboratory tests

Samples of serum were collected at the time of the clinical examinations in a fasting state. Serum was aliquoted and stored at -80°C until assayed in batches. Serum Klotho was measured using the Human Soluble α -Klotho Assay Kit (Immuno-Biological Laboratories Co. Ltd., Fujioka, Japan) with a sensitivity of 6.15 pg/mL. The immunoassays were performed according to the manufacturer's instructions. All other laboratory tests were performed in the hospital central laboratory using routine methods.

Statistical methods

Statistical analyses were performed using STATISTICA v. 10.0 software (StatSoft Polska, Kraków, Poland). The normality of the data distribution was checked with the Shapiro–Wilk test. The data is presented as medians and interquartile ranges or percentages, as appropriate. Differences between unpaired data were analyzed with the Mann–Whitney U test. Categorical data was analyzed with the χ^2 test. Correlations between variables were analyzed with Spearman's rank correlation coefficient. Differences were considered significant at $p < 0.05$.

Results

The study analyzed 57 consecutive PD patients. Serum levels of soluble Klotho ranged from 100 to 700 pg/mL. The patients were divided into 2 subgroups: those with Klotho levels below the median (260 pg/mL) and those with levels above the median. We decided on such subdivision of patients because there are no clear ranges of reference values for Klotho.⁴ The patients' characteristics in relation to their serum Klotho levels are shown in Table 1.

Clinical features of overhydration were observed in 19% of the patients (11/57). However, BIA found excessive hydration retention in as many as 44% of the patients (25/57). In addition, there was a significant difference in the distribution of those patients between the Klotho subgroups (Table 1). Surprisingly, there were no statistically significant differences in Klotho levels between patients with overhydration according to BIA and those without (250 (216–327) pg/mL vs 290 (223–399) pg/mL; $p = 0.172$).

The data revealed a tendency toward higher fluid overload in BIA in patients with lower levels of Klotho in serum

(Table 1), although these were not statistically significant differences. Also, patients with lower serum Klotho had significantly lower hematocrit and hemoglobin levels. These patients also tended to have lower residual diuresis. However, there was no relationship between serum Klotho levels and dialysis parameters (Table 1).

As expected, serum Klotho correlated negatively with overhydration according to BIA ($r = -0.27$; $p = 0.044$) (Fig. 1). Moreover, there was a positive correlation between Klotho and residual diuresis ($r = 0.26$; $p = 0.045$) (Fig. 2).

Table 1. Patients’ characteristics in relation to serum Klotho levels. Data are presented as medians (interquartile ranges) or as percentages

Variables	Lower levels of Klotho (<260 pg/mL) (n = 28)	Higher levels of Klotho (≥260 pg/mL) (n = 29)	Mann–Whitney or χ^2 test
Demographic and PD-related parameters			
Men [%]	14 (50)	14 (48)	0.896
Age [years]	60 (42–70)	55 (39–67)	0.375
BMI [kg/m ²]	24.4 (21.0–30.3)	26.0 (23.9–29.1)	0.664
Diabetic nephropathy, n [%]	8 (29)	7 (24)	0.704
DM [%]	11 (39)	9 (31)	0.514
Time on PD [months]	25 (15–38)	33 (16–68)	0.123
APD mode, n [%]	10 (36)	6 (21)	0.207
Ultrafiltration [mL/day]	1,200 (500–2,200)	1,000 (900–1,500)	0.766
Residual diuresis [mL/day]	1,300 (500–2,200)	1,650 (1,100–2,400)	0.054
Residual diuresis <500 mL/day [%]	7 (25)	1 (3)	0.019
Solute removal [Kt/V]	2.3 (2.1–3.5)	2.8 (2.3–3.3)	0.421
Creatinine clearance [L/week]	92.8 (75.4–120.2)	99.4 (68.8–136.1)	0.799
4-h D/P creatinine in PET	0.68 (0.58–0.72)	0.63 (0.55–0.71)	0.402
Transport status, n (% H/HA)	16 (57)	12 (41)	0.234
Blood tests and biochemical parameters			
Hematocrit [%]	33.1 (31.5–37.4)	37.1 (33.4–38.5)	0.018
Hemoglobin [g/dL]	11.1 (10.5–12.4)	12.5 (11.3–13.4)	0.016
CRP [mg/L]	5.6 (2.6–8.4)	2.7 (1.3–8.2)	0.123
Albumin [g/dL]	3.8 (3.5–4.1)	4.0 (3.7–4.2)	0.107
Total cholesterol [mg/dL]	184 (167–201)	198 (169–216)	0.263
Calcium [mmol/L]	9.1 (8.5–9.5)	9.0 (8.7–9.3)	0.936
Phosphorus [mmol/L]	5.3 (3.9–6.2)	5.1 (4.3–6.1)	0.707
PTH [pg/mL]	278 (178–401)	340 (299–490)	0.080
FGF-23 [pg/mL]	8.9 (3.2–41.6)	18.3 (5.6–44.4)	0.457
Hydration status			
OH in BIA [L]	2.0 (0.6–3.0)	0.8 (0.2–1.6)	0.066
OH in BIA [%]	2.3 (0.9–3.9)	1.0 (0.3–2.5)	0.056
Overhydration in BIA > 1.1 L [%]	16 (57)	9 (31)	0.047
Pts with edema, n [%]	7 (25)	4 (14)	0.284
SBP [mm Hg]	130 (120–150)	130 (120–145)	0.705
DBP [mm Hg]	80 (70–95)	80 (70–90)	0.497
Number of antihypertensives	3 (2–4)	4 (2–4)	0.215

BMI – body mass index; DM – diabetes mellitus; PD – peritoneal dialysis; APD – automated peritoneal dialysis; H – high; HA – high-average; CRP – C-reactive protein; PTH – parathyroid hormone; FGF-23 – fibroblast growth factor 23; OH – overhydration; BIA – bioimpedance analysis; SBP – systolic blood pressure; DBP – diastolic blood pressure.

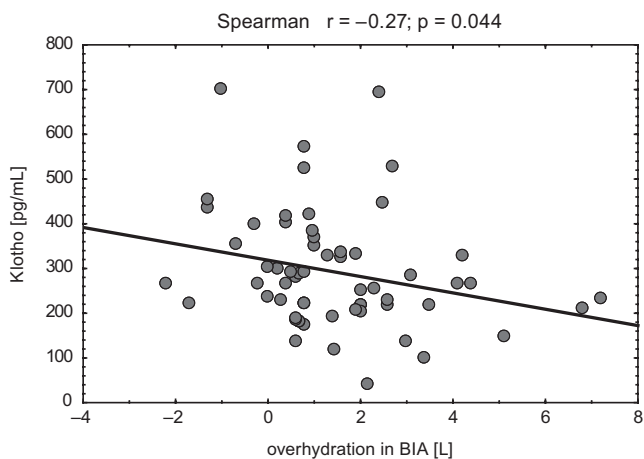


Fig. 1. Correlation between hydration status in bioimpedance analysis (BIA) and serum Klotho

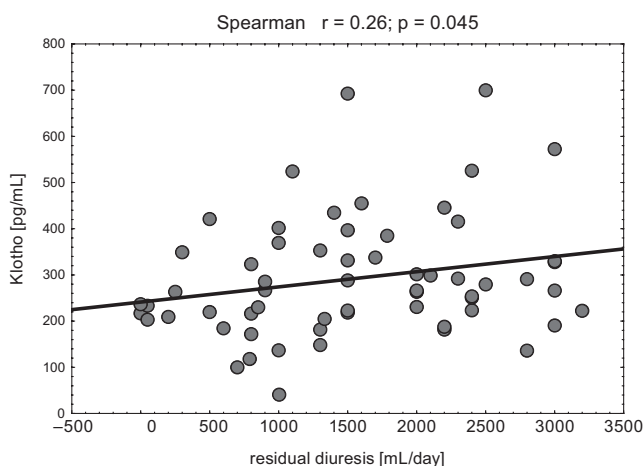


Fig. 2. Correlation between residual diuresis and serum Klotho

Discussion

The most important observation in our study was that serum soluble Klotho levels correlate inversely with hydration status in BIA. The results of the study suggest that residual urine output, but not dialysis parameters, could be associated with the levels of serum Klotho in PD patients.

Earlier studies indicated that serum soluble Klotho levels are positively associated with renal function and are significantly decreased in the later stages of CKD.^{14,15} At the same time, Klotho concentrations are probably independent of PD parameters themselves.¹⁶ However, the relationship between serum Klotho and residual renal function is not so obvious in PD patients.^{7,9} A previous study revealed that the total amount of urinary excreted Klotho, but not the serum level of soluble Klotho, may be a potential biomarker for assessing the residual renal function among PD patients.⁹ In 2012, Golembiewska et al. demonstrated that serum soluble Klotho concentrations

were negatively correlated with a 24-hour diuresis, but not with residual renal function.⁷

There has been a strong focus on residual renal function as a significant survival predictor for dialysis patients,^{17,18} but the precise mechanism by which residual diuresis is linked to morbidity and mortality among dialysis patients has yet to be determined.¹⁹ The presence of residual renal function is associated with better preservation of the renal endocrine and metabolic functions, and facilitates the maintenance of good hydration status.^{20,21} It is likely that residual urinary volume is the main predictor of overhydration in patients on PD.²² Moreover, our study demonstrated a significant correlation between residual urine output and hydration status ($r = -0.36$; $p = 0.004$).

It is possible that the relationship between residual diuresis and soluble Klotho in our study results from hydration status. However, to rule out the effect of dilution of serum Klotho, albumin concentrations were also assessed, and there was no relationship between Klotho levels and albumin concentrations. At the same time, we did not detect any correlation between overhydration in BIA and blood pressure, which should be influenced by an increase in plasma volume. This may suggest that overhydration is related to interstitial fluid retention rather than hypervolemia.²³ It is possible that overhydration per se affects soluble Klotho levels.

The introduction of BIA has made it possible to assess hydration status in PD patients more accurately.¹³ Recent studies have revealed that BIA-evaluated overhydration is common in dialysis patients, and is associated with loss of residual renal function and inflammation.^{24,25} Increasing evidence suggests that overhydration predicts all-cause mortality.²⁶ However, the relationship between overhydration and Klotho is not yet known. To the best of our knowledge, this is the first study evaluating the relationship between serum Klotho and hydration status in BIA in patients on PD.

Although this study provides new information on the relationship between residual diuresis, hydration status and soluble Klotho among PD subjects, the results should be interpreted within the context of the study limitations. The patient population was relatively small, which means that the study may be statistically underpowered. An additional limitation is that we cannot provide data on urinary and dialysate Klotho excretion. Further research is therefore needed.

Conclusions

Residual urine output, but not dialysis parameters, could be associated with the levels of serum soluble Klotho in PD patients. Soluble Klotho correlates inversely with hydration status in BIA.

References

1. Kuro-o M, Matsumura Y, Aizawa H, et al. Mutation of the mouse klotho gene leads to a syndrome resembling ageing. *Nature*. 1997;390(6655):45–51.
2. Olauson H, Mencke R, Hillebrands JL, Larsson TE. Tissue expression and source of circulating alphaKlotho. *Bone*. 2017;100:19–35.
3. Golembiewska E, Stepniewska J, Kabat-Koperska J, Kedzierska K, Domanski M, Ciechanowski K. The role of Klotho protein in chronic kidney disease: Studies in animals and humans. *Curr Protein Pept Sci*. 2016;17(8):821–826.
4. Wang Y, Sun Z. Current understanding of klotho. *Ageing Res Rev*. 2009;8(1):43–51.
5. Xu Y, Sun Z. Molecular basis of Klotho: From gene to function in aging. *Endocr Rev*. 2015;36(2):174–193.
6. Lim K, Lu TS, Molostvov G, et al. Vascular Klotho deficiency potentiates the development of human artery calcification and mediates resistance to fibroblast growth factor 23. *Circulation*. 2012;125(18):2243–2255.
7. Golembiewska E, Safranow K, Kabat-Koperska J, Myslak M, Ciechanowski K. Serum soluble Klotho protein level is associated with residual diuresis in incident peritoneal dialysis patients. *Acta Biochim Pol*. 2013;60(2):191–194.
8. Liu QF, Ye JM, Yu LX, et al. Plasma s-Klotho is related to kidney function and predicts adverse renal outcomes in patients with advanced chronic kidney disease. *J Investig Med*. 2017;66(3):669–675.
9. Akimoto T, Shiizaki K, Sugase T, et al. The relationship between the soluble Klotho protein and the residual renal function among peritoneal dialysis patients. *Clin Exp Nephrol*. 2012;16(3):442–447.
10. Gigante M, Lucarelli G, Divella C, et al. Soluble serum alphaKlotho is a potential predictive marker of disease progression in clear cell renal cell carcinoma. *Medicine (Baltimore)*. 2015;94(45):e1917.
11. Hu MC, Shi M, Zhang J, et al. Renal production, uptake, and handling of circulating alphaKlotho. *J Am Soc Nephrol*. 2016;27(1):79–90.
12. Twardowski ZJ, Nolph KD, Khanna R, et al. Peritoneal equilibration test. *Perit Dial Int*. 1987;7(3):138–148.
13. Davies SJ, Davenport A. The role of bioimpedance and biomarkers in helping to aid clinical decision-making of volume assessments in dialysis patients. *Kidney Int*. 2014;86(3):489–496.
14. Shimamura Y, Hamada K, Inoue K, et al. Serum levels of soluble secreted alpha-Klotho are decreased in the early stages of chronic kidney disease, making it a probable novel biomarker for early diagnosis. *Clin Exp Nephrol*. 2012;16(5):722–729.
15. Seibert E, Radler D, Ulrich C, Hanika S, Fiedler R, Girndt M. Serum klotho levels in acute kidney injury. *Clin Nephrol*. 2017;87 (2017)(4):173–179.
16. Oh HJ, Nam BY, Lee MJ, et al. Decreased circulating klotho levels in patients undergoing dialysis and relationship to oxidative stress and inflammation. *Perit Dial Int*. 2015;35(1):43–51.
17. Lee MJ, Park JT, Park KS, et al. Prognostic value of residual urine volume, GFR by 24-hour urine collection, and eGFR in patients receiving dialysis. *Clin J Am Soc Nephrol*. 2017;12(3):426–434.
18. Diaz-Buxo JA, White SA, Himmele R. The importance of residual renal function in peritoneal dialysis patients. *Adv Perit Dial*. 2013;29:19–24.
19. Liu X, Dai C. Advances in understanding and management of residual renal function in patients with chronic kidney disease. *Kidney Dis (Basel)*. 2017;2(4):187–196.
20. Sikorska D, Pawlaczyk K, Olewicz-Gawlik A, et al. The importance of residual renal function in peritoneal dialysis. *Int Urol Nephrol*. 2016;48(12):2101–2108.
21. Vilar E, Farrington K. Emerging importance of residual renal function in end-stage renal failure. *Semin Dial*. 2011;24(5):487–494.
22. Jung ES, Sung JY, Han SY, et al. Residual urinary volume is a predictor of overhydration in patients on peritoneal dialysis. *Tohoku J Exp Med*. 2014;233(4):295–300.
23. Sikorska D, Pawlaczyk K, Roszak M, et al. Preliminary observations on the association between serum IL-6 and hydration status and cardiovascular risk in patients treated with peritoneal dialysis. *Cytokine*. 2016;85:171–176.
24. Van Biesen W, Williams JD, Covic AC, et al. Fluid status in peritoneal dialysis patients: The European Body Composition Monitoring (EuroBCM) study cohort. *PLoS ONE*. 2011;6(2):e17148.
25. Fan S, Sayed RH, Davenport A. Extracellular volume expansion in peritoneal dialysis patients. *Int J Artif Organs*. 2012;35(5):338–345.
26. Paniagua R, Ventura MD, Avila-Diaz M, Hinojosa-Heredia H, Mendez-Duran A, Cueto-Manzano A, et al. NT-proBNP, fluid volume overload and dialysis modality are independent predictors of mortality in ESRD patients. *Nephrol Dial Transplant*. 2010;25(2):551–557.

Treatment of heart failure in the elderly in Poland. The results of the Polish part of EURObservational Research Programme: The Heart Failure Pilot Survey

Adam Rafał Poliwczak^{1,A–D,F}, Janusz Śmigiełski^{2,B,C,E}, Agnieszka Bała^{3,B,D}, Ewa Straburzyńska-Migaj^{4,B,E}, Agata Tymińska^{5,B,C},
Paweł Balsam^{5,A,B}, Krzysztof Ozierański^{5,B,C}, Agnieszka Kapłon-Cieślicka^{5,B,E}, Joanna Zaprutko^{6,B,C}, Jarosław Drożdż^{7,A,B,E,F}

¹ Department of Human Physiology, Medical University of Lodz, Poland

² State Higher Vocational School of Konin, Poland

³ Department of Internal Diseases and Clinical Pharmacology, Medical University of Lodz, Poland

⁴ 1st Department of Cardiology, Poznan University of Medical Sciences, Poland

⁵ 1st Chair and Department of Cardiology, Medical University of Warsaw, Poland

⁶ 2nd Department of Cardiology, Poznan University of Medical Sciences, Poland

⁷ Department of Cardiology, Medical University of Lodz, Poland

A – research concept and design; B – collection and/or assembly of data; C – data analysis and interpretation;

D – writing the article; E – critical revision of the article; F – final approval of the article

Advances in Clinical and Experimental Medicine, ISSN 1899–5276 (print), ISSN 2451–2680 (online)

Adv Clin Exp Med. 2019;28(10):1351–1358

Address for correspondence

Adam Poliwczak
E-mail: polczak@mp.pl

Funding sources

None declared

Conflict of interest

None declared

Received on August 13, 2018

Reviewed on December 9, 2018

Accepted on February 18, 2019

Published online on May 6, 2019

Cite as

Poliwczak R, Śmigiełski J, Bała A, et al. Treatment of heart failure in the elderly in Poland. The results of the Polish part of EURObservational Research Programme: The Heart Failure Pilot Survey. *Adv Clin Exp Med.* 2019;28(10):1351–1358. doi:10.17219/acem/104527

DOI

10.17219/acem/104527

Copyright

© 2019 by Wrocław Medical University

This is an article distributed under the terms of the Creative Commons Attribution Non-Commercial License (<http://creativecommons.org/licenses/by-nc-nd/4.0/>)

Abstract

Background. Pharmacotherapy remains the fundamental method of treating heart failure (HF). Treatment of the elderly is less based on the principles of evidence-based medicine (EBM) and doses do not reach the prescribed value.

Objectives. The aim of the study was to identify any distinct treatment of HF in the elderly compared to those under 65 years of age.

Material and methods. This study describes the Polish part of the EURObservational Research Programme: The Heart Failure Pilot Survey (ESC-HF Pilot). Eligibility to the program was limited to people with HF in 26 centers in Poland. After the first phase, more data was collected at 3 and 12 months. It covered a total of 893 people.

Results. Treatment of HF is conducted largely in accordance with the applicable guidelines. The percentage of people over 65 years of age who use angiotensin-converting-enzyme inhibitors/angiotensin-II receptor blockers (ACE-I/ARB), β -blockers and mineralocorticoid-antagonists remains high. Also, during the 12-month follow-up the frequency of the use of β -blockers did not decrease, and a decrease in the number subjects treated with ACE-I was compensated by increasing percentage of the use of ARB. A major problem also seems to be the appropriate treatment to prevent thromboembolic complications in the case of coexistence of atrial fibrillation (AF). There is a large group of older people who do not receive proper anticoagulation.

Conclusions. The study showed the existence of differences in the treatment of HF in the elderly. It partly does not proceed in accordance with the guidelines, especially in the presence of multiple comorbidities.

Key words: pharmacotherapy, elderly, heart failure treatment

Introduction

Despite significant progress, the length and quality of life of patients with heart failure (HF) remains insufficient. Heart failure is a major cause of hospitalization and disability in the elderly.^{1–4} In these patients, the prognosis deteriorates due to the coexistence of many other diseases. Making a proper diagnosis of HF based on the definition contained in the ESC guidelines may be problematic. Common symptoms such as shortness of breath, decreased exercise tolerance and peripheral edema may result from a variety of diseases.^{2–6} In clinical trials on HF treatment, older people, i.e., above 65 years, are underrepresented.^{7–10} Only a few of clinical trials have been dedicated to the elderly.¹¹ In previous studies, we found that treatment of the elderly is less based on the principles of EBM, and drug doses do not reach the prescribed value.^{12–14} Older people are more exposed to side effects and more at risk of possible interactions. This is related to changes in drug metabolism, impairment of kidney and liver function, and increased polypharmacy.¹⁵ Age is also an unfavorable prognostic factor in HF.¹⁶ According to the current standards, HF pharmacotherapy is based on ACE inhibitors/AT1 receptor-blockers, selected beta-blockers, mineralocorticoid receptor blockers, and ivabradine. It has been shown that these drug groups have a positive effect on prolonging survival. In addition, symptomatic and quality-of-life medicines are used, such as diuretics, digoxin and nitrates.³

Methods

This study describes the Polish part of the trial – EURObservational Research Programme: The Heart Failure Pilot Survey (ESC-HF Pilot). Its methodology has been described in previous publications.¹⁷ The study involved 136 cardiac centers in 12 European countries. In Poland, the study was conducted in 26 centers. Patients were enrolled between October 2009 and May 2010 and divided into 2 groups. The first group comprised patients who had previously been diagnosed with chronic HF and qualified during the next visit to the cardiology outpatient clinic. The second group consisted of patients admitted to hospital with acute HF, requiring administration of intravenous therapy with positive inotropic drugs, vasodilators and diuretics. There were no specific exclusion criteria of the study, except for age. All qualified patients had to be at least 18 years old. All participants expressed voluntary consent in accordance with the Declaration of Helsinki (1975) and the consent of the Commission of Bioethics, Medical University of Lodz (RNN/214/09/EC) was obtained. After the first phase, more data on the treatment and the fate of the participants was collected after 12 months.

The aim of this work was to analyze the treatment of HF and the use of additional treatment in the group of people

65 years of age and older in comparison with the rest of the population. We tried to find possible differences in the treatment of both groups.

Statistical methods

The data was verified for normality of distribution and equality of variances. The normality of the distribution was checked using the Shapiro-Wilk test. Comparison of gender, smoking status, place of treatment, HF etiology, presence of kidney disease, and other comorbidities, as well as population structure analysis was performed by using χ^2 test. The Student's t-test was used to compare the average age of participants. The statistical analysis was performed using STATISTICA v. 10 (StatSoft, Tulsa, USA). The results of the quantitative variables are presented as a mean \pm standard deviation (SD). Other results are presented as a percentage. The limit of statistical significance was set at $p < 0.05$.

Results

The study included a total of 893 people, including 650 (73%) hospitalized patients and 243 (27%) outpatients. The average age was 66.1 years (± 13.2 years). The basic information is summarized in Table 1. Women accounted for a total of 34% and men of 66% of all patients studied. Among outpatients, women accounted for 28%, men 72%. In the case of hospital patients, these proportions were 36% and 65%, respectively. Older people were characterized by a more severe HF assessed with the New York Heart Association Functional Classification (NYHA). Similarly, in the elderly, diabetes and atrial fibrillation (AF) were more common. Among patients with permanent AF, this was particularly evident in NYHA class II, where 19.15% of younger and 34.23% of the older patients were treated for this reason. There were no statistically significant differences in drug doses between patients with AF and sinus rhythm in individual age groups (Table 4).

Pharmacological treatment of patients at the time of inclusion in the study showed a statistically significant difference in the frequency of use of different groups of drugs. The study looked at the treatment that took place before the patient was enrolled into the study, during the initial observation and after 12 months.

In the case of ACE-I, any preparation from this group of drugs was taken by 69% younger patients and only 58% of people aged 65 ($p < 0.001$). Also, during the initial observation, this difference remained (82% vs 73%, $p < 0.005$). After 12 months of follow-up, 80% of younger patients and 68% of older patients were still taking ACE-I. The frequency of ARB adoption did not differ significantly, both before inclusion and during the study: it was 8% compared to 12% ($p = 0.760$) before inclusion and 11% compared to 12% ($p = 0.561$) at baseline for younger vs older patients.

Table 1. Basic characteristic of the studied population. It includes the percentage of women, etiologies of heart failure and the NYHA class, the place of treatment, the presence and basic treatment of diabetes and the presence and type of atrial fibrillation

Parameters	<65 years n = 386	≥65 years n = 507	p-value
Women	77 (20%)	223 (44%)	<0.001
CHF etiology:			
ischemic	182 (47%)	324 (64%)	<0.001
non-ischemic	204 (53%)	183 (36%)	<0.001
NYHA class:			
I	26 (7%)	14 (3%)	<0.001
II	156 (41%)	135 (27%)	<0.001
III	129 (34%)	260 (51%)	<0.001
IV	72 (19%)	97 (19%)	ns
Place of treatment:			
hospital	250 (65%)	400 (79%)	<0.001
outpatients	136 (35%)	107 (21%)	<0.001
Chronic kidney disease	42 (11%)	130 (26%)	<0.001
Smoking status:	n = 380	n = 487	
never	106 (28%)	248 (51%)	<0.001
current	76 (20%)	30 (6%)	<0.001
former	198 (52%)	209 (43%)	<0.001
Diabetes			
total	103 (27%)	195 (38%)	0.004
oral and diet	57 (15%)	107 (21%)	0.003
insulin	38 (10%)	79 (16%)	0.004
newly diagnosed	8 (2%)	9 (2%)	ns
Atrial fibrillation	n = 383	n = 507	
total	120 (31%)	241 (48%)	<0.001
paroxysmal	25 (7%)	75 (15%)	0.004
persistent	20 (5%)	29 (6%)	ns
permanent	75 (20%)	137 (27%)	0.005
Permanent atrial fibrillation vs sinus rhythm amount NYHA class n (%)			
I	0 (0%)/ 23 (100%)	2 (20%)/ 8 (80%)	ns
II	27 (19.15%)/ 114 (80.85%)	38 (34.23%)/ 73 (65.77%)	0.006
III	31 (30.10%)/ 72 (69.90%)	67 (32.84%)/ 137 (67.16%)	ns
IV	17 (25%)/ 51 (75%)	30 (38.96%)/ 47 (61.04%)	ns

After 12 months 16% of younger patients vs 21% of older ones ($p = 0.043$) continued to receive these drugs. Considering the frequency of using both classes of drugs together (ACE-I or ARB), before enrollment in the study, it was only 77% in the younger group and 69% in patients aged 65 years and older ($p < 0.001$). At baseline observation, it increased to 93% and 86%, respectively ($p = 0.006$). After 12 months, it was 96% and 89% ($p = 0.006$), respectively.

Another basic class of drugs for the treatment of HF was β -blockers. Before inclusion, frequency of β -blocker therapy was 77% in the group of younger and 69% in the group of older patients and they statistically differed significantly ($p = 0.007$). At baseline observation, the percentage of β -blocker therapy was 92% in younger patients and 89% in older ones, respectively, in both age groups. It did not differ statistically significantly ($p = 0.083$). After

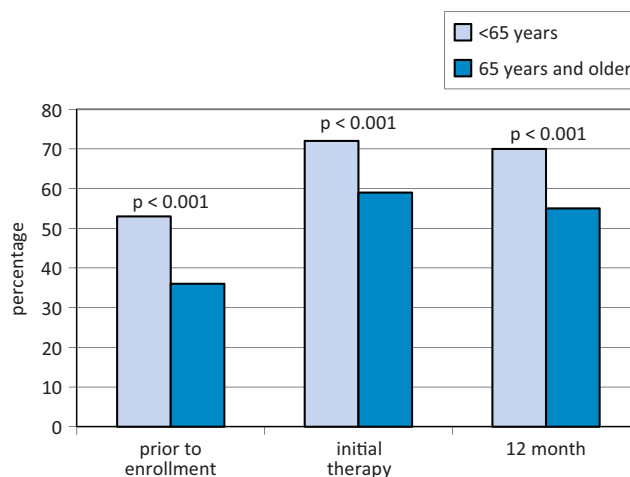


Fig. 1. The total use an aldosterone antagonist during the observation in different age groups

12 months, 93% of younger patients applied β -blockers vs 88% of the elderly. The difference again was statistically significant ($p < 0.005$).

In each step of the trial, we observed statistically significant more frequent use of aldosterone-antagonists in the younger group (Fig. 1).

In the case of diuretics, the frequency of their use did not differ significantly. It amounted, prior to enrollment, to 62% for younger patients and 63% for the elderly ($p = 0.745$). During initial observations, this frequency was respectively 83% vs 85% ($p = 0.466$). After 12 months, it was 74% vs 80% ($p = 0.241$). A relatively significant percentage of patients in both groups received a second diuretic, not an aldosterone-antagonist. Among those under 65 years of age, it was 10% compared to 5% for the group of patients 65 years and over ($p < 0.005$) prior to enrollment. In the initial observation, it increased to 25% vs 20% ($p = 0.093$).

Before inclusion, the percentage of patients treated with digoxin was 23% for younger ones and 16% for older ones ($p = 0.026$). During the initial follow-up, it was 33% and 24%, respectively. After 12 months, the proportion of patients treated with digoxin decreased to 27% in the younger patients and to 21% in the older group ($p = 0.062$).

Statins, which do not directly affect the course of HF treatment, are often used in the treatment of patients with HF. Before inclusion, the frequency of use of statins was the same, regardless of the age group – 54% for younger patients vs 53% for older ones ($p = 0.806$). During the initial observation, it increased to 65% vs 69% ($p = 0.160$), respectively. After 12 months, it remained high and amounted to 62% vs 62% ($p = 0.896$), respectively. On the other hand, the frequency of use of nitrates remained low. However, it was statistically significantly higher in the elderly 9% vs 21% ($p < 0.001$) prior to enrollment. During the initial follow-up, it was 13% for younger vs 27% for older patients ($p < 0.001$). After 12 months, in any age group, there was no longer anyone receiving nitrates. The percentage of people taking calcium channel blockers was

Table 2. The most commonly used drugs with basic groups in the treatment of heart failure. The division depending on the group of drugs, including ACE-I, ARB, beta-blockers, and aldosterone antagonists. Changes in the frequency of use of individual drugs during therapy

Medication		Prior to enrollment		Initial observation		After 12 months	
		<65 years [%]	≥65 years [%]	<65 years [%]	≥65 years [%]	<65 years [%]	≥65 years [%]
ACE-I	chinapril	3	3	3	2	1	2
	enalapril	7	10	3	4	2	8
	perindopril	15	22	14	15	14	13
	ramipril	60	51	68	65	71	65
	trandolapril	3	2	2	1	2	1
	lisinopril	3	4	3	2	5	4
	cilazapril	7	5	6	6	5	6
	captopril	2	3	1	5	0	0
ARB	losartan	50	68	51	56	41	44
	candesartan	28	7	23	5	29	10
	valsartan	9	17	21	32	24	40
	eprosartan	0	2	0	2	0	0
	telmisartan	9	7	5	5	5	6
	other	3	0	0	0	0	0
	Beta-blockers	carvedilol	55	41	58	47	57
metoprolol CR	19	20	19	19	16	12	
bisoprolol	19	31	18	28	22	30	
nebivolol	2	2	2	3	2	6	
other	5	6	3	3	3	4	
Aldosterone antagonists	spironolacton	80	89	76	84	68	85
	eplerenon	20	11	24	16	32	15

similar to the percentage of patients taking nitrates. It was higher in older people throughout the observation period. Before enrollment, 9% of younger patients were treated, compared to 15% in the older group ($p = 0.021$), and during the initial observation it increased up to 12% vs 18% ($p = 0.011$), respectively. Before enrollment into the study, half of the respondents took antiplatelet drugs. This percentage was 52% in the younger and 56% in the older group ($p = 0.231$). In the initial observation, it reached 61% vs 70% ($p = 0.006$), respectively. They are used more often by people over 65 years of age. After 12 months, it amounted to 60% vs 65% and did not differ significantly ($p = 0.197$). A similar percentage of people took oral anticoagulants prior to the study, i.e., 32% and 30% ($p = 0.474$), (younger vs older). In the initial follow-up, it was up to 43% vs 50% ($p = 0.530$), and after 12 months only 32% vs 34% ($p = 0.622$). A small percentage of patients with HF received antiarrhythmic drugs, mostly amiodarone. Also, a negligible percentage of patients received antidepressants. It was in fact 5% of younger patients vs 3% of older ones of patients ($p = 0.061$) prior to enrollment. In the initial observation, the percentage of people taking antidepressants was 8% of younger patients vs 4% of older ones ($p = 0.008$), being significantly higher in the younger group. A small percentage of patients received non-steroidal anti-inflammatory drugs. Before enrollment into the study, it amounted to 5% in the younger

and 7% in the older group ($p = 0.163$). In the initial observation, it did not change significantly and amounted to 2% vs 4% ($p = 0.181$), respectively. Taking into account the most important group of drugs involved in the HF treatment, Table 2 shows the most commonly used formulations of these groups of drugs. Table 3 presents the dose of the most commonly administered drugs that have been obtained in the register. The most commonly used ACE-I was ramipril and perindopril. Among ARBs, the most common was losartan, with a large proportion of valsartan and candesartan. Among β -blockers, the most commonly used preparation in each age group was carvedilol. Spironolactone is still a more frequently used preparation compared with the newer eplerenone.

The registry does not contain ivabradine and combinations of ARB and neprilysin inhibitor because at the time of data collection these drugs were not yet recommended for treatment of HF; they appeared only in the standards of ESC (2012 and 2016 version).^{3,18}

Discussion

The elderly require a specific approach in the treatment of HF. Despite the fact that in recent years social awareness about aging and older people in Europe has increased, in the case of treatment of HF, this is not fully reflected

Table 3. The average doses of individual preparations [mg] depending on the age of patients and changes in doses during therapy

Medication		Prior to enrollment		Initial observation		After 12 months	
		<65 years	≥65 years	<65 years	≥65 years	<65 years	≥65 years
ACE-I	enalapril	13 (n = 19)	16 (n = 27)	18 (n = 11)	19 (n = 16)	22 (n = 5)	16 (n = 18)
	perindopril	7 (n = 27)	6 (n = 54)	7 (n = 33)	6 (n = 46)	8 (n = 24)	7 (n = 27)
	ramipril	7 (n = 103)	7 (n = 102)	8 (n = 133)	8 (n = 161)	8 (n = 106)	8 (n = 110)
	trandolapril	2 (n = 5)	2 (n = 2)	2 (n = 5)	2 (n = 2)	2 (n = 4)	2 (n = 2)
	lisinopril	14 (n = 8)	13 (n = 13)	16 (n = 7)	15 (n = 7)	17 (n = 9)	16 (n = 8)
	captopril	38 (n = 2)	25 (n = 2)	50 (n = 1)	63 (n = 8)	–	–
ARB	losartan	49 (n = 15)	51 (n = 40)	51.4 (n = 22)	51 (n = 35)	53 (n = 18)	53 (n = 28)
	candesartan	12 (n = 9)	10 (n = 4)	12.6 (n = 10)	11 (n = 3)	10 (n = 12)	10 (n = 5)
	valsartan	107 (n = 3)	128 (n = 10)	106.7 (n = 9)	126 (n = 20)	108 (n = 10)	101 (n = 25)
	telmisartan	53 (n = 3)	60 (n = 4)	30.0 (n = 2)	53 (n = 3)	60 (n = 2)	50 (n = 4)
Beta-blockers	carvedilol	40 (n = 84)	35 (n = 34)	38 (n = 110)	32 (n = 55)	39 (n = 85)	32 (n = 58)
	metoprolol CR	75 (n = 56)	58 (n = 70)	70 (n = 66)	62 (n = 82)	88 (n = 41)	68 (n = 34)
	bisoprolol	6 (n = 40)	6 (n = 61)	6 (n = 45)	6 (n = 68)	7 (n = 43)	7 (n = 51)
	nebivolol	6 (n = 6)	5 (n = 3)	6 (n = 5)	5 (n = 7)	7 (n = 3)	5 (n = 11)
Aldosterone antagonists	spironolacton	37 (n = 164)	35 (n = 158)	47 (n = 210)	43 (n = 250)	39 (n = 129)	35 (n = 147)
	eplerenon	36 (n = 39)	33 (n = 20)	36 (n = 66)	31 (n = 46)	34 (n = 59)	29 (n = 27)

Table 4. The average doses of individual preparations [mg] depending on the age and atrial fibrillation status. There were no statistically significant differences in drug doses between patients with atrial fibrillation and sinus rhythm in individual age groups

Medication		<65 years		≥65 years	
		atrial fibrillation (permanent)	sinus rhythm	atrial fibrillation (permanent)	sinus rhythm
aACE-I	perindopril	4.9	6.0	5.6	5.5
	ramipril	4.8	5.7	5.3	5.5
ARB	losartan	37.5	46.2	56.3	50.0
	candesartan	16.5	11.0	8.0	12.0
	valsartan	120.0	–	112	133.3
Beta-blockers	carvedilol	27.5	26.0	20.1	17.8
	metoprolol CR	70.0	72.9	60.0	55.9
	bisoprolol	4.8	5.3	4.0	5.0

in the guidelines and recommendations on HF. In the European Society of Cardiology (ESC) recommendations in 2008,¹ only 1 paragraph is devoted to the treatment of HF in patients 65 years and older. Moreover, in the next update, from 2012 and 2016, it is not mentioned at all.^{3,18} The elderly are characterized by the frequent coexistence of various diseases. This was confirmed in our registry. Chronic kidney disease and diabetes occurred significantly more often. Also, in significantly more frequent cases, AF and HF were more advanced. This data is consistent with that obtained by Komajda et al.¹⁹ In this observation, patients older than 80 years were characterized by much more advanced changes and a higher incidence of comorbidities. Etiology of HF was consistent with previous observations. According to the POLCARD-HF registry conducted in Poland in 2003–2007, patients with HF and ischemic background were significantly older than those with non-ischemic cause of HF.²⁰

Treatment

One of the basic groups of drugs with proven efficacy used in the treatment of HF are ACE-I. The percentage of people treated with these preparations was high and statistically significantly different depending on the age group. At every stage of the follow-up, the percentage of people treated with ACE-I was higher in younger patients. Considering the use of ACE-I or ARB, the percentage of people taking these drugs was even higher, reaching over 95% in the younger group and almost 90% in the elderly. During the observation, the percentage of patients treated taking ACE-I declined, with a simultaneous increase in the use of the ARB. This may indicate the appearance of adverse effects of ACE-I, which led to a switch to an alternative therapy. The most troublesome adverse effect connected with ACE-I drugs is coughing. It occurs often, in from 5–21% to almost 50% of the treated

population.^{21–23} The frequency does not appear to depend on the age of the patients.²⁴ Perhaps this is one of the main reasons for the transition to the ARB treatment. The most important side effects of both ACE-I and ARBs include renal function deterioration. The studied elderly population was characterized by the presence of more than twice as frequent chronic kidney disease. This fact can decrease the frequency of use of ACE-I/ARBs. This may be one of the reasons for the existence of a group of patients who do not use any of these drug groups.

The most commonly used ACE-I in both age groups proved to be ramipril and perindopril. However, the doses of drugs recommended in the ESC guidelines for any of the preparations used were not achieved.^{3,14,18} These doses were similar and did not depend significantly on the age group. This fact concerning the Polish population coincided with the results obtained in the whole registry.¹⁷ As indicated by numerous publications, despite not achieving the recommended doses, the use of smaller doses also has a positive effect on the survival of patients with HF.^{25,26}

As in the case of the ACE-I/ARB, the frequency of used β -blockers also looks optimistic, reaching over 90% in younger and almost 90% in older patients. What is even more interesting is the fact that the frequency of β -blockers use did not decrease during the 12 month follow-up. Unfortunately, the drugs did not achieve recommended target dose. These observations are consistent with the general register.¹⁷ Of the 4 β -blockers with proven efficacy in the treatment of HF, only nebivolol is intended for the elderly population. Other β -blockers such as carvedilol, bisoprolol and metoprolol succinate do not show significant differences in the benefits derived from their use, depending on age. This is confirmed by a meta-analysis conducted by Dulin et al.²⁷ involving more than 12,000 patients. Similar results were obtained by Sin et al.²⁸ and Pascual-Figal et al.,²⁹ further indicating that this beneficial effect is not reduced in elderly patients with multiple comorbidities, including chronic obstructive pulmonary disease (COPD). Of course, special attention should be given to the correct initiation of treatment with β -blockers and possible side effects. Possible side effects did not translate into decreased frequency of β -blockers use after 12 months, remaining at a nearly 90% level. Among the β -blockers, carvedilol was the most common, regardless of the age group, which draws attention to a negligible proportion of patients treated with nebivolol despite SENIORS study results. In this case, there are no conditions capable of explaining this observation.

Among the aldosterone-antagonists, spironolactone still ranks highest in comparison to eplerenone. The frequency of the application of that class of drugs was significantly lower in older patients. This difference persisted throughout the observation period. After the publication of results research RALES³⁰ and EPHEsus^{31,32}, it became clear that they are a very valuable component in the treatment

of HF. Unfortunately, their use is limited by side effects, especially in the case of spironolactone. The most important side effect is connected to hyperkalemia, especially when combined with ACE-I/ARB. This risk considerably increases in the case of kidney damage, especially in creatinine clearance $50 < \text{mL/min}$, which is more common in older people.^{33,34} These people require more frequent monitoring of serum creatinine and potassium levels. A relatively high percentage of patients were treated with diuretics – loop or thiazide, of which 20% require 2 diuretics, not including aldosterone antagonists. This did not differ according to age. An interesting, though unexplained, issue remains the high percentage of people using these drugs in the younger age group. Perhaps this is due to a different etiology of HF, e.g., hypertension, where diuretics are one of the main therapeutic groups. This was consistent with the data for the entire registry, in which the frequency of the use of diuretics was 82%.¹⁷ In contrast, the frequency of diuretic therapy was less than that described by Komajda et al.,¹⁹ where it reached above 90%. Also, according to Zugck et al.,³⁵ the proportion of diuretics was 74.7–96.7%. The use of diuretics is associated with a number of possible side effects, including electrolyte disorder, deterioration of renal function and excessive dehydration.²⁴ Similarly, a relatively high percentage of people were treated with digoxin. Initially, it was 16% in the group of older people, and after 1 year of observation, it was even higher and amounted to 21%. A similar percentage of those using digoxin was noted by Cichocka-Radwan et al.³⁶ among people over 80 years of age, which was 13.7%. Interestingly, in our analysis, the frequency of digoxin use was higher in the group of younger people (under 65 years of age). Perhaps the explanation of this phenomenon should be sought in a greater number of diseases coexisting in the older age group, including disorders of kidney function, liver and electrolyte disorders that contraindicate this type of treatment.

One of the major problems in the treatment of HF is the coexistence of arrhythmias, particularly AF. The incidence of AF increases with age.^{37–39} In the general population aged 65 years and older, it is 7–8%, and 18% in the population over 85 years of age. The occurrence of AF significantly increases the risk of thromboembolic complications and requires additional treatment. According to the current guidelines, all individuals with HF aged 65 years or older require anticoagulation, preferably by means of oral anticoagulants. Also, most of the younger people, particularly women, also require such treatment in the absence of significant contraindications. In the present register, AF was present in almost half of the elderly, and nearly 1/3 of the younger patients. Oral anticoagulants in the 12 month follow-up were accepted by nearly 1/3 of younger patients and a similar percentage of elderly. As can be seen, there is a large group of older people who, despite the existence of clear indications, do not receive proper treatment. Perhaps this is due to the existence of contraindications or increased risk

of bleeding. This problem seems to require extra attention. What is positive is the less frequent treatment with drugs which lack proven efficacy, such as nitrates or digoxin. Unfortunately, there is still much to be done to achieve full implementation of the ESC recommendations. On the other hand, all the complex risks of pharmacotherapy in the elderly, with multiple comorbidities, should be taken into account. Elderly patients are also different from the younger ones in terms of their clinical profile, long-term prognosis and predictive factors.⁴⁰

Conclusions

The selected results described by the authors of the Polish part of the register of HF EURObservational Research Programme: The Heart Failure Pilot Survey (ESC-HF Pilot) do not differ from the results described for the entire registry. On this basis, we will attempt to put forth some conclusions:

1. The practice of treating HF is conducted largely in accordance with the applicable guidelines.
2. The percentage of people 65 years of age who use ACE-I/ARB, β -blockers and mineralocorticoid-antagonists remains high.
3. During the 12-month follow-up, the frequency of the use of β -blockers does not decrease, and a decrease in the number subjects treated with ACE-I is compensated by increasing percentage of the use of ARB.
4. A major problem seems to be the appropriate treatment to prevent thromboembolic complications in the case of AF coexistence. There is a large group of the elderly who do not receive proper anticoagulation.

Described attempts to draw wider conclusions are very cautious. The authors are aware of the limitations of the entire project. However, our study will contribute to improving both the efficiency and safety of the treatment of HF in the elderly in Poland.

ORCID iDs

Adam Rafał Poliwczyk  <https://orcid.org/0000-0002-5281-0318>
 Janusz Śmigieński  <https://orcid.org/0000-0003-0274-1446>
 Agnieszka Bała  <https://orcid.org/0000-0002-8060-524X>
 Ewa Straburzyńska-Migaj  <https://orcid.org/0000-0002-0545-3370>
 Agata Tymińska  <https://orcid.org/0000-0002-6195-1024>
 Paweł Balsam  <https://orcid.org/0000-0003-0441-8976>
 Krzysztof Ozierański  <https://orcid.org/0000-0002-3848-0922>
 Agnieszka Kapłon-Cieślicka  <https://orcid.org/0000-0003-2020-3027>
 Joanna Zaprutko  <https://orcid.org/0000-0001-9869-2428>
 Jarosław Drożdż  <https://orcid.org/0000-0002-0732-2104>

References

1. Dickstein K, Cohen-Solal A, Filippatos G, et al; ESC Committee for Practice Guidelines (CPG). ESC Guidelines for the diagnosis and treatment of acute and chronic heart failure 2008. The Task Force for the Diagnosis and Treatment of Acute and Chronic Heart Failure 2008 of the European Society of Cardiology. Developed in collaboration with the Heart Failure Association of the ESC (HFA) and endorsed by the European Society of Intensive Care Medicine (ESICM). *Eur J Heart Fail.* 2008;10(10):933–989.
2. Hunt SA, Abraham WT, Chin MH, et al. 2009 focused update incorporated into the ACC/AHA 2005 Guidelines for the Diagnosis and Management of Heart Failure in the Adults: A report of the American College of Cardiology Foundation/American Heart Association Task Force on Practice Guidelines. Developed in collaboration with the International Society for Heart and Lung Transplantation. *Circulation.* 2009;119(14):e391–479. doi:10.1161/CIRCULATIONAHA.109.192065
3. Ponikowski P, Voors AA, Anker SD, et al; ESC Scientific Document Group. 2016 ESC Guidelines for the diagnosis and treatment of acute and chronic heart failure: The Task Force for the diagnosis and treatment of acute and chronic heart failure of the European Society of Cardiology (ESC). Developed with the special contribution of the Heart Failure Association (HFA) of the ESC. *Eur Heart J.* 2016;37(27):2129–2200.
4. Manzano L, Escobar C, Cleland JG, Flather M. Diagnosis of elderly patients with heart failure. *Eur J Heart Fail.* 2012;14(10):1097–1103.
5. van Riet EE, Hoes AW, Limburg A, Landman MA, van der Hoeven H, Rutten FH. Prevalence of unrecognized heart failure in older persons with shortness of breath on exertion. *Eur J Heart Fail.* 2014;16(7):772–777. doi:10.1002/ejhf.110
6. Díez-Villanueva P, Alfonso F. Heart failure in the elderly. *J Geriatr Cardiol.* 2016;13:115–117. doi:10.11909/j.issn.1671-5411.2016.02.009
7. Jha SR, Ha HS, Hickman LD, et al. Frailty in advanced heart failure: A systematic review. *Heart Fail Rev.* 2015;20:553–560. doi:10.1007/s10741-015-9493-8
8. Metra M, Cotter G, El-Khorazaty J, et al. Acute heart failure in the elderly: Differences in clinical characteristics, outcomes, and prognostic factors in the VERITAS Study. *J Card Fail.* 2015;21:179–188. doi:10.1016/j.cardfail.2014.12.012
9. Mahjoub H, Rusinaru D, Soulière V, Durier C, Peltier M, Tribouilloy C. Long-term survival in patients older than 80 years hospitalized for heart failure. A 5-year prospective study. *Eur J Heart Fail.* 2008;10(1):78–84.
10. Cherubini A, Oristrell J, Pla X, et al. The persistent exclusion of older patients from ongoing clinical trials regarding heart failure. *Arch Intern Med.* 2011;171(6):550–556. doi:10.1001/archinternmed.2011.31
11. Flather MD, Shibata MC, Coats AJ, et al; SENIORS Investigators. Randomized trial to determine the effect of nebivolol on mortality and cardiovascular hospital admission in elderly patients with heart failure. *Eur Heart J.* 2005;26(3):215–225.
12. Gustafsson F, Torp-Pedersen C, Seibaek M, Burchardt H, Kober L; DIAMOND study group. Effect of age on short and long-term mortality in patients admitted to hospital with congestive heart failure. *Eur Heart J.* 2004;25(19):1711–1717.
13. Cohen-Solal A, Desnos M, Delahaye F, Emeriau JP, Hanania G. A national survey of heart failure in French hospitals. The Myocardopathy and Heart Failure Working Group of the French Society of Cardiology, the National College of General Hospital Cardiologists and the French Geriatrics Society. *Eur Heart J.* 2000;21(9):763–769.
14. Rywik TM, Kołodziej P, Targoński R, et al. Characteristics of the heart failure population in Poland: ZOPAN, a multicentre national programme. *Kardiologia Pol.* 2011;69(1):24–31.
15. Sztramko R, Chau V, Wong R. Adverse drug events and associated factors in heart failure therapy among the very elderly. *Can Geriatr J.* 2011;14(4):79–92.
16. Zaprutko J, Michalak M, Nowicka A, et al. Hospitalization length and prognosis in heart failure patients. *Kardiologia Pol.* 2017;75(4):519–526. doi:10.5603/KP.a2017.0088
17. Maggioni AP, Dahlström U, Filippatos G, et al; Heart Failure Association of ESC (HFA). EURObservational Research Programme: The Heart Failure Pilot Survey (ESC-HF Pilot). *Eur Heart J.* 2010;31:1023–1031.
18. McMurray JJ, Adamopoulos S, Anker SD, et al; ESC Committee for Practice Guidelines. ESC Guidelines for the diagnosis and treatment of acute and chronic heart failure 2012: The Task Force for the Diagnosis and Treatment of Acute and Chronic Heart Failure 2012 of the European Society of Cardiology. Developed in collaboration with the Heart Failure Association (HFA) of the ESC. *Eur Heart J.* 2012;33(14):1787–1847.
19. Komajda M, Hanon O, Hochadel M, et al. Contemporary management of octogenarians hospitalized for heart failure in Europe: Euro Heart Failure Survey II. *Eur Heart J.* 2009;30(4):478–486.
20. Zieliński T, Kurjata P, Korewicki J; participants of POLKARD-HF. Prognosis in patients with severe heart failure referred for heart transplantation-POLKARD-HF 2003–2007. *Int J Cardiol.* 2010;145(2):242–244.

21. Gokhale M, Girman C, Chen Y, Pate V, Funk MJ, Stürmer T. Comparison of diagnostic evaluations for cough among initiators of angiotensin converting enzyme inhibitors and angiotensin receptor blockers. *Pharmacoepidemiol Drug Saf.* 2016;25(5):512–520. doi:10.1002/pds.3977
22. Hallberg P, Nagy J, Karawajczyk M, et al. Comparison of clinical factors between patients with angiotensin-converting enzyme inhibitor-induced angioedema and cough. *Ann Pharmacother.* 2017;51(4):293–300. doi:10.1177/1060028016682251
23. Woo KS, Nicholls MG. High prevalence of persistent cough with angiotensin converting enzyme inhibitors in Chinese. *Br J Clin Pharmacol.* 1995;40(2):141–144.
24. Rich MW. Pharmacotherapy of heart failure in the elderly: Adverse events. *Heart Fail Rev.* 2012;17(4–5):589–595.
25. Packer M, Poole-Wilson PA, Armstrong PW, et al. Comparative effects of low and high doses of the angiotensin-converting enzyme inhibitor, lisinopril, on morbidity and mortality in chronic heart failure. ATLAS Study Group. *Circulation.* 1999;100(23):2312–2318.
26. Demers C, Mody A, Teo KK, McKelvie RS. ACE inhibitors in heart failure: What more do we need to know? *Am J Cardiovasc Drugs.* 2005;5(6):351–359.
27. Dulin BR, Haas SJ, Abraham WT, Krum H. Do elderly systolic heart failure patients benefit from beta blockers to the same extent as the non-elderly? Meta-analysis of 12,000 patients in large-scale clinical trials. *Am J Cardiol.* 2005;95(7):896–898.
28. Sin DD, McAlister FA. The effects of beta-blockers on morbidity and mortality in a population-based cohort of 11,942 elderly patients with heart failure. *Am J Med.* 2002;113(8):650–656.
29. Pascual-Figal DA, Redondo B, Caro C, et al. Comparison of late mortality in hospitalized patients >70 years of age with systolic heart failure receiving beta blockers versus those not receiving beta blockers. *Am J Cardiol.* 2008;102(12):1711–1717. doi:10.1016/j.amjcard.2008.07.059
30. Pitt B, Zannad F, Remme WJ, et al. The effect of spironolactone on morbidity and mortality in patients with severe heart failure. Randomized Aldactone Evaluation Study Investigators. *N Engl J Med.* 1999;341(10):709–717.
31. Pitt B, Remme W, Zannad F, et al; Eplerenone Post-Acute Myocardial Infarction Heart Failure Efficacy and Survival Study Investigators. Eplerenone, a selective aldosterone blocker, in patients with left ventricular dysfunction after myocardial infarction. *N Engl J Med.* 2003;348(14):1309–1321.
32. Krum H, Shi H, Pitt B, et al; EMPHASIS-HF Study Group. Clinical benefit of eplerenone in patients with mild symptoms of systolic heart failure already receiving optimal best practice background drug therapy: Analysis of the EMPHASIS-HF study. *Circ Heart Fail.* 2013;6(4):711–718. doi:10.1161/CIRCHEARTFAILURE.112.000173
33. Juurlink DN, Mamdani MM, Lee DS, et al. Rates of hyperkalemia after publication of the randomized aldactone evaluation study. *N Engl J Med.* 2004;351(6):543–551.
34. Eschalier R, McMurray JJ, Swedberg K, et al; EMPHASIS-HF Investigators. Safety and efficacy of eplerenone in patients at high risk for hyperkalemia and/or worsening renal function: Analyses of the EMPHASIS-HF study subgroups (Eplerenone in Mild Patients Hospitalization And Survival Study in Heart Failure). *J Am Coll Cardiol.* 2013;62(17):1585–1593. doi:10.1016/j.jacc.2013.04.086
35. Zugck C, Franke J, Gelbrich G, et al. Implementation of pharmacotherapy guidelines in heart failure: Experience from the German Competence Network Heart Failure. *Clin Res Cardiol.* 2012;101(4):263–272.
36. Cichoń-Radwan A, Lelonek M. Annual prognostic factors in chronic heart failure in patients over 80 years old. *Kardiol Pol.* 2017;75(2):164–173.
37. Chugh SS, Havmoeller R, Narayanan K, et al. Worldwide epidemiology of atrial fibrillation: A Global Burden of Disease 2010 Study. *Circulation.* 2014;129(8):837–847.
38. Fitzmaurice DA, Hobbs FD, Jowett S, et al. Screening versus routine practice in detection of atrial fibrillation in patients aged 65 or over: Cluster randomized controlled trial. *BMJ.* 2007;335(7616):383.
39. Schnabel RB, Yin X, Gona P, et al. 50-year trends in atrial fibrillation prevalence, incidence, risk factors, and mortality in the Framingham Heart Study: A cohort study. *Lancet.* 2015;386(9989):154–162.
40. Ozierański K, Balsam P, Tymińska A, et al. Heart failure in elderly patients: Differences in clinical characteristics and predictors of 1-year outcome in the Polish ESC-HF Long-Term Registry. *Pol Arch Med Wewn.* 2016;126(7–8):502–513.

A large single-institution retrospective analysis of aggressive B-cell lymphomas according to the 2016/2017 WHO classification

*Dorota Jesionek-Kupnicka^{1,A–D,F}, *Marcin Braun^{1,2,A–D,F}, Tadeusz Robak^{3,E,F}, Wojciech Kuncman^{1,E,F}, Radzislav Kordek^{1,E,F}

¹ Department of Pathology, Chair of Oncology, Medical University of Lodz, Poland

² Postgraduate School of Molecular Medicine, Medical University of Warsaw, Poland

³ Department of Hematology, Medical University of Lodz, Poland

A – research concept and design; B – collection and/or assembly of data; C – data analysis and interpretation;

D – writing the article; E – critical revision of the article; F – final approval of the article

Advances in Clinical and Experimental Medicine, ISSN 1899–5276 (print), ISSN 2451–2680 (online)

Adv Clin Exp Med. 2019;28(10):1359–1365

Address for correspondence

Marcin Braun

E-mail: braunmarcin@gmail.com

Funding sources

None declared

Conflict of interest

None declared

* These authors contributed equally to this work.

Received on August 27, 2018

Reviewed on March 10, 2019

Accepted on May 7, 2019

Published online on September 12, 2019

Cite as

Jesionek-Kupnicka D, Braun M, Robak T, Kuncman W, Kordek R. A large single-institution retrospective analysis of aggressive B-cell lymphomas according to the 2016/2017 WHO classification. *Adv Clin Exp Med.* 2019;28(10):1359–1365. doi:10.17219/acem/109200

DOI

10.17219/acem/109200

Copyright

© 2019 by Wrocław Medical University

This is an article distributed under the terms of the Creative Commons Attribution Non-Commercial License (<http://creativecommons.org/licenses/by-nc-nd/4.0/>)

Abstract

Background. High-grade B-cell lymphomas (HGBLs) comprise a new entity in the revised 2016/2017 World Health Organization Classification of Tumours of Haematopoietic and Lymphoid Tissues. The diagnosis of HGBL encompasses histopathology and immunohistochemistry, with additional molecular examination of the *BCL2/MYC* or *BCL6/MYC* rearrangement status.

Objectives. The aim of the study was to summarize our experience in the histopathological and immunohistochemical diagnosis of patients with aggressive B-cell lymphomas according to the revised 2016/2017 WHO classifications.

Material and methods. We reviewed our single-institution experience with accurate diagnoses of HGBL and diffuse large B-cell lymphoma (DLBCL) using the available histopathological and immunohistochemical tools. The timeframe was from January 1, 2017 to April 18, 2018.

Results. Out of 265 patients, 217 (81.9%) were diagnosed with DLBCL, 43 (16.2%) with HGBL/DLBCL and 5 (1.9%) with not otherwise specified HGBL (HGBL-NOS). Regarding concurrent expression of MYC and BCL2 and/or BCL6 (double expressors (DE) and triple expressors (TE)), more DE and TE cases were found in the HGBL/DLBCL group than in the DLBCL group (25.53% vs 8.47%, $p < 0.001$, for DE cases and 55.32% vs 6.21%, $p < 0.001$, for TE cases). All 48 (100.00%) of the HGBL-NOS and HGBL/DLBCL patients, and 26 (11.98%) of the DLBCL-DE/TE cases were recommended for molecular analysis.

Conclusions. Our findings show that a comprehensive histopathological and immunohistochemical examination may identify potential HGBL cases. This study emphasizes the need to introduce a suitable molecular examination for patients with HGBL morphology and/or double/triple expression of BCL2/BCL6/MYC proteins.

Key words: DLBCL, World Health Organization (WHO) 2016/2017 Classification Of Tumours Of Haematopoietic and Lymphoid Tissues, DLBCL/BL, HGBL, high grade B-cell lymphoma/diffuse large B-cell lymphoma

The revised 2016/2017 World Health Organization (WHO) Classification of Tumours of Haematopoietic and Lymphoid Tissues included new entities among aggressive B-cell lymphomas.^{1,2} The most significant changes were introduced by distinguishing a new category of high grade B-cell lymphomas (HGBLs), which were mainly derived from previous provisional categories, including unclassifiable B-cell lymphomas with features intermediate between diffuse large B-cell lymphoma (DLBCL) and Burkitt's lymphoma (BL) (BCLU), as well as from DLBCLs of classic morphology.^{1,2}

The HGBL category was created based on the differences between its pathogenesis and clinico-pathological features and those of DLBCL or BL.²⁻⁴ The poorer prognosis among HGBL patients in comparison to those with DLBCL or BL established a strong need to develop novel, more intensive therapies, as the standard regimen of rituximab, cyclophosphamide, vincristine, and doxorubicin (R-CHOP) is ineffective in HGBL patients.^{3,5-11} Although this new category is still highly heterogeneous, it creates an opportunity for a more accurate diagnosis and may ultimately lead to better treatment allocation or facilitate the search for new treatment strategies in randomized clinical trials.

An accurate diagnosis of HGBL encompasses standard histopathological and immunohistochemical analyses combined with molecular examination.^{2,4} Recently, Szumera-Ciećkiewicz et al. comprehensively summarized the current practical guidelines on differential diagnosis of aggressive B-cell lymphomas, including the proper differentiation of HGBL.⁴ In brief, the current protocols for DLBCL/HGBL/BL diagnosis require the following to be determined: 1) the morphology of the lymphoma cells; 2) the cell of origin (COO), using the immunohistochemistry-based Hans protocol; 3) an immunohistochemical analysis of BCL2, BCL6 and MYC expression, as well as Tdt and cyclin D1/SOX11 in cases with blastoid morphology; and 4) a fluorescent in situ examination of *BCL2/MYC* or *BCL6/MYC* rearrangements (Table 1).^{1,2,4} While the first

3 requirements are widely available in Polish histopathology laboratories, there is a deficiency in access to proper molecular examinations.

In this study we aimed to conduct a large retrospective single-institutional report on the morphological and immunohistochemical diagnosis of aggressive B-cell lymphomas in light of the revised 2016/2017 World Health Organization (WHO) Classification of Tumours of Haematopoietic and Lymphoid Tissues.

The work described in this article was carried out in accordance with the Code of Ethics of the World Medical Association (Declaration of Helsinki) for experiments involving humans; EU Directive 2010/63/EU for animal experiments; and uniform requirements for manuscripts submitted to biomedical journals.

Patients and methods

Study cohort

All aggressive B-cell lymphoma cases diagnosed at the Department of Pathology, Chair of Oncology, Medical University of Lodz, Poland, between January 1, 2017 and April 18, 2018 were included in the analysis. The review was restricted to cases classified as HGBL not otherwise specified (HGBL NOS – cases with clear blastoid morphology or not meeting the criteria for standard DLBCL or BL – Table 1), DLBCL and HGBL/DLBCL (a category for cases which in histopathological and immunohistochemical analysis appear to be HGBL, but no molecular confirmation was accessible). Formalin-fixed paraffin-embedded (FFPE) samples were collected, along with hematoxylin and eosin (H&E) and immunohistochemical slides. Finally, pathological data obtained from the patients was extracted into a pre-prepared Excel (v. 1907, Office 365; Microsoft Corp., Redmond, USA) spreadsheet. The required data encompassed the patient's age at diagnosis, sex, diagnosis,

Table 1. High grade B-cell lymphoma (HGBL) subtypes and diagnostic criteria according to the 2016/2017 WHO Classification of Tumours of Haematopoietic and Lymphoid Tissues

Subtype	Morphology features	Immunohistochemistry	FISH analysis for <i>BCL2/MYC</i> or <i>BCL6/MYC</i> rearrangements	Most common diagnosis according to the previous 2008 WHO classification
HGBL, NOS	Mandatory for diagnosis; blastoid or Burkitt-like (between BL and DLBCL)	GCB to ABC ratio ~ 2:1; DE/TE – most cases; negative for TdT and cyclin D1/SOX11	Not mandatory for diagnosis	DLBCL/BL
HGBL, DH/TH	Not mandatory for diagnosis; DLBCL – most cases, blastoid or Burkitt-like (between BL and DLBCL)	GCB – most cases, DE/TE – most cases, negative for TdT and cyclin D1/SOX11	Mandatory for diagnosis; positive for <i>BCL2/MYC</i> or <i>BCL6/MYC</i> rearrangement present	DLBCL
HGBL, DH/TH, transformed from FL	Mandatory for diagnosis; history of follicular lymphoma, DLBCL – most cases	GCB – most cases, DE/TE – most cases, negative for TdT and cyclin D1/SOX11	Mandatory for diagnosis; positive for <i>BCL2/MYC</i> or <i>BCL6/MYC</i> rearrangement present	DLBCL

NOS – not otherwise specified; DH – double-hit; TH – triple hit; GCB – germinal center B-cell phenotype; ABC – activated B-cell phenotype; DE – double expressor; TE – triple expressor; FISH – fluorescent in-situ hybridization; DLBCL/BL – unclassifiable B-cell lymphomas with features intermediate between diffuse large B-cell lymphoma (DLBCL) and Burkitt's lymphoma (BL).

morphology, the results of immunohistochemical analysis including COO classification, Ki67 proliferation index, as well as BCL2, BCL6 and MYC expression.

Pathological diagnostic approach

Since January 1, 2017, our institution has followed a new diagnostic protocol for all aggressive B-cell lymphomas. The protocol is in accordance with the 2016/2017 WHO Classification of Tumours of Haematopoietic and Lymphoid Tissues. In this protocol a diagnostic report of a lymphoma encompasses: 1) morphological texture (e.g., “high grade B-cell lymphoma with blastoid morphology”); 2) immunophenotype along with Ki67 proliferation index; 3) COO: germinal center B-cell phenotype (GCB) or activated B-cell phenotype (ABC), according to the Hans protocol¹²; 4) the status of immunoexpression of BCL2, BCL6 and/or MYC proteins (double expressor, triple expressor, non-double expressor); 5) a conclusion, including an indication whether the patient needs an additional molecular examination (e.g., “According to the 2016/2017 WHO

Classification of Tumours of Haematopoietic and Lymphoid Tissues, an additional fluorescence in situ hybridization (FISH) analysis should be performed on the sample for differential diagnosis between DLBCL and HGBL, DH/TH”). Examples of HGBL/DLBCL cases are shown in Fig. 1,2.

Immunohistochemistry

The standard panel of antibodies examined in patients with DLBCL, BL and HGBL covered CD20, CD3, BCL2, BCL6, MYC, CD10, MUM1, Ki67, cyclin D1, SOX11, TdT, CD5, CD38, and PAX5 (BSAP). Clones of the antibodies along with the manufacturers are listed in Table 2. Immunohistochemical analysis used monoclonal antibodies (FLEX Monoclonal Mouse Anti-Human, Dako A/S, Glostrup, Denmark) and EnVisionTMFLEX+ (Dako A/S) for the visualization. The tests were carried out using Autostainer Link 48 (Dako A/S).

The expression for all markers was reported as positive or negative, but for BCL2, BCL6, MYC, and Ki67 detailed

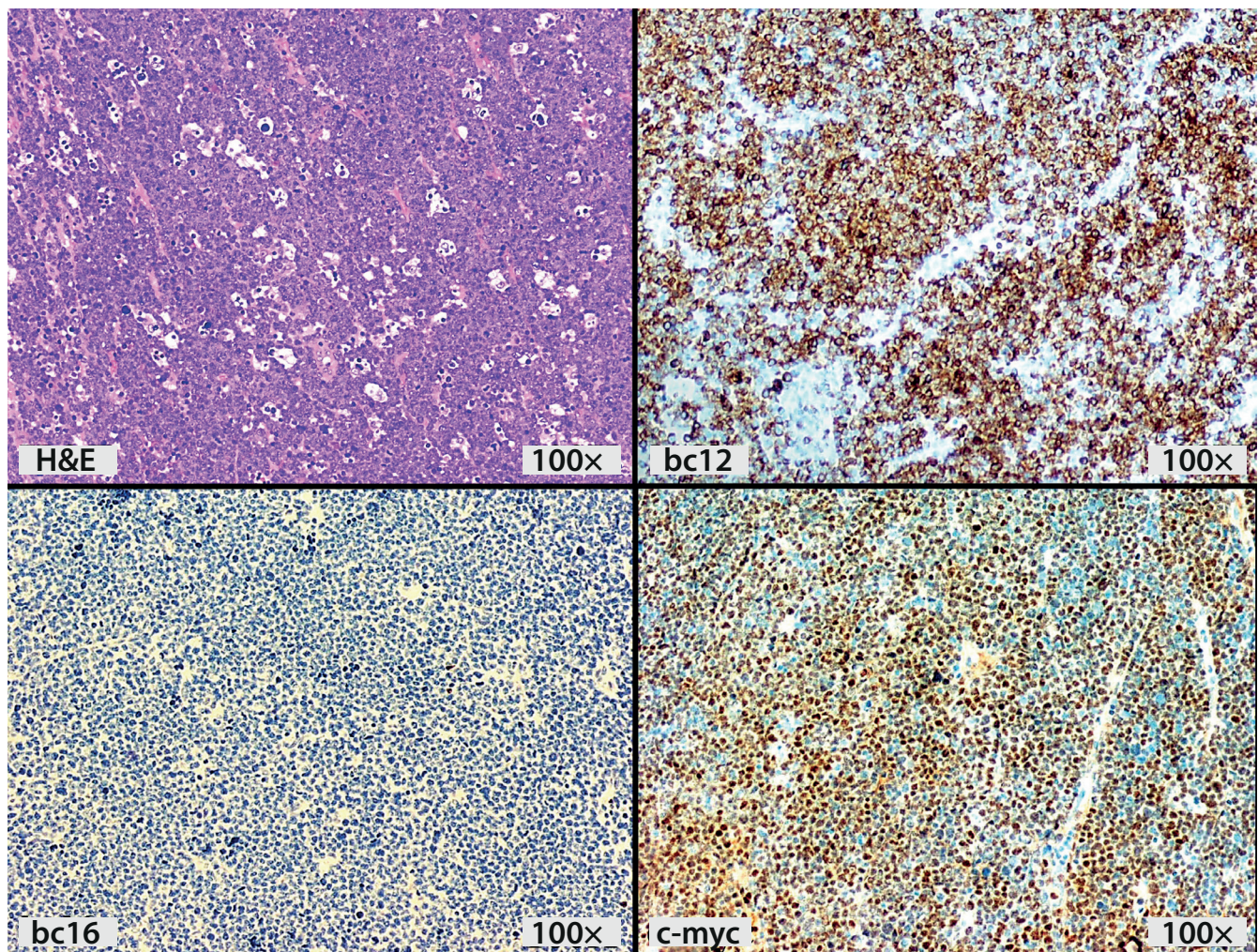


Fig. 1. Histopathological example of a high grade B-cell lymphoma not otherwise specified (HGBL NOS) with the starry-sky pattern. The case was of germinal center B-cell phenotype origin and revealed BCL2 and MYC expression without expression of BCL6

DE – double expressor.

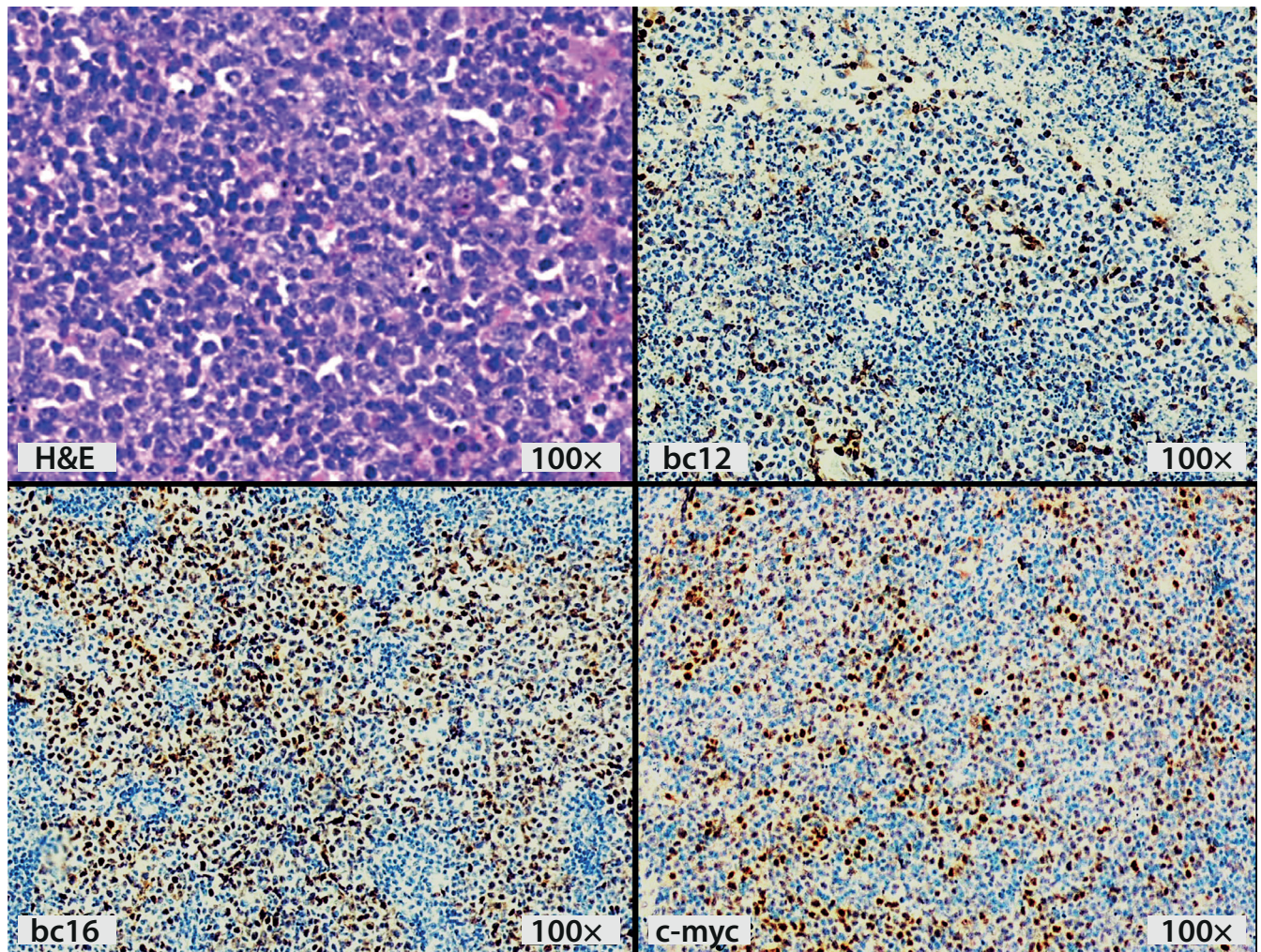


Fig. 2. Histopathological example of a high grade B-cell lymphoma not otherwise specified (HGBL NOS) with blastoid morphology. The case was of germinal center B-cell phenotype, revealed BCL6 and MYC expression without expression of BCL2 and was negative for TdT

DE – double expressor.

Table 2. List of antibodies used in the immunohistochemical analysis

Antibody	Clone	Company
BCL2	124	Dako
BCL6	PG-B6p	Dako
BSAP (PAX-5)	DAK-Pax5	Dako
CD3	Polyclonal rabbit	Dako
CD5	4C7	Dako
CD10	56C6	Dako
CD20	L26	Dako
CD38	SP149	Cell Marque
Cyclin D1	EP12	Dako
MYC	Y69	VENTANA
Ki-67	MIB-1	Dako
MUM-1	MUM1p	Dako
SOX-11	MRQ-58	Cell Marque
TdT	EP266	Dako

percentages of positive cells were reported in brackets. Cases were marked as positive under the following conditions: when more than 50% of the lymphoma cells were stained with anti-BCL2 antibody (cytoplasmic and nuclear staining), when more than 30% of the lymphoma cells were stained with BCL6 (nuclear staining) or when more than 40% of the lymphoma cells were stained with MYC (nuclear staining). The immunohistochemistry results were validated using positive and negative tissue controls in the whole series of immunostained slides.

Statistical analysis

Continuous variables were presented as medians followed by interquartile range (IQR), while nominal variables were presented as numbers followed by percentages in brackets. The Shapiro–Wilk test was used to assess the normality of distribution. Continuous variables were compared using the Mann–Whitney U test in case of non-normal distribution. Differences between categorical

variables were evaluated using the χ^2 or two-tailed Fisher's exact tests. The STATISTICA v. 12.5 PL software package (Statsoft Inc., Tulsa, USA) was used for the analysis. P-values <0.05 were considered statistically significant.

Results

Patients characteristics

Between January 1, 2017 and April 18, 2018, 265 patients were diagnosed with either DLBCL (n = 217, 81.88%), HGBL, NOS (n = 5, 1.89%), or HGBL/DLBCL (n = 43, 16.23%). The median age of the whole group was 69 years (IQR = 61.12–77.77). The HGBL/DLBCL patients were older than DLBCL patients; however, this result was not statistically significant. Almost ½ of the patients in each group were males.

All HGBL NOS cases presented a blastoid-pattern morphology and were either double or triple expressors. Due to the small number of cases, all 5 HGBL NOS cases were included with the HGBL/DLBCL patients. The details of the study group, along with comparisons between the DLBCL and HGBL/DLBCL patients, are presented in Table 3.

Table 3. Characteristics of the HGBL/DLBCL and DLBCL study population. Quantitative variables are presented as medians followed by quartiles in brackets and as numbers followed by percentages in brackets

Variable	HGBL/DLBCL (n = 48, 18.12%)	DLBCL (n = 217, 81.88%)	p-value (test)	Whole group (n = 265, 100.00%)
Age [years]	72.16 (64.28–80.19)	68.73 (60.57–76.15)	0.086 (Mann–Whitney U test)	68.89 (61.12–77.77)
Sex (males)	21 (45.65%)	99 (46.26%)	0.940 (χ^2)	120 (46.15%)
Hematology Center				
KMH	33 (68.75%)	99 (45.62%)	0.004 (χ^2)	132 (49.81%)
EC	15 (31.25%)	118 (54.38%)		133 (50.19%)
HGBL, NOS	5 (10.41%)	NA	NA	5 (1.89%)
Morphology				
blastoid	6 (12.50%)	NA	NA	6 (2.26%)
BL/DLBCL	14 (29.17%)	NA		14 (5.28%)
DLBCL	28 (58.33%)	245 (100.00%)		245 (92.45%)
Cell of origin				
GCB	14 (29.79%)	82 (40.20%)	0.186 (χ^2)	96 (38.25%)
ABC	33 (70.21%)	122 (59.80%)		155 (61.75%)
BCL2 (positive)	41 (87.23%)	115 (59.90%)	<0.001 (χ^2)	156 (65.27%)
BCL6 (positive)	34 (72.34%)	137 (66.83%)	0.466 (χ^2)	171 (67.86%)
MYC (positive)	38 (80.85%)	29 (16.48%)	<0.001 (χ^2)	67 (30.04%)
DE (positive)				
BCL2/MYC	9 (19.15%)	10 (5.65%)	0.005 (χ^2)	19 (8.48%)
BCL6/MYC	3 (6.38%)	5 (2.82%)		8 (3.57%)
TE (positive)	26 (55.32%)	11 (6.21%)	<0.001 (χ^2)	37 (16.52%)
Ki67 index	95.00 (90.00–100.00)	90.00 (75.00–90.00)	<0.001 (Mann–Whitney U test)	90.00 (80.00–95.00)

HGBL – high grade B-cell lymphoma; NOS – not otherwise specified; BL – Burkitt's lymphoma; GCB – germinal center B-cell phenotype; ABC – activated B-cell phenotype; DLBCL – diffuse large B-cell lymphoma; NA – not applicable; KMH – Kopernik Memorial Hospital; EC – external oncological centers; DE – double expressor; TE – triple expressor.

Lymphoma morphology

Within the HGBL/DLBCL group, 6 patients (12.50%) presented with partially blastoid morphological features, and 14 patients (29.17%) presented with BL morphological features, while more than ½ presented with standard DLBCL morphology (mainly centroblastic or immunoblastic).

Comparison of cell of origin of lymphomas and Ki67 index

The majority of the lymphomas displayed an immunophenotype characteristic of ABCs. This tendency was stable regardless of the study group. There were 33 ABCs (70.21%) in the HGBL/DLBCL group and 122 ABCs (59.80%) in the DLBCL group (p = 0.186).

The Ki67 proliferation index in the whole study group was high: 90% (IQR = 80–95%). It differed significantly between HGBL/DLBCL and DLBCL patients: 95% (90–100%) vs 90.00% (75–90%), respectively (p < 0.001).

Comparison of BCL2, BCL6 and MYC expression

The majority of the lymphomas studied displayed positivity for BCL2 and BCL6 expression: n = 156 (65.27%) and n = 171 (67.86%), respectively; and 67 patients (30.04%) were positive for MYC expression. The percentage of BCL6-positive lymphomas did not differ significantly between the study groups (p = 0.466). However, HGBL/DLBCL cases were more frequently BCL2-positive and MYC-positive than DLBCL cases: 41 (87.23%) vs 115 (59.90%) BCL2-positive cases (p < 0.001) and 38 (80.85%) vs 29 (16.48%) MYC-positive cases (p < 0.001).

Regarding concurrent expression of MYC and BCL2 and/or BCL6, more DE and TE cases were found in the HGBL/DLBCL group than in the DLBCL group: 12 (25.53%) vs 15 (8.47%) DE cases (p < 0.001) and 26 (55.32%) vs 11 (6.21%) TE cases (p < 0.001); DE and TE cases comprised 54 (20.40%) of the patients in the study.

Patients recommended for molecular analysis

We recommended fluorescence in situ hybridization (FISH) analysis for identifying *BCL2/MYC* and

BCL6/MYC rearrangements in all 48 (100%) of the HGBL/DLBCL cases and in 26 (11.98%) of the DLBCL cases, i.e., 74 (27.92%) of all the patients included in the study. As of the end of this study, none of the patients had been sent for molecular analysis.

Discussion

During the 18 months following the introductions of the revised 2016/2017 WHO Classification of Tumors of Haematopoietic and Lymphoid Tissues, our clinic recommended almost 20% of HGBL patients and 30% of HGBL/DLBCL-DE patients for FISH analysis for proper discrimination between HGBL, DH/TH and DLBCL. Considering the important clinical and biological differences between these diagnoses, we demonstrated a pressing need to apply the differential diagnosis of DLBCL and HGBL in the routine diagnosis of lymphomas in Poland.

The HGBL category was formally introduced in 2017 with the publication of the new WHO classifications; however, this distinct subgroup of lymphomas had been proposed a few years earlier.^{2,4,11} The most important morphological criterion (the blastoid pattern) and the additional immunohistochemical criteria (double- or triple- expression of *MYC*, *BCL2* and/or *BCL6*) are most often published in guidelines and reviews.^{3,4} Therefore, the present study separated all patients who were positive for the first or both criteria and labelled them as HGBL/DLBCL patients. No stringent criteria exist that can help to determine the additional molecular testing needed to separate HGBL DH/TH cases.^{1,3,4,13,14}

HGBL/DLBCL patients constituted almost 20% of our study group. This percentage is a little lower than literature values (in the largest cohorts, 30% of DLBCL cases were classified as HGBL/DLBCL; 6% were confirmed as HGBL-DH after molecular testing).²⁻⁴ In our study, the discrepancy was eliminated when DLBCL DE/TE cases were included in the group recommended for additional testing.²⁻⁴ The inclusion of DLBCL DE/TE for additional molecular assessment is clearly substantiated by recent reports on DLBCL DH cases within the DLBCL DE/TE group.^{3,4,15,16}

Most of the morphological and immunohistochemical characteristics identified in the group were consistent with those presented in previous reports; however, 2 were found to be intriguingly different. Firstly, almost 70% of the HGBL/DLBCL group displayed an ABC subtype phenotype when we assessed the COO using the Hans algorithm. The opposite GCB-to-ABC ratio is typically presented in the literature, with the value reaching as high as 100% GCB in true HGBL DH (*BCL2/MYC* rearranged) cases.⁴ The older age of the HGBL/DLBCL patients in our study (median age: 72 years) may explain this discrepancy, as ABC cases are more common among older patients.⁴ Another possible explanation is that our sample included

a lower percentage of DE/TE cases among the ABC DLBCLs than reported previously.^{3,5,7} Secondly, while a significantly higher Ki67 proliferation index was found in the HGBL/DLBCL group than in the DLBCL group in the present study, previous reports indicate no significant differences in this parameter, and advise against using it as a differential criterion for HGBL and DLBCL cases.^{1,2,4,5} We agree with these observations, because despite the statistical significance, the absolute differences in Ki67 proliferation index in our study were around 5%.

The need for detection of HGBL is reinforced not only by the different pathogenesis of HGBL and DLBCL, but also by the important clinical differences between HGBL and DLBCL mentioned previously.^{1,3} In comparison with DLBCL patients, HGBL (DH/TH or NOS) patients are characterized by shorter overall and event/progression-free survival, and are more frequently associated with poor prognostic factors, such as age at diagnosis, high IPI scores and advanced disease.^{3,4} Moreover, diagnoses of HGBL (DH/TH or NOS) may soon become predictive for treatment allocation, especially among younger patients; most studies indicate that this group should be treated more intensively than with a standard R-CHOP regimen.^{3,5,17,18} However, it must be emphasized that trials of more intensive or novel regimens in HGBL have reported inconsistent results, and the evidence is still not strong enough to prepare distinct treatment guidelines for HGBL patients.^{2,3,15,19-23} This further emphasizes the need for better distinction of HGBL as a highly heterogeneous, provisional category of lymphomas, which should be investigated further.


The major limitation of our study is its lack of FISH analysis of HGBL/DLBCL and DLBCL DE/TE cases, which might be valuable for the final diagnosis. We plan to conduct this type of examination whenever possible in the future. A second limitation concerns the limited amount of clinical data and follow-up. We did not present these data in this report because the scope of the study was restricted to the diagnostic aspect of HGBL/DLBCL. In addition, our pathology department treats patients from several regional oncology centers and gathering such a large volume of data would be excessively time-consuming. Finally, the patients in our study were diagnosed following January 1, 2017 and no accurate conclusions could be drawn in such a short time since the diagnosis. We plan to update the report with clinical and molecular details in the near future.


Conclusions


Our findings show that comprehensive histopathological and immunohistochemical examinations can identify potential HGBL cases. As many as 20% of our HGBL/DLBCL patients would need FISH examination for *BCL2/MYC* or *BCL6/MYC* rearrangements. This is the strongest justification for the need to introduce appropriate examinations among patients with high grade B-cell lymphomas.


ORCID iDs

Dorota Jesionek-Kupnicka  <https://orcid.org/0000-0001-9319-9570>

Marcin Braun  <https://orcid.org/0000-0003-3804-7042>

Tadeusz Robak  <https://orcid.org/0000-0002-3411-6357>

Wojciech Kuncman  <https://orcid.org/0000-0003-1117-4463>

Radzislaw Kordek  <https://orcid.org/0000-0003-4724-3627>

References

- Swerdlow S, Campo E, Harris N, et al. *WHO Classification of Tumours of Haematopoietic and Lymphoid Tissues*. Revised 4th ed. Lyon, France: IARC Press; 2017.
- Swerdlow SH, Campo E, Pileri SA, et al. The 2016 revision of the World Health Organization classification of lymphoid neoplasms. *Blood*. 2016;127(20):2375–2390. doi:10.1182/blood-2016-01-643569
- Sesques P, Johnson NA. Approach to the diagnosis and treatment of high-grade B-cell lymphomas with MYC and BCL2 and/or BCL6 rearrangements. *Blood*. 2017;129(3):280–288. doi:10.1182/blood-2016-02-636316
- Szumera-Ciećkiewicz A, Rymkiewicz G, Grygalewicz B, et al. Comprehensive histopathological diagnostics of aggressive B-cell lymphomas based on the updated criteria of the World Health Organization's 2017 classification. *Polish J Pathol*. 2017;69(1):1–19. doi:10.5114/PJP.2018.75332
- Johnson NA, Slack GW, Savage KJ, et al. Concurrent expression of MYC and BCL2 in diffuse large B-cell lymphoma treated with rituximab plus cyclophosphamide, doxorubicin, vincristine, and prednisone. *J Clin Oncol*. 2012;30(28):3452–3459. doi:10.1200/JCO.2011.41.0985
- Green TM, Young KH, Visco C, et al. Immunohistochemical double-hit score is a strong predictor of outcome in patients with diffuse large B-cell lymphoma treated with rituximab plus cyclophosphamide, doxorubicin, vincristine, and prednisone. *J Clin Oncol*. 2012;30(28):3460–3467. doi:10.1200/JCO.2011.41.4342
- Hu S, Xu-Monette ZY, Tzankov A, et al. MYC/BCL2 protein coexpression contributes to the inferior survival of activated B-cell subtype of diffuse large B-cell lymphoma and demonstrates high-risk gene expression signatures: A report from the International DLBCL Rituximab-CHOP Consortium Program. *Blood*. 2013;121(20):4021–4031. doi:10.1182/blood-2012-10-460063
- Yan L-X, Liu Y-H, Luo D-L, et al. MYC expression in concert with BCL2 and BCL6 expression predicts outcome in Chinese patients with diffuse large B-cell lymphoma, not otherwise specified. *PLoS One*. 2014; 9(8):e104068. doi:10.1371/journal.pone.0104068
- Horn H, Ziepert M, Becher C, et al; German High-Grade Non-Hodgkin Lymphoma Study Group. MYC status in concert with BCL2 and BCL6 expression predicts outcome in diffuse large B-cell lymphoma. *Blood*. 2013;121(12):2253–2263. doi:10.1182/blood-2012-06-435842
- Perry AM, Alvarado-Bernal Y, Laurini JA, et al. MYC and BCL2 protein expression predicts survival in patients with diffuse large B-cell lymphoma treated with rituximab. *Br J Haematol*. 2014;165(3):382–391. doi:10.1111/bjh.12763
- Macpherson N, Lesack D, Klasa R, et al. Small noncleaved, non-Burkitt's (Burkitt-like) lymphoma: Cytogenetics predict outcome and reflect clinical presentation. *J Clin Oncol*. 1999;17(5):1559–1567. doi:10.1200/JCO.1999.17.5.1558
- Hans CP, Weisenburger DD, Greiner TC, et al. Confirmation of the molecular classification of diffuse large B-cell lymphoma by immunohistochemistry using a tissue microarray. *Blood*. 2004;103(1):275–282. doi:10.1182/blood-2003-05-1545
- Cheah CY, Oki Y, Westin JR, Turturro F. A clinician's guide to double hit lymphomas. *Br J Haematol*. 2015;168(6):784–795. doi:10.1111/bjh.13276
- Pedersen MØ, Gang AO, Brown P, et al. Real world data on young patients with high-risk diffuse large B-cell lymphoma treated with R-CHOP or R-CHOEP – MYC, BCL2 and BCL6 as prognostic biomarkers. *PLoS One*. 2017;12(10):e0186983. doi:10.1371/journal.pone.0186983
- Scott DW, King RL, Staiger AM, et al. High grade B-cell lymphoma with MYC and BCL2 and/or BCL6 rearrangements with diffuse large B-cell lymphoma morphology. *Blood*. 2018;131(20):2060–2064. doi:10.1182/blood-2017-12-820605
- Li S, Young KH, Medeiros LJ. Diffuse large B-cell lymphoma. *Pathology*. 2018;50(1):74–87. doi:10.1016/j.pathol.2017.09.006
- Howlett C, Snedecor SJ, Landsburg DJ, et al. Front-line, dose-escalated immunochemotherapy is associated with a significant progression-free survival advantage in patients with double-hit lymphomas: A systematic review and meta-analysis. *Br J Haematol*. 2015;170(4):504–514. doi:10.1111/bjh.13463
- Petrich AM, Gandhi M, Jovanovic B, et al. Impact of induction regimen and stem cell transplantation on outcomes in double-hit lymphoma: A multicenter retrospective analysis. *Blood*. 2014;124(15):2354–2361. doi:10.1182/blood-2014-05-578963
- Johnson NA, Savage KJ, Ludkovski O, et al. Lymphomas with concurrent BCL2 and MYC translocations: The critical factors associated with survival. *Blood*. 2009;114(11):2273–2279. doi:10.1182/blood-2009-03-212191
- Puvvada SD, Stiff PJ, Leblanc M, et al. Outcomes of MYC-associated lymphomas after R-CHOP with and without consolidative autologous stem cell transplant: Subset analysis of randomized trial intergroup SWOG S9704. *Br J Haematol*. 2016;174(5):686–691. doi:10.1111/bjh.14100
- Staiger AM, Ziepert M, Horn H, et al; German High-Grade Lymphoma Study Group. Clinical impact of the cell-of-origin classification and the MYC/BCL2 dual expresser status in diffuse large B-cell lymphoma treated within prospective clinical trials of the German High-Grade non-Hodgkin's Lymphoma Study Group. *J Clin Oncol*. 2017;35(22):2515–2526. doi:10.1200/JCO.2016.70.3660
- Rosenthal A, Younes A. High grade B-cell lymphoma with rearrangements of MYC and BCL2 and/or BCL6: Double hit and triple hit lymphomas and double expressing lymphoma. *Blood Rev*. 2017;31(2):37–42. doi:10.1016/j.blre.2016.09.004

Pupil autoregulation impairment as an early marker of glaucomatous damage

Marta Anna Szmigiel^{1,A–F}, Joanna Wiktoria Przeździecka-Dołyk^{1,2,A–F}, Jacek Olszewski^{1,C,E,F}, Henryk Kasprzak^{1,A,C–F}

¹ Department of Optics and Photonics, Faculty of Fundamental Problems of Technology, Wrocław University of Science and Technology, Poland

² Department and Clinic of Ophthalmology, Wrocław Medical University, Poland

A – research concept and design; B – collection and/or assembly of data; C – data analysis and interpretation;

D – writing the article; E – critical revision of the article; F – final approval of the article

Advances in Clinical and Experimental Medicine, ISSN 1899–5276 (print), ISSN 2451–2680 (online)

Adv Clin Exp Med. 2019;28(10):1367–1375

Address for correspondence

Marta Szmigiel

E-mail: marta.szmigiel@pwr.edu.pl

Funding sources

M. Szmigiel acknowledges that part of this work was supported by the National Science Centre conferred on the basis of decision No. DEC-2013/11/N/ST7/00366.

Conflict of interest

None declared

Received on October 14, 2018

Reviewed on January 24, 2019

Accepted on May 14, 2019

Published online on September 11, 2019

Cite as

Szmigiel MA, Przeździecka-Dołyk JW, Olszewski J, Kasprzak H. Pupil autoregulation impairment as an early marker of glaucomatous damage. *Adv Clin Exp Med.* 2019;28(10):1367–1375. doi:10.17219/acem/109343

DOI

10.17219/acem/109343

Copyright

© 2019 by Wrocław Medical University

This is an article distributed under the terms of the Creative Commons Attribution Non-Commercial License (<http://creativecommons.org/licenses/by-nc-nd/4.0/>)

Abstract

Background. Glaucoma, a degenerative and progressive disease, leads to structural and functional changes in the optic nerve head and retinal ganglion cells (RGCs), while the vasculature of the iris stays intact.

Objectives. The aim of this study was to determine whether the coherence level associated with pupil geometry and peripheral arterial pulsation can be the basis for differentiating glaucoma and glaucoma-suspected patients from a control group.

Material and methods. This is an investigator-initiated, single-center prospective cohort study. Patients with diagnosed glaucoma (glaucoma group – GG) or glaucoma suspects (glaucoma suspects group – GSG), as well as healthy participants (control group – CG), were prospectively enrolled in the study. Glaucoma-diagnosed patients and glaucoma suspects who converted to glaucoma within 5 years were included. All patients underwent a full ophthalmological examination that included measurements of the thicknesses of the retinal nerve fiber layer (RNFL) and the ganglion cell complex (GCC) along with other parameters. A custom-made pupilometer was synchronized with a pulsometer to simultaneously record an image of the pupil and the peripheral arterial pulsation signal. All readings were processed with a script developed by the researchers. The main indicator of an increased influence of the vascular structures of the iris on pupil geometry in the patients and CG were the coherence levels (levC) between parameters describing the pupillary shape and peripheral arterial pulsation.

Results. Differences in the median value of the levCpS, levCpE and levCpθ parameters between the GG and GSG compared to the CG were found ($p < 0.001$). During the follow-up period, a larger decrease was observed in RNFL thickness and GCC thickness in the GSG than in the GG ($p < 0.05$). Strong correlations were found between levCpS and RNFL and GCC loss among the GSG group ($p < 0.001$), while in the GG this parameter correlated with RNFL and GCC thickness ($p < 0.001$).

Conclusions. This is the first attempt to relate changes in the neuronal signaling pathways in glaucoma to the vascular-dependent changes of pupil geometry. The findings presented herein suggest that this approach can be used to determine which glaucoma suspects have autonomic system impairment in the eye, increasing their probability of glaucoma conversion.

Key words: glaucoma, retinal nerve fiber layer, pupil, ganglion cell complex, peripheral arterial pulsation

Introduction

Glaucoma is the most common type of optic neuropathy. According to the World Health Organization (WHO), it represents one of the leading causes of irreversible blindness in developed countries, along with age-related macular degeneration and diabetic retinopathy.^{1,2} The pathomechanism of glaucomatous optic neuropathy has not been fully explained. This degenerative and progressive disease leads to structural and functional changes in both the optic nerve head and in the retinal ganglion cells (RGCs).

Although the majority of RGCs are involved in cortical image processing and recognition, there is a small group of RGCs that project the lateral geniculate nucleus, the pretectal olivary nucleus and the suprachiasmatic nucleus. This non-image-forming pathway (Fig. 1A) is managed by a different type of RGCs, called intrinsically photosensitive RGCs (ipRGCs), comprising approx. 0.8–3% of the total RGC population in the human retina. Assuming that

the total number of RGCs in the human retina is approx. 1.2 million, only 9.6–36 thousand RGCs contain melanopsin and are intrinsically photosensitive.^{3–5} In a healthy retina, a light impulse – after being transduced into a biochemical impulse – is transmitted via the cortical and non-image-forming pathways towards the appropriate centers in the brain. However, in the glaucomatous retina, the same light impulse causes less pronounced cortical and non-image-forming input towards the brain due to the presence of fewer RGCs in the retina (Fig. 1A). Non-image forming input is transmitted through the optic tract to the pretectal nucleus, where it acts as an excitatory impulse for the Edinger–Westphal nucleus. The impulses from this nucleus travel through the oculomotor nerve (its parasympathetic part) to the ciliary ganglion and, after switching to the post-synaptic neuron, as short ciliary nerves to the iris. Arousal of the sympathetic part of reticular formation results in inhibitory impulses that travel from the hypothalamus to the Edinger–Westphal nucleus. Simultaneously, arousal

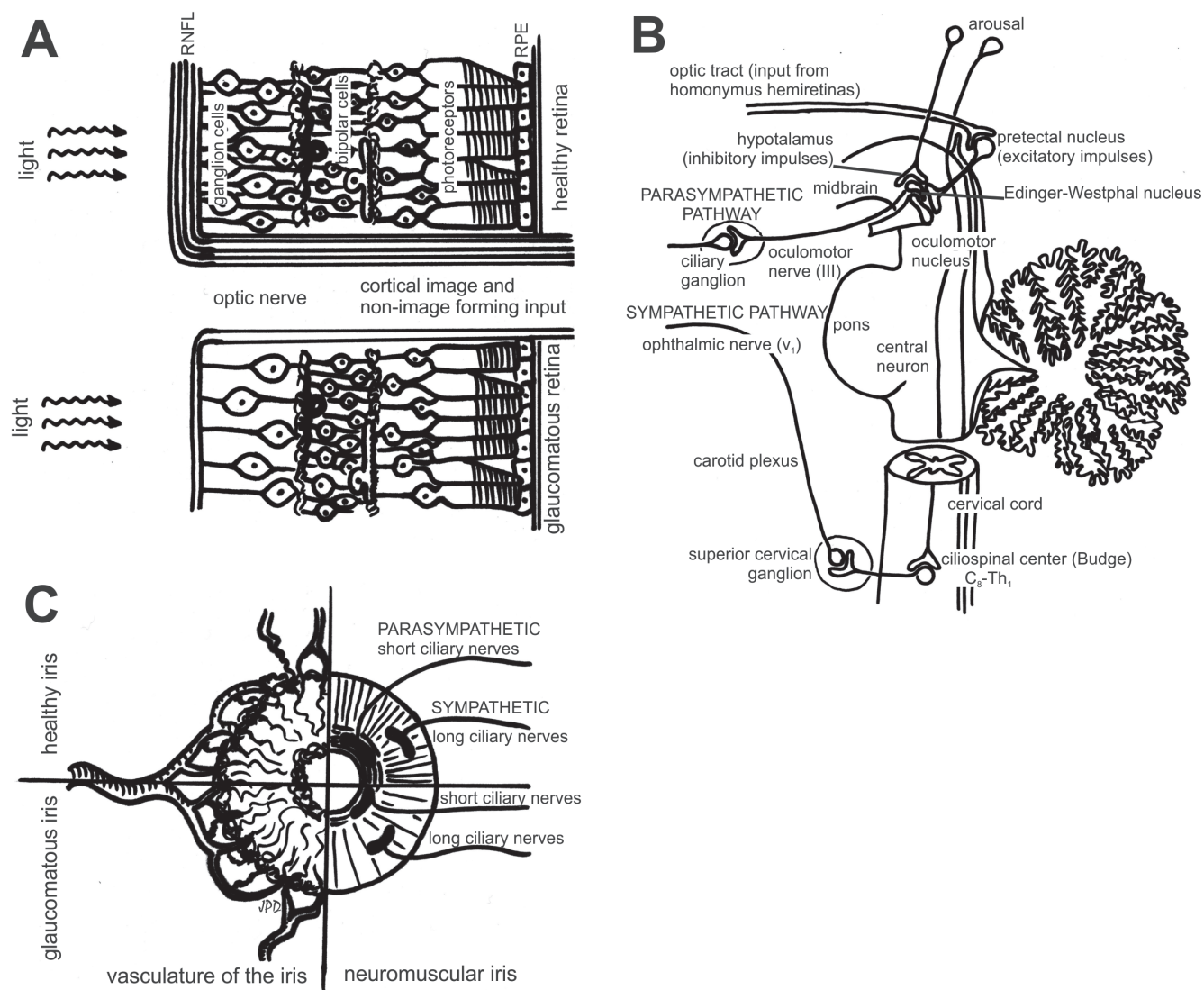


Fig. 1. Healthy (top) and glaucomatous (bottom) retina with important cells for cortical image and non-image forming input (A), non-image forming pathways in brain and spinal cord (B) and healthy (top) and glaucomatous (bottom) iris with vascular (left) and neuromuscular (right) (C) anatomic features

of the sympathetic part of the reticular formation is transmitted through the cervical cord to the ciliospinal center located in the C₈–Th₁. The sympathetic presynaptic nerve leaves the spinal cord and forms synapses in the superior cervical ganglion. The postsynaptic sympathetic nerves form the carotid plexus and travel upward with this vessel, then along with the ophthalmic nerve (V₁) they enter the tissues of the eye as long ciliary nerves (Fig. 1B).

In the iris as well, there are differences between glaucomatous and normal neuromuscular structures. The reduced input from RGCs in glaucomatous patients results in muscle atrophy due to insufficient impulse creation when compared to a healthy eye, but the vasculatures of glaucomatous and healthy irises are similar. The peripheral arterial pulsation, while invisible in a healthy eye, becomes pronounced in a glaucomatous one. This provides the background for our study (Fig. 1C).

In 2002, Hattar et al. and Berson et al. simultaneously described a new type of photoreceptor that expresses the photopigment melanopsin (also known as opsin 4 or OPN4).^{6,7} In recent years, the investigators have shown that light transmission to the hypothalamic suprachiasmatic nucleus or the post-illumination pupillary light response (PLR) is compromised as a result of ipRGC damage in glaucoma. Gracitelli et al. showed that there is a positive association between ipRGCs and retinal nerve fiber layer (RNFL) thinning in glaucoma. In addition, it has also been proven that the severity of glaucoma reflected by a standard automated perimeter mean deviation worse than 12 dB was associated with a worse pupillary response.^{5,8,9} The correlation between ipRGCs and RNFL is represented in Fig. 1A, demonstrating a significant reduction in the number of RGCs and in RNFL thickness in a glaucomatous retina. Kuze et al. suggested that electroretinography (ERG) may be a promising method in treating a variety of pathological conditions in which ipRGC disorders are possible. In that study, glaucomatous patients showed diminished responses of the ipRGCs in ERG.⁴ The reduced blue-red post-illumination pupil response indicates a characteristic impairment of the melanopsin-driven pathway of ipRGCs in patients with glaucoma. Other studies have shown that reduced maximal relative amplitude and increased slope of the response during exposure to the 4-second red stimulus suggest a disturbed synaptic function and an altered interaction between outer photoreceptors, RGCs and ipRGCs.^{10,11} In glaucomatous patients, the diminished input from hemiretinas results in lower excitatory impulses being projected from the pretectal nucleus to the Westphal–Edinger nucleus (Fig. 1B). This results in a decrease of the parasympathetic pathway activity transmitted to the iris muscles which contract the pupil (Fig. 1B,C).

Detection of the pupil edge is used to determine the parameters that describe the pupil and its changes over time in an unequivocal and comparable manner. Pupil geometry is quite complex¹² and is characterized by rapid changes in its geometrical parameters over time,¹³ with a constant

level of light and constant conditions of its stimulation. For various lighting conditions, the pupil can grow in area even several times larger. Normal pupil diameter in bright light varies in adults from 2 mm to 4 mm and in dim light from 4 mm to 8 mm. Even with constant lighting, the shape and size of the pupil are variable. Measurements of pupil diameter after dark adaptation and during pulsing light stimulation are presented in a study by Gooley et al.¹⁴ In a paper by Winn et al.,¹⁵ the authors measured the variation of pupil diameter over time for different, constant levels of illumination. This effect is most often associated with the pulsation of blood in its blood vessels. Some authors have carried out studies of pupil size along with other signals. That led to a description of the relationship between fluctuations in pupil diameter and heart rate¹⁶ or fluctuations in pupil diameter and respiratory fluctuations.¹⁷ The size of the pupil also changes as a result of the accommodation reflex.

On the other hand, apart from neovascular glaucoma, no changes in iris vasculature have been reported. The effect of a pulse wave in the peripheral tissues has been described several times in the past. Pulse wave is the spread of arterial deformation, which is caused by a change in blood volume that is pushed from the heart with every heartbeat. It propagates at a speed of 5–8 m/s, while the blood flow rate is around 0.5 m/s.

Dynamic changes in pupil size have been used to objectively measure the influence of chronic stress. In a study by Al Abdi et al.,¹⁸ a device for physiological measurements was developed to diagnose chronic stress, based on blunted reactivity of the autonomic nervous system to cognitive load. The authors documented blunted cognitive-load-induced changes in pulse wave amplitude, galvanic skin response and pupil diameter in stressed subjects in comparison with non-stressed ones. Preliminary results have demonstrated the ability of these methods to objectively detect chronic stress. The most interesting aspect is the work by Al Abdi et al. who proved that pupil diameter is under the control of the autonomic system and that a degradation of the autonomic system is strongly represented in the ability of the pupil to change its geometry.

We hypothesize that the impaired autonomic regulation of pupil size in glaucoma and glaucoma suspects is an early sign of this disease and, therefore, the vasculature of the iris has an impact on short-term changes in pupil shape. This is caused by pulse wave propagation to distant tissues – when the autonomic innervation (sympathetic and parasympathetic pathways) is impaired, iris muscles atrophy. Under these conditions, the autonomic regulation of systemic circulation overcomes local regulation of pupil size represented by the neuromuscular unit in the iris to the point at which it can be detected (Fig. 1).

To the best of our knowledge, this is the first study that addresses the correlation between peripheral arterial pulsation and pupil size and shape changes in early glaucoma detection.

Material and methods

Study design

This was an investigator-initiated, single-center prospective cohort study conducted at the Department of Optics and Photonics, Wrocław University of Science and Technology, and Department of Ophthalmology, Wrocław Medical University, Poland. The project was approved by the Ethics Committee of the Wrocław Medical University (approval No. KB 246/2017) and it adhered to the tenets of the Declaration of Helsinki.

Study population

Patients with diagnosed glaucoma or glaucoma suspects were prospectively enrolled in the study. The included patients were those who were diagnosed with glaucoma and glaucoma suspects who converted to glaucoma within 5 years from inclusion. Detailed inclusion and exclusion criteria can be found in Table 1. All patients underwent a complete ophthalmological examination, including slit-lamp biomicroscopy, funduscopy and gonioscopy, as well as visual field testing using a standard white-on-white visual field (Humphrey Field Analyzer (HFA) II 750; 24-2 Swedish interactive threshold algorithm; Carl Zeiss Meditec, Dublin, USA) and RNFL thickness measurement using a Spectralis OCT (Heidelberg Engineering, Heidelberg, Germany). Additionally, the retinal ganglion cell complex (GCC) was assessed using an RtVue AngioOCT (Optovue, Fremont, USA). The following baseline data were recorded: age, gender, best-corrected visual acuity, preoperative IOP with Goldmann applanation tonometry, and medication score.

The study population was divided into 3 groups: 25 eyes in the glaucoma suspect group (GSG), 22 eyes in the glaucoma group (GG) and 28 eyes in the control group (CG). Subjects were fully informed of the purpose of the study and about all the procedures and their requirements. Informed consent was obtained from the patients before any measurements were taken.

Experimental measurements

The patient's head was stabilized in a rigid head rest, designed and built by the researchers. The patient was asked to gaze at the motionless fixation point and to abstain from blinking for up to 14 s. Thanks to this eye fixation, an assumption about the constant impact of corneal refraction on the pupil image was made. If possible, the examination was carried out on both eyes of each patient. However, the study included people during the post-operative period (cataract) or who were already monocular; hence, it was not possible to examine both eyes of each person in each case.

The main component of the system for recording images of the human pupil was a fast CMOS camera (AOS S-PRI; AOS Technologies AG, Baden, Switzerland).¹⁹ Together with the photo lens, it ensures an optimal image size of the pupil on the image sensor (800 × 600 pixels). Acceptable contrast was obtained by means of retro-illumination registered by the camera. To preclude the pupils responding to the lighting system, infrared illumination was used. Peripheral arterial pulsation was synchronously recorded with the recording of video sequences of the pupils with the use of an MLT1010 pulsometer attached to the subject's finger (AD Instruments, Sydney, Australia). The sequences were recorded at a speed of 200 fps and the peripheral arterial pulsation signal had a rate of 200 Hz.

The video sequence was divided into single frames (up to 2,700 frames), and each of them was numerically analyzed with the use of Matlab R2015b (The MathWorks, Inc., Natick, USA). Border points of the pupil were selected automatically using an edge detection procedure (Fig. 2). Due to differences in magnification of the pupil, the pupil size was calibrated for each sequence. The pupil image was treated as a filled plane figure. The shape of the pupil was approximated with the best fitting ellipse, understood as the ellipse with the same second moments of inertia as the pupil shape (Fig. 2). The area of the pupil approximated by the ellipse (S) and the length of its major and minor semi-axes (a and b , respectively) were determined. Based on the major and minor semi-axes, the eccentricity (ϵ) was determined with the use of the following equation:

$$\epsilon = \sqrt{\frac{a^2 - b^2}{a^2}} \quad (1)$$

Table 1. Inclusion and exclusion criteria

Inclusion criteria	Exclusion criteria
<ol style="list-style-type: none"> 18 years of age or older. Diagnosis of glaucoma or glaucoma suspect done previously and re-assessed during screening by ophthalmologist. Medicated IOP $\geq 15 \leq 35$ mm Hg. Subjects in glaucoma group taking 1–5 IOP-lowering medications. Conversion to glaucoma diagnosed within a 5-year period (from the time of recordings) in glaucoma suspect group. Signed informed consent. 	<ol style="list-style-type: none"> Active inflammation (e.g., blepharitis, conjunctivitis, keratitis, or uveitis). Active iris neovascularization or neovascularization of the iris within the previous 6 months. Anterior chamber intraocular lens. Presence of intraocular silicone oil. Vitreous present in the anterior chamber. Impaired episcleral venous drainage (e.g., Sturge–Weber or nanophthalmos or other evidence of elevated venous pressure). History of dermatological keloid formation. Previous photorefractive keratectomy (PRK).

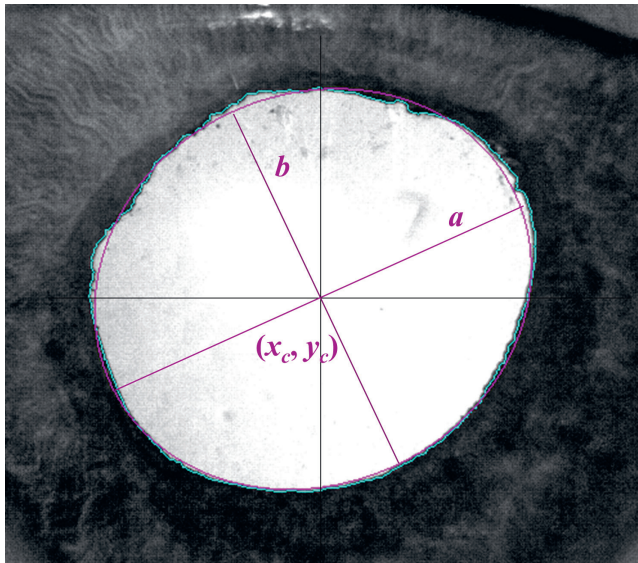


Fig. 2. Exemplary pupillary edge of iris (light blue corrugated line) with the best fitted ellipse (purple line) and its parameters: (x_c, y_c) – center of the ellipse, a – major and b – minor semi-axis

The temporal variability of the parameters S and ε , as well as the peripheral arterial pulsation (p), was subjected to further analysis.

Numerical analysis

All analyzed signals were subjected to spectral analysis using fast Fourier transform (FFT) and correlation analysis with the use of the coherence function between pairs of recorded signals. Values of the coherence function are always in the range of 0 to 1. Higher values of the coherence function between 2 signals means higher spectral correlation between the signals.

Two of the signals, S and p , analyzed over time for exemplary sequence, are shown in Fig. 3. Their basic registered

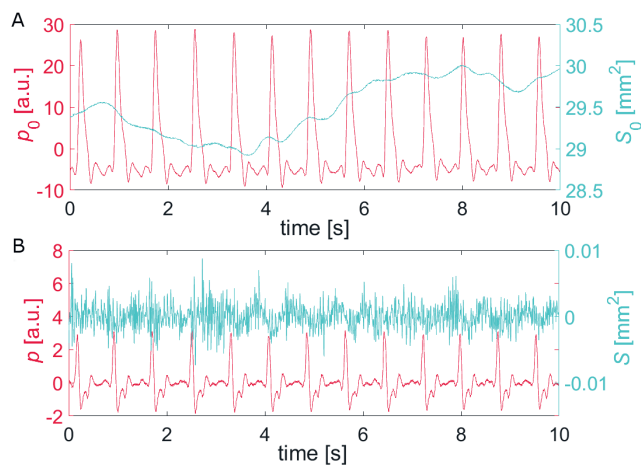


Fig. 3. Examples of basic signals p and S A) in their basic registered form p_0 and S_0 and B) differentiated signals for further analysis p and S

p – the peripheral arterial pulsation signal; S – the area of the eye pupil; p_0 – basic registered peripheral arterial pulsation signal; S_0 – basic registered area of the eye pupil.

form, marked with subscript 0 – that is, p_0 and S_0 – is presented in Fig. 3A. Figure 3B shows their differentiated forms for further analysis, denoted as S and p , respectively, in order to better visualize the effect of higher frequencies.

Periodograms (marked as PFT) of the modified signals calculated by the use of FFT are presented in Fig. 4A. Peaks in the PFT periodograms stand for characteristic frequencies present in the signal. However, the components with that frequency may appear at different times in the analyzed signals. The coherence function allows frequencies present in both signals at the same time to be located with the use of Welch’s overlapped averaged periodogram.²⁰ The coherence function between the 2 modified signals presented in Fig. 3B²¹ is shown in Fig. 4B. To determine and quantitatively compare correlations between 2 analyzed signals, the average value of the coherence function above 0.5 was determined. This parameter, called coherence level, was defined as:

$$\text{lev}C_{z_1z_2} = \frac{\sum_{i=1}^j C_{z_1z_2}^*(i)}{j} \quad (2)$$

where

$$C_{z_1z_2}^*(i) = \begin{cases} C_{z_1z_2}(i) & \text{for } C_{z_1z_2}(i) \geq 0.5 \\ 0 & \text{for } C_{z_1z_2}(i) < 0.5 \end{cases} \quad (3)$$

and where z_1, z_2 represent pairs of parameters and i denotes the next values $i = 1, 2, \dots, j$ of frequencies in the range of 0–40 Hz for which the coherence value has been determined. A graphical interpretation of the coherence level is shown in Fig. 4B, though for better visualization the graph presents only values up to 20 Hz. The points above the red line at the level of 0.5 were taken into consideration when determining the value of the coherence level. The coherence level parameter is with some approximation proportional

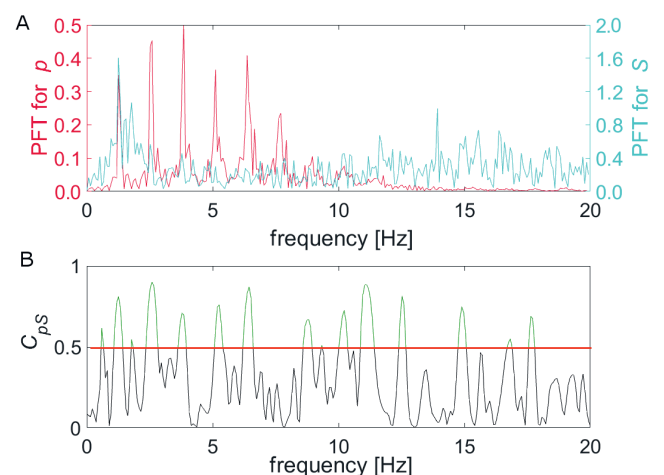


Fig. 4. A) PFT periodograms for p and S signals and B) coherence function with marked values to calculate coherence level

p – peripheral arterial pulsation signal; S – area of the eye pupil; C_{ps} – coherence function between p and S ; $\text{lev}C_{ps}$ – coherence level.

to the area below the coherence function and above the line indicating the coherence level equal to 0.5. It was assumed that the coherence values $C_{z_1z_2}$ below 0.5 do not indicate a significant correlation between the signals analyzed. Thus, the coherence level parameter describes the characteristic coherence level in the range 0–40 Hz.

Outcome measures

The primary outcome measure was the coherence level between the systemic pulsation signal and the change in the area of the pupil. Secondary outcome measures included correlations between RNFL and GCC thicknesses and the coherence level, as well as correlations between the coherence level and the change in RNFL and GCC thicknesses over the 5-year follow-up period.

Statistical analysis

Almost each participant of all 3 groups –GG, GSG and CG – was recorded at least twice; analysis of variance (ANOVA) factorial analyses were performed to determine the existence of any connection between the 1st and 2nd recordings. Descriptive statistics for each parameter, such as RNFL, GCC and their change over the years, and the coherence levels, including median and 95% confidence intervals (95% CI) for the median, were used. The crosstabs with relative risk and odds ratio (OR) analysis using z-scores were conducted for all parameters. Comparisons of 2 independent samples were performed with the Mann–Whitney test and, for multiple independent samples, an ANOVA Kruskal–Wallis test was used. In all analyses, statistical significance was recognized if $p < 0.05$ for primary and

$p < 0.001$ for secondary outcome measures. The analysis of correlations was conducted by means of Spearman's R test ($p < 0.001$). In the next step, the Stepwise Model Builder from STATISTICA v. 13.3 (StatSoft Inc., Tulsa, USA) for linear regression was used, in which the next variable was added only if the overall fitness of the model was improved with a significance level of $p < 0.05$. Some of the abovementioned calculations were made in Matlab R2015b (The MathWorks, Inc., Natick, USA) as well.

Results

The characteristics of the study population are described in Table 2. Figure 5 shows box-plot charts for 3 of the values of the coherence level: $levC_{ps}$, $levC_{pe}$ and $levC_{s\epsilon}$. Please note that the vertical axis of Fig. 5C is expressed in different units than the other 2 graphs.

Statistical analysis revealed a significant difference between CG and both the GSG and GG for all 3 coherence level parameters (Fig. 5). The median value of $levC_{ps}$ in the GG (0.102) was much higher than that of the CG (0.038; $p < 0.001$). Moreover, the GSG had a higher median value (0.086) than the CG ($p < 0.001$). The median values of $levC_{pe}$

Table 2. Characteristics of subjects in the study groups

Parameter	GSG	GG	CG
Number of eyes measured	25	22	28
Age median (IQR) [years]	64 (35–72)	63 (53–70)	31 (24–41)
Female/male ratio	16:9	15:7	15:13

GSG – glaucoma suspect group; GG – glaucoma group; CG – control group; IQR – interquartile range.

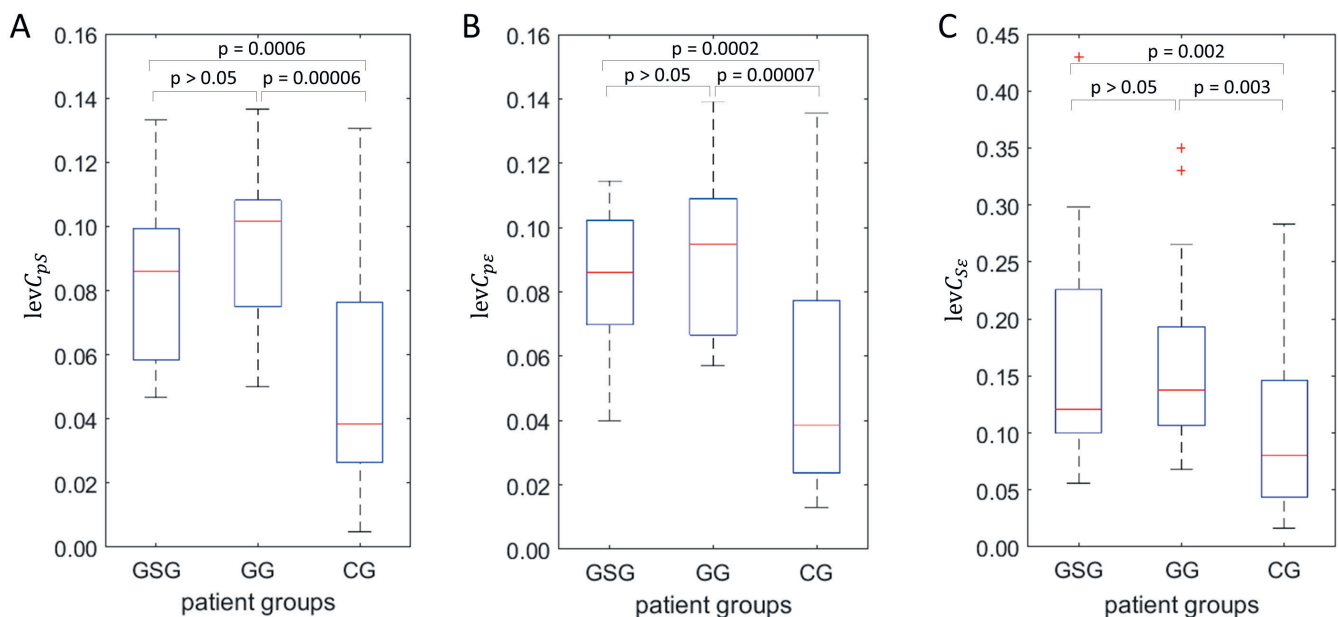


Fig. 5. Box-plot for $levC$ calculated for pair of signals: A) p and S , B) p and ϵ and C) S and ϵ for analyzed patient groups

GG – glaucoma group; GSG – glaucoma suspect group; CG – control group; IQR – interquartile range; HR – heart rate; $levC$ – coherence level; p – peripheral arterial pulsation; S – area of the pupil; ϵ – eccentricity; * $p < 0.05$; ** $p < 0.01$; *** $p < 0.001$.

Table 3. Summary of differences between GG and GSG groups (change in RNFL and GCC thickness were observed during follow-up period)

Parameter median and IQR	GG (n = 22)	GSG (n = 25)	p-value
Observation time [years]	4 (3.5–5.0)	3 (2.56–4.10)	p > 0.05
RNFL [μm]	70 (56–86)	95 (86–97)	0.001384
ΔRNFL [μm]	4.6 (4.2–5.2)	6.3 (5.4–7.1)	0.000006
ΔRNFL ^y [μm/year]	0.94 (0.84–1.20)	0.66 (0.54–0.71)	0.000010
GCC [μm]	81 (72–88)	91 (88–98)	0.001026
ΔGCC [μm]	4.45 (4.1–5.1)	7.0 (5.2–8.1)	0.000007
ΔGCC ^y [μm/year]	1.26 (0.95–1.39)	1.34 (1.05–1.57)	0.000021

IQR – interquartile range; GG – glaucoma group; GSG – glaucoma suspect group; RNFL – retinal nerve fiber layer; ΔRNFL – loss of retinal nerve fiber layer; ΔRNFL^y – loss of retinal nerve fiber layer per year; GCC – ganglion cell complex; ΔGCC – loss of ganglion cell complex; ΔGCC^y – loss of ganglion cell complex per year.

for both the GSG (0.086) and GG (0.095) were higher than that of the CG (0.038; p < 0.001). The differences in median values of levC_{ps} for both the GSG (0.121) and GG (0.138) were significantly higher in comparison to the CG (0.080; p < 0.01).

Clinical data of RNFL thickness and GCC thickness measured at the initial examination and reviewed during the 5-year observational period are summarized in Table 3. The loss of retinal nerve fiber layer (ΔRNFL) calculated for each measured eye separately represents the difference between RNFL thickness values at 2 points in time, when the pupil was measured and after up to 5 years, which was when the GSG patients had converted to glaucoma.

In regards to the GG patients, the median observation time was 4 years (95% CI = 3.5–5.0). The value ΔRNFL^y represents ΔRNFL per year. The same applies to GCC, the loss of ganglion cell complex (ΔGCC) and the yearly loss of ganglion cell complex (ΔGCC^y).

During the follow-up period, there was a larger decrease in RNFL and GCC thickness in the GSG than in the GG (p < 0.05). When it comes to the GSG, it should be stressed that the observation period was different for each patient. If a patient classified as GSG developed a visual field defect, the researcher was able to diagnose glaucoma and treatment was introduced; therefore, a change in RNFL and GCC thickness per year was calculated in a different timeframe for each patient. The median time that was required to detect conversion towards glaucoma was 3 years (95% CI = 2.56–4.10). Additionally, it should be highlighted that this is the first study to describe the change in GCC thickness in GSG patients. Interestingly, when the coherence levels were compared to the clinical data, there were strong correlations in GG and GSG. It is worth mentioning that the correlations between the coherence levels were stronger in the GSG (e.g., ΔRNFL thickness (r = 0.732; p < 0.0001) or ΔGCC thickness (r = 0.6491; p < 0.0001), while in the GG it was not statistically significant). The correlation between levC and RNFL thickness (r = -0.7539; p < 0.0001) and GCC thickness (r = -0.6509; p = 0.001) in the GG is presented in Fig. 6A,B. This progression was not observed in the GG during follow-up (ΔRNFL and ΔGCC thicknesses were not statistically significant). Additionally, as the patients from the GSG developed visual field defects during the observation period which resulted in a change of diagnosis toward glaucoma, we therefore focused on presenting the changes in RNFL and GCC thicknesses in the GSG during this time (Fig. 6C,D).

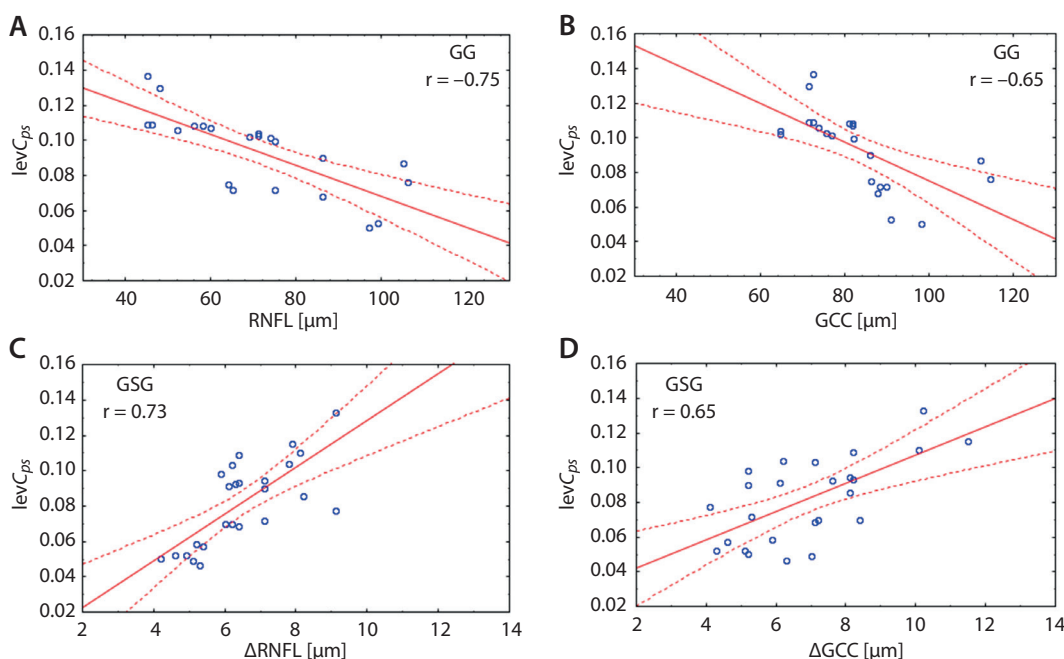


Fig. 6. Correlations between levC and different clinical indicator of progression in glaucomatous (A and B) and glaucoma suspect group (C and D)

levC – coherence level; p – peripheral arterial pulsation; S – area of the pupil; RNFL – retinal nerve fiber layer; ΔRNFL – loss of retinal nerve fiber layer; GCC – ganglion cell complex; ΔGCC – loss of ganglion cell complex; GG – glaucoma group; GSG – glaucoma suspect group.

Discussion

Taking into account the neuromuscular regulation of pupil size in a normal iris, the influence of peripheral arterial pulsation on the pupillary margin of the iris will be minimal. The situation is different in glaucomatous eyes, where the non-image-forming pathway that controls pupil size is impaired due to the loss of ipRGCs (Fig. 1). In glaucoma, the pupillary margin is affected by peripheral arterial pulsation, thus periodic changes in pupil size and shape that are consistent with the heartbeat can be found in those patients.

While decreased pupil constriction in response to red or blue stimuli was reported in the glaucoma group, in the ocular hypertension (OH) group, similar changes were not found by Kelbsch et al. It is worth mentioning that in our study, during the 5-year follow-up period all but 1 patient from the glaucoma suspect group converted to glaucoma, while in the research published by Kelbsch et al. no such data is available.¹⁰ Additionally, the results of the Ocular Hypertension Treatment Study (OHTS) provide clinically important information on the rate of conversion from OH to glaucoma during the 5-year follow-up period. Quoting the OHTS, “the cumulative probability of developing primary open angle glaucoma (POAG) was reduced by 60% among participants randomized to receive typical ocular hypotensive medication compared with those randomized to observation (hazard ratio = 0.40; 95% CI = 0.27–0.59). At 60 months, the cumulative probability of developing POAG was 4.4% in the medication group and 9.5% in the observation group”.²² Assuming that the German group included 16 patients with OH, only 1 or 2 of them would convert to glaucoma over the 5 years of follow-up if left untreated.

In a paper by Calcagni et al.,²³ heart rate, blood pressure, respiration, peripheral blood flow, and pupil diameter were simultaneously measured in constant light conditions in order to determine whether there is any correlation between those signals, particularly whether fluctuations in blood pressure contribute to spontaneous pupil fluctuations. It was noted that stimulation of the carotid baroreceptors induced pupil size fluctuations. On the other hand, taking into account that the sympathetic pathway of non-image-forming input signals from ipRGCs are led through the carotid plexus, it is likely that carotid sinus baroreceptors are stimulated at the same time as the carotid plexus axons from non-image-forming homonymous hemiretinal signals. Due to this probability, it is an extremely difficult task to distinguish between those 2 stimulations.

In the current study, we report on 5 years of follow-up observation of changes in RNFL and GCC thickness. In the GG, the rate of thickness change ΔRNFL^y was $0.94 \mu\text{m}/\text{year}$, while for ΔGCC^y it was $0.66 \mu\text{m}/\text{year}$. However, in the GSG, both measurements were higher: $1.26 \mu\text{m}/\text{year}$ and $1.34 \mu\text{m}/\text{year}$ for ΔRNFL^y and ΔGCC^y


thicknesses, respectively. Similar results for glaucomatous patients were presented by Hammel et al. In their work, glaucomatous eyes were characterized by a mean rate of global circumpapillary ΔRNFL^y thickness change of $-0.98 \mu\text{m}/\text{year}$ and a normalized global circumpapillary ΔRNFL^y change of $-1.7\%/ \text{year}$. Changes in RNFL thickness occurred significantly faster than the average macular GCC change ($-0.57 \mu\text{m}/\text{year}$) and normalized macular GCC change ($-1.3\%/ \text{year}$).²⁴ In a paper by Kim et al., RNFL and GCC thicknesses were observed over a 3-year period and the rates were estimated to be on the level of $-1.23 \mu\text{m}/\text{year}$ and $1.53 \mu\text{m}/\text{year}$, respectively.²⁵ Additionally, the temporal relationship between GCC loss and RNFL loss in glaucomatous patients was confirmed.^{25,26} It is important to mention that in our work, we also observed a patient who was considered a glaucoma suspect at the beginning of the study and who converted to glaucoma during the follow-up period. In the GSG, the RNFL and GCC losses were greater than in the GG; however, this patient was not treated prior to their conversion. In this regard, interesting studies were published by Sehi et al. and Miki et al. In their work, Sehi et al. observed 310 glaucoma suspects and pre-perimetric glaucoma patients for over 3.3 years. In 89 eyes, visual field progression was found, and RNFL progression was reported in 101 eyes. Miki et al. compared 454 eyes of 294 glaucoma suspects during a 2.2-year follow-up period. The estimated mean rate of global RNFL loss was significantly faster in eyes developing visual field defects compared with eyes that did not ($-2.02 \mu\text{m}/\text{year}$ vs $-0.82 \mu\text{m}/\text{year}$; $p < 0.001$).^{27,28} We found slightly less deterioration in RNFL thickness than has been previously presented, though our study group was smaller and we introduced treatment with 2 anti-glaucoma drugs at once. This approach may play an important role in the early inhibition of GCC and RNFL loss.

This is the first time the coherence level between peripheral arterial pulsation and change in pupil geometry was measured. To the best of our knowledge, this is the first attempt to relate changes in the neuronal signaling pathways in glaucoma to the vascular-dependent changes of pupil geometry. The findings suggest that this approach could be used to define which glaucoma suspect patients have alterations in the autoregulation of pupil geometry which increase their likelihood of converting to glaucoma. This alternate autoregulation of pupil geometry might be due to autonomic system impairment in the eye, but this hypothesis needs to be examined further. In the future, the methodology presented by our group can open up a wide range of new approaches to glaucoma neurodegeneration. Further research is still needed, including electrophysiological tests. It is worth mentioning that the measurement is relatively brief – 12 s. Additionally, during recording no provocative tests, such as flashes of red or blue light under specific conditions, were required to evoke ipRGC potentials.

ORCID iDs

Marta Anna Szmigiel  <https://orcid.org/0000-0002-2823-4859>

Joanna Wiktorja Przędzicka-Dołyk

 <https://orcid.org/0000-0002-1099-4876>

Jacek Olszewski  <https://orcid.org/0000-0002-8978-6059>

Henryk Kasprzak  <https://orcid.org/0000-0002-4241-1954>

References

- Parihar JKS. Glaucoma: The 'black hole' of irreversible blindness. *Med J Armed Forces India*. 2016;72(1):3–4.
- World Health Organization. Vision impairment and blindness. <https://www.who.int/news-room/fact-sheets/detail/blindness-and-visual-impairment>. Accessed February 23, 2019.
- Gracitelli CPB, Duque-Chica GL, Moura AL, et al. Relationship between daytime sleepiness and intrinsically photosensitive retinal ganglion cells in glaucomatous disease. *J Ophthalmol*. 2016;2016:5317371.
- Kuze M, Morita T, Fukuda Y, Kondo M, Tsubota K, Ayaki M. Electrophysiological responses from intrinsically photosensitive retinal ganglion cells are diminished in glaucoma patients. *J Optom*. 2017;10(4):226–232.
- Gracitelli CPB, Duque-Chica GL, Moura AL, et al. A positive association between intrinsically photosensitive retinal ganglion cells and retinal nerve fiber layer thinning in glaucoma. *Invest Ophthalmol Vis Sci*. 2014;55(12):7997–8005.
- Hattar S, Liao HW, Takao M, Berson DM, Yau KW. Melanopsin-containing retinal ganglion cells: Architecture, projections, and intrinsic photosensitivity. *Science*. 2002;295(5557):1065–1070.
- Berson DM, Dunn FA, Takao M. Phototransduction by retinal ganglion cells that set the circadian clock. *Science*. 2002;295(5557):1070–1073.
- Rukmini AV, Milea D, Baskaran M, et al. Pupillary responses to high-irradiance blue light correlate with glaucoma severity. *Ophthalmology*. 2015;122(9):1777–1785.
- El-Danaf RN, Huberman AD. Characteristic patterns of dendritic remodeling in early-stage glaucoma: Evidence from genetically identified retinal ganglion cell types. *J Neurosci*. 2015;35(6):2329–2343.
- Kelbsch C, Maeda F, Strasser T, et al. Pupillary responses driven by ipRGCs and classical photoreceptors are impaired in glaucoma. *Graefes Arch Clin Exp Ophthalmol*. 2016;254(7):1361–1370.
- Kankipati L, Girkin CA, Gamlin PD. The post-illumination pupil response is reduced in glaucoma patients. *Invest Ophthalmol Vis Sci*. 2011;52(5):2287–2292.
- Wyatt HJ. The form of the human pupil. *Vision Res*. 1995;35(14):2021–2036.
- Nowak W, Hachoł A, Kasprzak H. Time-frequency analysis of spontaneous fluctuation of the pupil size of the human eye. *Optica Applicata*. 2008;38(2):469–480.
- Gooley JJ, Ho Mien I, St Hilaire MA, et al. Melanopsin and rod-cone photoreceptors play different roles in mediating pupillary light responses during exposure to continuous light in humans. *J Neurosci*. 2012;32(41):14242–14253.
- Winn B, Whitaker D, Elliott DB, Phillips NJ. Factors affecting light-adapted pupil size in normal human subjects. *Invest Ophthalmol Vis Sci*. 1994;35(3):1132–1137.
- Yoshida H, Mizuta H, Gouhara T, Suzuki Y, Yana K, Okuyama F. Statistical properties of simultaneously recorded fluctuations in pupil diameter and heart rate. Proceedings of 17th International Conference of the Engineering in Medicine and Biology Society (IEEE 1995), Montreal, Canada:165–166.
- Yoshida, H, Yana K, Okuyama F, Tokoro T. Time-varying properties of respiratory fluctuations in pupil diameter of human eyes. *Methods Inf Med*. 1994;33(1):46–48.
- Al Abdi RM, Alhitary AE, Abdul Hay EW, Al-Bashir AK. Objective detection of chronic stress using physiological parameters. *Med Biol Eng Comput*. 2018;56(12):2273–2286.
- Szmigiel M, Kasprzak H. Distribution of parameters of elliptic approximation of the human pupil. *Optica Applicata*. 2015;45(1):41–50.
- Welch P. The use of fast Fourier transform for the estimation of power spectra: A method based on time averaging over short, modified periodograms. *IEEE Transactions on Audio and Electroacoustics*. 1967;15(2):70–73.
- Szmigiel MA, Kasprzak H, Klysik A. Dependences between kinetics of the human eye pupil and blood pulsation. In: Applications of Digital Image Processing XXXIX, International Society for Optics and Photonics, August 29 – September 1, 2016, San Diego, USA, art. 99712V, s. 1–9; SPIE Proceedings Series, vol. 9971.
- Gordon MO, Beiser JA, Brandt JD, et al. The Ocular Hypertension Treatment Study: Baseline factors that predict the onset of primary open-angle glaucoma. *Arch Ophthalmol*. 2002;120(6):714–720.
- Calcagini G, Censi F, Lino S, Cerutti S. Spontaneous fluctuations of human pupil reflect central autonomic rhythms. *Methods Inf Med*. 2000;39(2):142–145.
- Hammel N, Belghith A, Weinreb RN, Medeiros FA, Mendoza N, Zangwill LM. Comparing the rates of retinal nerve fiber layer and ganglion cell-inner plexiform layer loss in healthy eyes and in glaucoma eyes. *Am J Ophthalmol*. 2017;178:38–50.
- Kim YK, Ha A, Na KI, Kim HJ, Jeoung JW, Park KH. Temporal relation between macular ganglion cell-inner plexiform layer loss and peripapillary retinal nerve fiber layer loss in glaucoma. *Ophthalmology*. 2017;124(7):1056–1064.
- Lee WJ, Kim YK, Park KH, Jeoung JW. Trend-based analysis of ganglion cell-inner plexiform layer thickness changes on optical coherence tomography in glaucoma progression. *Ophthalmology*. 2017;124(9):1383–1391.
- Miki A, Medeiros FA, Weinreb RN, et al. Rates of retinal nerve fiber layer thinning in glaucoma suspect eyes. *Ophthalmology*. 2014;121(7):1350–1358.
- Sehi M, Zhang X, Greenfield DS, et al. Retinal nerve fiber layer atrophy is associated with visual field loss over time in glaucoma suspect and glaucomatous eyes. *Am J Ophthalmol*. 2013;155(1):73–82.e1.

The effect of the population-based cervical cancer screening program on 5-year survival in cervical cancer patients in Lower Silesia

Dominika Zielecka-Dębska^{1,5,A-E}, Jerzy Błaszczyk^{2,A,B,D,E}, Dawid Błaszczyk^{3,B,C,E},
Jolanta Szelachowska^{1,5,C-E}, Krystian Lichon^{1,5,A,B,D,E}, Adam Maciejczyk^{1,5,D,E}, Rafał Matkowski^{4,5,A,D-F}

¹ Radiotherapy Department, Lower Silesian Oncology Centre in Wrocław, Poland

² Department of Epidemiology and Lower Silesian Cancer Registry, Lower Silesian Oncology Centre in Wrocław, Poland

³ Lower Silesian Coordinating Center for Preventive Programs, Lower Silesian Oncology Centre in Wrocław, Poland

⁴ Breast Unit, Lower Silesian Oncology Centre in Wrocław, Poland

⁵ Department of Oncology, Faculty of Medicine, Wrocław Medical University, Poland

A – research concept and design; B – collection and/or assembly of data; C – data analysis and interpretation;
D – writing the article; E – critical revision of the article; F – final approval of the article

Advances in Clinical and Experimental Medicine, ISSN 1899–5276 (print), ISSN 2451–2680 (online)

Adv Clin Exp Med. 2019;28(10):1377–1383

Address for correspondence

Dominika Zielecka-Dębska
E-mail: zielecka.d@gmail.com

Funding sources

The research project was fully sponsored
by the Ministry of Science and Higher Education
of Poland with grant No. ST.C280.17.010.

Conflict of interest

None declared

Received on April 10, 2019

Reviewed on May 21, 2019

Accepted on May 31, 2019

Published online on October 22, 2019

Cite as

Zielecka-Dębska D, Błaszczyk J, Błaszczyk D, et al. The effect
of the population-based cervical cancer screening program
on 5-year survival in cervical cancer patients in Lower Silesia.
Adv Clin Exp Med. 2019;28(10):1377–1383.
doi:10.17219/acem/109759

DOI

10.17219/acem/109759

Copyright

© 2019 by Wrocław Medical University
This is an article distributed under the terms of the
Creative Commons Attribution Non-Commercial License
(<http://creativecommons.org/licenses/by-nc-nd/4.0/>)

Abstract

Background. Poland is considered among the European countries with an average incidence of cervical cancer (CC; about 3,000–3,500/year) and at the same time with high mortality (5-year survival rate – 55.2%). For this reason, in 2006 Poland introduced a Population-Based Cervical Cancer Prevention and Early Detection Program addressed to women aged 25–59 years, in which a cytological test is carried out every 3 years.

Objectives. The aim of the study was to assess the changes in the curability of CC patients brought by the introduction of the Screening Program in the Lower Silesian voivodeship and to identify the subpopulation of women for whom activities aimed at increasing adherence rates must be intensified.

Material and methods. The 5-year relative survival in 3,586 CC patients from 2000–2010 registered in the Lower Silesian Cancer Registry was analyzed.

Results. In the Lower Silesian voivodeship, a 55.1% 5-year survival rate was recorded in 2000–2004 and 70.5% in 2010. The highest increase in 5-year relative survival rates was found in rural communities (from 53.1% in 2000–2004 to 77.7% in 2010) and in Wrocław (56.8% and 74.2%, respectively). In the study group, the number of patients with invasive CC (C53) detected in the local stage of the disease increased systematically from 61.5% in 2000–2004 to 74.3% in 2010.

Conclusions. The introduction of the population-based screening program improved the curability rate in CC patients in the Lower Silesian voivodeship. In order to maintain the recent positive trends, further education should be continued, and activities aimed at increasing adherence to screening tests should be intensified, especially in urban-rural communities.

Key words: cervical cancer, screening tests, cancer epidemiology

Introduction

Epidemiological statistics list Poland as a country with an increased risk of cervical cancer (CC), where incidence and mortality rates are among the highest in the European Union.^{1,2} Cervical cancer accounts for about 6.5% of all cancers in Polish women; it ranks 6th for incidence and 8th for mortality.³ Increased incidence of CC is observed in women aged over 20 years, and peak incidence falls in the age range of 49–54 years.¹ The risk of death from CC in low-income populations, including these in Poland, is around 2–4%.⁴ For the above reasons, this issue is of key importance for social and economic stability of Poland.⁵ In 2006, Poland introduced the Population-Based Cervical Cancer Prevention and Early Detection Program addressed to women aged 25–59 years, whose basic aim is to provide women with a possibility to have a cytology test performed every 3 years free of charge.^{6,7} The primary function of cytology screening is to diagnose and treat precancerous lesions and preinvasive cancer, as well as invasive cancer at an early stage, which helps avoid the cancer or ensure effective treatment.^{5,8,9} In highly developed countries such as Finland, Germany or Sweden, where screening tests were introduced back in the 1960s, the mortality rate of CC decreased by over 80%.^{3,10} However, Poland has not managed to reach the optimal percentage of target population adherence, hence CC screening is not fully effective yet.¹¹ The fact that women rarely use screening tests offered by the healthcare system signifies women's poor health-related awareness and the lack of effects of educational activities undertaken by the government and healthcare system.¹²

Objectives

The aim of the present study was to assess the changes in curability (5-year relative survival) of CC patients (C53 – malignant neoplasm of cervix uteri and D06 – carcinoma

in situ of cervix uteri according to ICD-10 classification) after introduction of the population-based screening in the Lower Silesian voivodeship, identify the subpopulation of women for whom activities aimed at increasing adherence to screening tests must be intensified and determine whether there is a positive trend in CC curability despite low adherence to the screening tests.

Material and methods

The 5-year survival rates in 3,586 CC patients (C53 and D06) from 2000–2010 as registered in the Lower Silesian Cancer Registry (LSCR) were analyzed. According to the registry, 271–374 cases were diagnosed annually in the Lower Silesian voivodeship. To exclude the influence of age on 5-year survival, the values of relative survival were calculated based on the life expectancy tables. Statistical calculations were performed using Microsoft Excel 2013 (Microsoft Corp., Armonk, USA) and the χ^2 test with the Yates's correction.

Ethical permission was not applied because the work is based on retrospective data from the LSCR. Our research did not have any influence on patient treatment and survival. No non-routine procedures were performed in the study, so consent from the patients was not taken. The data comes from the LSCR, which is a governmental institution.

Results

The 5-year relative survival rate in CC patients (C53 and D06) in the Lower Silesian voivodeship has been increasing steadily. It increased from 55.1% in 2000–2004 to 60.5% in 2005–2009, and in 2010 it reached 70.8% (Table 1) ($p < 0.00001$). At the same time, the number of cancers diagnosed at the pre-invasive stage (in situ cancers – D06)

Table 1. Five-year survival in cervical cancer patients in the Lower Silesian voivodeship in 2000–2010

Year	Number of C53+D06 cancers	5-year survival	Observed survival [%]	Relative survival [%]	Number of C53 cancers	5-year survival	Observed survival [%]	Relative survival [%]	Number of D06 cancers	%
2000	311	146	46.9	49.5	301	138	45.8	48.3	10	3.2
2001	341	179	52.5	55.4	332	171	51.5	54.4	9	2.6
2002	282	161	57.1	60.3	279	158	56.6	59.7	3	1.1
2003	271	139	51.3	54.2	258	127	49.2	51.9	13	4.8
2004	313	168	53.7	56.7	292	150	51.4	54.3	21	6.7
2005	314	166	52.9	55.3	294	148	50.3	52.6	20	6.4
2006	326	173	53.1	55.5	278	128	46.0	48.1	48	14.7
2007	338	183	54.1	56.5	283	132	46.6	48.7	55	16.3
2008	374	226	60.4	63.1	275	129	46.9	49.0	99	26.5
2009	357	230	64.4	67.3	245	121	49.4	51.6	112	31.4
2010	359	242	67.4	70.8	257	144	56.0	58.8	102	28.4

increased in a statistically significant manner in the analyzed group of patients ($p < 0.00001$), which greatly improved 5-year survival.

In the group of patients diagnosed with pre-invasive (D06) and invasive (C53) cancer, an upward trend in 5-year survival by 1.5% per year in 2000–2010 was observed (linear trend: $y = 1.5 \cdot x + 46.8$). We also found a steady increase in the survival rate in invasive CC (C53) patients by 1% per year, which is described by the trend $y = 0.03 \cdot x + 49.8$ (Fig. 1). In the group of patients diagnosed with invasive CC (C53) a linear reduction in the standardized mortality rate was observed in the years 2000–2015 (Fig. 2).¹³ Between 2000 and 2005, in the Lower Silesian voivodeship, an average number of 142 deaths of women due to invasive CC

were reported, in 2006–2010 and in 2011–2015 it was 138 and 133, respectively (trend: almost 1 person/year) (Fig. 2).

As the next step, we analyzed the differences in 5-year relative survival rates depending on the patients' residence. The highest increase in relative curability rates was definitely noted in rural communities (from 53.1% in 2000–2004 through 61.5% in 2005–2009 to 77.7% in 2010) and Wrocław (56.8%, 64.4% and 74.2%, respectively) (Table 2). The reasons for this were both a higher number of pre-invasive CC (D06) detected as shown in Table 1 and Table 3, and a better prognosis for invasive CC (Table 4). Both of these were an expected consequence of screening tests.

In the following years, a steady increase in the number of patients treated at the Lower Silesian Oncology Center

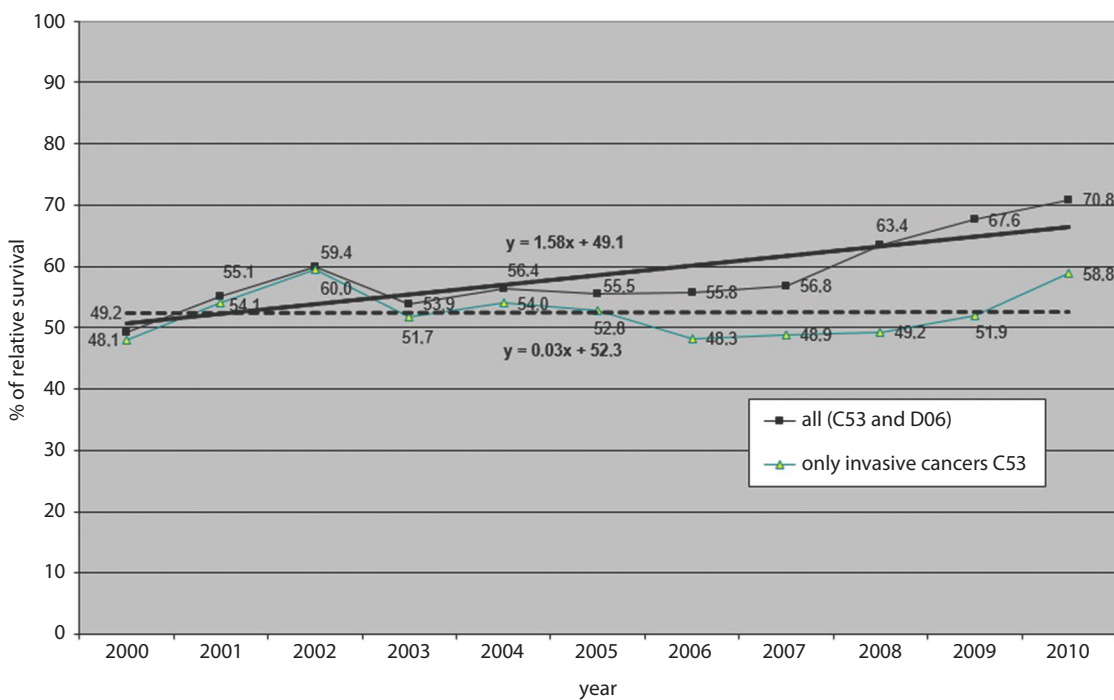


Fig. 1. Five-year relative survival in cervical cancer patients in the Lower Silesian voivodeship in 2000–2010

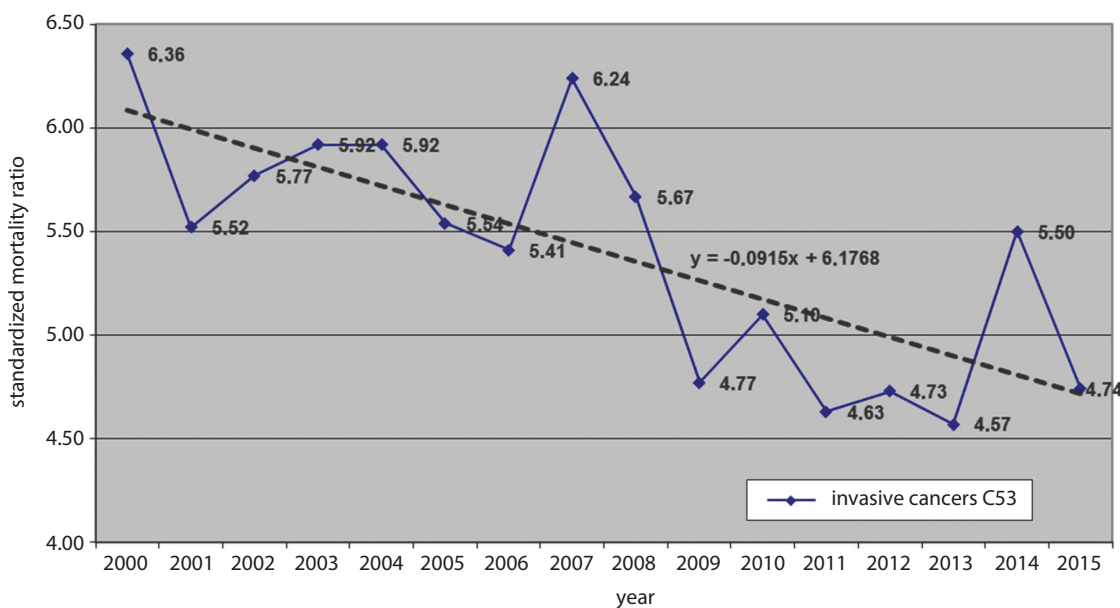


Fig. 2. Standardized mortality rate in invasive cervical cancer patients in the Lower Silesian voivodeship in 2000–2015¹³

Table 2. C53 and D06 (relative) survival by administrative unit

Administrative unit	2000–2004			2005–2009			2010		
	number of cancers	5-year survival	[%]	number of cancers	5-year survival	[%]	number of cancers	5-year survival	[%]
Urban community of Wrocław	321	172	56.8	389	236	64.4	68	48	74.2
Other urban communities	560	306	57.6	611	327	56.7	132	87	68.8
Rural community	296	150	53.1	293	171	61.5	69	52	77.7
Town in an urban-rural community	208	95	49.0	222	128	60.5	43	25	60.9
Rural area in an urban-rural community	133	70	55.4	194	116	63.1	47	30	67.7

Table 3. Incidence of D06 in situ cancers

Administrative unit	2000–2004			2005–2009			2010		
	number of all cancers	number of D06 cancers	[%]	number of all cancers	number of D06 cancers	[%]	number of all cancers	number of D06 cancers	[%]
Urban community of Wrocław	321	6	1.9	389	96	24.7	68	17	25.0
Other urban communities	560	25	4.5	611	104	17.0	132	40	30.3
Rural community	296	11	3.7	293	56	19.1	69	24	34.8
Town in an urban-rural community	208	6	2.9	222	35	15.8	43	10	23.3
Rural area in an urban-rural community	133	8	6.0	194	43	22.2	47	11	23.4

Table 4. Only invasive cancers C53 (relative) survival by administrative unit

Administrative unit	2000–2004			2005–2009			2010		
	number of cancers	5-year survival	[%]	number of cancers	5-year survival	[%]	number of cancers	5-year survival	[%]
Urban community of Wrocław	315	167	56.3	293	148	54.4	51	32	66.8
Other urban communities	535	284	56.1	507	225	47.4	92	48	53.3
Rural community	285	141	51.9	237	116	52.1	45	28	64.5
Town in an urban-rural community	202	89	47.4	187	94	53.1	33	17	54.5
Rural area in an urban-rural community	125	63	53.2	151	75	53.1	36	19	56.9

Table 5. Number of patients treated at LSOC by place of residence

Administrative unit	2005–2009			2010		
	number of cancers	number of patients treated at LSOC	[%]	number of cancers	number of patients treated at LSOC	[%]
Urban community of Wrocław	389	212	54.5	68	52	76.5
Other urban communities	611	179	29.3	132	63	47.7
Rural community	293	127	43.3	69	40	58.0
Town in an urban-rural community	222	91	41.0	43	32	74.4
Village in an urban-rural community	194	74	38.1	47	31	66.0
Total	1,709	683	40.0	359	218	60.7

* treated at LSOC by any method, also after surgery performed outside LSOC (but receiving radiotherapy and/or chemotherapy at LSOC); LSOC – Lower Silesian Oncology Center.

in Wrocław (LSOC), which is the referral center for Lower Silesia, was observed. In 2005–2009, 40% of all CC patients from Lower Silesia were treated at the LSOC, whereas in 2010 this number was as high as 60.7%. Such a large change in the number of patients treated at the LSOC probably resulted from the fact that the patients who had undergone screening were referred for multi-specialist

consultation to a full-profile reference center and then received treatment at the LSOC.

Table 5 shows the percentage of patients treated at the LSOC by place of residence. Treatment in the LSOC was most often selected by residents of Wrocław (54.5% in 2005–2009 and 76.5% in 2010), while residents of small and medium-sized towns were treated in the LSOC the least frequently (29.3%

Table 6. Five-year (relative) survival, any treatment method, all cancers (C53 and D06)

Period	Treated at LSOC	5-year survival	[%]	Treated only outside LSOC	5-year survival	[%]
2005–2009	683	463	70.8	1,026	515	53.5
2010	218	141	67.5	141	101	75.0

LSOC – Lower Silesian Oncology Center.

Table 7. Five-year (relative) survival rates, any treatment used, only invasive cancers (C53)

Period	Treated at LSOC	5-year survival	[%]	Treated only outside LSOC	5-year survival	[%]
2005–2009	536	322	63.2	839	336	43.2
2010	175	102	61.2	82	42	55.1

LSOC – Lower Silesian Oncology Center.

in 2005–2009 and 47.7% in 2010), which was most probably due to the fact that municipal hospitals have departments dedicated to the care of gynecology patients.

Another factor that was analyzed was the impact of experience of the hospital center where the patients received treatment on the curability. Firstly, it is worth noting that before 2008 the LSOC was the only entity that provided oncological radiotherapy services in the Lower Silesian voivodeship. Surgical procedures and systemic treatment in the analyzed period were carried out in various centers in the voivodeship, including the LSOC. Out of the 3,586 patients reported to the LSCR, 1,831 had undergone a surgical procedure, radiotherapy was used in 1,915 patients and 1,022 patients received systemic therapy. No treatment was used in 181 (5%) patients out of the 3,586 patients diagnosed with CC – these were the patients who were not eligible for treatment due to comorbidities or advanced disease. This data was excluded from the analysis. In the study period, we found a significant increase of the 5-year survival rate in the patients treated outside the LSOC (from 53.5% to 75.0%) (Table 6). This increase was undoubtedly attributed to the higher percentage of in situ cancers (D06) that were detected and treated, as well as a decreasing percentage of patients with invasive CC in this group (C53 accounted for 58.2% of diagnoses). By contrast, in patients referred to the reference center (LSOC) for treatment, invasive cancers (C53) still accounted for a high percentage of diagnoses (as high as 80.3%) (Tables 6,7). At the same time, prognosis in patients with invasive CC (C53) who were treated outside the LSOC remained significantly worse, with 5-year survival of 43.2% in 2005–2009 and 55.1% in 2010, whereas in patients treated at the LSOC it was 63.2% in 2005–2009 and 61.2% in 2010 (Table 7). The analysis showed that the treatment results discussed above, namely the 5-year-survival rate in patients with invasive CC (C53) treated outside the LSOC in the study period (2005–2010), were statistically lower ($p < 0.00001$) than for the patients treated at the LSOC. We observed a systematic increase of the percentage, from 61.5% in 2000–2004 through 68.7% in 2005–2009 to 74.3% in 2010, of patients with invasive CC (C53) detected in the local stage of the disease (Table 8).

Table 8. Advancement of invasive cervical cancer (C53)

Period	Number and percentage	Local disease	Regional disease	Metastatic disease
2000–2004	n	643	227	176
	%	61.5	21.7	16.8
2005–2009	n	748	184	157
	%	68.7	16.9	14.4
2010	n	159	31	24
	%	74.3	14.5	11.2

In 2005–2009 in the Lower Silesian voivodeship, we recorded a 63.2% 5-year survival rate among patients diagnosed with invasive CC (C53) treated at the LSOC, and a 43.2% 5-year survival rate in patients treated outside the LSOC. In this group, 69% were patients diagnosed with the local stage of the disease, 17% – with regional stage of the disease and 14% – with generalized disease (Table 9). According to the 25th Annual FIGO (Fédération internationale de gynécologie et d’obstétrique – International Federation of Gynecology and Obstetrics) Report, in Europe the 5-year survival rate in patients with invasive CC (C53) is 82% for the local, 42% for regional and 17% for generalized stages.¹⁴ Taking into account the disease advancement data, the expected relative survival rates in patients from our voivodeship can be calculated using the European standard¹⁴: $0.69 \cdot 82\% + 0.17 \cdot 42\% + 0.14 \cdot 17\% = 66.1\%$.

The above calculations suggest that 5-year survival rate in the patients receiving treatment at the reference center (LSOC) is at the European level (63.2%). Unfortunately, a much worse prognosis is observed in the patients treated outside the LSOC (43.2%).

Discussion

About 60,000 new cases of CC are diagnosed each year in Europe and as many as half of those patients die.¹⁵ Large-scale studies have shown that screening in women aged

Table 9. Five-year relative survival (RSC) in 1995–1999 and 2000–2007^{21,22}

Country	RSC 1995–1999 [%]	RSC 2000–2007 [%]	Change [%]
Northern Europe	71.6	71.5	–0.1
Denmark	69.5	70.7	1.2
Finland	67.9	69.0	1.1
Iceland	76.7	84.6	7.9
Norway	72.8	75.6	2.8
Sweden	71.0	69.9	–1.1
UK and Ireland	65.2	66.6	1.4
Ireland	65.3	66.3	1.0
UK (England)	65.2	66.8	1.6
UK (Northern Ireland)	68.6	71.8	3.2
UK (Scotland)	67.5	66.1	–1.4
UK (Wales)	59.3	63.1	3.8
Central Europe	69.2	68.0	–1.2
Austria	67.5	68.3	0.8
Belgium	69.3	70.2	0.9
France	69.6	63.5	–6.1
Germany	65.0	66.8	1.8
Switzerland	70.6	66.7	–3.9
the Netherlands	73.2	70.3	–2.9
Southern Europe	65.3	66.9	1.6
Croatia	–	68.0	–
Italy	65.6	66.8	1.2
Malta	64.8	54.7	–11.1
Portugal	58.0	63.8	5.8
Slovenia	71.8	75.5	3.7
Spain	66.1	66.1	0
Eastern Europe	63.7	60.3	–3.4
Bulgaria	–	54.8	–
Czech Republic	72.0	67.1	–4.9
Estonia	–	65.6	–
Latvia	–	52.0	–
Lithuania	–	58.9	–
Poland*	53.3	55.2	1.9
Slovakia	65.8	66.5	0.7
European average	64.7	65.4	0.7

* Lower Silesian and Świętokrzyskie voivodeship as well as city of Kraków participated in the study.

21–65 years with a cytology test significantly reduces the CC incidence and mortality rate.^{16,17} Although widely available, free-of-charge prophylactic cytology tests has been available in Poland for a few years and access to diagnostic tests has become easier, the number of new cases remains high despite the downward trend.¹⁸ The reason behind the low adherence of the target population to screening cytology tests is low awareness of the benefits of such tests, as well as insufficient knowledge among the target group about

the screening tests offered.^{19,20} It should also be underlined that some cases of CC develop despite women's participation in screening (adenocarcinomas), and some of the cases occur in groups not covered by regular screening.¹⁵ In order to compare the effectiveness of conducted activities aimed at reducing mortality from malignant neoplasms, EURO-CARE studies were conducted in Europe. In the EURO-CARE-5 study (2000–2007), an average of 65.4% for 5-year relative survival was obtained, with the highest values found in Northern Europe (71.5% on average) and Central Europe (68%), and the lowest values noted in Eastern Europe (60.3%).²¹ In comparison with survival rates in 1995–1999, no unequivocal increase in survival rates was noted in Europe or in individual countries (Table 9).²²

The 5-year survival rate in Poland in 2000–2007 (55.2%) was among the lowest in Europe, being almost 10% lower than the average for Europe, and almost 30% lower than the average for Iceland.²¹ In 1995–1999, this rate in Poland was lower by a further 1.9%.

In the Lower Silesian voivodeship in 2000–2004, relative survival was 55.1%, in 2005–2009 it was 60.5% and in 2010 it was 70.5%. It is worth noting that if a survival rate of over 70% is maintained in the following years, the Lower Silesian voivodeship may rank high in the planned EURO-CARE-6 study because only 8 European countries had a rate value of over 70% (Table 9) in EURO-CARE-5.²¹ Considering the upward trend in detecting in situ cancers, an extremely beneficial effect of population-based screening on 5-year survival rate in CC patients is observed (Table 4). The highest increase in the relative curability rates was noted among patients residing in rural communities (from 53.1% in 2000–2004 through 61.5% in 2005–2009 to 77.7% in 2010) and in Wrocław. While in the case of Wrocław better results may be attributed to easily available cytology test and screening information, the deciding factor in rural communes might have been the provision of free of charge medical service and significantly and gradually rising public awareness regarding cancer prevention. At the same time, it is unclear why such a major effect of screening was not observed in communal towns, i.e., small and medium-sized towns. The higher 5-year survival rate in CC patients was accompanied by a higher percentage of patients undergoing treatment at the LSOC. In 2010, compared to 2005–2009, the number of patients treated at the LSOC increased by over 20% from 40% to 60.7% of all cancer patients in the Lower Silesian voivodeship. The authors believe that centralized therapy in the center with the most extensive experience in the treatment of CC contributed to better treatment outcomes for the patients.

Conclusions

The 5-year survival rate in 2000–2007 in Poland (55.2%) was among the lowest ones in Europe, being almost 10% lower than the European average. In the Lower Silesian

voivodeship, a 55.1% 5-year survival rate was recorded in 2000–2004, 60.5% in 2005–2009 and 70.5% in 2010. The highest increase in relative survival rates was found in rural communities (from 53.1% in 2000–2004 through 61.5% in 2005–2009 to 77.7% in 2010) and in Wrocław (56.8%, 64.4% and 74.2%, respectively). In the group under study, the number of patients with invasive CC (C53) detected in the local stage of the disease increased systematically from 61.5% in 2000–2004 through 68.7% in 2005–2009 to 74.3% in 2010. Five-year relative survival rates in Lower Silesian patients receiving treatment at the LSOC (63.2% and 61.2%) were significantly better than those in patients treated in other centers (43.2% and 55.1%) and close to the expected relative survival rates for Lower Silesian patients with invasive cancers (66.1%). In conclusion, the introduction of the population-based screening program improved the curability rate for CC patients in the Lower Silesian voivodeship. However, to ensure that the recent positive trends are continued, women must be educated further, and activities aimed at increasing adherence to screening tests must be intensified, particularly in urban-rural communities. At the same time, patients diagnosed with CC must be systemically referred to highly specialized centers where comprehensive treatment is provided.

ORCID iDs

Dominika Zielecka-Dębska  <https://orcid.org/0000-0001-6731-5400>
 Jerzy Błaszczyk  <https://orcid.org/0000-0002-9331-9728>
 Dawid Błaszczyk  <https://orcid.org/0000-0001-7396-1660>
 Jolanta Szelachowska  <https://orcid.org/0000-0003-3254-6625>
 Krystian Lichoń  <https://orcid.org/0000-0002-9311-7069>
 Adam Maciejczyk  <https://orcid.org/0000-0002-7047-0433>
 Rafał Matkowski  <https://orcid.org/0000-0002-1705-5097>

References

- Barnaś E, Borowiec-Domka E, Kądziołka J, Grzegorzczak J. Factors affecting the response-rate to cytology examinations of women in the Subcarpathian region, National Programme of Cervical Cancer Prophylaxis [in Polish]. *Probl Hig Epidemiol*. 2008;89(4):482–486.
- World Health Organization, Department of Information, Evidence and Research. Mortality database. <http://www-dep.iarc.fr/WHOdb/table2.asp> of subordinate document. Accessed March 31, 2019.
- Nowicki A, Borowa I, Maruszak M. Women health behaviours regarding prevention and early detection of precancerous lesions and cervical carcinoma [in Polish]. *Ginek Pol*. 2008;79(12):840–849.
- Denny L, Kuhn L, De Souza M, Pollack AE, Dupree W, Wright TC Jr. Screen-and-treat approaches for cervical cancer prevention in low-resource settings: A randomized controlled trial. *JAMA*. 2005;294(17):2173–2181.
- Goldie SJ, Gaffikin L, Goldhaber-Fiebert JD, et al; Alliance for Cervical Cancer Prevention Cost Working Group. Cost-effectiveness of cervical-cancer screening in five developing countries. *N Engl J Med*. 2005;353(20):2158–2168.
- Mariańczyk K, Steuden S. Expectations and intentions of health behaviours as factors determining performance of preventive Pap smear among women aged over 45 [in Polish]. *Psychoonkologia*. 2011;2:55–64.
- Nowakowski A, Wojciechowska U, Wieszczy P, Cybulski M, Kamiński MF, Didkowska J. Trends in cervical cancer incidence and mortality in Poland: Is there an impact of the introduction of the organised screening? *Eur J Epidemiol*. 2017;32(6):529–532.
- Gustafsson L, Ponten J, Zack M, Adami H-O. International incidence rates of invasive cervical cancer after introduction of cytological screening. *Cancer Causes Control*. 1997;8(5):755–763.
- Spaczyński M, Karowicz-Bilinska A, Kędzia W, et al. Costs of Population Cervical Cancer Screening Program in Poland between 2007–2009 [in Polish]. *Ginek Pol*. 2010;81(10):750–756.
- Anttila A, Pukkala E, Söderman B, Kallio M, Nieminen P, Hakama M. Effect of organised screening on cervical cancer incidence and mortality in Finland, 1963–1995: Recent increase in cervical cancer incidence. *Int J Cancer*. 1999;83(1):59–65.
- Zielecka D, Lichoń K, Maciejczyk A, Błaszczyk J, Błaszczyk D, Matkowski R. Wpływ cytologicznych badań przesiewowych na zachorowania na raka szyjki macicy w województwie dolnośląskim w latach 2005–2014. *Postepy Hig Med Dosw*. 2018;72:13–20.
- Słowiecka A, Wiraszka G. Women's attitudes towards reproductive system disease prevention. *Eur J Clin Invest*. 2013;1:50–60.
- Wojciechowska U, Didkowska J. Zachorowania i zgony na nowotwory złośliwe w Polsce. In: Krajowy Rejestr Nowotworów, Centrum Onkologii – Instytut im. Marii Skłodowskiej-Curie. <http://onkologia.org.pl/raporty/of> subordinate document. Accessed March 27, 2019.
- Sergio P. *25th Annual Report on the Results of Treatment of Gynecological Cancer*. London, UK: Elsevier Health Sciences; 2003.
- Spaczyński M, Nowak-Markwitz E, Witold K. Cervical cancer screening in Poland and worldwide [in Polish]. *Ginek Pol*. 2007;78(5):354–360.
- Moyer VA; U.S. Preventive Services Task Force. Screening for Cervical Cancer: U.S. Preventive Services Task Force Recommendation Statement. *Ann Intern Med*. 2012;156(12):880–891.
- Dillner J, Rebolj M, Birembaut P, et al. Long term predictive values of cytology and human papillomavirus testing in cervical cancer screening: Joint European cohort study. *BMJ*. 2008;337:1756–1833.
- Karczmarek-Borowska B, Grądalska-Lampart M. Cervical cancer incidence and mortality rates including the screening program results in the Podkarpackie Region between 1999–2010 [in Polish]. *Ginek Pol*. 2013;84(11):930–937.
- Tuchowska P, Worach-Kardas H, Marcinkowski JT. The most frequent malignant tumors in Poland: The main risk factors and opportunities to optimize preventive measures [in Polish]. *Probl Hig Epidemiol*. 2013;94(2):166–171.
- Wrześniewska M, Adamczyk-Gruszka O, Gruszka J, Bąk B. Diagnostic and therapeutic possibilities in the prophylaxis of cervical cancer [in Polish]. *Stud Med*. 2013;29(1):109–116.
- Sant M, Chirlaque Lopez MD, Agresti R, et al; EUROCARE-5 Working Group. Survival of women with cancers of breast and genital organs in Europe 1999–2007: Results of the EUROCARE-5 study. *Eur J Cancer*. 2015;51(15):2191–2205.
- Berrino F, De Angelis R, Sant M, et al; EUROCARE-4 Working Group. Survival for eight major cancers and all cancers combined for European adults diagnosed in 1995–99: Results of the EUROCARE-4 study. *Lancet Oncol*. 2007;8(9):773–783.

Therapy compliance in children with phenylketonuria younger than 5 years: A cohort study

Dariusz Walkowiak^{1,A–F}, Anna Bukowska-Posadzy^{2,3,B,C,E,F}, Łukasz Kałużny^{2,B,C,E,F},
Mariusz Ołtarzewski^{4,B,C,E,F}, Rafał Staszewski^{1,C,E,F}, Michał Musielak^{5,A,E,F}, Jarosław Walkowiak^{2,A,C–F}

¹ Department of Organization and Management in Health Care, Poznan University of Medical Sciences, Poland

² Department of Pediatric Gastroenterology and Metabolic Diseases, Poznan University of Medical Sciences, Poland

³ Department of Clinical Psychology, Poznan University of Medical Sciences, Poland

⁴ Department of Screening Tests, Institute of Mother and Child, Warszawa, Poland

⁵ Department of Social Sciences, Poznan University of Medical Sciences, Poland

A – research concept and design; B – collection and/or assembly of data; C – data analysis and interpretation;
D – writing the article; E – critical revision of the article; F – final approval of the article

Advances in Clinical and Experimental Medicine, ISSN 1899–5276 (print), ISSN 2451–2680 (online)

Adv Clin Exp Med. 2019;28(10):1385–1391

Address for correspondence

Dariusz Walkowiak
E-mail: dariuszwalkowiak@ump.edu.pl

Funding sources

None declared

Conflict of interest

None declared

Received on September 12, 2018

Reviewed on September 30, 2018

Accepted on February 18, 2019

Published online on August 30, 2019

Cite as

Walkowiak D, Bukowska-Posadzy A, Kałużny Ł, et al.
Therapy compliance in children with phenylketonuria
younger than 5 years: A cohort study. *Adv Clin Exp Med.*
2019;28(10):1385–1391. doi:10.17219/acem/104536

DOI

10.17219/acem/104536

Copyright

© 2019 by Wrocław Medical University
This is an article distributed under the terms of the
Creative Commons Attribution Non-Commercial License
(<http://creativecommons.org/licenses/by-nc-nd/4.0/>)

Abstract

Background. Phenylketonuria (PKU) is a metabolic disease. It is manifested by a complete or partial inability to convert phenylalanine (Phe) to tyrosine and leads to increased concentrations of Phe in the blood and in other tissues, including the brain, causing irreversible neurological damage if left untreated. Low-phenylalanine diet is a key component of classical PKU therapy.

Objectives. The objective of this study was to assess the effectiveness of classical phenylketonuria therapy and compliance with doctors' recommendations in the first 5 years of life.

Material and methods. Data was collected from all diagnosed and treated patients (n = 57) born 1999–2010. Phenylalanine blood levels, the number of visits to a specialist outpatients' center, the number of blood tests, as well as socioeconomic status (SES) and parents' education level have been analyzed, and potential relationships have been assessed.

Results. In the 1st year of life patients visited their doctors (odds ratio (OR) = 6.8267; 95% confidence interval (95% CI) = 2.827–16.5163; p < 0.0001) and had their blood collected (OR = 2.7875; 95% CI = 1.0467–7.4234; p < 0.0402) significantly more frequently than in the 2nd year. This tendency persisted into subsequent years. Similarly, in infancy they had statistically significantly lower odds of exceeding more than 40% of their Phe levels over therapeutic range than 1 year later (OR = 3.6078; 95% CI = 1.4859–8.7599; p < 0.0046). No PKU child had more than 70% of Phe levels over the therapeutic range in the 1st year of life, whereas 4 years later there were 18 such children. Phe levels were correlated with the number of visits to a specialist (p = 0.39) and the number of Phe blood tests with index of dietary control (p = –0.33). The effectiveness of therapy and compliance with the doctor's recommendations seem to depend neither on the level of education of the patient's parents nor on their SES.

Conclusions. Therapy effectiveness and patients' compliance in PKU is very good in infancy. However, both deteriorate in subsequent years. Moreover, they do not seem to depend on the family background.

Key words: compliance, diet, phenylketonuria, inborn errors of metabolism, phenylalanine

Introduction

Phenylketonuria (PKU) is currently regarded as a model inborn error of metabolism, which, if the treatment is not started immediately after birth, leads to irreversible damage to the central nervous system. Metabolic pediatrics often uses the experience gained in treating that illness over the years, from extending screening of the newborn, through the strategies of medical care for diagnosed patients, to the control of the effectiveness of the therapy.¹ A constitutive element of the strategy of complex care of patients suffering from PKU is the creation of an effective system of medical and dietary supervision that allows the patients to function in society under the conditions as close as possible to those of their healthy peers. Research conducted over the years has shown certain deficits in treated patients with PKU. At the same time, however, we are confident that to achieve the best outcomes, PKU must be diagnosed early, and the low-phenylalanine (Phe) diet effectively implemented. The strategy of medical care for patients with PKU includes, among others, the monitoring of the serum Phe levels, effectively planned and carried out visits to a dietician, and medical and psychological examinations. Both for the parents of a PKU child and for the doctor, the results of blood tests are the first step in the evaluation of the effectiveness of the treatment, and they allow the doctor and parents to modify the child's diet in order to achieve the best therapeutic effect.

In 1956 Blainey and Gulliford drew attention to the diet non-compliance during the homestay of PKU children.² Because they were among the first specialists working with PKU patients, one can say that the problems with the diet compliance are almost as old as the treatment of the disease itself. On the other hand, despite the time that has since passed, it is still believed that "compliance assessment measures remain inadequately defined. The direct assessment of blood Phe concentration is perhaps the best overall measure, but there is no universal agreement about the number of Phe concentrations that should be within target range and frequency or timing of measurement."³

Objectives

The purpose of this article was twofold. Firstly, the effectiveness of PKU therapy in the first 5 years of life of a patient has been assessed on the basis of Phe levels in blood, the compliance with dietary recommendations based upon the number of visits to a specialist and the number of blood tests. In particular, we have analyzed how the values of these parameters change in time, and whether there is any internal correlation among them. Secondly, we attempted to verify a hypothesis about a link between these 3 parameters and the family background of a patient as expressed by the parental educational level and the socioeconomic status (SES) of the family.

Material and methods

A retrospective longitudinal study was conducted in a group of classical PKU patients, diagnosed from May 1999 to September 2010, who were admitted for diagnosis and treatment at the Department of Pediatric Gastroenterology and Metabolic Diseases at the Poznan University of Medical Sciences, a reference unit for PKU patients from western Poland. For the purposes of our analysis, patients with classical PKU were defined as those who require a low-phenylalanine diet to maintain plasma Phe levels within the target range of 2–6 mg% (120–360 $\mu\text{mol/L}$) and whose Phe levels without diet exceed 20 mg% (1200 $\mu\text{mol/L}$).^{4,5} The inclusion criteria were the following: neonatal diagnosis carried out with the colorimetric method, classical PKU diagnosed and continuous treatment for at least 5 years. The exclusion criterion was a chronic or acute disease which may influence PKU treatment. Our department is taking care of 57 PKU patients (37 girls and 20 boys) born between May 1999 and September 2010. All 57 patients participated in the study, with no one excluded from this group. There were 2 more PKU patients diagnosed in this period: a girl who died at the age of 2 of another disease, and a boy whose parents after 1 year of diet refused any further treatment for their son.

All records of each patient's visit to a specialist were collected from the clinical documentation for comparison with recommendations regarding the number of visits. The parents of a PKU child are informed that for the first 3 years of life the child should visit a specialist every 3 months. Later in life the control should be carried out every 6 months. The compliance percentages with these recommendations were calculated for each year of the child's life separately. We also collected information about the SES and educational level of the parents of all the patients.

We evaluated all the blood Phe concentrations collected during the first 5 years of the children's lives, with the exception made for the 1st month, because Phe concentrations in this period are unstable. For each patient, we counted the number of tests to compare it with the recommendations. The 5-year index of dietary control (IDC) was calculated as the mean of the 12-month medians. The percentage of Phe concentrations which were within the therapeutic range was analyzed for each patient and each year of life.

Since this was an exploratory study, sample size was not calculated and all the available data was gathered. The Shapiro–Wilk test was applied to determine the normality of the data distribution. Results are expressed as medians and interquartile ranges (IQRs; means \pm SD). The odds ratio (OR) was calculated to compare the following: 1) the percentage of results beyond the therapeutic range taken from the data from the first 5 years of life, 2) the number of medical visits and Phe blood sampling (compared were the the results for the years of life grouped into two groups: one group comprising the 1st, the 2nd and the 3rd year of life, and the other – the 4th and the 5th years, the assumption being that

recommendations for patients aged 1–3 years differ from those for 4–5 years of life). The 95% confidence intervals (95% CI) were calculated to estimate the precision of the OR.

Spearman’s rank correlation coefficient was calculated to determine possible correlations between, on the one hand, the educational level of the mother, the educational level of the father, the SES of the family and the sex of the child, and on the other hand, the following parameters: the number of visits to a specialist and the frequency of Phe blood monitoring. Then, possible correlations between all the 6 abovementioned factors, and both IDC and the percentage of Phe concentrations within the therapeutic range were also tested with Spearman’s coefficient.

The level of significance was set at $p < 0.05$. Statistical analysis was performed using STATISTICA v. 12 (StatSoft Inc., Tulsa, USA).

The study adhered to the Declaration of Helsinki and was approved by the Bioethical Committee at the Poznan University of Medical Sciences (approval No. 268/15).

Results

During the first 5 years of life, 57 PKU children visited a specialist 806 times and had their blood monitored for Phe 7,638 times. The mean number of visits to the specialist over the first 5 years of life was 14.1 (range: 6–29).

In the 1st year of life, the mean number of visits was 4.7, decreasing to 2.5 in the 3rd year and to 1.7 in the 5th year (Table 1). As the recommended number of visits was lower in year 4 and 5, the lowest mean percentage of the recommended number of visits was in the 3rd year – 62%.

The mean number of blood Phe monitoring in the 1st year was 44.4 (range: 7–73) (Table 2). In the 5th year, the mean number of blood Phe monitoring decreased to 15.3. In the 4th and 5th year, there were children with no blood Phe monitoring at all. The mean number of blood Phe monitoring during the first 5 years varied from 21 to 239, so from 10% to 115% of the recommended value, with the mean value of 137 (66%).

During the 1st year of life, 32 patients out of 57 (56%) had less than 20% of Phe blood test results over the therapeutic range of 6 mg% (Table 3). During the 5th year of life, there were only 15 (26%) such patients. We found no PKU child with more than 70% of Phe blood test results over the therapeutic range in the 1st year of life. In the 5th year of life, there were 18 such children. During the 1st year, the mean value of blood Phe concentrations was 3.6 mg%, and the median was 3.2 (Table 3). In the consecutive years, the mean value increased, reaching 7.1 mg% in the 5th year, and the median increased to 5.7 mg%. The maximum value was observed in the 4th year (5.9 mg%).

During the 1st year of life, patients had statistically significantly lower odds of exceeding Phe therapeutic range

Table 1. Number of visits to a specialist

Years of life		1 st	2 nd	3 rd	4 th	5 th	1 st –5 th
Number of visits to a specialist	range	2–9	0–8	0–7	0–5	0–4	6–29
	median (IQR)	5 (4–5)	3 (2–4)	2 (2–3)	2 (1–3)	2 (1–2)	14 (11–17)
	mean (SD)	4.7 (1.4)	3.3 (1.4)	2.5 (1.3)	1.9 (1.1)	1.7 (0.9)	14.1 (4.4)
Recommended number of visits		4	4	4	2	2	16
Number of visit as % of recommendations	range	50–225	0–200	0–175	0–250	0–200	37–150
	median (IQR)	125 (100–125)	75 (50–100)	50 (50–75)	100 (50–150)	100 (50–100)	87 (69–106)
	mean (SD)	117 (35)	82 (35)	62 (32)	95 (55)	85 (45)	88 (27)

IQR – interquartile range; SD – standard deviation.

Table 2. Number of Phe blood tests

Years of life		1 st	2 nd	3 rd	4 th	5 th	1 st –5 th
Number of blood Phe tests	range	7–73	3–58	1–52	0–48	0–46	21–239
	median (IQR)	47 (35–55)	34 (21–45)	25 (13–36)	15 (10–26)	13 (8–19)	137 (92–175)
	mean (SD)	44.4 (14.6)	32.5 (15.1)	24.7 (13.6)	18.1 (10.4)	15.3 (8.6)	134 (54)
Recommended number of blood tests		52	52	52	26	26	208
Number of blood tests as % of recommendations	range	13–140	6–111	2–100	0–185	0–177	10–115
	median (IQR)	90 (67–106)	65 (40–86)	48 (25–69)	58 (38–100)	50 (31–73)	66 (44–84)
	mean (SD)	85 (28)	62 (29)	47 (26)	70 (40)	59 (33)	64 (26)

IQR – interquartile range; SD – standard deviation.

Table 3. Phe blood levels over the therapeutic range and mean Phe blood concentrations

Number of patients with Phe levels over the therapeutic range					
Abnormal results	Years of life				
	1 st	2 nd	3 rd	4 th	5 th
<20%	32	23	21	20	15
21–40%	16	11	11	9	14
41–70%	9	15	10	14	10
>70%	0	8	15	14	18
Mean blood Phe concentrations [mg%]					
Years of life	1 st	2 nd	3 rd	4 th	5 th
Range	1.4–7.7	2.6–13.2	1.3–24.7	2.6–24.7	2.1–24.8
Median (IQR)	3.2 (2.6–4.4)	4.5 (3.6–6.9)	5.1 (3.9–8.9)	5.9 (4.0–7.4)	5.7 (4.2–8.3)
Mean (SD)	3.6 (1.6)	5.5 (2.4)	6.5 (4.3)	6.6 (4.2)	7.1 (4.7)

IQR – interquartile range; SD – standard deviation.

Table 4. Comparison of Phe levels and parental compliance between particular years

Phe levels over therapeutic range (OR (95% CI))				
Percentage	Years of life			
	2 nd vs 1 st	3 rd vs 1 st	4 th vs 1 st	5 th vs 1 st
<20%	1.8922 (0.8991–3.9823) 0.0930	2.1943 (1.0359–4.6480) 0.0402	2.3680 (1.1133–5.0368) 0.0252	3.5840 (1.6295–7.8829) 0.0015
<40%	3.6078 (1.4859–8.7599) 0.0046	4.1667 (1.7222–10.0807) 0.0015	5.1494 (2.1333–12.4299) 0.0003	5.1494 (2.1333–12.4299) 0.0003
Parental compliance (OR (95% CI))				
Event	Years of life			
	2 nd vs 1 st	3 rd vs 1 st	3 rd vs 2 nd	5 th vs 4 th
Visits	6.8267 (2.8217–16.5163) <0.0001	20.0000 (7.6948–51.9831) <0.0001	2.9297 (1.2850–6.6795) 0.0106	1.0751 (0.5099–2.2669) 0.8491
Phe blood tests	2.7875 (1.0467–7.4234) 0.0402	10.7317 (2.3363–49.2947) 0.0023	3.8500 (0.7638–19.4057) 0.1024	3.7143 (1.2478–11.0558) 0.0184

OR – odds ratio; CI – confidence interval.

than later in life (Table 4). Statistically significant OR were found between the number of visits to a specialist and a number of blood Phe tests in the 1st vs 2nd and 3rd year of life. No relationship was found between, on the one hand, the parental educational level and the SES of the family, and on the other, the number of visits to the specialist and the frequency of Phe blood monitoring (Table 5).

Statistically significant correlations were found between, on the one hand, the percentage of Phe concentrations within the therapeutic range and IDC, and on the other, the number of visits to the specialist and the frequency of Phe blood monitoring (Table 5). No statistically significant correlations of the parental educational level and the SES of the family with the percentage of Phe concentrations within the therapeutic range and IDC were documented.

Discussion

In this unique study comprising all PKU patients treated in our department, we aimed to assess the effectiveness of therapy and compliance with specialists' recommendations in the first years of life. It is worth emphasizing that although treatment control of PKU patients in infancy was very good, still many parents did not strictly follow given dietary recommendations. In subsequent years, significant deterioration was observed, which points to the need of further parental education and intensification of medical care. Unexpectedly, we did not observe any impact of parental education or socioeconomic status.

In an analysis of rare diseases, including inborn errors of metabolism, a common obstacle in achieving reliable results of tests is the size of the study group and

Table 5. Correlations between Phe levels, family background and the number of visits and frequency of blood testing

Variable	% of measured Phe levels within therapeutic range		IDC		Number of visits		Number of blood tests	
	ρ	p	ρ	p	ρ	p	ρ	p
Educational level of mother	0.20	0.14	-0.04	0.77	0.08	0.55	0.11	0.41
Educational level of father	0.21	0.12	-0.11	0.40	-0.05	0.72	0.02	0.89
SES	0.18	0.19	-0.12	0.36	0.13	0.32	0.20	0.14
Number of visits to the specialist	0.39	0.003	-0.30	0.02	-	-	-	-
Number of blood tests	0.26	0.05	-0.33	0.01	-	-	-	-

Phe – phenylalanine; IDC – index of dietary control; SES – socioeconomic status.

its representativeness for the entire patient population. If the survey covers only a part of the patient population, the risk of bias increases. The present study is unique, because 100% of the treated PKU patients in our hospital were included in the study and the whole experimental group was enrolled on the basis of uniform criteria. This allowed for a reliable assessment of patient compliance (the number of visits and blood tests, and especially the concentration of Phe) in the largest PKU patients group to date.

The literature concerning the number of medical visits and practices associated with it during the treatment of PKU is not too extensive. There is no doubt that of crucial importance is the number and schedule of a PKU patient's visits to a specialist, because it is during those visits that knowledge about the disease is transmitted; these visits exert a disciplinary influence on the parents and contribute to the correction of their misconceptions drawn, e.g., from the Internet. Similarly to the recommendations on the number of blood tests, there are also recommendations on the minimal frequency of visits to a specialist. The PKU Consensus Development Conference Statement, released in 2000, suggests "regular and frequent visits to a PKU clinic".⁶ The National Society for Phenylketonuria (UK) recommends as a minimum, until 2 years of life, a 3-monthly review, for patients aged less than 5 years – a 4-monthly review, and later – a 6-monthly review.⁷ German recommendations⁸ suggest at least 1 clinical monitoring per quarter until 4 years of age and every 3–6 months until 12 years of age. The analysis done by van Spronsen et al.,⁹ conducted in 17 European PKU centers in 12 countries, as a suggested frequency of clinical evaluation in the 1st year of life gives from 2 to 12 (with the most frequent value 9), and for the next 3 years of life from 1 to 6 visits per year (with the most frequent value being 4). In the recently published European guidelines for the diagnosis and management of patients with PKU,¹⁰ the researchers suggest a visit to a specialist every 2 months in the 1st year of life, and then twice per year until 12 years of age. In Poznań, parents are informed that for the first 3 years of life, children should visit a specialist

every 3 months. Later in life, control should be carried out every 6 months.

In the group that took part in the present study, the average number of visits to the specialist in the first 5 years of life was 14.1 (while the recommended number was 16). More than 50% of the patients did not comply with the recommendations. One-third of the visits (269 of 806) took place in the 1st year of life. A significant part of the analyzed group also had periods without medical examination, sometimes even exceeding 1 year. The analysis of the visits is hindered by random events, such as, e.g., infections, which can cause a temporary increase of Phe in the blood, and hence should lead to a visit to a specialist. Circumstances not directly related to the disease (such as the need to obtain a certificate for the purposes of the foundation supporting PKU children) could also have had an impact on the number of visits. Despite all the factors that influenced the number of visits in this study, we observed a significant correlation between the number of visits and the number of blood tests ($\rho = 0.44$ at $p = 0.0006$). The analysis of our data disaggregated by years revealed a correlation only in the 3rd, 4th and 5th year of the children's life.

It is quite difficult to compare our analysis of the number of Phe blood tests with the results of other studies due to the different attitudes to research and organization of healthcare in various countries, as well as to the different ways of presenting the results. One of such studies was conducted over 1 year in 9 European countries and in Turkey.¹¹ Unfortunately, due to the low number of patients in the particular age groups in some of the analyzed countries (in 7 of the countries the surveyed group of children aged up to 1 year included 6 or fewer children), it is impossible to make accurate comparisons. While in the youngest age group (up to 1 year), the median number of blood tests even exceeded the recommendations, it decreased in subsequent periods. Moreover, since the study lasted for only 1 year, there was no follow-up data. In 2002, the results of the research performed in 4 PKU clinics in the UK and Australia¹² were published. The authors reviewed the available data from the years

1994–2000 in a group of 178 patients aged 0–4 years, and of 137 patients aged 5–9 years. The median percentage of following the recommendations regarding the number of Phe blood tests in the first 4 years of life was 81%, with the IQR 63–90%. For children aged 5–9 years, the median was 86%, and the IQR 58–113%. In our results for the Poznań center, the median for the first 5 years of life was 65%, with the IQR 44–84%. The same parameters for the 4-year period were respectively 67% (the median) and 46–86% (IQR). In 2004, Waitzman et al. presented the results of their analysis of the frequency of Phe blood tests in 59 patients aged 8 years in 4 PKU centers in the USA. The study covered the years 1980–1995.¹³ The researchers found that each week of delay in carrying out the Phe test increased the probability of exceeding the recommended Phe concentration by 10%. They also emphasized that the recommendations for test frequency issued by the US Medical Research Council Working Party on Phenylketonuria¹⁴ were not supported by any formal analysis. Viau et al.^{15,16} presented the results of a group of 55 patients, in which the average annual number of blood Phe samples was 16.5. The minimum value was 5 and the maximum was 62. Calculated according to this methodology, the average for the Poznań center was 26.7, with correspondingly lower maximum and higher minimum values.

In 2013, Hartnett et al.¹⁷ presented data on compliance to the recommendations regarding the number of Phe tests in a hospital in Vancouver, Canada. The median percentage of compliance in the first 6 months of life of the children was 98% (range: 74–125%), until the end of the 1st year – 87% (55–117%) and until 12 years of age – 90% (44–127%). One of the conclusions of the Canadian study was the following: “Concomitant with the increase in Phe levels, there was a reduced frequency of blood Phe monitoring as patients with PKU aged”.¹⁶ In the Poznań center, the median percentage of compliance in the 1st year was 90% (range: 19–140%). In 2011, Cotugno et al.¹⁸ observed a tendency in mothers with lower education to underestimate Phe in meals, resulting in missing the target Phe range. In their study of patients in Brazil, Vieira et al.¹⁹ considered the level of dietary compliance in patients up to 13 years old to be satisfactory if a patient’s yearly median of Phe test results was lower than 6 mg%. It was found that 11 out of the 25 PKU patients in this group adhered to the diet.

In 1971, Acosta and Wenz²⁰ carried out an analysis of the diet adherence in a group of 101 PKU children. As an “excellent” result they defined 75% of the Phe blood levels within the target range of 2–6 mg%, as a “good” range – 75% of the blood levels within the range of 2–12 mg% and as “poor” – 75% of the Phe levels above 12 mg%. Noteworthy is the fact that the results do not cover the whole range of potential Phe values. The group with the best results included 49% of children under 1 year of age. The group with the worst results included 40% of children over 10 years of age. Children diagnosed early had better blood

test results. In 1996, Cabalska et al.²¹ stated that the results can be considered very good if Phe levels for at least 75% of the observation time are in the range of 4–6 mg%. The results of Phe were considered good if for at least 75% of the observation time they were included in the range of 6–12 mg%. Bad results were those of more than 12 mg% for 75% of the observation time.

German Collaborative Study of Children Treated for Phenylketonuria (PKU)²² in the group of 89 children as good results described those with a median of 4.3 mg% in the 1st and 2nd year of life, and 5 mg% in the 5th (there were 42 such children). In the intermediate group, 35 children were classified, with a median of 5 mg% in the 1st, 5.8 mg% in the 2nd and 7.4 mg% in the 5th year of life. Poor results of 12 children were those with a median of 5.6 mg% in the 1st year, 7.4 mg% in the 2nd and 10.7 mg% in the 5th year. The comparison of our results with the results of the German Collaborative Study is extremely difficult due to the passage of time and to the differences in target blood Phe. Our study showed that the blood Phe level defined in the German study as good was reached by 83% (44 out of 53) of Poznań patients in the 1st year of life, by 51% (27 out of 53) in the 2nd year and up to 43% in the 5th year. By comparison, the German results for the first 5 years of life were 46%. Overall, our results confirm the findings of the German Collaborative Study that in the 5th year of life more than 12% of patients have results that greatly diverge from those suggested in the recommendations. Somewhat thought-provoking in the German report was that results with a median over the recommended Phe levels given in the German recommendations, which is 4 mg%, were considered good.

Fisch et al.²³ presented data from a survey in 111 PKU clinics in the USA and Canada. In 20% of the surveyed hospitals, the non-compliance level was 20 mg%, in 13% of hospitals – 15 mg% and in 28% of hospitals – 10 mg%. In the 1st year of life, 43% of children had target Phe blood level under 5 mg%, and 51% – between 6 and 10 mg%. Van Spronsen et al.¹⁰ recommend out-of-the-ordinary intervention, such as increased intensity of monitoring or social worker supervision, if in patients under 12 years of age more than 50% of Phe concentrations are out of the target range for at least 6 months. Hartnett et al.¹⁷ presented the Phe test results from the years 1991–2009. The authors assumed that good Phe control was when more than 60% of Phe test results were within the treatment range (2–6 mg%); fair control – with 30–60% such results; and poor control – when less than 30% of Phe tests were within the treatment range. Of the 33 patients in the 1st year of life, 13 had good results, 16 – fair and 4 – poor. In the group from 2 to 6 years of age, 11 out of 29 patients had good results, 17 – fair and 1 – poor. In 12 patients (36%), the average concentration of Phe from the 2nd month of life to the end of the 1st year exceeded 6 mg%; till the 6th year of life 8 (26%) such patients were found. In the Poznań center, there were 15% (8 of 53) of children between 2 and 12 months of life with an average

Phe concentration higher than 6 mg%, 6 children (11%) had a good control and 21 (40%) – fair control. The difference was not statistically significant.

The major strength of this unique study is that all PKU patients remaining under care in our hospital were included. The majority of PKU studies comprised only a part of all patients remaining under care, which may have resulted in a significant bias, as it is more likely for researchers to have access to (and therefore include) patients who more strictly follow recommendations.

There are several limitations to this study. Firstly, we have studied the first 5 years of life, and therefore all the conclusions apply only to the 0–5 years age group. It would be desirable to expand the study onto older age groups of PKU patients as well. Secondly, our work focused on Phe concentrations in blood, the number of visits to a specialist and the number of blood tests, but we did not take into account the cognitive and intellectual functions, whose inclusion might have enriched the overall picture. Thirdly, the possibility cannot be excluded that patients implement the prescribed diet only shortly before blood sampling and that the Phe levels measured do not correspond to the real Phe values in the periods of time between tests.

In summary, the treatment control of PKU patients is the best in infancy, although many parents do not strictly follow the doctors' advice. In the next 4 years, over half of the patients fail to visit a specialist as many times as required, and even more fail to reach the recommended number of blood tests. Similar observations have been made regarding dietary compliance, as measured by Phe concentrations. In nearly half of the patients older than 12 months, similar percentages of correct and incorrect Phe concentrations have been detected. The process of control and therapy does not seem to depend on the level of education of the patient's parents, nor on their SES. Phenylalanine levels, however, remain correlated with the number of visits to a specialist and the number of Phe blood tests carried out.

Conclusions

Therapy effectiveness and patients' compliance in PKU is very good in infancy. However, both deteriorate in subsequent years. Moreover, they do not seem to depend on the family background. This reveals the need for systemic improvement of treatment control.

ORCID iDs

Dariusz Walkowiak  <https://orcid.org/0000-0001-8874-2401>
 Anna Bukowska-Posadzy  <https://orcid.org/0000-0003-0749-0316>
 Łukasz Kałużny  <https://orcid.org/0000-0002-0340-5914>
 Mariusz Ołtarzewski  <https://orcid.org/0000-0002-3353-723X>
 Rafał Staszewski  <https://orcid.org/0000-0001-9062-0737>
 Michał Musielak  <https://orcid.org/0000-0003-4952-0384>
 Jarosław Walkowiak  <https://orcid.org/0000-0001-5813-5707>

References

- Blau N, Van Spronsen FJ, Levy HL. Phenylketonuria. *Lancet*. 2010; 376(9750):1417–1427.
- Blainey JD, Gulliford R. Phenylalanine-restricted diets in the treatment of phenylketonuria. *Arch Dis Child*. 1956;31(160):452–466.
- MacDonald A, Gokmen-Ozel H, van Rijn M, Burgard P. The reality of dietary compliance in the management of phenylketonuria. *J Inher Metab Dis*. 2010;33(6):665–670.
- Güttler F. Hyperphenylalaninemia: Diagnosis and classification of the various types of phenylalanine hydroxylase deficiency in childhood. *Acta Paediatr Scand Suppl*. 1980;280:1–80.
- Trefz FK, Schmidt H, Bartholome K, Mahle M, Mathis P, Pecht G. Differential diagnosis and significance of various hyperphenylalaninemias. In: Bickel H, Wachtel U, eds. *Inherited Diseases of Amino Acid Metabolism*. Stuttgart, West Germany: Georg Thieme Verlag KG; 1985:86–100.
- Phenylketonuria: Screening and Management. NIH Consensus Statement 2000 October 16–18;17:1–27.
- Management of PKU. A Consensus Document for the Diagnosis and Management of Children, Adolescents and Adults with Phenylketonuria. London, UK: The National Society for Phenylketonuria (UK) Ltd.; 2014.
- Burgard P, Bremer HJ, Bührdel P, et al. Rationale for the German recommendations for phenylalanine level control in phenylketonuria 1997. *Eur J Pediatr*. 1999;158(1):46–54.
- van Spronsen FJ, Ahring Kiær K, Gizewska M. PKU: What is daily practice in various centres in Europe? *J Inher Metab Dis*. 2009;32(1):58–64.
- van Spronsen FJ, van Wegberg AM, Ahring K, et al. Key European guidelines for the diagnosis and management of patients with phenylketonuria. *Lancet Diabetes Endocrinol*. 2017;5(9):743–756. doi:10.1016/S2213-8587(16)30320-5
- Ahring K, Bélanger-Quintana A, Dokoupil K, et al. Blood phenylalanine control in phenylketonuria: A survey of 10 European centres. *Eur J Clin Nutr*. 2011;65(2):275–278.
- Walter JH, White FJ, Hall SK, et al. How practical are recommendations for dietary control in phenylketonuria? *Lancet*. 2002;60(9326):55–57.
- Waitzman N, Bilginsoy C, Leonard CO, Ernst SL, Prince A. *The Effect of Phenylalanine Test Frequency on Management of Phenylketonuria (PKU)*. Working paper No: 2004-3. Salt Lake City, UT: University of Utah, Department of Economics; 2004.
- Recommendations on the dietary management of phenylketonuria. Report of Medical Research Council Working Party on Phenylketonuria. *Arch Dis Child*. 1993;68(3):426–427.
- Viau KS. *Correlation of Age-Specific Phenylalanine Levels on Intellectual Outcome in Patients with Phenylketonuria* [doctoral dissertation]. All Graduate Theses and Dissertations. Paper 739. Logan UT: Utah State University; 2010.
- Viau KS, Wengreen HJ, Ernst SL, Cantor NL, Furtado LV, Longo N. Correlation of age-specific phenylalanine levels with intellectual outcome in patients with phenylketonuria. *J Inher Metab Dis*. 2011;34(4):963–971.
- Hartnett C, Salvarinova-Zivkovic R, Yap-Todos E, et al. Long-term outcomes of blood phenylalanine concentrations in children with classical phenylketonuria. *Mol Genet Metab*. 2013;108(4):255–258.
- Cotugno G, Nicolò R, Cappelletti S, Goffredo BM, Vici Dionisi C, Di Ciommo V. Adherence to diet and quality of life in patients with phenylketonuria. *Acta Paediatr*. 2011;100(8):1144–1149.
- Vieira TA, Nalin T, Krug BC, Bittar CM, Netto CBO, Schwartz IVD. Adherence to treatment of phenylketonuria: A study in southern Brazilian patients. *J Inborn Errors Metab Screen*. 2015;3:1–7.
- Acosta PB, Wenz E. Nutrition in Phenylketonuria. In: Bickel H, Hudson FP, Woolf LE, eds. *Phenylketonuria and Some Other Inborn Errors of Amino Acid Metabolism*. Stuttgart, West Germany: Georg Thieme Verlag KG; 1971:181–96.
- Cabalska MB, Nowaczewska I, Sendecka E, Zorska K. Longitudinal study on early diagnosis and treatment of phenylketonuria in Poland. *Eur J Pediatr*. 1996;155 (Suppl 1):S53–S55.
- Burgard P, Schmidt E, Rupp A, Schneider W, Bremer H. Intellectual development of the patients of the German Collaborative Study of children treated for phenylketonuria. *Eur J Pediatr*. 1996;55 (Suppl 1): S33–S38.
- Fisch RO, Matalon R, Weisberg S, Michals K. Phenylketonuria: Current dietary treatment practices in the United States and Canada. *J Am Coll Nutr*. 1997;16(2):147–151.

Urotensin receptor antagonist palosuran attenuates cyclosporine-a-induced nephrotoxicity in rats

Murat Olukman^{1,A,D}, Cenk Can^{1,C}, Deniz Coşkunsever^{1,B}, Yiğit Uyanıkgil^{3,B},
Türker Çavuşoğlu^{2,B}, Eser Sözmen^{2,B}, Soner Duman^{3,E}, Fatma Gül Çelenk^{2,C}, Sibel Ülker^{1,D,F}

¹ Department of Medical Pharmacology, Faculty of Medicine, Ege University, Izmir, Turkey

² Department of Histology and Embriology, Faculty of Medicine, Ege University, Izmir, Turkey

³ Department of Medical Biochemistry, Faculty of Medicine, Ege University, Izmir, Turkey

⁴ Department of Nephrology, Faculty of Medicine, Ege University, Izmir, Turkey

⁵ Department of Medical Genetics, Faculty of Medicine, Ege University, Izmir, Turkey

A – research concept and design; B – collection and/or assembly of data; C – data analysis and interpretation;

D – writing the article; E – critical revision of the article; F – final approval of the article

Advances in Clinical and Experimental Medicine, ISSN 1899–5276 (print), ISSN 2451–2680 (online)

Adv Clin Exp Med. 2019;28(10):1393–1401

Address for correspondence

Murat Olukman

E-mail: murat.olukman@ege.edu.tr

Funding sources

None declared

Conflict of interest

None declared

Received on May 22, 2018

Reviewed on August 17, 2018

Accepted on February 18, 2019

Published online on September 13, 2019

Cite as

Olukman M, Can C, Coşkunsever D, et al. Urotensin receptor antagonist palosuran attenuates cyclosporine-a-induced nephrotoxicity in rats. *Adv Clin Exp Med.* 2019;28(10):1393–1401. doi:10.17219/acem/104544

DOI

10.17219/acem/104544

Copyright

© 2019 by Wrocław Medical University

This is an article distributed under the terms of the

Creative Commons Attribution Non-Commercial License

(<http://creativecommons.org/licenses/by-nc-nd/4.0/>)

Abstract

Background. Cyclosporine-A (CsA) is widely used for immunosuppressive therapy in renal transplantation. Nephrotoxicity is the main dose-limiting undesirable consequence of CsA. Urotensin II (U-II), a novel peptide with a powerful influence on vascular biology, has been added to the list of potential renal vascular regulators. Upregulation of the urotensin receptors and elevation of plasma U-II levels are thought to possibly play a role in the etiology of renal failure.

Objectives. The present study examines this hypothesis by evaluating renal function and histology with regard to the potential role of U-II and its antagonist, palosuran, in the pathogenesis of CsA-induced nephrotoxicity in rats.

Material and methods. Male Sprague–Dawley rats were treated with CsA (15 mg/kg, for 21 days, intraperitoneally) or CsA + palosuran (300 mg/kg, for 21 days). Renal function was measured and histopathology, U-II immunostaining and protein detection with western blotting of the kidneys were performed.

Results. Cyclosporine-A administration caused a marked decline in creatinine clearance (Ccr). Fractional sodium excretion (FE_{Na}) tended to increase in the CsA-treated rats. Plasma U-II levels decreased in the CsA-treated rats. Cyclosporine-A treatment resulted in a marked deterioration in renal histology and an increase in the expression of U-II protein in the kidneys. Palosuran's improvement of renal function manifested as a significant decrease in serum creatinine levels and a significant increase in urine creatinine levels, resulting in a marked increase in Ccr. Palosuran produced a significant normalization of kidney histology and prevented an increase in U-II expression.

Conclusions. Cyclosporine-A-induced renal impairment was accompanied by an increase in U-II expression in kidneys and a contrary decrease in systemic U-II levels. Palosuran improved the condition of rats suffering from renal dysfunction by preventing the decrease in renal U-II expression without affecting the systemic levels of U-II. The protective effect of palosuran in CsA nephrotoxicity is possibly independent of its U-II receptor antagonism.

Key words: nephrotoxicity, urotensin-II, cyclosporine-A, palosuran, experiment

Introduction

Cyclosporine-A (CsA) is a calcineurine inhibitor that is widely used for immunosuppressive therapy in renal transplantation patients.¹ However, clinical usage of this immunosuppressant is often restricted by its side effects. Nephrotoxicity is the main dose-limiting undesirable consequence of CsA treatment, which may lead to irreversible damage in both glomerular and tubular structures. Chronic CsA treatment causes functional and structural nephrotoxicity characterized by glomerular sclerosis, tubulointerstitial fibrosis and tubular atrophy,² whereas acute CsA nephrotoxicity induces a reversible reduction of the glomerular filtration rate (GFR) and renal blood flow, which is thought to result from afferent arteriolar vasoconstriction.³ The initial vasoconstriction caused by CsA is related to the imbalance between various modulators of renal vascular tonus, such as the powerful vasodilators prostacyclin and nitric oxide^{4,5} and/or the vasoconstrictor factors angiotensin II and endothelin.⁶

Recently, urotensin II (U-II), a novel peptide with potent influences on vascular biology, was added to the list of potential renal vascular regulators. This peptide has been defined as the most potent vasoconstrictor to date and is a ligand for the Gq protein U-II receptor (UTR), originally known as the GPR14 receptor.⁷ Urotensin II and UTR are expressed in a large number of tissues and organs^{8,9} and pharmacological studies have shown that U-II plays a potent vasoactive role in the cardiovascular system.^{10,11} In addition to its potent direct vascular actions, U-II contributes to the control of renal function^{12–15} and, therefore, is involved in cardiorenal disease states. Upregulation of the UTR receptors and elevation of plasma U-II levels have been postulated to play a possible role in the etiology of renal failure, congestive heart failure, diabetes mellitus, and systemic and portal hypertension.^{16–18} This suggestion has led to the development of different UTR antagonists in recent years.¹⁹ Among these, the selective UTR antagonist palosuran (ACT-058362C; 1-[2-(4-Benzyl-4-hydroxy-piperidin-1-yl)-ethyl]-3-(2-methyl-quinolin-4-yl)-urea sulfate) has been shown to display renoprotective properties with beneficial recruitment on both glomerular and tubulointerstitial damage in experimental models of renal failure.^{20,21} In rats with ischemic acute renal failure, acute administration of palosuran significantly attenuated renal glomerular and tubular dysfunction, prevented increases in serum creatinine concentration and lessened the decrease in GFR.²¹ In addition, it has been shown that chronic palosuran treatment prevented the progressive increase in albuminuria, renal dysfunction and tubular and tubulointerstitial lesions in diabetic rats.²¹

Given the potential renoprotective effects of palosuran, we sought to examine whether this UTR antagonist might be useful in providing protection against CsA-induced nephrotoxicity. The present study therefore examines this

hypothesis by evaluating renal function and histology with regard to the potential role of U-II in the pathogenesis of CsA-induced nephrotoxicity in rats.

Material and methods

Experiment design

Male Wistar rats (Ege University Animal Center, Izmir, Turkey) weighing 240–270 g were used in the study in order to exclude the confounding effect of sex-dependent factors (i.e., fluctuation in estrogen/progesterone levels during the menstruation cycle). This hormone fluctuation may influence an experiment, including X-chromosome and female sex hormone levels. All rats were fed standard rat food and water ad libitum under controlled environmental conditions (12-hour light/dark photo-period and a room temperature of $21 \pm 2^\circ\text{C}$). The rats were randomly assigned to 5 experimental groups of 6 animals each:

Group 1 (Control): received daily intraperitoneal (i.p.) injections of saline solution for 21 days;

Group 2 (CsA) received CsA (15 mg/kg/day, i.p.) for 21 days²²;

Group 3 (CsA+palosuran) received CsA (15 mg/kg/day, i.p.) + palosuran (300 mg/kg/day, orally) for 21 days²¹;

Group 4 (Vehicle) received a CsA vehicle (40 mg of Cremophor EL dissolved in 33% alcohol, i.p.) at volumes equivalent to corresponding CsA doses for 21 days;

Group 5 (Palosuran) received palosuran (300 mg/kg/day, orally) with concomitant daily i.p. injections of saline solution for 21 days.

The CsA used was a commercially available, injectable preparation (Sandimmune-parenteral[®]). Palosuran was dissolved in distilled water and administered directly into the stomach through an intragastric cannula.

Functional studies

One day prior to sacrifice at the end of the treatment period, the rats were kept separately in metabolic cages; urine samples were collected over a 24-hour period for electrolyte and clearance studies. At sacrifice, blood samples were obtained by direct intracardiac puncture under anesthesia and the kidneys were removed for further studies and rinsed in ice-cold physiological saline. The blood samples were immediately centrifuged at 4°C and the plasma samples were stored at -70°C until the biochemical analysis was performed.

Urine and plasma analysis

The concentrations of creatinine, sodium and potassium in the urine and plasma were measured with enzymatic assay, as were the U-II levels. The creatinine clearance rate (Ccr), the fractional excretion of sodium and

the renal failure index were calculated using standard methods. The Ccr was calculated using the following formula: $Ccr = UV/P/1440$, where Ccr is the clearance in mL/min, U is the 24-hour urinary concentration of creatinine in mg/dL, V is the 24-hour urine volume in mL and P is the plasma concentration of creatinine in mg/L. Whole-blood CsA levels were measured using a Cloned Enzyme Donor Immunoassay (CEDIA; Microgenics Corporation, Fremont, USA) using an automatic analyzer (Hitachi 912, Hitachi Ltd, Tokyo, Japan). Since the last dose of CsA was given 24 h prior to sacrifice, all CsA levels measured were trough concentrations (Co).

SDS-PAGE electrophoresis and western blotting

The kidney tissue was homogenized in lysis buffer (20 mM of Tris-HCl, pH 7.5, 2 mM of EGTA, 5 mM of EDTA, 10 mM of dithiothreitol, 0.5 mg/mL of aprotinin, 0.001 mg/mL of pepstatin, 0.001 mg/mL of leupeptin, and 0.5 mM of PMSF) on ice, then centrifuged at 14,000 rpm at 4°C for 30 min to remove the insoluble pellet. Protein concentration in the supernatant was measured spectrophotometrically using the Lowry method. Sixty micrograms of protein were loaded on 8% SDS-PAGE gel. The resolved proteins were transferred to 0.2- μ m nitrocellulose membranes and the blots were blocked in 5% non-fat dried milk for 1 h at 25°C to saturate non-specific protein binding. The membranes were incubated with primary antibodies (anti U-II; 20 μ L, anti- β -actin; 1:20,000; Abcam, Cambridge, UK) overnight at 4°C. After extensive washing, the blots were incubated in horseradish peroxidase-linked secondary antibodies (anti-mouse IgG, 1:10,000 for actin; 1:3,000 for anti U-II) for 1 h at 25°C. The blots were covered with an ECL Plus[®] chemiluminescence detection kit (Amersham Pharmacia, Piscataway, USA) and then exposed to X-ray film. The autoradiographs were analyzed with scanning densitometry with subtraction of the background counts measured outside loaded lanes, and the intensity of the signal was measured with image analysis software (Image Quant TL v2003, Amersham Biosciences, Piscataway, USA). The data is presented as the ratio of U-II band density to β -actin band density.

Morphology

When the rats were sacrificed, the kidneys were removed, dissected and immersed in 4% buffered paraformaldehyde for 24 h at room temperature. The tissues were dehydrated in a gradual alcohol series (80–95–100%) and embedded in paraffin. For light microscopy, the paraffin sections were cut into 5- μ m thick slices in microtome (Leica RM 2145; Leica Camera AG, Wetzlar, Germany) and stained with hematoxylin and eosin (H&E) to characterize general cellular patterns.

Immunohistochemistry

Immunocytochemical staining was performed on 5- μ m sections of the formaldehyde-fixed, paraffin-embedded renal tissue. The sections were stained at the same time to avoid possible variation over time. After deparaffinization in xylol and rehydration with distilled water, the sections were kept in a citrate buffer (0.3% citrate, pH 6.0) in a microwave oven at 90 W for 5 min and at 360 W for 15 min. After washing the sections in phosphate-buffered saline (PBS), they were exposed to normal horse serum for 30 min to block nonspecific immunoglobulin transfer, followed by overnight incubation with anti-U-II primary antibody (dilution 1:1000) at 4°C in a humidified chamber (Abcam, KIMERA Medical, İstanbul). Endogenous peroxidase activity in the rat kidney was blocked with H₂O₂ (3% in H₂O for 10 min). The sections were then incubated with a biotinylated horse-antimouse secondary antibody (1:200) for 30 min at room temperature and washed with horseradish peroxidase conjugated streptavidin for 30 min. All sections were visualized with 3,3'-diaminobenzidine tetrahydrochloride/H₂O₂. Finally, the sections were counterstained with Mayer's hemotoxylin, dehydrated in an increasing series of alcohol (95% for 2 min and 100%, for 2 min \times 3) and kept in xylol for 2 min 3 times just before being mounted in Entellan. The stained sections were scanned with an Olympus BX-51 microscope (Olympus Corp., Tokyo, USA) and images were taken with an Olympus C-5050 digital camera (Olympus Corp.). The images were analyzed in Image-Pro Express v. 4.5.1.3 software (Media Cybernetics Inc., Cambridge, UK). All digital quantification (Image-Pro Plus, v. 6.0, Media Cybernetics Inc.) and assessments were performed in a blinded manner. Tubular injury was graded (0–3) based on the presence of tubular atrophy and the presence/degree of isometric tubular vacuolization: 0 – no changes present, grade 1 – \leq 25% to 50% and grade 3 – $>$ 50% tubular injury involvement. Interstitial fibrosis was scored as a sign of architectural destruction: 0 – no changes present, grade 1 – 25%, grade 2 – 26% to 50% and grade 3 – $>$ 50% tubular injury involvement.²³

Drugs and reagents

The CsA (Sandimmune-parenteral[®]) was a kind gift from Novartis (Istanbul, Turkey). The palosuran was obtained from Actelion Pharmaceutical (Allschwil, Switzerland). All reagents used for western blotting and immunohistochemistry were of analytical grade.

Data analysis

The results are expressed as mean \pm standard error of the mean (SEM) of the groups. The differences between the means of the groups were assessed by one-way analysis of variance (ANOVA) with a subsequent Tukey's test. Associations between different variables were determined

with linear regression analysis and Spearman's correlation coefficient was calculated between these variables. Results were considered significantly significant when $p < 0.05$.

Results

Effects of CsA and palosuran on urine and serum output

The biochemical parameters of all experimental groups are summarized in Table 1. Injection of CsA at a dose of 15 mg/kg/day for 21 days resulted in a whole-blood trough CsA concentration of $1,022.00 \pm 97.10$ ng/mL. Palosuran treatment in the rats decreased the CsA concentration significantly (822.08 ± 115.72 ng/mL; $p < 0.05$). However, both concentrations were markedly higher than the targeted therapeutic concentration of CsA

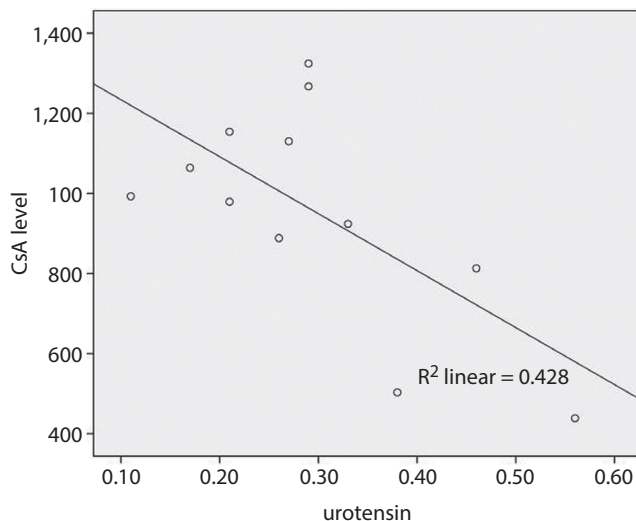


Fig. 1. Correlation between serum urotensin-II (U-II) and cyclosporine-A (CsA) levels. Spearman's rank correlation test revealed a correlation between serum U-II levels and CsA levels ($R^2 = 0.428$)

(250–400 ng/mL), indicating that the dosage used in our study maintained toxic trough concentrations.²⁴ Cyclosporine-A administration caused a marked deterioration of renal function in the rats, characterized by a significant decline in Ccr with a concomitant increase in serum creatinine levels. Fractional sodium excretion (FE_{Na}) tended to increase in the CsA-treated rats; however, the difference was not statistically significant. No effect of CsA was found on the other renal functional parameters compared to the control group. The vehicle of CsA did not significantly alter any of the parameters, either.

Administration of palosuran along with CsA led to an improvement in renal function, manifested as a significant decrease in serum creatinine levels and a significant increase in urine creatinine levels, resulting in a marked increase in Ccr. However, FE_{Na} showed a noteworthy decrease in these animals.

Palosuran caused no significant changes in the parameters tested when given to the control rats. The serum and urine levels of Na and K were comparable among all groups.

Plasma U-II levels were significantly lower in the CsA-treated rats in comparison to the control rats (Table 1). However, there was no correlation between the measured serum levels of CsA and the plasma levels of U-II in the CsA-treated rats (Fig. 1). Concomitant administration of palosuran and CsA did not further lower the U-II levels. The palosuran-treated control rats also revealed no significant differences in terms of U-II levels when compared to the naïve controls.

When the correlation of serum U-II levels with each parameter used to validate renal function was calculated, only a negative correlation with serum creatinine level was found (Fig. 2).

Histopathological changes of kidneys

The photomicrographs of kidneys from all groups are shown in Fig. 3. The microscopic findings of vehicle-treated

Table 1. Biochemical parameters of experimental groups. Data is expressed as mean \pm SEM; n = 6 in each group

Parameters	Control	CsA	CsA + palosuran	Vehicle	Palosuran + control
Urine volume [mL/day]	5.15 \pm 1.25	4.27 \pm 0.85	3.36 \pm 0.49	5.11 \pm 1.23	6.11 \pm 1.31
Urine creatinine [mg/dL]	87.30 \pm 13.20	68.58 \pm 9.39	152.60 \pm 19.25*	78.87 \pm 11.72	72.10 \pm 11.40
Urine Na [mEq/L]	104.62 \pm 16.75	72.94 \pm 19.95	63.00 \pm 8.26	100.04 \pm 25.48	86.60 \pm 14.51
Urine K [mEq/L]	165.86 \pm 22.70	140.05 \pm 9.10	189.13 \pm 28.68	145.20 \pm 17.87	180.51 \pm 22.91
Serum creatinine [mg/dL]	0.62 \pm 0.03	1.06 \pm 0.18*	0.65 \pm 0.03 [#]	0.54 \pm 0.03	0.56 \pm 0.02
Serum Na [mEq/L]	139.70 \pm 0.52	141.53 \pm 0.46	140.70 \pm 0.65	140.43 \pm 0.63	142.0 \pm 0.86
Serum K [mEq/L]	5.41 \pm 0.14	5.84 \pm 0.22	4.87 \pm 0.17	5.46 \pm 0.12	5.50 \pm 0.03
Ccr [mL/min/100 g body weight]	0.45 \pm 0.02	0.19 \pm 0.03*	0.50 \pm 0.04 [#]	0.43 \pm 0.06	0.43 \pm 0.05
FE_{Na} [%]	0.53 \pm 0.05	0.71 \pm 0.12	0.19 \pm 0.01* [#]	0.51 \pm 0.10	1.64 \pm 0.12*
Plasma urotensin level [ng/mL]	0.57 \pm 0.04	0.30 \pm 0.04*	0.29 \pm 0.06	0.50 \pm 0.04	0.59 \pm 0.04

* $p < 0.05$ when compared to the control group; [#] $p < 0.05$ when compared to the CsA group. CsA – cyclosporine; Ccr – creatinine clearance; FE_{Na} – fractional sodium excretion.

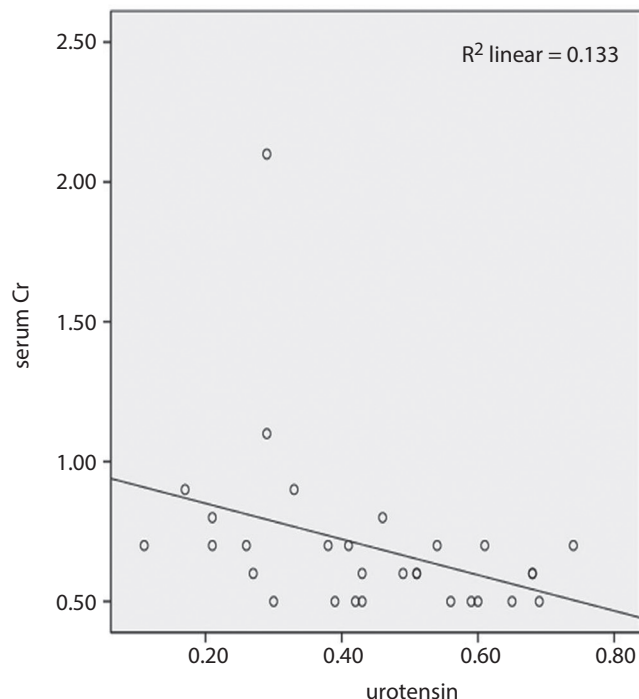


Fig. 2. Correlation between serum urotensin-II (U-II) and creatinine (Cr) levels. Spearman's rank correlation test revealed a correlation between serum U-II levels and Cr levels ($R^2 = 0.133$)

rats showed essentially normal architecture. Cyclosporine-A treatment resulted in a marked deterioration in renal histology. The sections from the CsA-treated rat kidneys revealed derangements in both glomerular and tubular structures. Extensive mononuclear cell infiltration was observed in both perivascular and peritubular areas, mostly in the mid-cortex and the corticomedullary junctions. The cortical areas were characterized by diffuse peritubular capillary congestion and hemorrhagic foci. Vacuolization signs compatible with dilatation were observed in Bowman's space and the glomeruli. A foamy and vacuolated appearance of the parenchymal cell cytoplasm was noted in the distal and – more prominently – in the proximal tubules, and pyknotic nuclei were found in the tubular cells. Examination of the medullar sections revealed dilatation and tubular disintegration in all parts of the loop of Henle.

Simultaneous administration of CsA and palosuran produced a significant normalization of the kidney histology. Hemorrhagic foci and peritubular capillary congestion were seen less in the cortex and areas of mononuclear cell infiltration were sporadically found in the corticomedullary junction. The glomerular structures did not reveal signs of dilatation and the diameter of the glomerulus remained normal.

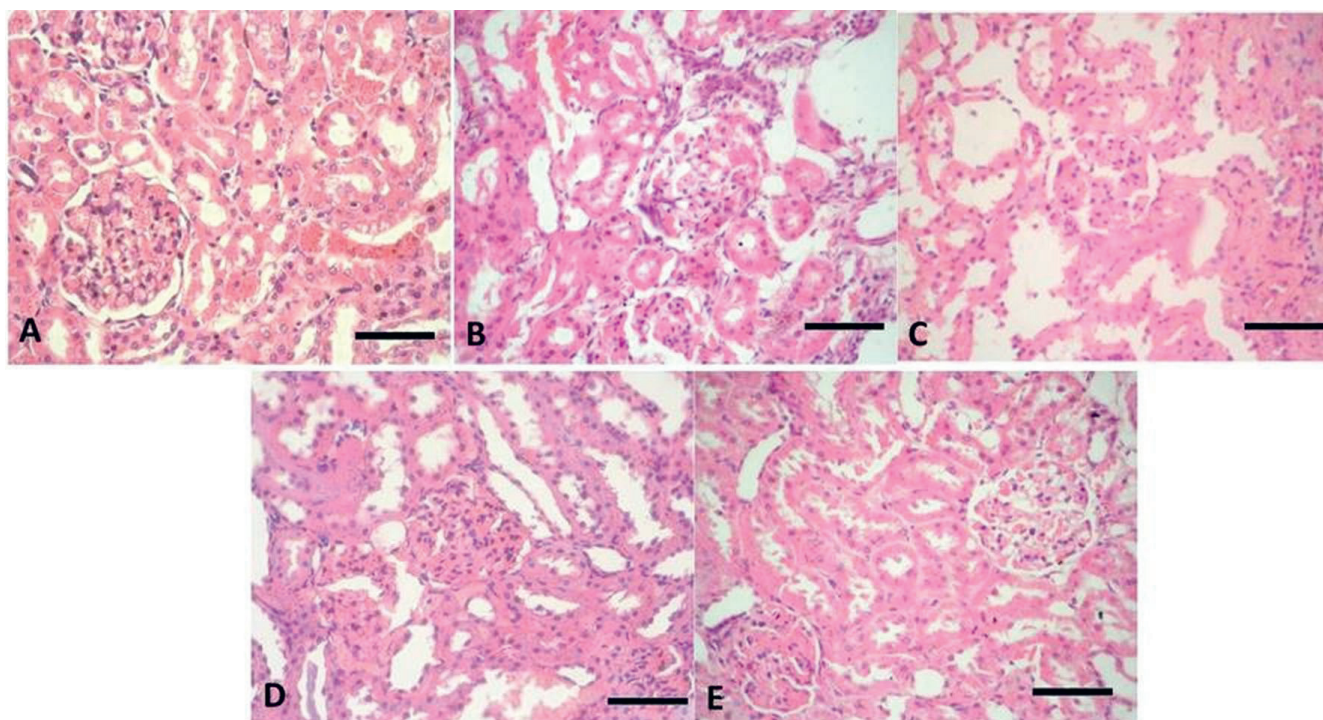


Fig. 3. Representative photomicrographs of histopathological findings in rat kidneys stained with H&E, showing structural renal injury induced with cyclosporine-A (CsA) and the effect of palosuran treatment: (A) control, (B) CsA, (C) CsA + palosuran, (D) vehicle, and (E) palosuran-treated. Extensive mononuclear cell infiltration is visible in both the perivascular and peritubular areas. Peritubular capillary congestion and hemorrhagic foci are visible in the cortex, as well as signs of vacuolization compatible with dilatation in Bowman's space and glomeruli. The foamy appearance characteristic of vacuolated parenchymal cell cytoplasm is visible in the distal and proximal tubules. Pyknotic nuclei were characteristic in tubular cells. The simultaneous administration of palosuran and CsA produced a significant normalization of the kidney histology (C). Minimal hemorrhagic foci and peritubular capillary congestion are visible in the cortex, and scattered areas of mononuclear cell infiltration are present in the corticomedullary junction. The glomerular structures do not reveal signs of dilatation and the diameter of the glomerulus is normal. The scale bar is 50 μ for $\times 100$ and 125 μ for $\times 40$ magnification; $n = 4$ in each group. Representative experiments are shown

Treatment of the rats with palosuran alone did not significantly affect kidney histology when compared to the untreated control kidneys; only minimal structural derangements were observed. The kidneys from the palosuran-treated rats revealed rare foci of congestion in perivascular and peritubular areas and sporadic areas of mononuclear cell infiltration in the corticomedullary junction. Minimal signs of dilatation and vacuolization in Bowman's capsules were observed.

Immunohistochemical findings of the kidneys

Incubation of kidney sections with an antibody against Urotensin II caused staining in different regions of the kidney. In control preparations, immunoreactivity was detected predominantly in the proximal tubules and it gradually decreased in the distal sections (Fig. 4), whereas no immunostaining was detected in the glomerular structure. Medullary collecting tubules and the loop of Henle were stained positively for U-II. Figure 4B shows that U-II immunoreactivity was greatest in the CsA-treated rat kidneys. U-II immunostaining was most remarkable in the distal and proximal tubules, but also appeared in the glomerular region. Immunostaining of kidneys from both palosuran- and vehicle-treated control kidneys also showed staining in the tubular sections and slight

staining in the glomerular sections, but immunoreactivity was considerably less when compared to the CsA group. The expression of U-II decreased dramatically with concomitant palosuran and CsA treatment in rat kidneys. The proximal and distal tubular sections from these rats showed a staining pattern similar to the control kidneys except for the minimal staining in the glomeruli.

Effects of palosuran on U-II protein expression in renal tissue

Cyclosporine-A treatment resulted in a significant increase in the expression of U-II protein in the kidneys ($p < 0.05$, Fig. 5). The addition of palosuran to CsA treatment significantly prevented the increase in U-II expression ($p < 0.05$). The administration of a CsA vehicle or palosuran alone to the rats did not change U-II protein expression.

Discussion

In the current study, the CsA-treated animals showed a marked decline in creatinine clearance along with an elevation of serum creatinine levels. Histological examination of the kidneys from these rats revealed derangements in both the glomerular and tubular structures. These

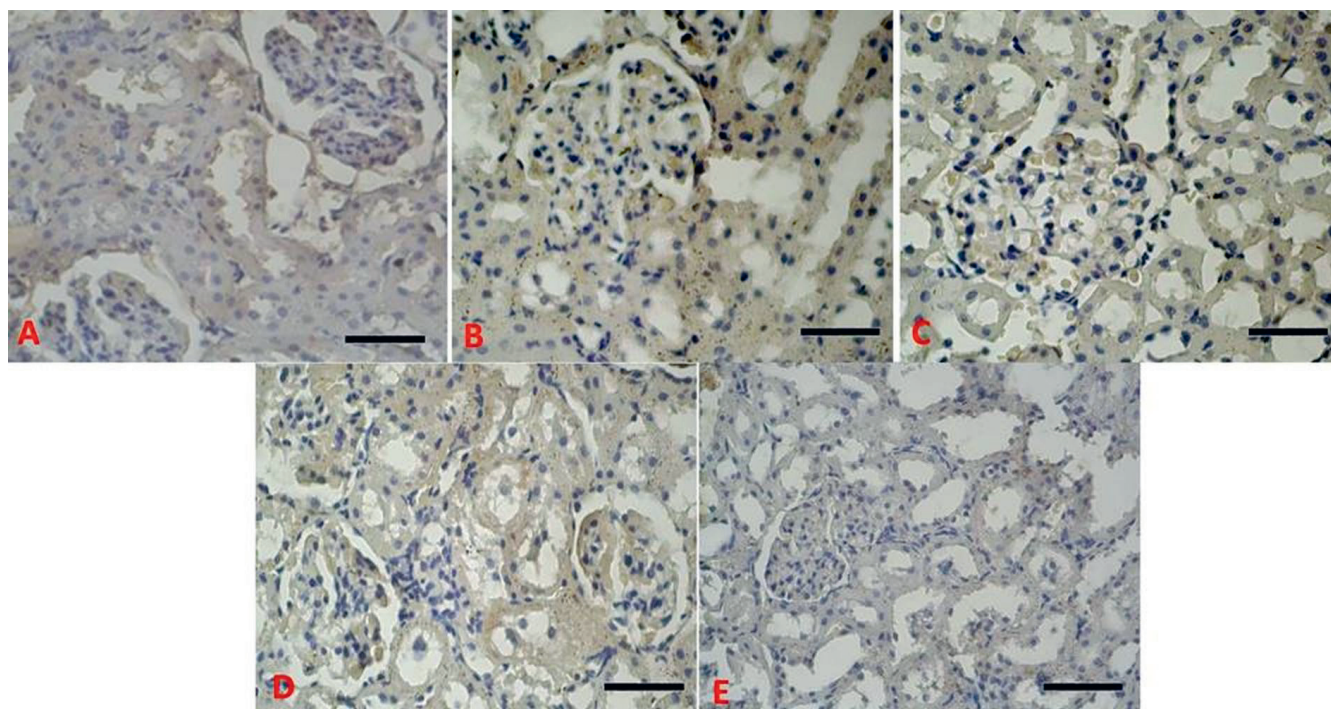


Fig. 4. Immunohistochemical localization of U-II in kidney sections of the experimental groups as follows: (A) control, (B) CsA, (C) CsA + palosuran, (D) vehicle, and (E) palosuran-treated. The CsA-treated animals show remarkable immunostaining in the distal and proximal tubules and in the glomerular region when compared to controls. The expression of U-II decreased abundantly with concomitant palosuran treatment in CsA-administered rat kidneys. The proximal and distal tubular sections from these rats showed a similar staining pattern with the control kidneys except for minimal staining in the glomerules. Immunostaining of kidneys from both palosuran- and vehicle-treated control kidneys also showed staining in the tubular area and faintly in the glomerular sections, though immunoreactivity was considerably less when compared to the CsA group. The scale bar is 50 μ for $\times 100$ and 125 μ for $\times 40$ magnification; $n = 4$ in each group. Representative experiments are shown

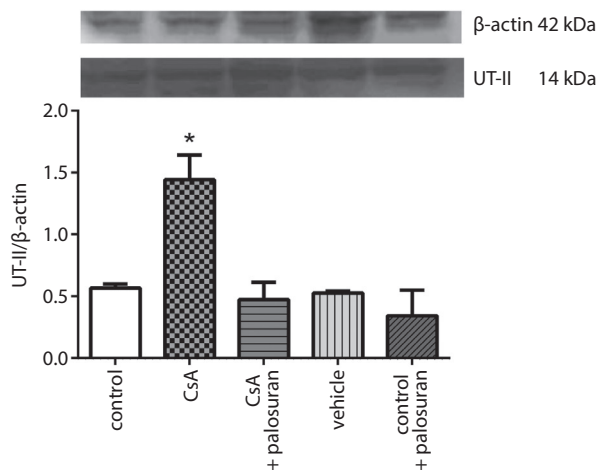


Fig. 5. Expression of urotensin II (U-II) protein in the kidneys of rats treated with cyclosporine (CsA) alone and in combination with palosuran for 21 days. The control group was composed of healthy rats receiving daily intraperitoneal (i.p.) injections of saline solution for 21 days. The vehicle group received i.p. injections of 40 mg of Cremophor EL dissolved in 33% alcohol at volumes equivalent to corresponding CsA doses for 21 days; * $p < 0.05$ when compared to controls and # $p < 0.05$ when compared to CsA; $n = 4$

findings are in agreement with the well-known pattern of acute CsA nephrotoxicity and they support previous reports on CsA-induced renal dysfunction and morphological changes.²² Alterations in renal hemodynamics and glomerular and/or tubular structures play important roles in CsA-induced renal dysfunction.²⁵ Cyclosporine-A-induced nephrotoxicity is characterized by a marked reduction in renal blood flow and a reduction in glomerular filtration rate, which in turn leads to elevated serum creatinine levels and decreased serum Ccr.²⁶ Consistent with these reports, our findings mimicked the initial phase of CsA-induced renal complications.

The vasoconstrictor effect of CsA on renal vasculature is involved in chronic CsA nephrotoxicity as well.²⁷ The major mechanism of CsA action on GFR is vasoconstriction in afferent arterioles through the mediation of contractile factors (i.e., angiotensin II and endothelin).²⁶ We have hypothesized that a newly identified modulator, U-II, may also contribute to CsA-induced nephrotoxicity and, if so, the selective UTR antagonist palosuran may be useful in preventing CsA-induced nephrotoxicity. Indeed, palosuran treatment showed a significant improvement in both functional and structural changes induced by CsA. It prevented a CsA-induced decrease in Ccr, leading to a concomitant decrease in serum creatinine. Moreover, the morphological derangements in both the glomerular and tubular structures induced by CsA were attenuated by palosuran treatment.

This data agrees in part with previous data reporting the possible renoprotective potential of palosuran with beneficial effects on both glomerular and tubulointerstitial damage in renal ischemia/reperfusion²⁰ and diabetes-induced renal injury.²¹ Palosuran increases renal blood flow without changing the filtration fraction, has a pre- and post-glomerular vasodilator effect and delays

the development of proteinuria and renal damage in diabetic rats, thus suggesting a possible role as a U-II receptor antagonist.²¹

Although the impact of U-II on the kidneys is mainly mediated by its effects on vascular smooth muscle cells, its direct effect on the renal tubular cells and collecting ducts should also be considered. The immunolocalization of UTR in renal tubular cells suggests that U-II may act as an autocrine or paracrine regulator of the water and electrolyte transport in the tubular cells.¹⁸ Our immunohistological studies revealed increased U-II immunoreactivity in the CsA-treated rat kidneys. Urotensin II immunostaining was most notable in the distal and proximal tubules, though sporadic staining was noticed in the glomerular region as well. The expression of U-II decreased markedly in the rat kidneys treated concomitantly with palosuran and CsA. This finding also suggests a possible relationship between the increased U-II expression in kidneys and renal dysfunction. Hence, the expression of U-II mRNA in the kidney was enhanced in a model of chronic renal failure in rats.¹⁸ The principal site of U-II receptor expression in a rat kidney is the medulla, especially the tubular component of the kidney. Urotensin II was found mostly in the epithelial cells of tubules and ducts, with a greater density in the distal convoluted tubules in normal human kidneys; only focal immunoreactivity, however, was found in the endothelial cells of the glomeruli.¹⁸

Taken together, these findings suggest the possibility that although glomerular hemodynamic responses appear to dominate the effect of U-II on renal structures, the renal U-II system may also play a role in renal tubular function and electrolyte handling. In our study, palosuran caused a significant decrease in FE_{Na} , considering the natriuretic effect of U-II in CsA-treated rats at first glance. However, the studies on the role of U-II on renal electrolyte handling have provided conflicting results depending on the study protocols and rat species. For example, bolus injections of rat U-II in low concentrations leads to dose-related reductions in both GFR and sodium excretion rate, but only a modest reduction in GFR and no change in sodium excretion has been reported.²⁸ Contrarily, U-II infusion caused a profound reduction in GFR accompanied by antidiuresis and antinatriuresis.²⁹ Urotensin-II changes urinary electrolytes in a dose-dependent manner: at lower infusion rates it reduces electrolyte reabsorption. However, the fractional excretion of electrolytes was not altered by a UTR antagonist, urantide, suggesting that endogenous U-II may have little influence on tubular function in different rat strains.³⁰

This last observation suggests the possibility that the effects of exogenously administered U-II do not necessarily mimic the exact effects of endogenously elevated levels of the mediator. The same might be true for antagonists as well, since different UTR antagonists exert different effects on the functional parameters of tubules regardless of the antagonistic capacity.³¹ For example, palosuran

treatment caused an increase in sodium excretion in cirrhotic bile duct-ligated rats compared with untreated counterparts.³² This natriuretic effect was accompanied by an increase in urine volume, an effect that was not observed in our study.

It seems that the effects of UTR antagonists on renal function do not necessarily have to be attributable to their U-II antagonistic properties alone, but the unintended effects of these antagonists should also be taken into account.³³ Although palosuran exerted profound effects on both the functional and morphological parameters of the CsA-treated kidneys in our study, it did not cause significant changes on those parameters in the control rats. Thus, it is highly likely that the protective effect of palosuran in our model of CsA nephrotoxicity is independent of its U-II receptor antagonism. Indeed, palosuran inhibits U-II binding in membrane preparations with nearly equal potency as native U-II; however, its antagonistic activity is significantly less in intact cells.³³ The dosing regimens used in the previous nephropathy models in which palosuran was reported to be effective²⁰ were unable to inhibit rat U-II in vitro and the data from these studies does not convincingly demonstrate selective in vivo UTR blockade by palosuran.¹⁵ Moreover, recent studies have revealed that several actions of palosuran could not be replicated using another UTR antagonist, SB-701411.^{34,35} These observations taken together suggest a lack of UTR receptor affinity and an “off-target” effect of palosuran in its renoprotective properties.

Cyclosporine-A treatment decreased mean serum U-II levels significantly and U-II levels demonstrated a negative correlation with serum creatinine levels, suggesting that the U-II system was potentially downregulated in the CsA-treated rats. However, the measured serum levels of CsA did not show any correlation with the plasma levels of U-II. On the other hand, although palosuran attenuated the derangements in functional and morphological parameters of CsA-induced renal dysfunction, it did not affect the decreased plasma U-II levels. These findings strengthen the hypothesis that the beneficial effect of palosuran observed in the present study was independent of its U-II receptor antagonism. It is well-known that there are differences in plasma U-II concentration between healthy subjects and patients with renal¹⁷ and heart failure.^{36,37} However, it has been controversial whether the U-II system in the kidney acts protectively or harmfully in kidney diseases. Although U-II levels are usually higher in patients than in controls, higher levels can also be found in renal transplant patients³⁸ and they may correlate well with a decreased chance of adverse outcome, suggesting a protective role of U-II against cardiovascular events in renal disease states.^{38–40} Mosenkis et al. observed that plasma U-II concentrations were higher in controls than in subjects with end-stage renal disease undergoing hemodialysis or those with chronic renal disease, and that U-II correlated negatively with serum creatinine and positively with Ccr, suggesting a positive correlation between U-II concentration and renal function.³⁸

The kidney is a major source of U-II, and urinary concentrations of U-II are significantly higher with renal tubular disease due to either reduced renal clearance or increased renal production.⁸ When acute symptoms arise, U-II is temporarily upregulated in order to repair the damage caused, but it later returns to its normal levels. This would explain how the upregulation of U-II is an inverse predictor of adverse clinical outcome in patients with acute coronary syndromes.³⁹ Chronically high U-II levels, on the other hand, can lead to the development of several diseases, including cardiovascular disease and kidney disease.³¹

Conclusions

The present study demonstrated that exposure of healthy rats to toxic doses of CsA for 21 days resulted in a deterioration of both renal glomerular and tubular functions as well as a drop in Ccr. Cyclosporine-A-induced renal impairment was accompanied by an increase in U-II expression in kidneys and a contrary decrease in systemic U-II levels. The UTR antagonist palosuran mitigated renal dysfunction by preventing the decrease in renal U-II expression without affecting systemic levels of U-II. Its lack of an effect on the U-II system suggests that local U-II expression in the kidneys contributes to CsA-induced renal impairment. The protective effect of palosuran in our model of CsA nephrotoxicity is possibly independent of its U-II receptor antagonism, meaning that further research should be conducted to define the actual mechanisms of palosuran's action in various disease models.

Ethics approval and consent to participate

The project was approved by the Local Animal Care and Ethics Committee of Ege University, whose policies conform to the Guide for the Care and Use of Laboratory Animals published by the US National Institutes of Health (NIH Publication No. 85-23, revised 1996) and the present study was approved by the Institutional Animal Ethical Committee of Ege University (License No. 2010-26, 26/02/2010).

References

1. Bennett WM, DeMattos A, Meyer MM, Andoh T, Barry JM. Chronic cyclosporine nephropathy: The Achilles' heel of immunosuppressive therapy. *Kidney Int.* 1996;50(4):1089–1100.
2. Liptak P, Ivanyi B. Primer: Histopathology of calcineurin-inhibitor toxicity in renal allografts. *Nat Clin Pract Nephrol.* 2006;2(7):398–404; quiz following 404.
3. Barros EJ, Boim MA, Ajzen H, Ramos OL, Schor N. Glomerular hemodynamics and hormonal participation on cyclosporine nephrotoxicity. *Kidney Int.* 1987;32(1):19–25.
4. Perico N, Zoja C, Benigni A, Ghilardi F, Gualandris L, Remuzzi G. Effect of short-term cyclosporine administration in rats on renin-angiotensin and thromboxane A2: Possible relevance to the reduction in glomerular filtration rate. *J Pharmacol Exp Ther.* 1986;239(1):229–235.

5. Bobadilla NA, Gamba G, Tapia E, et al. Role of NO in cyclosporin nephrotoxicity: Effects of chronic NO inhibition and NO synthases gene expression. *Am J Physiol*. 1998;274(4 Pt 2):F791–798.
6. Capasso G, Unwin R, Ciani F, et al. Inhibition of neutral endopeptidase potentiates the effects of atrial natriuretic peptide on acute cyclosporin-induced nephrotoxicity. *Nephron*. 2000;86(3):298–305.
7. Ames RS, Sarau HM, Chambers JK, et al. Human urotensin-II is a potent vasoconstrictor and agonist for the orphan receptor GPR14. *Nature*. 1999;401(6750):282–286.
8. Matsushita M, Shichiri M, Imai T, et al. Co-expression of urotensin II and its receptor (GPR14) in human cardiovascular and renal tissues. *J Hypertens*. 2001;19(12):2185–2190.
9. Maguire JJ, Kuc RE, Davenport AP. Orphan-receptor ligand human urotensin II: Receptor localization in human tissues and comparison of vasoconstrictor responses with endothelin-1. *Br J Pharmacol*. 2000;131(3):441–446.
10. Douglas SA, Naselsky D, Ao Z, et al. Identification and pharmacological characterization of native, functional human urotensin-II receptors in rhabdomyosarcoma cell lines. *Br J Pharmacol*. 2004;142(6):921–932.
11. Gardiner SM, March JE, Kemp PA, et al. Regional heterogeneity in the haemodynamic responses to urotensin II infusion in relation to UT receptor localisation. *Br J Pharmacol*. 2006;147(6):612–621.
12. Langham RG, Kelly DJ. Urotensin II and the kidney. *Curr Opin Nephrol Hypertens*. 2013;22(1):107–112.
13. Langham RG, Kelly DJ, Gow RM, et al. Increased expression of urotensin II and urotensin II receptor in human diabetic nephropathy. *Am J Kidney Dis*. 2004;44(5):826–831.
14. Totsune K, Takahashi K, Arihara Z, et al. Elevated plasma levels of immunoreactive urotensin II and its increased urinary excretion in patients with Type 2 diabetes mellitus: Association with progress of diabetic nephropathy. *Peptides*. 2004;25(10):1809–1814.
15. Tölle M, van der Giet M. Cardiorenovascular effects of urotensin II and the relevance of the UT receptor. *Peptides*. 2008;29(5):743–763.
16. Watanabe T, Arita S, Shiraishi Y, et al. Human urotensin II promotes hypertension and atherosclerotic cardiovascular diseases. *Curr Med Chem*. 2009;16(5):550–563.
17. Totsune K, Takahashi K, Arihara Z, Sone M, Ito S, Murakami O. Increased plasma urotensin II levels in patients with diabetes mellitus. *Clin Sci (Lond)*. 2003;104(1):1–5.
18. Mori N, Hirose T, Nakayama T, et al. Increased expression of urotensin II-related peptide and its receptor in kidney with hypertension or renal failure. *Peptides*. 2009;30(2):400–408.
19. Douglas SA, Dhanak D, Johns DG. From ‘gills to pills’: Urotensin-II as a regulator of mammalian cardiorenal function. *Trends Pharmacol Sci*. 2004;25(2):76–85.
20. Clozel M, Binkert C, Birker-Robaczewska M, et al. Pharmacology of the urotensin-II receptor antagonist palosuran (ACT-058362; 1-[2-(4-benzyl-4-hydroxy-piperidin-1-yl)-ethyl]-3-(2-methyl-quinolin-4-yl)-urea sulfate salt): First demonstration of a pathophysiological role of the urotensin system. *J Pharmacol Exp Ther*. 2004;311(1):204–212.
21. Clozel M, Hess P, Qiu C, Ding SS, Rey M. The urotensin-II receptor antagonist palosuran improves pancreatic and renal function in diabetic rats. *J Pharmacol Exp Ther*. 2006;316(3):1115–1121.
22. Capasso G, Di Gennaro CI, Della Ragione F, et al. In vivo effect of the natural antioxidant hydroxytyrosol on cyclosporine nephrotoxicity in rats. *Nephrol Dial Transplant*. 2008;23(4):1186–1195.
23. Takasu C, Vaziri ND, Li S, et al. Treatment with dimethyl fumarate attenuates calcineurin inhibitor-induced nephrotoxicity. *Transplantation*. 2015;99(6):1144–1150.
24. Jorga A, Holt DW, Johnston A. Therapeutic drug monitoring of cyclosporine. *Transplant Proc*. 2004;36(2 Suppl):396S–403S.
25. Nankivell BJ, Borrows RJ, Fung CL, O’Connell PJ, Allen RD, Chapman JR. The natural history of chronic allograft nephropathy. *N Engl J Med*. 2003;349(24):2326–2333.
26. Thomson SC, Tucker BJ, Gabbai F, Blantz RC. Functional effects on glomerular hemodynamics of short-term chronic cyclosporine in male rats. *J Clin Invest*. 1989;83(3):960–969.
27. Shihab FS, Yi H, Bennett WM, Andoh TF. Effect of nitric oxide modulation on TGF-beta1 and matrix proteins in chronic cyclosporine nephrotoxicity. *Kidney Int*. 2000;58(3):1174–1185.
28. Ovcharenko E, Abassi Z, Rubinstein I, Kaballa A, Hoffman A, Winaver J. Renal effects of human urotensin-II in rats with experimental congestive heart failure. *Nephrol Dial Transplant*. 2006;21(5):1205–1211.
29. Abdel-Razik AE, Forty EJ, Balment RJ, Ashton N. Renal haemodynamic and tubular actions of urotensin II in the rat. *J Endocrinol*. 2008;198(3):617–624.
30. Song W, Abdel-Razik AE, Lu W, et al. Urotensin II and renal function in the rat. *Kidney Int*. 2006;69(8):1360–1368.
31. Tsoukas P, Kane E, Giaid A. Potential clinical implications of the urotensin II receptor antagonists. *Front Pharmacol*. 2011;2:38.
32. Trebicka J, Leifeld L, Hennenberg M, et al. Hemodynamic effects of urotensin II and its specific receptor antagonist palosuran in cirrhotic rats. *Hepatology*. 2008;47(4):1264–1276.
33. Behm DJ, McAtee JJ, Dodson JW, et al. Palosuran inhibits binding to primate UT receptors in cell membranes but demonstrates differential activity in intact cells and vascular tissues. *Br J Pharmacol*. 2008;155(3):374–386.
34. Albertin G, Casale V, Ziolkowska A, et al. Urotensin-II and U11-receptor expression and function in the rat adrenal cortex. *Int J Mol Med*. 2006;17(6):1111–1115.
35. Spinazzi R, Albertin G, Nico B, et al. Urotensin-II and its receptor (UT-R) are expressed in rat brain endothelial cells, and urotensin-II via UT-R stimulates angiogenesis in vivo and in vitro. *Int J Mol Med*. 2006;18(6):1107–1112.
36. Douglas SA, Tayara L, Ohlstein EH, Halawa N, Giaid A. Congestive heart failure and expression of myocardial urotensin II. *Lancet*. 2002;359(9322):1990–1997.
37. Richards AM, Charles C. Urotensin II in the cardiovascular system. *Peptides*. 2004;25(10):1795–1802.
38. Mosenkis A, Kallem RR, Danoff TM, Aiyar N, Bazeley J, Townsend RR. Renal impairment, hypertension and plasma urotensin II. *Nephrol Dial Transplant*. 2011;26(2):609–614.
39. Khan SQ, Bhandari SS, Quinn P, Davies JE, Ng LL. Urotensin II is raised in acute myocardial infarction and low levels predict risk of adverse clinical outcome in humans. *Int J Cardiol*. 2007;117(3):323–328.
40. Zoccali C, Mallamaci F, Tripepi G, Cutrupi S, Pizzini P, Malatino L. Urotensin II is an inverse predictor of incident cardiovascular events in end-stage renal disease. *Kidney Int*. 2006;69(7):1253–1258.

A new measurement site for echocardiographic epicardial adipose tissue thickness and its value in predicting metabolic syndrome

Meng Wang^{1,2,B,D}, Liang Zhao^{1,3,C,D}, Hao Liang^{4,B,C}, Chunyuan Zhang^{5,B,E}, Liying Guan^{6,E}, Minglong Li^{1,A,F}

¹ Department of Endocrinology, Shandong Provincial Hospital Affiliated to Shandong University, Jinan, China

² Department of Endocrinology, Yidu Central Hospital of Weifang, China

³ Second Department of Endocrinology, Central Hospital of Taian, China

⁴ Department of Ultrasonic Diagnosis and Treatment, Shandong Provincial Hospital Affiliated to Shandong University, Jinan, China

⁵ Health Management Center, Yidu Central Hospital of Weifang, China

⁶ Health Management Center, Shandong Provincial Hospital Affiliated to Shandong University, Jinan, China

A – research concept and design; B – collection and/or assembly of data; C – data analysis and interpretation; D – writing the article; E – critical revision of the article; F – final approval of the article

Advances in Clinical and Experimental Medicine, ISSN 1899–5276 (print), ISSN 2451–2680 (online)

Adv Clin Exp Med. 2019;28(10):1403–1408

Address for correspondence

Minglong Li
E-mail: liminglong_doctors@163.com

Funding sources

None declared

Conflict of interest

None declared

Received on August 11, 2018
Reviewed on December 27, 2018
Accepted on February 18, 2019

Published online on August 30, 2019

Cite as

Wang M, Zhao L, Liang H, Zhang C, Guan L, Li M. A new measurement site for echocardiographic epicardial adipose tissue thickness and its value in predicting metabolic syndrome. *Adv Clin Exp Med.* 2019;28(10):1403–1408. doi:10.17219/acem/104526

DOI

10.17219/acem/104526

Copyright

© 2019 by Wrocław Medical University
This is an article distributed under the terms of the Creative Commons Attribution Non-Commercial License (<http://creativecommons.org/licenses/by-nc-nd/4.0/>)

Abstract

Background. Echocardiographic epicardial adipose tissue (EAT) thickness is defined as the thickness of the low-isoechoic area on the free wall of the right ventricle in the parasternal long-axis and short-axis views. Recent studies have suggested that it might support current risk stratification strategies in identifying an increased risk of metabolic syndrome.

Objectives. The aim of this study is to explore a new measurement site which can better reflect EAT thickness and to assess its value in predicting metabolic syndrome.

Material and methods. A total of 975 Chinese adults were measured for EAT thickness on the right ventricular anterior free wall (EAT-rv) and on the anterior interventricular groove (EAT-ivg) with echocardiography. The correlation between EAT thickness and metabolic syndrome was analyzed, as was the agreement between epicardial adipose volume (EAV) and EAT thickness. Independent risk factors of EAT thickness were identified and the predictive value of EAT thickness was assessed.

Results. Epicardial adipose tissue thickness was higher in older participants and those with obesity, diabetes, hypertension, hypertriglyceridemia, and metabolic syndrome, and it was lower in male participants. The EAT-ivg was higher in the participants with hypo-high-density-lipoprotein cholesterolemia than in those without the disorder, but the EAT-rv values were not statistically different. The kappa value was 0.524 between EAT-rv and EAV, and 0.783 between EAT-ivg and EAV. Advanced age, large waist circumference and female gender were independent risk factors of high EAT-ivg, while high-density-lipoprotein (HDL) cholesterol was a protective factor. The EAT-ivg was associated with metabolic syndrome. The area under the curve of EAT-ivg applied in predicting metabolic syndrome was greater than that of EAT-rv (0.715 vs 0.648).

Conclusions. The EAT-ivg was more consistent with EAV than EAT-rv, was independently associated with metabolic syndrome and had a higher value in predicting metabolic syndrome than EAT-rv. Therefore, the anterior interventricular groove can serve as a new measurement site which better reflects EAT thickness.

Key words: metabolic syndrome, echocardiography, epicardial adipose tissue, consistency, predictive value

Introduction

Epicardial adipose tissue (EAT) is the visceral thoracic fat depot that surrounds the heart, located between the myocardium and the visceral pericardium. It has been reported that EAT is associated with multiple pathological states, including metabolic syndrome, T2DM, atrial fibrillation, and coronary artery disease.^{1–3} Recent studies have shown that EAT thickness measured with echocardiography may play a limited additional role supporting current risk stratification strategies in identifying individuals at an increased risk of metabolic syndrome.^{4,5} Moreover, measurements of EAT thickness attained by echocardiography and computed tomography (CT) are inconsistent.^{6,7} This fact may be explained by the poor distribution of EAT at the measurement site. Echocardiographic EAT thickness has been defined as the thickness of the low-isoechoic area on the free wall of the right ventricle in the parasternal long-axis and short-axis views,^{8,9} but the distribution of EAT is unbalanced and is concentrated primarily in the interventricular and atrioventricular grooves rather than in the free wall of the right ventricle.⁷ Therefore, there is clinical value in finding a new measurement site for echocardiographic EAT thickness which can better reflect the risk of metabolic syndrome. In addition, Salami et al. have confirmed that there are significant racial differences in the distribution of EAT.¹⁰

A large-sample investigation of EAT thickness in Chinese adults has not yet been published. In this study, a total of 975 Chinese adults were measured for EAT thickness on the right ventricular anterior free wall (EAT-rv) and on the anterior interventricular groove (EAT-ivg). Distribution of EAT and its consistency with epicardial adipose volume (EAV) were described, and its independent association with metabolic syndrome and its value in predicting metabolic syndrome were analyzed. The aims were to explore a new measurement site which can better reflect EAT thickness and to assess its value in predicting metabolic syndrome.

Material and methods

Participants

A total of 986 Chinese adults receiving a general check-up at the Health Management Center of Shandong Provincial Hospital between January 2017 and September 2017 were enrolled in the study. The exclusion criteria consisted of the following: 1) age <18 years or >75 years; 2) atrial fibrillation; 3) serum creatinine level >2 mg/dL; 4) hypothyroidism; 5) current or past use of glucagon-like peptide (GLP)-1, SGLT2 inhibitors, thiazolidinediones, fibrates, statins, or insulins; 6) coronary heart disease; and 7) advanced malignant tumors. Transthoracic 2-dimensional echocardiography was performed in all participants, and 11 participants were excluded because of inadequate image quality. This study was approved by the ethics committee of Shandong

Provincial Hospital, China (approval No. 2016024138), and all participants provided their written informed consent.

Measurement of EAT thickness

Transthoracic 2-dimensional echocardiography was performed with a Philips iU22 ultrasound system and an s5-1 matrix-array transducer (Phillips Healthcare, Bothell, USA) according to the recommendations of the European and American Societies of Echocardiography.^{11,12} All participants were placed in the left lateral decubitus position. Ultrasonic images were stored in specialized workstations where EAT thickness was measured by the same reader. According to recommendations by Iacobellis et al., EAT thickness on the right ventricular anterior free wall (EAT-rv) was measured,^{8,9} as shown in Fig. 1. In addition, EAT thickness on the anterior interventricular groove (EAT-ivg) at the midchordal level and the tip of the papillary muscle from the parasternal short-axis view was measured as a new measurement site, as shown in Fig. 2. The average value of 3 cardiac cycles for each echocardiographic view was used for analysis.

Quantification of epicardial adipose volume

Among these 975 participants, 120 were randomly selected for cardiac dual-source computer tomography (DSCT). Cardiac DSCT was performed using a 128-slice DSCT scanner (Siemens AG, Munich, Germany). Image reconstructions were performed at 75% RR intervals. A density ranging from –30 to –190 Hounsfield units was employed to identify adipose tissue. The pericardium was manually traced from the right pulmonary artery to the diaphragm in order to determine a region of interest. Epicardial adipose volume was assessed using a dedicated workstation (Syngo.via v. VB10A; Siemens) by the same experienced CT diagnostic physician.

Diagnosis of metabolic syndrome

Metabolic syndrome was determined according to the recommendations of the Chinese Diabetes Society,¹³ including: 1) obesity, i.e., body mass index (BMI) ≥ 25 kg/m²; 2) fasting blood glucose level ≥ 6.1 mmol/L or the use of antidiabetic medication; 3) triglyceride level ≥ 1.7 mmol/L; 4) high-density-lipoprotein (HDL) cholesterol count <1.04 mmol/L; and 5) blood pressure higher than 130/85 mm Hg or the use of hypotension medication. Metabolic syndrome was diagnosed when a patient had at least 3 of the above 5 components.

Statistical analysis

All analyses were performed using SPSS software v. 22.0 (IBM Corp., Armonk, USA). Continuous variables with

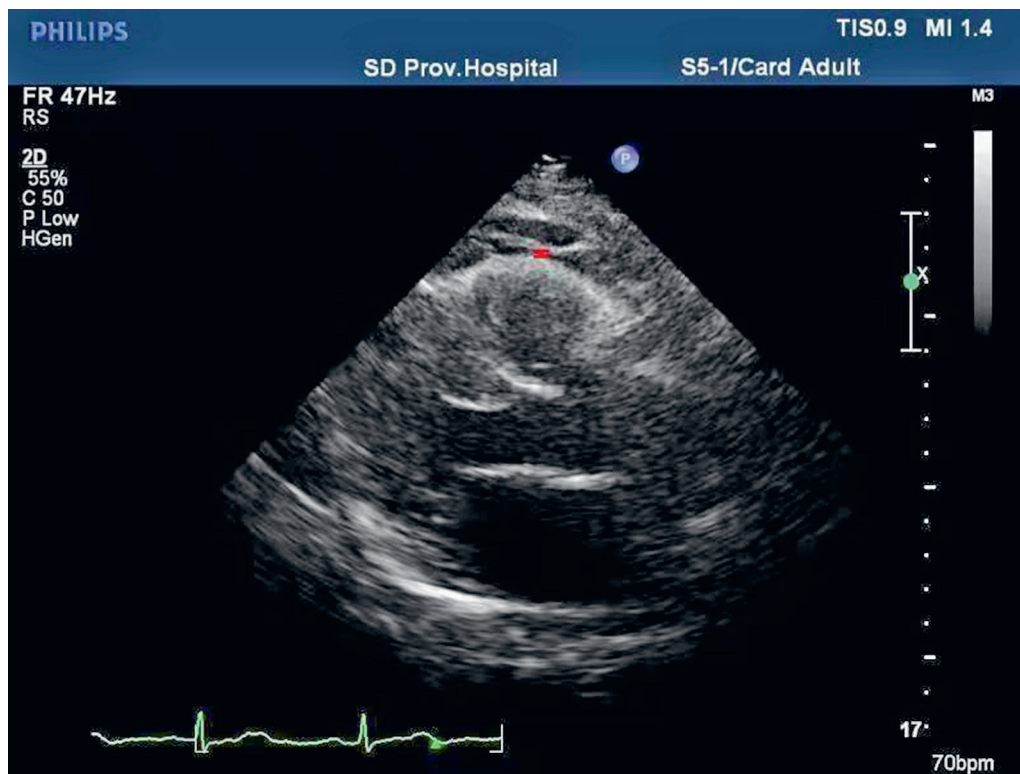


Fig. 1. Measurement of EAT-rv on the right ventricular anterior free wall during end-systole, according to recommendations by Iacobellis et al. The red line shows the measurement distance

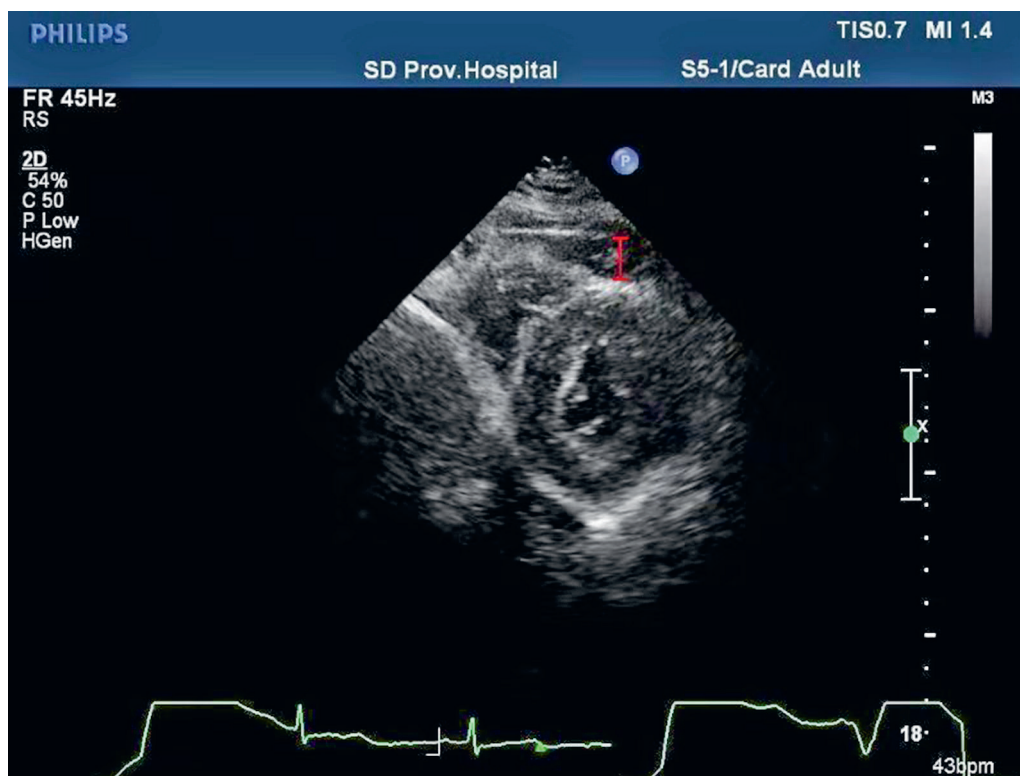


Fig. 2. Measurement of EAT-ivg on the anterior interventricular groove in the parasternal short-axis view. The red line shows the measurement distance

normal distribution were expressed as means \pm standard deviations (SDs) and those without normal distribution as 25th–75th percentiles (P25–P75). The EAT thicknesses were compared between groups using the Kruskal–Wallis test. Non-conditional logistic regression analysis was performed to determine the association between metabolic syndrome and EAT thickness. The EAV and EAT thickness

were grouped according to tertiles, and consistency was determined with κ statistics. Ordered logistic regression was used to identify independent risk factors of EAT thickness (quartiles). The predictive value of EAT thickness was evaluated with a receiver operating characteristic (ROC) curve, and the areas under the curve (AUC) were compared with the Z-test. Significance was set at $p < 0.05$.

Results

Distribution of EAT thickness

The mean age of all participants ($n = 975$) was 55.58 ± 11.78 years; their EAT-rv was 3.01 (2.09 – 3.90) and their EAT-ivg was 5.27 (4.01 – 6.86). EAT-ivg was greater than EAT-rv ($p < 0.05$). The distribution of EAT thickness in all participants is shown in Table 1. Epicardial adipose tissue thickness was higher in older participants and in those with obesity, diabetes, hypertension, hypertriglyceridemia, and metabolic syndrome; it was lower among the male participants. However, EAT-ivg was higher in participants with hypo-high-density-lipoprotein cholesterolemia than in those without this condition, and EAT-rv was not statistically different between the participants with and without hypo-high-density-lipoprotein cholesterolemia.

Table 1. Distribution of EAT thickness in all participants (data expressed as median (P25–P75))

Parameter	n	EAT-rv [mm]	EAT-ivg [mm]
Sex			
male	431	2.66 (2.02–3.65)	5.19 (3.70–6.63)
female	544	3.17 (2.18–4.05)*	5.38 (4.06–7.21) [§]
Age [years]			
≤45	211	2.03 (1.47–2.91)	3.93 (2.65–5.00)
46–55	248	2.63 (2.03–3.48)	5.04 (3.74–6.13)
56–65	282	3.22 (2.36–3.95)	6.07 (4.54–7.26)
66–75	234	3.73 (3.02–4.55)*	6.49 (5.05–8.28)*
BMI [kg/m ²]			
≤23.9	375	2.78 (2.02–3.73)	4.72 (3.28–6.27)
24.0–27.9	434	3.02 (2.10–3.90)	5.36 (4.08–7.00)
≥28	165	3.41 (2.32–4.35)*	6.41 (4.88–7.92)*
Diabetes			
yes	169	3.39 (2.32–4.18)*	6.35 (4.29–8.20)*
no	805	2.92 (2.04–3.82)	5.09 (3.83–6.67)
Hypertension			
yes	458	3.35 (2.52–4.22)*	6.22 (4.76–7.58)*
no	517	2.49 (1.92–3.45)	4.23 (3.20–6.16)
Hypertriglyceridemia			
yes	354	3.23 (2.30–4.09)*	5.96 (4.42–7.30)*
no	621	2.69 (2.02–3.64)	4.90 (3.49–6.56)
Hypo-high-density-lipoprotein cholesterolemia			
yes	212	3.11 (2.10–3.90)	5.72 (4.35–7.18)*
no	763	2.91 (2.03–3.79)	5.05 (3.77–6.82)
Metabolic syndrome			
yes	362	3.42 (2.48–4.24)*	6.44 (5.04–7.93)*
no	613	2.67 (2.02–3.63)	4.70 (3.29–6.25)

* $p < 0.001$; [§] $p < 0.05$. EAT – epicardial adipose tissue; EAT-rv – EAT thickness on the right ventricular anterior free wall; EAT-ivg – EAT thickness on the anterior interventricular groove; BMI – body mass index.

Consistency between EAT thickness and EAV

The κ value between EAT-rv and EAV was 0.524 ($p < 0.05$), and that between EAT-ivg and EAV it was 0.783 ($p < 0.05$) (Table 2 and 3).

Table 2. Agreement analysis by tertiles of EAT-rv and EAV

Tertiles of EAV [mL]	Tertiles of EAT-rv [mm]		
	<2.32	2.32–3.65	>3.65
<45.3	16 (13.33%)	12 (10.00%)	12 (10.00%)
45.3–66.2	13 (10.83%)	17 (14.17%)	10 (8.33%)
>66.2	11 (9.17%)	11 (9.17%)	18 (15.00%)

EAT – epicardial adipose tissue; EAT-rv – EAT thickness on the right ventricular anterior free wall; EAV – epicardial adipose volume.

Table 3. Agreement analysis by tertiles of EAT-ivg and EAV

Tertiles of EAV [mL]	Tertiles of EAT-ivg [mm]		
	<4.43	4.43–6.67	>6.67
<45.3	19 (15.83%)	11 (9.17%)	10 (8.33%)
45.3–66.2	12 (10.00%)	18 (15.00%)	10 (8.33%)
>66.2	9 (7.50%)	11 (9.17%)	20 (16.67%)

EAT – epicardial adipose tissue; EAT-ivg – EAT thickness on the anterior interventricular groove; EAV – epicardial adipose volume.

Risk factors of EAT-ivg

As shown in Table 4, ordered logistic regression analysis showed that advanced age, large waist circumference and female gender were independent risk factors of high EAT-ivg, and HDL cholesterol was a protective factor. On the other hand, BMI, triglyceride, HDL cholesterol, uric acid, creatinine, estimated glomerular filtration rate (eGFR), and HbA1c levels, hypertension, diabetes, and lifestyle (including eating habits, smoking and exercise habit) were not statistically significant.

Table 4. Risk factors of high EAT-ivg

Parameter	Wald statistic	ORs (95% CI)	p-value
Age [years]	29.977	1.061 (1.037–1.086)	<0.001
HDL cholesterol [mmol/L]	6.379	0.431 (0.225–0.825)	<0.05
Waist circumference [cm]	11.283	1.116 (1.048–1.187)	<0.05
Female gender	13.642	2.674 (1.559–4.587)	<0.001

OR – odds ratio; 95% CI – 95% confidence interval; HDL cholesterol – high-density-lipoprotein cholesterol.

Association between EAT thickness and metabolic syndrome

As shown in Table 5, non-conditional logistic regression analysis revealed that EAT-ivg was associated with metabolic syndrome, and the crude, age-adjusted,

Table 5. Association between EAT metrics and metabolic syndrome

Parameter	EAT-rv	p-value	EAT-ivg	p-value
Crude OR	1.337 (1.162–1.538)	<0.001	1.628 (1.498–1.770)	<0.001
Age-adjusted OR	1.306 (1.124–1.518)	<0.001	1.569 (1.457–1.690)	<0.001
Age- and waist-circumference-adjusted OR	1.163 (0.985–1.374)	0.075	1.363 (1.221–1.520)	<0.001
Age-, waist-circumference- and BMI-adjusted OR	1.116 (0.938–1.329)	0.217	1.331 (1.182–1.498)	<0.001

EAT – epicardial adipose tissue; EAT-rv – EAT thickness on the right ventricular anterior free wall; EAT-ivg – EAT thickness on the anterior interventricular groove; BMI – body mass index; OR – odds ratio.

age- and waist-circumference-adjusted and age-, waist-circumference- and BMI-adjusted odds ratios (ORs) were 1.628, 1.529, 1.363, and 1.331, respectively. The EAT-rv was associated with metabolic syndrome when only age was adjusted for.

Value of EAT thickness applied in predicting metabolic syndrome

As shown in Fig. 3, the AUC of EAT-rv applied in predicting metabolic syndrome was 0.648 (standard error: 0.018), and the AUC of EAT-ivg was 0.715 (standard error: 0.017). A Z-test showed that the AUC of EAT-ivg was greater than that of EAT-rv ($p < 0.05$).

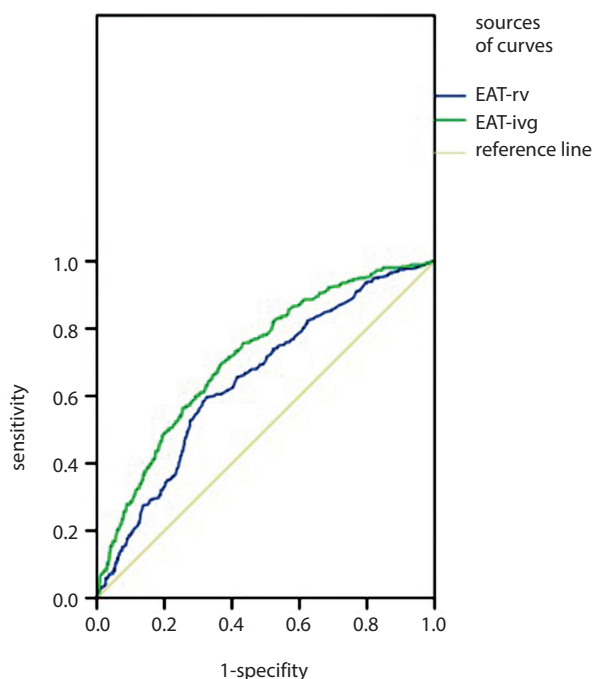


Fig. 3. The AUC of EAT-rv and EAT-ivg applied in predicting metabolic syndrome

Discussion

To our knowledge, this is the first large-scale clinical study to investigate the distribution of EAT and its association with metabolic syndrome. In this study, we explored a new measurement site for echocardiographic

EAT thickness (EAT-ivg), which was greater than EAT-rv. The median values for EAT-ivg and EAT-rv were 5.27 (4.01–6.86) and 3.01 (2.09–3.90), respectively. The EAT-rv values found among our sample of the Chinese population were similar to those of South Koreans,¹⁴ but lower than values measured among Caucasians.¹⁵ This racial difference was also confirmed by Fox et al.¹⁶ Our results show that EAT thickness was higher in older people and lower in males, a finding which is consistent with a study by Graeff et al.⁴ Both clinical studies and autopsies confirmed that EAT thickness significantly correlates with aging.^{15,17} As for gender difference, our results were consistent with the study by Baragetti et al.,¹⁸ but opposite to the study by Calabuig et al.¹⁵ This discrepancy could be explained by the fact that the latter study did not include multivariate analysis.

In 2003, Iacobellis et al. first measured EAT thickness on the right ventricle anterior free wall (EAT-rv) with echocardiography, which showed an excellent agreement with MRI epicardial measurements and a significant association with metabolic syndrome.⁸ However, the association was reduced when the size of the study population was increased and multivariate analysis was performed.^{4,15} In our study, EAT-rv also lacked a significant correlation with metabolic syndrome after multivariate analysis, but EAT-ivg did significantly correlate with metabolic syndrome. In addition, the κ value between EAT-rv and EAV was lower than that of EAT-ivg and EAV, and the AUC for the application of EAT-rv in predicting metabolic syndrome was lower than that of EAT-ivg. Therefore, EAT-ivg is a better index for echocardiographic EAT thickness and is more valuable in predicting metabolic syndrome.

We also analyzed the independent risk factors of EAT thickness. In addition to age and sex, waist circumference – a commonly used assessment tool for visceral fat – was also an independent risk factor. This conclusion is consistent with previous reports.^{4,5,15} High-density-lipoprotein cholesterol is a protective factor of EAT thickness, according to our results. In a cross-sectional study of 72 hemodialysis patients, a low HDL cholesterol level was identified as an independent risk factor of elevated EAT thickness.¹⁹ A meta-analysis showed that there was a highly significant ($p < 0.001$) correlation between EAT thickness and HDL cholesterol.⁵ Our results confirm the previous findings.

One advantage of this study was employing an echocardiogram to measure EAT thickness in different locations, and then to compare them with EAV as measured with CT. The distribution of EAT thickness was asymmetrical, and the EAT on the anterior interventricular groove was thicker than on the right ventricle anterior free wall. We chose the anterior interventricular groove as the anatomic landmark in the parasternal short-axis view because this landmark was the most definitive and had the maximum distribution of EAT we could find using transthoracic echocardiography. We also compared EAT-rv and EAT-ivg with EAV. Their κ coefficients were small, which was similar to a study by Kim et al.,²⁰ but EAT-ivg had a larger κ coefficient than EAT-rv. This meant that EAT-ivg correlated more strongly with EAV than EAT-rv.

There were also some limitations in our study. Firstly, the participants were people undergoing physical examination, which may have led to selection bias. Secondly, cardiac magnetic resonance is considered the gold standard and it can more accurately assess epicardial fat than transthoracic echocardiography and cardiac DSCT. However, it is expensive and difficult to perform in clinical practice for a large-scale cohort. Thirdly, we did not measure visceral fat because it is also difficult to measure in a large population.

Conclusions

In summary, EAT-ivg had a stronger agreement with EAV than EAT-rv, it was independently associated with metabolic syndrome and it was more valuable in predicting metabolic syndrome than EAT-rv. Therefore, the anterior interventricular groove can serve as a new measurement site which can better reflect EAT thickness.

ORCID iDs

Meng Wang  <https://orcid.org/0000-0002-7663-6756>
 Liang Zhao  <https://orcid.org/0000-0003-1230-2199>
 Hao Liang  <https://orcid.org/0000-0002-8902-6199>
 Chunyuan Zhang  <https://orcid.org/0000-0001-7832-7714>
 Liying Guan  <https://orcid.org/0000-0001-9648-6698>
 Minglong Li  <https://orcid.org/0000-0003-3870-5519>

References

- Al Chekakie MO, Welles CC, Metoyer R, et al. Pericardial fat is independently associated with human atrial fibrillation. *J Am Coll Cardiol*. 2010;56(10):784–788.
- Clément K, Basdevant A, Dutour A. Weight of pericardial fat on coronary artery disease. *Arterioscler Thromb Vasc Biol*. 2009;29(5):615–616.
- Ouwens DM, Sell H, Greulich S, Eckel J. The role of epicardial and perivascular adipose tissue in the pathophysiology of cardiovascular disease. *J Cell Mol Med*. 2010;14(9):2223–2234.
- Graeff DB, Foppa M, Pires JC, et al. Epicardial fat thickness: Distribution and association with diabetes mellitus, hypertension and the metabolic syndrome in the ELSA-Brasil study. *Int J Cardiovasc Imaging*. 2016;32(4):563–572.
- Rabkin SW. The relationship between epicardial fat and indices of obesity and the metabolic syndrome: A systematic review and meta-analysis. *Metab Syndr Relat Disord*. 2014;12(1):31–42.
- Kim BJ, Kim HS, Kang JG, Kim BS, Kang JH. Association of epicardial fat volume and nonalcoholic fatty liver disease with metabolic syndrome: From the CAESAR study. *J Clin Lipidol*. 2016;10(6):1423–1430.e1.
- Wang TD, Lee WJ, Shih FY, et al. Relations of epicardial adipose tissue measured by multidetector computed tomography to components of the metabolic syndrome are region-specific and independent of anthropometric indexes and intraabdominal visceral fat. *J Clin Endocrinol Metab*. 2009;94(2):662–669.
- Iacobellis G, Assael F, Ribaudo MC, et al. Epicardial fat from echocardiography: A new method for visceral adipose tissue prediction. *Obes Res*. 2003;11(2):304–310.
- Iacobellis G, Willens HJ. Echocardiographic epicardial fat: A review of research and clinical applications. *J Am Soc Echocardiogr*. 2009;22(12):1311–1319; quiz 1417–1418.
- Salami SS, Tucciarone M, Bess R, et al. Race and epicardial fat: The impact of anthropometric measurements, percent body fat and sex. *Ethn Dis*. 2013;23(3):281–285.
- Gottdiener JS, Bednarz J, Devereux R, et al; American Society of Echocardiography. American Society of Echocardiography recommendations for use of echocardiography in clinical trials. *J Am Soc Echocardiogr*. 2004;17(10):1086–1119.
- Lang RM, Bierig M, Devereux RB, et al; American Society of Echocardiography's Nomenclature and Standards Committee; Task Force on Chamber Quantification; American College of Cardiology Echocardiography Committee; American Heart Association; European Association of Echocardiography, European Society of Cardiology. Recommendations for chamber quantification. *Eur J Echocardiogr*. 2006;7(2):79–108.
- Xing Y, Xu S, Jia A, et al. Recommendations for revision of Chinese diagnostic criteria for metabolic syndrome: A nationwide study. *J Diabetes*. 2018;10(3):232–239.
- Kim BJ, Kim BS, Kang JH. Echocardiographic epicardial fat thickness is associated with coronary artery calcification: Results from the CAESAR study. *Circ J*. 2015;79(4):818–824.
- Calabuig A, Barba J, Guembe MJ, et al. Epicardial adipose tissue in the general middle-aged population and its association with metabolic syndrome. *Rev Esp Cardiol (Engl Ed)*. 2017;70(4):254–260.
- Fox CS, White CC, Lohman K, et al. Genome-wide association of pericardial fat identifies a unique locus for ectopic fat. *PLoS Genet*. 2012;8(5):e1002705.
- Silaghi A, Piercecchi-Marti MD, Grino M, et al. Epicardial adipose tissue extent: Relationship with age, body fat distribution, and coronary artery disease. *Obesity (Silver Spring)*. 2008;16(11):2424–2430.
- Baragetti A, Pisano G, Bertelli C, et al. Subclinical atherosclerosis is associated with epicardial fat thickness and hepatic steatosis in the general population. *Nutr Metab Cardiovasc Dis*. 2016;26(2):141–153.
- Abdallah E, El-Shishtawy S, Sherif N, Ali A, El-Bendary O. Assessment of the relationship between serum paraoxonase activity and epicardial adipose tissue in hemodialysis patients. *Int Urol Nephrol*. 2017;49(2):329–335.
- Kim BJ, Kang JG, Lee SH, et al. Relationship of echocardiographic epicardial fat thickness and epicardial fat volume by computed tomography with coronary artery calcification: Data from the CAESAR study. *Arch Med Res*. 2017;48(4):352–359.

Effectiveness and safety of intracoronary papaverine, alprostadil, and high dosages of nicorandil and adenosine triphosphate for measurement of the index of coronary microcirculatory resistance in a pig model

Tianbing Duan^{1,2,A–F}, Jinxia Zhang^{2,B}, Dingcheng Xiang^{2,A,E}, Rui Song^{2,C}, Ranran Kong^{2,C}, Dingli Xu^{1,A,F}

¹ Department of Cardiology, Nanfang Hospital, Southern Medical University, Guangzhou, China

² Department of Cardiology, Guangzhou General Hospital of Guangzhou Military Command, China

A – research concept and design; B – collection and/or assembly of data; C – data analysis and interpretation;

D – writing the article; E – critical revision of the article; F – final approval of the article

Advances in Clinical and Experimental Medicine, ISSN 1899–5276 (print), ISSN 2451–2680 (online)

Adv Clin Exp Med. 2019;28(10):1409–1418

Address for correspondence

Dingli Xu

E-mail: dinglixu@fimmu.com

Funding sources

This study was supported by BEIJING TIDE PHARMACEUTICAL CO., LTD. (Beijing, China) but was designed and implemented independently by Guangzhou General Hospital of Guangzhou Military Command. We declare that none of the authors has any financial and personal relationships with other people or organizations that can inappropriately influence the quality of the work presented in this manuscript. There is no professional or other personal interest of any nature or kind in any product, service and/or company that may be construed as influencing the position presented in this manuscript.

Conflict of interest

None declared

Received on June 26, 2018

Reviewed on September 6, 2018

Accepted on February 18, 2019

Published online on October 22, 2019

Cite as

Duan T, Zhang J, Xiang S, Song R, Kong R, Xu D. Effectiveness and safety of intracoronary papaverine, alprostadil, and high dosages of nicorandil and adenosine triphosphate for measurement of the index of coronary microcirculatory resistance in a pig model. *Adv Clin Exp Med.* 2019;28(10):1409–1418. doi:10.17219/acem/104541

DOI

10.17219/acem/104541

Copyright

© 2019 by Wrocław Medical University

This is an article distributed under the terms of the Creative Commons Attribution Non-Commercial License (<http://creativecommons.org/licenses/by-nc-nd/4.0/>)

Abstract

Background. Papaverine is used to induce maximal hyperemia for index of coronary microcirculatory resistance (IMR) measurement in animal experiments, although it can lead to polymorphic ventricular tachycardia and ventricular fibrillation.

Objectives. This study investigated the effect of an intracoronary (IC) bolus of high adenosine triphosphate (ATP) and nicorandil doses for IMR measurement and explored the possibility of inducing maximal hyperemia with an IC alprostadil bolus.

Material and methods. Index of coronary microcirculatory resistance was measured in a hyperemic state induced by 7 experimental conditions in 21 pigs (IC bolus of papaverine (18 mg), ATP (40 µg, 80 µg, 160 µg, and 240 µg), and nicorandil (2 mg and 4 mg)). The 7 conditions were induced sequentially, and the average IMR was calculated. Because of the long-term hyperemic condition in the pilot experiments, the IMR was measured 1, 3, 5, 8, and 10 min after an IC bolus of alprostadil (10 µg) in another 7 pigs.

Results. The IMR induced by 240 µg of ATP or 4 mg of nicorandil was not significantly different from that induced by 18 mg of papaverine (both $p > 0.05$). A strong linear correlation was observed between IMRs with papaverine (18 mg) and nicorandil (4 mg) ($R^2 = 0.936$, $p < 0.001$) and with papaverine (18 mg) and ATP (240 µg) ($R^2 = 0.838$, $p < 0.05$). The IC bolus of nicorandil (4 mg) produced the smallest changes, whereas papaverine caused the most significant changes in mean blood pressure and heart rate ($p < 0.05$). Tachypnea and transient ST depression were more common with increasing ATP dosages (especially 240 µg). Alprostadil (5 min) yielded a significant hyperemic response but reduced baseline blood pressure by almost 40% for a long time.

Conclusions. Intracoronary bolus administration of 4 mg of nicorandil was better than 18 mg of papaverine or 240 µg of ATP for induction of maximal hyperemia and IMR measurement in a pig model, whereas alprostadil was not suitable for IMR measurement.

Key words: papaverine, alprostadil, adenosine triphosphate, index of microcirculatory resistance, nicorandil

Introduction

ST-segment elevation myocardial infarction (STEMI) usually results from acute thrombotic occlusion of a coronary artery and is the leading cause of death or loss of ability to live independently.¹ The goal of reperfusion therapy with fibrinolytic drugs or primary percutaneous coronary intervention (PPCI) is to restore blood flow to ischemic areas. Although total ischemia times have improved significantly recently for patients undergoing PPCI, in-hospital mortality and heart failure have remained virtually unchanged.² As a result, addressing coronary microvascular functional and structural obstructions, which occur frequently even after prompt epicardial recanalization of the infarct-related artery and increase the risk of cardiovascular events regardless of the epicardial disease status, is an unmet need.³

The index of coronary microcirculatory resistance (IMR) is a pressure-temperature sensor guidewire-based measurement that is performed during cardiac catheterization.⁴ The IMR is a specific quantitative measurement used to assess coronary microvasculature function and shows a high predictive capacity for the extent and severity of myocardial infarction in patients with STEMI.^{5,6} Accurate IMR calculation requires a maximal steady state of coronary hyperemia.

Papaverine is the most commonly used pharmacological agent and the gold standard for induction of maximal hyperemia in animal experiments.⁷ The peak effect occurs 10–30 s after administration, with a plateau duration of approx. 45–60 s.⁸ However, papaverine may induce Q-T prolongation, which can lead to polymorphic ventricular tachycardia and ventricular fibrillation.^{9,10} In addition, an intracoronary (IC) bolus of papaverine induces a significant increase in coronary venous lactate in both animal experiments and patients with normal coronary arteries, which suggests that papaverine may produce myocardial ischemia.^{11–13} Adenosine triphosphate (ATP) is a precursor of adenosine that has a short half-life in plasma and is rapidly degraded into adenosine diphosphate, adenosine monophosphate and adenosine. Significant coronary vasodilation effects of ATP have been proposed to depend on its degradation to adenosine via stimulation of adenosine receptor A2a and not the direct action of ATP.¹⁴ In a clinical setting, intravenous ATP ($140 \mu\text{g}\cdot\text{kg}^{-1}\cdot\text{min}^{-1}$) can induce a complete, true, steady-state hyperemia and enable a pressure pullback maneuver, although the optimal dosage of ATP administered via IC bolus to induce a maximal hyperemic condition is controversial¹⁵; thus, the ideal dosage of the IC ATP bolus needs to be further explored. However, no study has investigated the hyperemic effect induced by larger dosages of ATP for IMR measurement in animal experiments.

Compared with continuous intravenous infusion of adenosine for IMR measurement, administration of a IC bolus of nicorandil (2 mg) is a simple, safe and effective method to induce steady-state hyperemia for invasive physiological evaluation in a cardiac catheterization laboratory, but the effectiveness of larger dosages of nicorandil has not

been reported.¹⁶ Alprostadil, which is a coronary vasodilator that acts on the microvascular system, was reported to be safe and vasoprotective in patients with pulmonary hypertension or chronic heart failure.^{17,18} Therefore, could alprostadil be a new agent to induce coronary hyperemia?

Due to the difficulty in studying coronary microvascular dysfunction in patients with STEMI immediately after PPCI, animal experimentation is the proper research approach. Therefore, in this study, we used papaverine as the control group in a pig model to compare the effectiveness and safety of inducing hyperemia with larger dosages of ATP and nicorandil and the feasibility and the practicality of inducing coronary hyperemia with an IC bolus of alprostadil for measurement of the IMR. Our results provide insights into the optimal administration method and dosage needed to achieve hyperemia and accurately measure the IMR in animal experiments.

Material and methods

Protocol

The Institutional Animal Care and Use Committee of Guangzhou General Hospital of Guangzhou Military Command approved the study protocol. All studies were performed in accordance with the Animal Research Reporting In Vivo Experiments (ARRIVE) guidelines for

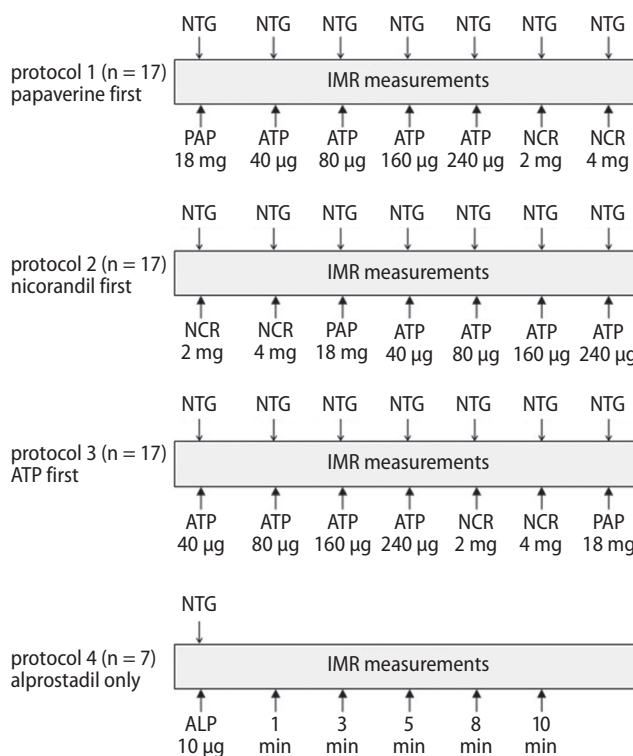


Fig. 1. Outline of the hyperemic stimuli protocol

NTG – nitroglycerine; PAP – papaverine; NCR – nicorandil; ATP – adenosine triphosphate; ALP – alprostadil; IMR – index of microcirculatory resistance.

the reporting of animal experiments.¹⁹ The IMR was measured following induction by 7 experimental conditions in 21 pigs (IC bolus of papaverine (18 mg), ATP (40 µg, 80 µg, 160 µg, and 240 µg) and nicorandil (2 mg and 4 mg)). To exclude the possible influence of the sequence of pharmacological agents, measurements of the above 3 drugs were performed in sequential order (i.e., ATP and nicorandil were followed by papaverine in the 1st measurement, papaverine and ATP were followed by nicorandil in the 2nd measurement, and nicorandil and papaverine were followed by ATP in the 3rd measurement). In addition, due to the long hyperemic condition induced in the pilot experiments, the measurement of the IMR induced by 10 µg of alprostadil was measured in an additional 7 pigs. An IC bolus of nitroglycerine (200 µg) was administered before each IMR measurement. Details of the experimental protocol are summarized in Fig. 1.

Animal preparation

Five days before the measurement, all 28 pigs received aspirin (5 mg/kg nightly), clopidogrel (5 mg/kg daily), perindopril (4 mg daily), and atorvastatin calcium (20 mg nightly). General anesthesia was induced by intramuscular injection of a mixture of ketamine (200 mg), Su-mian-xin (1.5 mL, mixture of haloperidol, xylidinothiazole and dihydroetorphine) and midazolam (10 mg), and then maintained with a mixture of 8 mL of 0.9% sodium chloride, 2 mL of ketamine (100 mg) and 40 mL of Propofol delivered continuously with a medical syringe pump through a marginal ear vein (8–18 mL per h). Oxygen was supplied at a rate of 2 L/min. Penicillin (4.8 million units) was injected 30 min before the experiment. After local injection of 10 mL of lidocaine in the inguinal area, the right femoral artery was exposed and isolated after skin incision and separation of subcutaneous tissue, and then a 6-French (6-F) size sheath was placed in the artery. A 6-F JR3.5 guide catheter was inserted into the left coronary artery through the arterial sheath. Then, the animals were heparinized (100 U/kg IC, with another 2500 U added every h). Finally, a baseline angiography was performed.

IMR measurement

After calibration, a 0.014-inch-diameter coronary pressure wire (St. Jude Medical Systems, Saint Paul, USA) was advanced into the distal area of the left anterior descending coronary artery (LAD). The mean aortic pressure (Pa), mean distal pressure of the LAD (Pd) and mean transit time (Tmn, in seconds) of a 3×3 mL bolus of room-temperature saline injected into the coronary artery were recorded at baseline through the 6-F guide catheter and the pressure wire. Then, a mixture of 0.9% sodium chloride and 1 hyperemic drug was injected into the left coronary artery through the 6-F JR3.5 guide catheter to induce maximal hyperemia. When the maximal steady state of coronary hyperemia was

reached, a 3×3 mL bolus of room-temperature saline was injected into the coronary artery, and the Pa, Pd and Tmn were recorded. The IMR was calculated as the mean Tmn multiplied by the Pd. The next measurement could not be made until the Pa, Pd and heart rate recovered from the hyperemic level to the baseline level after an interval of several minutes. Seven conditions were investigated; under each condition, the IMR was measured as described above in sequential order, and the average IMR value was calculated for analyses among the 21 pigs. In addition, the time of the pressure drop from the basic to the maximal hyperemic state and the duration of the maximal hyperemic condition were recorded under every condition. The IMR induced by alprostadil (10 µg) was measured in another 7 pigs due to the long hyperemic condition at 1, 3, 5, 8, and 10 min after the IC bolus. In all cases, a 12-lead real-time electrocardiogram (ECG) monitor system recorded the total ECG waveform, including the ventricular premature beats, ventricular tachycardia, ventricular fibrillation and ECG ST and T wave changes.

Statistical analyses

All statistical analyses were performed using SPSS v. 21.0 (IBM Corp., Armonk, USA). Categorical data was presented as a frequency or a percentage, and differences among groups were analyzed using the χ^2 test. Continuous data was presented as medians with standard deviations (SD) or medians and interquartile ranges (25th–75th). Differences in the IMR obtained with different hyperemic methods were analyzed using repeated measures analysis of variance (ANOVA). If the overall difference was significant, then a pairwise comparison was conducted. The Bland–Altman plot of the IMR was used to compare 2 hyperemic effects. A p-value <0.05 (two-sided) was considered significant.

Results

Study animals

A total of 28 pigs with an average body weight of 21.2 ±2.1 kg received IMR measurements. Twenty-one pigs were induced by papaverine (18 mg) and different doses of ATP (40 µg, 80 µg, 160 µg, and 240 µg) and nicorandil (2 mg and 4 mg) through IC bolus administration. Conversely, 7 pigs were induced by alprostadil alone. Four pigs died during the experiment, each due to one of the following reasons: hemorrhagic shock, an anesthesia accident, left main coronary thrombosis, and reperfusion arrhythmia. A total of 51 measurements were completed for each hyperemic drug dosage when the maximal hyperemic condition was induced in 17 pigs. In another 7 pigs, the time required for the recovery of the Pa, Pd and heart rate from the hyperemic to the baseline level after an IC bolus of alprostadil was almost 32 min, and a significant hyperemic

Table 1. Comparison between 4 drugs used to induce hyperemia

	Papaverine 18 mg (n = 51)	ATP 240 µg (n = 51)	Nicorandil 4 mg (n = 51)	Alprostadil ▲ 10 µg (n = 7)	p-value
Baseline characteristics					
Male [%]	17 (80.9%)	17 (80.9%)	17 (80.9%)	7 (100%)	
Body weight [kg]	21.7 (19.5–23.4)	21.7 (19.5–23.4)	21.7 (19.5–23.4)	24.0 (21.5–25.3)	
Death [%]	4 (14.3%)	4 (14.3%)	4 (14.3%)	0 (0%)	
Baseline Pa [mm Hg]	110 (101–120)	109 (101–118)	110 (102–121)	101 (97–108)	0.211
Baseline Pd [mm Hg]	108 (99–117)	107 (99–117)	109 (101–118)	98 (91–104)	0.116
Baseline HR	78 (72–85)	80 (75–88)	81 (78–85)	72 (64–77)	0.059
Hyperemic efficacy					
FFR	0.95 (0.94–0.96)	0.92 (0.89–0.97)	0.92 (0.90–0.95)	0.95 (0.94–0.96)	0.000
IMR	11.5 (9.8–13.1)	11.6 (10.0–12.9)	11.3 (9.2–13.7)	9.6 (7.2–11.5)	0.213
CFR	4.1 (3.9–4.4)	3.6 (3.3–3.8)	4.1 (3.8–4.3)	3.5 (3.1–3.9)*	0.000
Time to the lowest IMR [s]	15.7 (14.0–17.0)	12.8 (11.0–14.0)	17.7 (16.0–20.0)		0.000
Plateau time [s]	49.0 (49.0–52.0)	24.7 (22.0–27.0)	30.3 (27.0–33.0)		0.000
Tmn [s]	0.16 (0.13–0.19)	0.15 (0.13–0.17)	0.14 (0.11–0.16)	0.15 (0.12–0.16)	0.005
Side effects					
ΔPa [mm Hg]	33 (29–36)	26 (20–30)	19 (14–21)	33 (31–39)	0.000
ΔHeart rate	38 (32–45)	27 (25–29)	20 (18–23)	26 (22–29)	0.000
R** >20, n [%]	2 (11.7)	11 (64.7)	1 (5.9)	7 (100)	
ΔPR interval [ms]	0 (0)	0 (0)	0 (0)	0 (0)	
ST depression, n [%]	0 (0)	4 (23.5)	0 (0)	0 (0)	
Serious AV-nodal block, n [%]	0 (0)	0 (0)	0 (0)	0 (0)	

Values given are medians (interquartile range, 25th–75th) or rate.

▲ the value obtained 5 min after alprostadil administration.

* the value obtained 1 min after alprostadil administration.

**R – respiratory rate; Pa – mean aortic pressure; Pd – mean distal pressure of the left anterior descending coronary artery; FFR – fractional flow reserve; IMR – index of microcirculatory resistance; CFR – coronary flow reserve; Tmn – transit mean time; ΔPa – difference in the mean aortic pressure between the maximal hyperemic condition and the baseline level; ΔHR – difference in the heart rate between the maximal hyperemic condition and the baseline level; AV – nodal block, atrioventricular block.

condition continued for nearly 10 min; therefore, the IMR was measured 1, 3, 5, 8, and 10 min after alprostadil administration. The hyperemic efficacies of the 4 drugs are presented in Table 1.

IMR induced by ATP

A significant decrease was observed in the IMR with increasing ATP dosages from 40 µg to 240 µg (p-value for trend <0.05). No significant difference was observed in the IMR induced by 240 µg of ATP compared to that induced by 18 mg of papaverine (11.6 ± 2.2 vs 11.5 ± 2.4, p > 0.05), but a significant difference was found in the IMRs induced by 40 µg, 80 µg and 160 µg of ATP (22.2 ± 7.9, 15.3 ± 4.5 and 13.2 ± 3.3, respectively, vs 11.5 ± 2.4, all p < 0.05). A strong linear correlation was found between the IMRs induced with the IC bolus of papaverine (18 mg) and ATP (240 µg) ($R^2 = 0.838$, $y = 0.812x + 2.219$, p < 0.05). The agreement between the 2 sets of measurements was good, with a mean difference of 0.06 and SD of 0.44. In all measurements, the values of 1.9% (1/51) of the measurements were beyond

the 95% confidence interval (95% CI). As the ATP dosage increased, the fractional flow reserve (FFR) gradually decreased (p-value for trend <0.05) and the coronary flow reserve (CFR) increased from the lowest measurement at the 40 µg dosage to the highest at 240 µg (p-value for trend <0.05). Similar to the IMR, significant differences were found in the FFR and CFR induced by 240 µg of ATP compared with those induced by papaverine (both p < 0.05). Under the 240 µg dosage, a significant difference in the decreases in the mean arterial pressure and heart rate change were found between papaverine and ATP (p < 0.05). Detailed results are illustrated in Fig. 2, 3 and 5.

IMR induced by nicorandil

The IMR induced by nicorandil (2 mg) was higher than that induced by papaverine (18 mg) (13.6 ± 2.1 vs 11.5 ± 2.4, p < 0.05), whereas the IMR induced by the IC bolus of nicorandil (4 mg) (11.3 ± 2.0) was nearly equal to that induced by the IC bolus of papaverine (18 mg) (11.5 ± 2.4) (p = 0.999). A strong linear correlation was found between

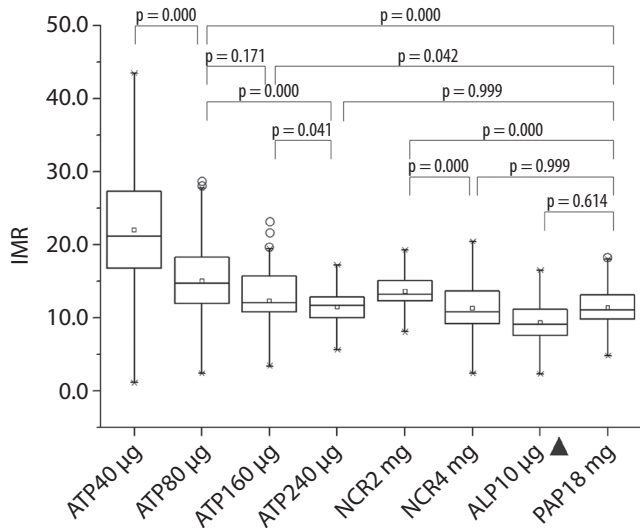


Fig. 2. Comparison of the IMR induced by an IC bolus of ATP, NCR, ALP and PAP in the non-stenotic LAD

PAP – papaverine; NCR – nicorandil; ATP – adenosine triphosphate; ALP – alprostadil; IMR – index of microcirculatory resistance.

▲ The IMR value was measured under the hyperemic condition 5 min after administration of alprostadil.

the IMRs with the IC bolus of papaverine (18 mg) and nicorandil (4 mg) ($R^2 = 0.936$, $y = 1.071x - 0.987$, $p < 0.001$). The agreement between the 2 sets of measurements was good, with a mean difference of 0.17 and a SD of 0.45. In all measurements, the values of 3.9% (2/51) of the measurements were beyond the 95% CI. A significant difference was observed in the FFR between the groups that received the IC bolus of nicorandil (4 mg) and papaverine (18 mg) ($p < 0.05$), but these differences were not found in the CFR ($p > 0.05$). Compared to the IC bolus of papaverine, fewer

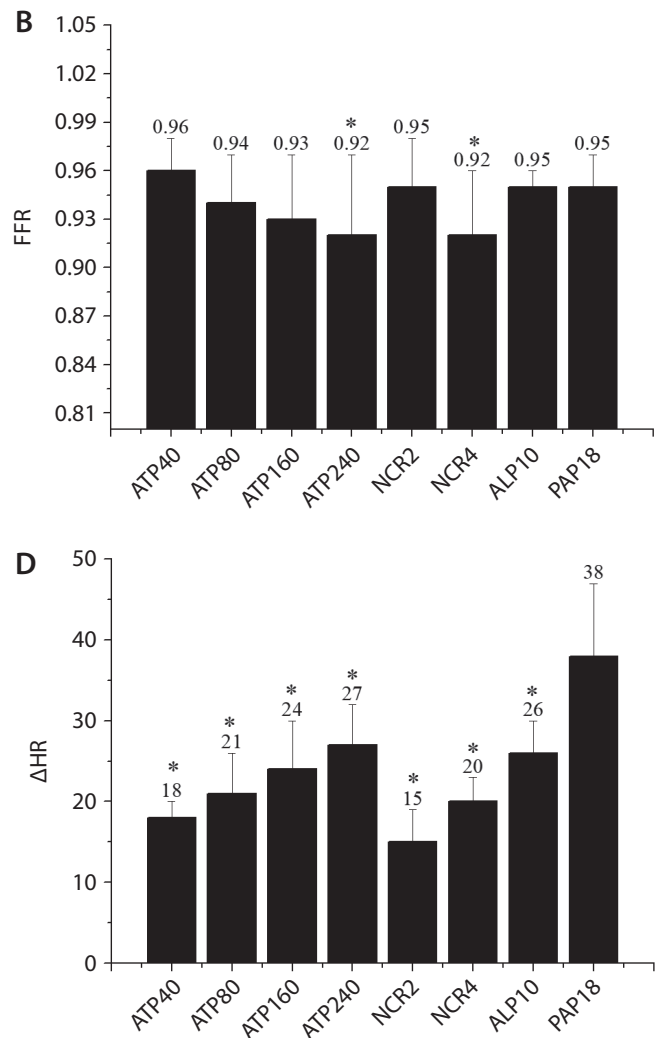
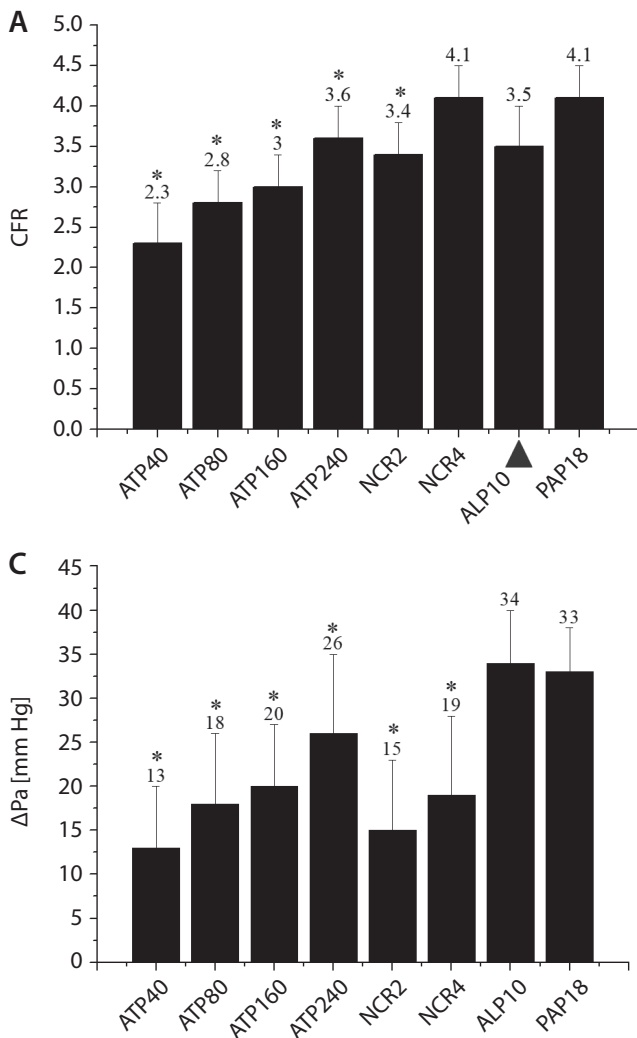


Fig. 3. Comparison of the CFR, FFR, ΔPa, and ΔHR induced by an IC bolus of ATP, NCR, ALP, and PAP in the non-stenotic left coronary artery

CFR – coronary flow reserve; FFR – fractional flow reserve; ΔPa – difference in the mean aortic pressure between the maximal hyperemic condition and the baseline level; ΔHR – difference in the heart rate between the maximal hyperemic condition and the baseline level.

The units of ATP40 (ATP80, ATP160, ATP240, ALP10) and NCR2 (NCR4, PAP18) were µg, and mg, respectively.

*Compared with 18 mg of papaverine, $p < 0.05$.

▲ The CFR value obtained 1 min after alprostadil administration.

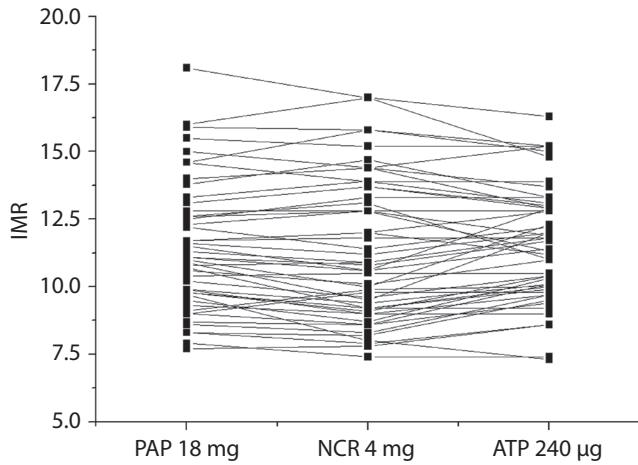


Fig. 4. Individual IMR values obtained after inducing hyperemia with papaverine (18 mg), ATP (240 µg) and nicorandil (4 mg)

Abbreviations are as described in Fig. 1.

changes were detected in the mean blood pressure and heart rate in the measurements that received the IC bolus of nicorandil (both $p < 0.05$). Detailed results are illustrated in Fig. 2, 3 and 5.

Individual IMR values among the papaverine (18 mg), ATP (240 µg) and nicorandil (4 mg) hyperemic induction groups are shown in Fig. 4.

IMR induced by alprostadil

After receiving an IC bolus of alprostadil (10 µg), the IMR decreased gradually and bottomed out within 5 min before increasing slowly. Compared with papaverine, alprostadil yielded a stronger hyperemic response with a lower IMR (5 min), but the difference did not reach significance (9.6 ± 2.2 vs 11.5 ± 2.4 , $p = 0.639$). The IC bolus of alprostadil caused large changes in the mean blood pressure, including an almost 40% reduction compared with the baseline blood pressure, and the heart rate also changed greatly. Detailed results are illustrated in Fig. 3 and 6.

Side effects during induction of maximal hyperemia

Of the 4 drugs, the IC bolus of nicorandil (4 mg) produced the smallest changes in the mean blood pressure and heart rate; in contrast, alprostadil and papaverine caused the most

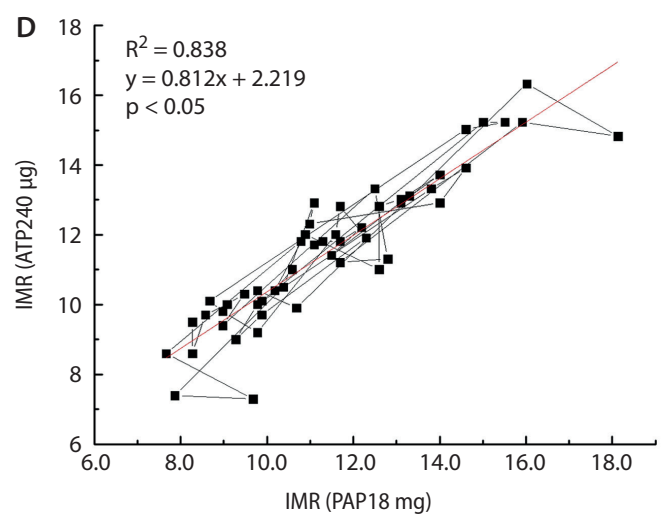
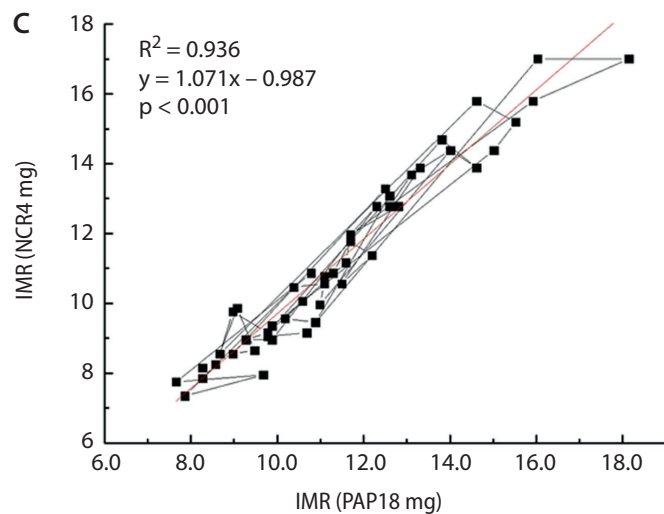
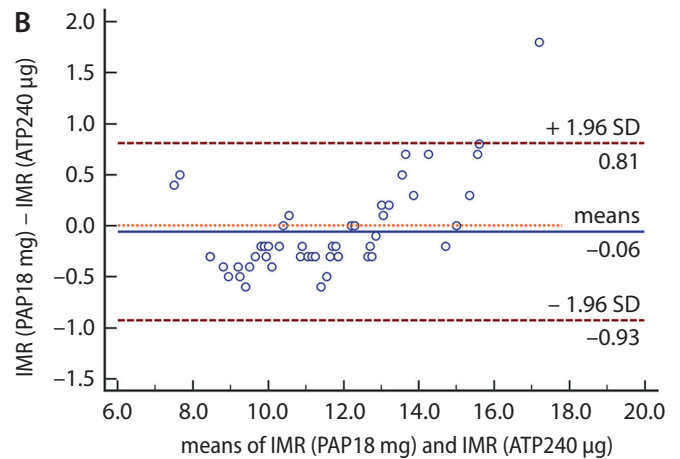
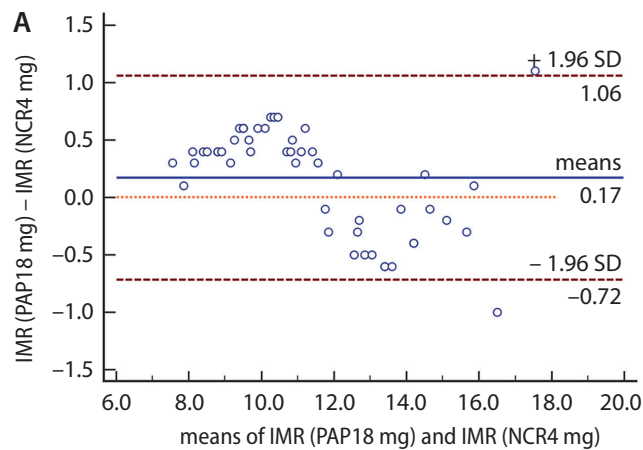


Fig. 5. Bland–Altman plots (A, B) and correlations (C, D) of IMR induced by an IC bolus of nicorandil (NCR, 4 mg), ATP (240 µg) and papaverine (PAP, 18 mg)

Abbreviations are as described in Fig. 1.

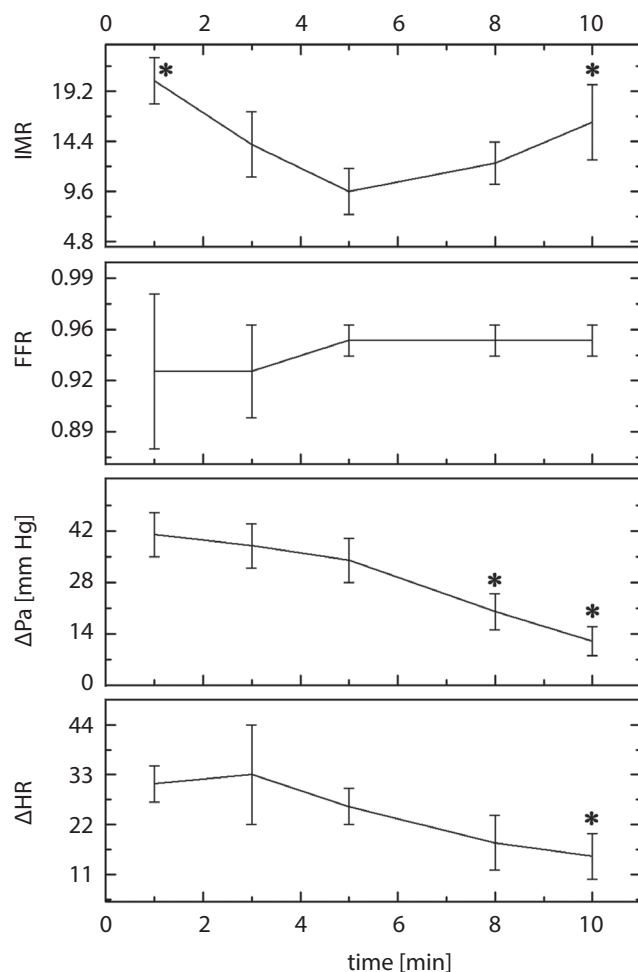


Fig. 6. Comparison of the IMR, FFR, Δ Pa and Δ HR under hyperemic conditions at 1, 3, 5, 8, and 10 min after administration of an IC bolus of alprostadil (10 μ g) in the non-stenotic left coronary artery

Abbreviations are as described in Fig. 1.

* Compared with the value obtained 5 min after administration of an IC bolus of alprostadil, $p < 0.05$.

significant changes in the mean blood pressure and heart rate, respectively ($p < 0.05$). Side effects were more common with increasing ATP dosages, especially at the 240 μ g dose, including tachypnea and transient ST depression. No significant changes in the PR, QRS or QT intervals on the ECG were noted, even at the highest dose administered, and no atrioventricular blocks occurred. Detailed results are illustrated in Table 1 and Fig. 3 and 6.

Discussion

In patients with STEMI, coronary microvasculature dysfunction occurs after complete reperfusion with a prevalence ranging from 5% to 50%.²⁰ Consistent evidence has shown that coronary microvasculature dysfunction has a strong negative impact on the prognosis, including effects on the potential benefits of percutaneous coronary intervention and an increase in the risk of early post-infarction

complications, adverse left ventricular remodeling, late-onset heart failure, and mortality.^{21–23} Identifying a simple, reliable and convenient method to independently diagnose coronary microvasculature dysfunction is crucial for the initiation of timely treatment and effective restoration of microcirculation function. The IMR is a specific quantitative indicator for the assessment of coronary microvasculature function that is applied in most physiological assessments of myocardial blood flow but requires a maximal steady coronary hyperemic condition to achieve accurate measurement.^{3,24}

Although perfusion of myocardial tissues has been restored in a timely manner and the condition of patients with STEMI has improved, they remain in critical condition and still need close observation to maintain life. There are many difficulties in the study of coronary microvascular dysfunction in patients with STEMI immediately after reperfusion. Therefore, investigations of the assessment methods in animal models and interventional studies of coronary microcirculation dysfunction after experimental STEMI could have great value. An ideal animal model should present with cardinal signs and pathology that resemble the human disease. Quality preclinical data offers valuable insights for translational research. Pigs resemble humans in the context of minimal preexisting coronary collaterals and similar coronary anatomy and physiology and, therefore, are commonly used in animal experiments of myocardial infarction.²⁵ In this study, we compared the hyperemic effects of different pharmaceutical agents on IMR measurements using a pig model.

As a precursor of adenosine, ATP is equivalent to adenosine for both CFR and FFR measurements. The current recommendation for IC ATP dosing is 60 μ g in the left coronary artery; if necessary, the dosage can be increased incrementally by 30 μ g to a maximum of 150 μ g.²⁶ However, the ideal dosage of the IC route is a controversial issue that has been addressed in several clinical reports.^{27–30}

According to previous reports^{14,15} that used 18 mg of papaverine as the control group, we compared the differences in the IMRs induced by 40 μ g, 80 μ g, 160 μ g, and 240 μ g of ATP via the left coronary artery. A significant dose-dependent relationship was observed with hyperemia, with the higher dosage yielding a better hyperemic response. The higher dosage of ATP resulted in a significantly lower IMR than the lower dosages. The lowest IMR was induced by 240 μ g of ATP, and the highest was induced by 40 μ g of ATP. Based on the IMR measured following IC infusion of 240 μ g of ATP, this condition was the only experimental condition that generated hyperemia comparable to that obtained with 18 mg of papaverine, whereas 40 μ g, 80 μ g and 160 μ g of ATP did not induce comparable states. Meanwhile, significant differences in the IMR were induced by the 4 ATP dosages. No difference in the IMR was found between the groups administered the IC bolus of ATP (240 μ g) and papaverine (18 mg); and a strong linear correlation existed between the IMRs induced with the IC bolus

of papaverine (18 mg) and ATP (240 μ g), although only 1 IMR value was beyond the 95% conformance scope. This result indicated that the hyperemic effects on the IMR induced by the 2 agents were equivalent. Similar to the IMR, significant differences were found in the FFR and CFR induced by 240 μ g of ATP compared with the effects induced by papaverine. These results showed that the current recommended dosage of IC ATP is not sufficient in animal experiments; thus, a higher dosage is essential to ensure an adequate hyperemic response. This conclusion is supported by several studies. Jeremias et al. compared the effect of ATP on the measurement of the CFR in 6 healthy mongrel dogs. Their results showed a dose-dependent relationship of the CFR with IC administration of ATP via the non-stenotic left circumflex coronary artery, with the largest value induced by the maximal dosage.²⁷ Casella et al. suggested that an IC bolus dosage up to 150 μ g should be better; for the standard doses, 10% measurement values may be underestimated.²⁸ Leone et al. demonstrated that only much higher doses (600 μ g) produced real hyperemic efficacy.²⁹ Lower doses of the drug are associated with an inferior diagnostic accuracy, and thus, a higher dosage may be required.

The FFR dropped slightly as the ATP dosage increased. The mean FFR values were very similar under all experimental conditions, and the difference between the highest and lowest values was only 0.04. This finding also differed from those of some previous studies on epicardial coronary stenosis,^{31,32} including angiographically intermediate stenosis, multivessel disease, and sequential stenosis. The discrepancy could result from the epicardial arteries being normal in our study. This finding indicated that the effects of different administration dosages on the normal epicardial coronary artery were similar. Unlike the FFR, the CFR increased slightly as the ATP dosage increased, and significant differences in the CFR were observed between the groups that received the IC bolus of ATP (40 μ g, 80 μ g and 160 μ g) and papaverine (18 mg).

Due to opening of ATP-sensitive potassium channels in coronary resistant arterioles and its possession of a nitrate moiety effect, nicorandil has been used as an anti-anginal drug for several years.^{33–35} Recently, nicorandil has been used for invasive physiological assessments as a novel hyperemic agent in the cardiac catheterization laboratory.^{36,37} In our study, 2 mg of nicorandil yielded a weaker hyperemic response with a higher IMR than 4 mg of nicorandil or 18 mg of papaverine, indicating that maximal hyperemia in the animal body was not achieved by lower dosages. No difference in the IMR was induced between the IC bolus of nicorandil (4 mg) and papaverine (18 mg), and a strong linear correlation existed between the IMRs obtained with the IC bolus of papaverine (18 mg) and nicorandil (4 mg), with only 2 IMR values beyond the 95% conformance scope. This finding indicated that the hyperemic effects on the IMRs induced by the 2 agents were equivalent. The FFR value induced by 4 mg of nicorandil

was much lower than that of papaverine, but no significant difference in the CFR was observed.

Our results showed that the effect of nicorandil on inducing maximal hyperemia appeared to contradict the results of some previous studies. Jang et al. compared the effect of nicorandil on the measurement of the IMR and FFR with adenosine as the clinical agent.¹⁶ The study suggested that the hyperemic effect of an IC bolus of 2 mg was equal to that of the IV standard dosage of adenosine and was superior to the effect of an IC bolus of adenosine (80 μ g), Tanaka et al. reported that no further decrease occurred in the FFR at nicorandil doses over 2 mg.³⁸

Several factors may explain the differences between the clinical setting and the experimental results, such as intrinsic differences in coronary anatomy, differences in drug metabolism or different heart sizes between pigs and humans. Some studies have reported that despite the similarity of the coronary arterial system with respect to morphology and size and even the capillary diameter between pigs and humans, slight differences exist.^{25,39} In addition, in our study, we used IMR instead of FFR or CFR as the main observation index, which was different from previous studies. The IMR is a reliable measurement that has been specifically dedicated to assessing coronary microvascular dysfunction, and changes in the IMR reflect fluctuations of the microcirculation condition induced by hyperemic agents in the same vessel. Conversely, as a modification of the translesional pressure gradient, the FFR detects clinically relevant lumen narrowing of the epicardial coronary artery.

The IC bolus of nicorandil (4 mg) and ATP (240 μ g) were both slower in reaching maximal hyperemia than papaverine. However, the hyperemic duration was longer than that obtained with an IC bolus of papaverine. The peak effect time of maximal coronary hyperemia for ATP (240 μ g) and nicorandil (4 mg) lasted 25 s, whereas the peak effect time of papaverine was 20 s. In our study, an average of 4 s was required to finish injecting a 1 \times 3 mL bolus of room-temperature saline into the coronary artery, and thus, the peak effect time was adequate for experienced hands (but not new learners) to conduct measurements of a 3 \times 3 mL bolus of saline during the experiments.

Alprostadil is a potent systemic vasodilator with important endogenous flow-regulating activity to maintain blood flow to vital organs.⁴⁰ This study is the first to evaluate the coronary hyperemic effect of alprostadil via IC bolus in IMR measurements in pigs. After administration of an IC bolus of alprostadil, the systemic blood pressure decreased immediately; the fastest rate reduction was nearly 30–40% in the first 2 min, and the significantly lower pressure lasted for more than 10 min. Thirty-two minutes later, the systemic blood pressure recovered from the hyperemic condition to the baseline level. As a result, IMR measurements were performed in an additional 7 pigs at 1, 3, 5, 8, and 10 min after the IC bolus. The maximal hyperemic effect of alprostadil occurred 5 min after administration. Alprostadil produced a lower IMR than papaverine,

but the difference in the IMR was not significant between the 2 drugs. The significant disadvantages of an IC bolus of alprostadil were drastic fluctuation of blood pressure and the long hyperemic duration time, which might influence vital organ perfusion. Thus, administration of an IC bolus of alprostadil is not suitable to produce a hyperemic response for IMR measurement.

During the experiments, blood pressure and heart rate were the most vulnerable measurements. Alprostadil caused the most severe decrease in the mean blood pressure, and papaverine led to the largest increase in the heart rate and decrease in the mean blood pressure. Conversely, an IC bolus of nicorandil (4 mg) produced the smallest changes in the mean blood pressure and heart rate, whereas the influence of ATP was at the mid-level of the 4 pharmaceutical agents. The most notable side effect of IC administration of ATP was a slight increase in tachypnea and transient ST depression. We did not observe any atrioventricular block or other changes in the PR and QRS intervals on the ECG, even at the highest dose. Therefore, as a safe and effective agent, 4 mg of nicorandil seems to be useful in animals with lower blood pressure, and 240 µg of ATP is a safe and valid agent to induce hyperemia via IC bolus administration, although it produced more side effects than nicorandil.

The study has several limitations that need to be addressed. Firstly, the dose-response relationship could be further confirmed by including other dosages of ATP, such as 180 µg, 200 µg or 220 µg. Secondly, we investigated only the hyperemic state in the left coronary artery in this study and did not examine that of the right coronary artery. Future studies will be required to confirm our results in the right coronary artery. Thirdly, the left coronary arteries of pigs were normal in this experiment without angiographic stenosis (i.e., 40–70%). Whether the results of normal arteries are same as those obtained with arteries with lesions is unclear.

Conclusions

In conclusion, both ATP and nicorandil are safe drugs that can achieve coronary hyperemia for the measurement of IMR in the left coronary artery; importantly, only higher dosages (240 µg of ATP or 4 mg of nicorandil) produced a hyperemic condition equivalent to papaverine in animal experiments, and nicorandil had fewer side effects than papaverine and ATP. Alprostadil is not suitable for inducing maximal hyperemia due to the severe decrease in blood pressure.

References

- Li J, Li X, Wang Q, et al. ST-segment elevation myocardial infarction in China from 2001 to 2011 (the China PEACE-Retrospective Acute Myocardial Infarction Study): A retrospective analysis of hospital data. *Lancet*. 2015;385(9966):441–451.
- Menees DS, Peterson ED, Wang Y, et al. Door-to-balloon time and mortality among patients undergoing primary PCI. *N Eng J Med*. 2013;369(10):901–909.
- Niccoli G, Scalone G, Lerman A, Crea F. Coronary microvascular obstruction in acute myocardial infarction. *Eur Heart J*. 2016;37(13):1024–1033.
- Fearon W, Balsam L, Farouque H, et al. Novel index for invasively assessing the coronary microcirculation. *Circulation*. 2003;107(25):3129–3132.
- McGeoch R, Watkins S, Berry C, et al. The index of microcirculatory resistance measured acutely predicts the extent and severity of myocardial infarction in patients with ST-segment elevation myocardial infarction. *JACC Cardiovasc Interv*. 2010;3(7):715–722.
- Cuculi F, De Maria G, Meier P, et al. Impact of microvascular obstruction on the assessment of coronary flow reserve, index of microcirculatory resistance, and fractional flow reserve after ST-segment elevation myocardial infarction. *J Am Coll Cardiol*. 2014;64(18):1894–1904.
- Vrolix M, Piessens J, De Geest H. Torsades de pointes after intracoronary papaverine. *Eur Heart J*. 1991;12(2):273–276.
- van der Voort PH, van Hagen E, Hendrix G, van Gelder B, Bech JW, Pijls NH. Comparison of intravenous adenosine to intracoronary papaverine for calculation of pressure-derived fractional flow reserve. *Cathet Cardiovasc Diagn*. 1996;39(2):120–125.
- Wilson RF, White CW. Serious ventricular dysrhythmias after intracoronary papaverine. *Am J Cardiol*. 1988;62(17):1301–1302.
- Kern MJ, Deligonul U, Serota H, Gudipati C, Buckingham T. Ventricular arrhythmia due to intracoronary papaverine: Analysis of QT intervals and coronary vasodilatory reserve. *Cathet Cardiovasc Diagn*. 1990;19(4):229–236.
- Christensen CW, Rosen LB, Gal RA, Haseeb M, Lassar TA, Port SC. Coronary vasodilator reserve. Comparison of the effects of papaverine and adenosine on coronary flow, ventricular function, and myocardial metabolism. *Circulation*. 1991;83(1):294–303.
- Takeuchi M, Nohtomi Y, Kuroiwa A. Intracoronary papaverine induced myocardial lactate production in patients with angiographically normal coronary arteries. *Cathet Cardiovasc Diagn*. 1996;39(2):126–130.
- Egashira K, Inou T, Hirooka Y, Yamada A, Urabe Y, Takeshita A. Evidence of impaired endothelium-dependent coronary vasodilatation in patients with angina pectoris and normal coronary angiograms. *N Engl J Med*. 1993;328(23):1659–1664.
- De Bruyne B, Pijls NH, Barbato E, et al. Intracoronary and intravenous adenosine 5'-triphosphate, adenosine, papaverine, and contrast medium to assess fractional flow reserve in humans. *Circulation*. 2003;107(14):1877–1883.
- Layland J, Carrick D, Lee M, Oldroyd K, Berry C. Adenosine: Physiology, pharmacology, and clinical applications. *JACC Cardiovasc Interv*. 2014;7(6):581–591.
- Jang H, Koo B, Lee H, et al. Safety and efficacy of a novel hyperaemic agent, intracoronary nicorandil, for invasive physiological assessments in the cardiac catheterization laboratory. *Eur Heart J*. 2013;34(27):2055–2062.
- Gupta V, Rawat A, Ahsan F. Feasibility study of aerosolized prostaglandin E1 microspheres as a noninvasive therapy for pulmonary arterial hypertension. *J Pharm Sci*. 2010;99(10):1774–1789.
- Hülsmann M, Stefanelli T, Berger R, et al. Response of right ventricular function to prostaglandin e1 infusion predicts outcome for severe chronic heart failure patients awaiting urgent transplantation. *J Heart Lung Transplant*. 2000;19(10):939–945.
- Kilkenny C, Browne W, Cuthill I, Emerson M, Altman D. Improving bioscience research reporting the ARRIVE guidelines for reporting animal research. *PLoS Biol*. 2010;8(6):e1000412.
- Niccoli G, Burzotta F, Galiuto L, Crea F. Myocardial no-reflow in humans. *J Am Coll Cardiol*. 2009;54(4):281–292.
- Fearon W, Shah M, Ng M, et al. Predictive value of the index of microcirculatory resistance in patients with ST-segment elevation myocardial infarction. *J Am Coll Cardiol*. 2008;51(5):560–565.
- Ndrepepa G, Tiroch K, Fusaro M, et al. 5-year prognostic value of no-reflow phenomenon after percutaneous coronary intervention in patients with acute myocardial infarction. *J Am Coll Cardiol*. 2010;55(21):2383–2389.
- Hamirani Y, Wong A, Kramer C, Salerno M. Effect of microvascular obstruction and intramyocardial hemorrhage by CMR on LV remodeling and outcomes after myocardial infarction: A systematic review and meta-analysis. *JACC Cardiovasc Imaging*. 2014;7(9):940–952.

24. Ng M, Yeung A, Fearon W. Invasive assessment of the coronary microcirculation: superior reproducibility and less hemodynamic dependence of index of microcirculatory resistance compared with coronary flow reserve. *Circulation*. 2006;113(17):2054–2061.
25. Kumar M, Kasala ER, Bodduluru LN, et al. Animal models of myocardial infarction: Mainstay in clinical translation. *Regul Toxicol Pharmacol*. 2016;76:221–230.
26. Kern MJ, Lerman A, Bech JW, et al; American Heart Association Committee on Diagnostic and Interventional Cardiac Catheterization, Council on Clinical Cardiology. Physiological assessment of coronary artery disease in the cardiac catheterization laboratory: A scientific statement from the American Heart Association Committee on Diagnostic and Interventional Cardiac Catheterization, Council on Clinical Cardiology. *Circulation*. 2006;114(12):1321–1341.
27. Jeremias A, Filardo S, Whitbourn R, et al. Effects of intravenous and intracoronary adenosine 5'-triphosphate as compared with adenosine on coronary flow and pressure dynamics. *Circulation*. 2000;101(3):318–323.
28. Casella G, Leibig M, Schiele TM, et al. Are high doses of intracoronary adenosine an alternative to standard Intravenous adenosine for the assessment of fractional flow reserve? *Am Heart J*. 2004;148(4):590–595.
29. Leone AM, Porto I, De Caterina A, et al. Maximal hyperemia in the assessment of fractional flow reserve: intracoronary adenosine versus intracoronary sodium nitroprusside versus intravenous adenosine: The NASCI (Nitroprussiato versus Adenosina nelle Stenosi Coronariche Intermedie) study. *JACC Cardiovasc Interv*. 2012;5(4):402–408.
30. De Luca G, Venegoni L, Iorio S, Giuliani L, Marino P. Effects of increasing doses of intracoronary adenosine on the assessment of fractional flow reserve. *JACC Cardiovasc Interv*. 2011;4(10):1079–1084.
31. Pijls N, Sels J. Functional measurement of coronary stenosis. *J Am Coll Cardiol*. 2012;59(12):1045–1057.
32. Drenjancevic I, Koller A, Selthofer-Relatic K, Grizelj I, Cavka A. Assessment of coronary hemodynamics and vascular function. *Prog Cardiovasc Dis*. 2015;57(5):423–430.
33. Markham A, Plosker G, Goa KL. Nicorandil: An updated review of its use in ischemic heart disease with emphasis on its cardioprotective effects. *Drugs*. 2000;60(4):955–974.
34. Miyazawa A, Ikari Y, Tanabe K, et al. Intracoronary nicorandil prior to reperfusion in acute myocardial infarction. *EuroIntervention*. 2006;2(2):211–217.
35. Hirohata A, Yamamoto K, Hirose E, et al. Nicorandil prevents microvascular dysfunction resulting from PCI in patients with stable angina pectoris: A randomised study. *EuroIntervention*. 2014;9(9):1050–1056.
36. Lee J, Kato D, Oi M, et al. Safety and efficacy of intracoronary nicorandil as hyperaemic agent for invasive physiological assessment: A patient-level pooled analysis. *EuroIntervention*. 2016;12(2):e208–215.
37. Kobayashi Y, Okura H, Neishi Y, et al. Additive value of nicorandil on ATP for further inducing hyperemia in patients with an intermediate coronary artery stenosis. *Coron Artery Dis*. 2017;28(2):104–109.
38. Tanaka N, Takahashi Y, Ishihara H, Kawakami T, Ono H. Usefulness and safety of intracoronary administration of nicorandil for evaluating fractional flow reserve in Japanese patients. *Clin Cardiol*. 2015;38(1):20–24.
39. Pijls N, van Son J, Kirkeeide R, De Bruyne B, Gould K. Experimental basis of determining maximum coronary, myocardial, and collateral blood flow by pressure measurements for assessing functional stenosis severity before and after percutaneous transluminal coronary angioplasty. *Circulation*. 1993;87(4):1354–1367.
40. Miller SB. Prostaglandins in health and disease: An overview. *Semin Arthritis Rheum*. 2006;36(1):37–49.

Anemia on admission and long-term mortality risk in patients with acute ischemic stroke

Tanja Hojs Fabjan^{1,4,A–F}, Meta Penko^{2,A–C,E,F}, Radovan Hojs^{3,4,A,C,E,F}

¹ Department of Neurology, University Medical Centre, Maribor, Slovenia

² Clinic of Internal Medicine, Department of Cardiology, University Medical Centre, Maribor, Slovenia

³ Clinic of Internal Medicine, Department of Nephrology, University Medical Centre, Maribor, Slovenia

⁴ Faculty of Medicine, University of Maribor, Slovenia

A – research concept and design; B – collection and/or assembly of data; C – data analysis and interpretation;

D – writing the article; E – critical revision of the article; F – final approval of the article

Advances in Clinical and Experimental Medicine, ISSN 1899–5276 (print), ISSN 2451–2680 (online)

Adv Clin Exp Med. 2019;28(10):1419–1424

Address for correspondence

Tanja Hojs Fabjan

E-mail: tanja.hojs@gmail.com

Funding sources

This work was partly supported by Slovenian Research Agency (ARRS); project “Chronic renal failure – new risk factor for stroke” (grant No. L3-9376).

Conflict of interest

None declared

Received on January 16, 2018

Reviewed on September 9, 2018

Accepted on February 18, 2019

Published online on September 16, 2019

Abstract

Background. Anemia is associated with adverse outcomes in patients with acute myocardial infarction and congestive heart failure. Additionally, it has been shown that anemia increases the short-term mortality risk in patients with acute stroke.

Objectives. The aim of our study was to determine the importance of anemia as a long-term mortality risk factor by itself or in combination with other risk factors.

Material and methods. We included 390 Caucasian patients with acute ischemic stroke in our study. Their progress was followed from the day of their admission until their death or a max. of 1,669 days. Stroke and anemia were defined according to the World Health Organization (WHO) criteria.

Results. Anemia was present in 57 (14.6%) patients. The patients with anemia were older ($p < 0.01$) and more likely to be female ($p < 0.001$). They had higher NIHSS scores on admission ($p < 0.001$) and discharge ($p < 0.001$), lower estimated glomerular filtration rates (eGFRs) ($p < 0.001$), lower serum LDL cholesterol ($p < 0.01$) and lower serum albumin levels ($p < 0.001$), while their serum C-reactive protein (CRP) levels were higher ($p < 0.001$). The Kaplan–Meier curves showed that patients with anemia had higher mortality ($p < 0.001$). Cox’s regression analysis revealed that anemia at admission was a predictor of long-term mortality in these patients (hazard ratio (HR) = 2.448, 95% confidence interval (95% CI) = 1.773–3.490; $p < 0.001$). Anemia remained a strong predictor of mortality after adjusting for other risk factors as well.

Conclusions. Anemia was frequent among our patients and was an independent predictor of long-term mortality even after adjusting for other risk factors.

Key words: risk factors, acute ischemic stroke, anemia, long-term mortality

Cite as

Hojs Fabjan T, Penko M, Hojs R. Anemia on admission and long-term mortality risk in patients with acute ischemic stroke. *Adv Clin Exp Med.* 2019;28(10):1419–1424. doi:10.17219/acem/104540

DOI

10.17219/acem/104540

Copyright

© 2019 by Wrocław Medical University

This is an article distributed under the terms of the Creative Commons Attribution Non-Commercial License (<http://creativecommons.org/licenses/by-nc-nd/4.0/>)

Introduction

Cerebral oxygen delivery depends on cerebral blood flow and arterial oxygen content.¹ Arterial oxygen content is primarily determined by hemoglobin levels.¹ Anemia, defined as low hemoglobin levels, may further impair oxygen delivery to the brain as well as, being associated with decreased oxygen-carrying ability, cause an inflammatory response, impaired cerebrovascular autoregulation and alterations in blood viscosity.^{1,2} Anemia is associated with decreased physical performance or disability and increased mortality regardless of the underlying cause of the low hemoglobin.^{3,4}

In previous studies, it has been shown that anemia is associated with adverse outcomes in patients with acute myocardial infarction and congestive heart failure.^{5–7} Additionally, it has been found that anemia increases the short-term mortality risk in patients with stroke. Li et al. in a meta-analysis of 13 cohort studies, found that anemia was an independent predictor of unfavorable outcomes in patients who have had a stroke.⁸ In 11 studies of this meta-analysis, patients were followed-up after a period of 48 h to 1 year, while in the remaining studies they were followed-up for 2 or 3 years.⁸ The latter 2 studies were from Taiwan and included a Chinese population.^{9,10} Data about the effect of anemia on long-term mortality (over 3 years) in patients with acute ischemic stroke is lacking, especially among Caucasians.

The aim of our study was to evaluate the influence of anemia on long-term mortality in patients suffering from acute ischemic stroke. The importance of other traditional and non-traditional factors on mortality risk was also evaluated.

Patients and methods

We included 390 Caucasian patients with acute ischemic stroke who were hospitalized at our department from January 2005 to January 2006. Patients were followed from the day of their admission until their death or for a max. of 56 months (from 1 to 1,669 days). No patient was lost to follow-up. Ischemic stroke was defined according to World Health Organization (WHO) criteria¹¹ and was diagnosed if the patient had had an appropriate clinical event and had a brain computed tomography (CT) that was either normal or showed a compatible low-density lesion. Events resolving completely within 24 h were diagnosed as a transitory ischemic attack (TIA) and these patients were excluded from the study. A neurologist reviewed all cases. During admission, a quantitative measurement of neurological deficit was performed according to the National Institutes of Health Stroke Scale (NIHSS1).¹² The same measurement was done on the day of discharge from the hospital (NIHSS2).

We collected blood samples from all patients. At admission, hemoglobin and serum creatinine were measured with routine laboratory methods. Anemia was defined using

the WHO criteria as a blood hemoglobin level <120 g/L in women and <130 g/L in men.¹³ The estimated glomerular filtration rate (eGFR) was calculated using the Chronic Kidney Disease Epidemiology Collaboration (CKD-EPI) equation.¹⁴ All other blood samples were taken in the first 24 h. Serum cholesterol (low-density-lipoprotein cholesterol (LDL cholesterol)), serum triglyceride, serum glycated hemoglobin (HbA1c), serum high-sensitivity C-reactive protein (hsCRP), serum albumin, serum lipoprotein(a), and serum homocysteine levels were measured with routine laboratory methods.

Diabetes mellitus was diagnosed if the patient had already been treated for diabetes mellitus (such information was obtained using a questionnaire from the patients and/or their relatives) or if their fasting glucose level during their hospitalization was higher than 7 mmol/L.¹⁵ Arterial hypertension was diagnosed if the patient had already been treated for hypertension (according to a questionnaire and/or their relatives) or if their average blood pressure value was ≥ 140 mm Hg systolic or ≥ 90 mm Hg diastolic, based on 3 different measurements during hospitalization.¹⁶ In the questionnaire, we also gathered data on smoking habits in order to divide the patients into 2 subgroups: current smokers and non-smokers. Atrial fibrillation was confirmed with a standard 12-lead electrocardiogram.

The study was approved by the National Ethics Committee of the Republic of Slovenia. Informed consent was obtained from each patient. The study was carried out in adherence with the Declaration of Helsinki.

Statistical analysis

SPSS for Windows software v. 24.0.0.0 (IBM Corp., Armonk, USA) was used to analyze the data. Arithmetic mean values and standard deviations (SD) were calculated. Characteristics of patients with and without anemia were compared using the t-test or the χ^2 test, where appropriate. Survival rates in patients with and without anemia were analyzed using Kaplan–Meier survival curves. A Cox multivariable regression analysis was used to discover predictors of long-term mortality. In the 1st model, variables which are known to be associated with higher mortality in the general population and/or in stroke patients were included: anemia; age; gender; presence of hypertension, diabetes or atrial fibrillation; smoking status; NIHSS1 and NIHSS2 scores; serum lipid (LDL cholesterol and triglycerides) and serum HbA1c levels; and eGFRs (CKD-EPI equation). In the 2nd model, along with the previous variables, serum hsCRP and serum albumin levels were included, since they – as markers of inflammation/malnutrition – have been associated with higher mortality in previous studies of stroke patients. In the 3rd model, serum lipoprotein(a) and serum homocysteine were added to all of the variables from the 2nd model. Serum lipoprotein(a) and serum homocysteine are accepted as newer non-traditional mortality risk factors. A value of $p < 0.05$ was considered to be statistically significant.

Results

In our study, 390 patients with acute ischemic stroke were included; 183 (46.9%) women and 207 (53.1%) men. Anemia was present in 57 (14.6%) patients. The baseline characteristics of all patients and patients with and without anemia are presented in Table 1.

Patients with anemia were older ($p < 0.01$) at the onset of stroke and more likely to be female ($p < 0.001$); they had higher NIHSS scores on admission ($p < 0.001$) and discharge ($p < 0.001$), and they had lower eGFRs ($p < 0.001$) and lower serum LDL cholesterol ($p < 0.01$), lower serum albumin ($p < 0.001$) and higher serum hsCRP levels ($p < 0.001$). There was no significant difference in smoking status, the presence of diabetes, hypertension or atrial fibrillation or serum HbA1c, serum triglyceride, serum lipoprotein(a), or serum homocysteine levels.

All patients were followed-up from the day of their admission to the hospital until their death or for a max. of 1,669 days. During the follow-up period, 191 (49%) patients died. The Kaplan–Meier survival analysis for patients with and without anemia showed statistically different survival curves; patients with anemia had higher mortality in the observation period (log-rank test; $p < 0.001$) (Fig. 1).

The patients who died were more likely to have anemia ($p < 0.001$) at the onset of their stroke; they were older ($p < 0.001$) and more likely to be female ($p < 0.025$); they had higher NIHSS scores on admission ($p < 0.001$) and discharge ($p < 0.001$), lower eGFRs ($p < 0.001$), lower serum LDL cholesterol ($p < 0.007$) and serum albumin levels

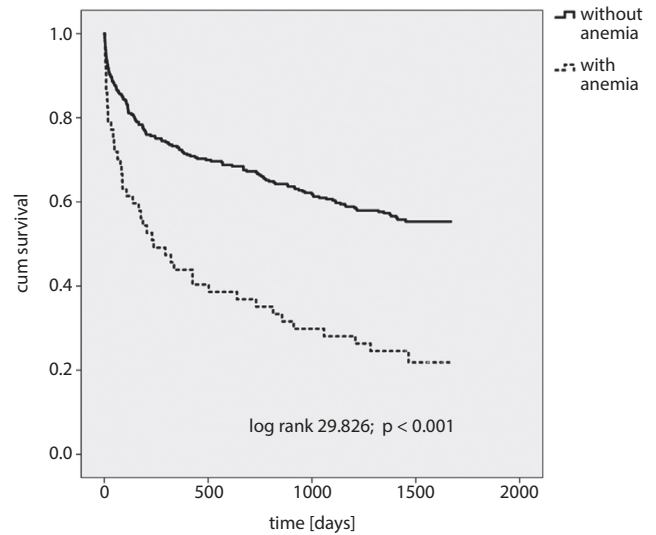


Fig. 1. Kaplan–Meier estimates for the survival of patients with anemia (broken line) and without anemia (solid line)

($p < 0.001$), while they had higher serum hsCRP ($p < 0.001$) and serum homocysteine levels ($p < 0.001$) (Table 2).

There was no significant difference in smoking status, the presence of diabetes, hypertension or atrial fibrillation or serum HbA1c, serum triglyceride, or serum lipoprotein(a) levels (Table 2).

According to the Cox regression analysis, anemia at admission was associated with long-term mortality in patients suffering from acute ischemic stroke (hazard ratio (HR) = 2.448, 95% confidence interval (95% CI) = 1.773–3.490; $p < 0.001$). Anemia also remained a strong

Table 1. Baseline characteristics of the patients included in our study (all patients grouped by presence of anemia)

Variable	All patients	With anemia	Without anemia
Age [years], mean \pm SD	70.97 \pm 11.64	74.63 \pm 12.09	70.35 \pm 11.46*
Gender (women/men), n (%)	183/207 (46.9)	44/13 (77.2)	139/194 (41.7)*
Hypertension (yes/no (%))	313/77 (80.3)	47/10 (82.5)	266/67 (79.9)
Diabetes mellitus/presence (yes/no (%))	100/290 (25.6)	12/42 (21.1)	88/245 (26.4)
HbA1c [mmol/L], mean \pm SD	6.39 \pm 1.43	6.43 \pm 1.54	6.38 \pm 1.42
Smoking/presence (yes/no (%))	61/329 (15.6)	6/52 (10.5)	55/278 (16.5)
Atrial fibrillation/presence (yes/no (%))	81/309 (20.8)	9/48 (15.8)	72/261 (21.6)
NIHSS1 (score), mean \pm SD	9.60 \pm 5.31	11.86 \pm 6.52	9.21 \pm 4.98*
NIHSS2 (score), mean \pm SD	8.07 \pm 7.44	11.28 \pm 7.99	7.53 \pm 7.21*
LDL cholesterol [mmol/L], mean \pm SD	3.17 \pm 1.08	2.73 \pm 0.98	3.25 \pm 1.08*
Triglycerides [mmol/L], mean \pm SD	1.92 \pm 2.23	1.71 \pm 1.54	1.96 \pm 2.32
eGFR [mL/min/1.73 m ²], mean \pm SD	63.38 \pm 20.16	54.04 \pm 25.83	64.98 \pm 18.60*
hsCRP [mg/L], mean \pm SD	17.68 \pm 35.91	34.87 \pm 44.49	14.73 \pm 33.42*
Albumin [g/L], mean \pm SD	40.08 \pm 5.05	34.61 \pm 5.27	41.01 \pm 4.38*
Lipoprotein(a) [g/L], mean \pm SD	0.29 \pm 0.36	0.33 \pm 0.40	0.28 \pm 0.35
Homocysteine [μ mol/L], mean \pm SD	13.18 \pm 6.23	13.96 \pm 5.41	13.05 \pm 6.35

* – statistically significant difference between patients with and without anemia; SD – standard deviation; LDL – low-density lipoprotein; HbA1c – glycated hemoglobin; NIHSS1 – National Institutes of Health Stroke Scale at admission; NIHSS2 – National Institutes of Health Stroke Scale at discharge; eGFR – estimated glomerular filtration rate; hsCRP – high-sensitivity C-reactive protein.

Table 2. Data of patients included in our study grouped by survival

Variable	Died	Survived	p-value
Anemia (yes/no (%))	44/147 (23.0)	13/186 (6.5)	0.001
Age [years], mean \pm SD	74.93 \pm 10.39	67.18 \pm 11.53	0.001
Gender (women/men), n (%)	101/90 (52.9)	82/117 (46.2)	0.025
Hypertension (yes/no (%))	155/36 (81.2)	158/41 (79.4)	NS
Diabetes mellitus (yes/no (%))	52/139 (27.2)	48/151 (24.1)	NS
HbA1c [mmol/L], mean \pm SD	6.43 \pm 1.36	6.34 \pm 1.50	NS
Smoking (yes/no (%))	25/166 (13.1)	36/163 (18.1)	NS
Atrial fibrillation (yes/no (%))	53/138 (27.7)	28/171 (14.1)	NS
NIHSS1 (score), mean \pm SD	11.95 \pm 8.56	7.78 \pm 3.91	0.001
NIHSS2 (score), mean \pm SD	11.95 \pm 8.56	4.36 \pm 3.17	0.001
LDL cholesterol [mmol/L], mean \pm SD	3.02 \pm 0.96	3.32 \pm 1.17	0.007
Triglycerides [mmol/L], mean \pm SD	1.73 \pm 1.80	2.11 \pm 2.56	NS
eGFR [mL/min/1.73 m ²], mean \pm SD	58.95 \pm 21.47	67.63 \pm 17.87	0.001
hsCRP [mg/L], mean \pm SD	25.67 \pm 37.87	10.00 \pm 32.18	0.001
Albumin [g/L], mean \pm SD	38.22 \pm 5.36	41.86 \pm 3.99	0.001
Lipoprotein(a) [g/L], mean \pm SD	0.28 \pm 0.36	0.29 \pm 0.35	NS
Homocysteine [μ mol/L], mean \pm SD	14.25 \pm 7.05	12.16 \pm 5.13	0.001

SD – standard deviation; LDL – low-density lipoprotein; HbA1c – glycated hemoglobin; NIHSS1 – National Institutes of Health Stroke Scale at admission; NIHSS2 – National Institutes of Health Stroke Scale at discharge; eGFR – estimated glomerular filtration rate; hsCRP – high-sensitivity C-reactive protein; NS – not statistically significant.

Table 3. Predictors of mortality in Cox regression analysis models

Variable	Model 1		Model 2		Model 3	
	HR (95% CI)	p-value	HR (95% CI)	p-value	HR (95% CI)	p-value
Anemia	1.949 (1.235–3.077)	0.004	1.721 (1.056–2.805)	0.029	1.718 (1.055–2.800)	0.03
Age	1.047 (1.024–1.069)	0.001	1.045 (1.023–1.068)	0.001	1.044 (1.021–1.067)	0.001
Female gender	1.689 (1.146–2.490)	0.008	1.745 (1.181–2.580)	0.005	1.700 (1.145–2.523)	0.008
LDL cholesterol	0.831 (0.706–0.978)	0.026	–	–	–	–
eGFR	0.989 (0.980–0.998)	0.021	0.991 (0.981–1.000)	0.049	–	–
NIHSS1	0.950 (0.918–0.982)	0.003	0.946 (0.914–0.980)	0.022	0.946 (0.914–0.980)	0.002
NIHSS2	1.226 (1.188–1.265)	0.001	1.223 (1.185–1.263)	0.001	1.224 (1.185–1.263)	0.001

HR – hazard ratio; 95% CI – 95% confidence interval; LDL – low-density lipoprotein; eGFR – estimated glomerular filtration rate; NIHSS1 – National Institutes of Health Stroke Scale at admission; NIHSS2 – National Institutes of Health Stroke Scale at discharge.

Model 1 included anemia, age, gender, the presence of hypertension, diabetes and atrial fibrillation, smoking status and NIHSS1, NIHSS2, serum LDL cholesterol, serum triglyceride, eGFR (CKD-EPI equation), and serum HbA1c levels. Model 2 included the previous variables plus serum hsCRP and serum albumin levels. Model 3 included the variables from the 2nd model plus serum lipoprotein(a) and serum homocysteine levels.

predictor of mortality in all 3 adjusted Cox regression models (Table 3).

With the Cox multivariable regression analysis in the 1st model, anemia, age, female gender, eGFR, NIHSS1 and NIHSS2 scores, and serum LDL cholesterol level were predictors of long-term mortality (Table 3). In the 2nd model, anemia, age, female gender, eGFR, and NIHSS1 and NIHSS2 scores remained predictors of long-term mortality (Table 3). In the 3rd

model, anemia, age, female gender, and NIHSS1 and NIHSS2 scores were predictors of long-term mortality (Table 3).

Discussion

To the best of our knowledge, this is the first study to demonstrate the importance of anemia in predicting long-term

mortality in patients with acute ischemic stroke. In our study, patients were followed-up from their admission to the hospital until their death or for a max. of 56 months (up to 1,669 days). Anemia at admission was more common among patients who later died than among the patients who survived. The Kaplan–Meier survival analysis showed higher mortality among patients with anemia in the observation period. The stroke patients with anemia had an increased risk of mortality compared to the patients without anemia in a univariate analysis (HR = 1.949; 95% CI = 1.235–3.077). Anemia remained an independent predictor of long-term mortality even after adjustments for known traditional – and some novel, non-traditional – risk factors (HR = 1.721–1.718) (Table 3).

In some previous studies, inconsistent results about the impact of anemia on mortality in patients with stroke have been reported.^{10,17,18} In 2016, a meta-analysis of cohort studies was published and it was clearly shown that anemia is an independent risk factor of unfavorable short-term outcomes in patients who have had a stroke.⁸ Thirteen studies were included in that meta-analysis.⁸ Patients with acute ischemic or acute hemorrhagic strokes – or both – were included.⁸ It is also important to note that 2 of 11 studies found that anemia is not always associated with mortality. Sico et al. found that anemia is independently associated with an outcome only in patients with a less severe stroke, defined as NIHSS < 10 at admission.¹⁹ They suggested a J-shaped relationship between hematocrit level and a poor prognosis in patients with severe stroke.¹⁹ In a study by Hao et al., anemia was not an independent predictor of the combined outcome of death and disability at 12 months.²⁰ In 11 of the studies included in the meta-analysis, patients were followed-up from 48 h up to 1 year.⁸ In the other 2 studies, patients were followed-up for 2 or 3 years and the authors concluded that there were still no long-term effects of anemia at that point.^{8–10} Both of the latter, longer studies were from Taiwan and studied a Chinese population.^{9,10}

In 2016, a paper by Barlas et al. was published.²¹ The authors analyzed their own data and conducted a meta-analysis of some previously published studies. They included in their retrospective analysis 8,013 stroke patients consecutively admitted over 11 years (86.7% had an ischemic stroke).²¹ Follow-up was obtained by electronic linkage and was ended at 365 days for all patients.²¹ Anemia was associated with an increased risk of short-term mortality.²¹ They included 20 studies in their meta-analysis; in 9 of them, the patients had ischemic stroke, in 6 studies the patients had hemorrhagic stroke, and in 5 the patients had suffered both types of stroke.²¹ In one study, the patients were followed-up on for 3 years, while in all the others the follow-up period was up to 1 year. The study that lasted for 3 years was from Taiwan and included a Chinese population. Meta-analyses of pooled results showed that anemia is associated with an increased risk of mortality in patients with ischemic stroke.²¹ In our study, the patients were followed for much longer and this is the only study where Caucasian patients were followed-up on for more than 1 year.

The prevalence of anemia in acute stroke patients varies from 0.11% to 39.40%. In a meta-analysis by Li et al., the pooled prevalence of anemia was 21.9%.⁸ In our study, the prevalence of anemia was 14.6%. This is still significantly higher than the reported prevalence of 7% in the general elderly population.²² The patients with anemia at admission were older and more likely to be female and with a higher neurological deficit (visible in NIHSS). Similar results were found in some but not all previous studies.^{10,20,23} In a laboratory analysis, patients with anemia had significantly lower eGFRs and lower serum LDL cholesterol, lower serum albumin and higher serum CRP levels. This laboratory data suggests that anemia is possibly part of the malnutrition-inflammation syndrome that is associated with advanced atherosclerosis.²⁴ This is frequently seen in patients with renal dysfunction, which was also more common in our study among patients with anemia.^{24,25} Old age and renal dysfunction were also found more frequently in patients with anemia than in those without, in some previous studies.^{10,20} In a study by Milionis et al., old age, lower eGFRs and lower total cholesterol and higher CRP levels were found in patients with anemia.²⁰ There was no significant difference in smoking status or the presence of diabetes, hypertension or atrial fibrillation in patients with or without anemia in our study. Similar results were found in most previous studies.^{10,19,20} In a study by Milionis et al., there was no difference in the presence of hypertension and smoking but patients with anemia more frequently suffered from diabetes and atrial fibrillation.²³

During the follow-up period, 49% of our patients died. Anemia was significantly more frequent among the patients who died. The patients who died were older and more likely to be female, they had higher NIHSS scores, lower eGFRs, lower serum LDL cholesterol and serum albumin levels, while they had higher serum hsCRP and serum homocysteine levels. In many previous studies where anemia was not included in the analysis, old age, higher NIHSS scores and renal dysfunction were predictors of short- and long-term mortality in patients with acute ischemic stroke.^{25–27} Laboratory data from our study – and some previous ones – suggests that mortality, like anemia, is associated with malnutrition-inflammation syndrome.^{8,24} Some other explanations about how anemia is associated with the outcome of acute ischemic stroke have also been proposed. Anemia leads to low blood oxygen content, which may cause subsequent cerebral ischemia.²⁸ Furthermore, anemia may induce a hyperkinetic circulatory state and upregulate the endothelial adhesion molecule genes, which may lead to a thrombus.²⁹ In addition, blood flow augmentation and turbulence may result in the migration of an existing thrombus, thus producing an artery-to-artery embolism.²⁹ Further studies are needed about the mechanism behind how anemia influences short- and long-term mortality in patients with acute ischemic stroke. There is only a single study examining the relationship between a specific morphological type

of anemia and mortality.³⁰ In that study, normochromic normocytic anemia was associated with inpatient mortality, 90-day mortality and a longer length of hospital stay in patients with ischemic stroke.³⁰ The study also found an association between hypochromic microcytic anemia and both 90-day mortality and longer length of stay in these patients.³⁰ The exact causes of normochromic normocytic and hypochromic microcytic anemia were not explained in this study.

Our study had some limitations which should be considered. Firstly, this is a single-center study. Secondly, only Caucasians were included in our study, thus limiting the generalizability of our findings. Thirdly, we had no information on the etiology or duration of anemia prior to the stroke or on further treatment during the follow-up period. The subtypes of anemia were not analyzed. Finally, the effect of unmeasured confounding variables (frailty, cognitive function, etc.) or complex interactions between covariates cannot be ruled out.

Conclusions

Anemia was frequent in patients who suffered from an acute ischemic stroke. Patients with anemia at admission had higher mortality during the observation period. Anemia was an independent predictor of long-term mortality in a univariate analysis and after adjustments for many other risk factors.

References

- Dhar R, Zazulia AR, Videen TO, Zipfel GJ, Derdeyn CP, Diringner MN. Red blood cell transfusion increases cerebral oxygen delivery in anemic patients with subarachnoid hemorrhage. *Stroke*. 2009;40(9):3039–3044.
- Ferrucci L, Guralnik JM, Woodman RC, et al. Proinflammatory state and circulating erythropoietin in persons with and without anemia. *Am J Med*. 2005;118(11):1288.
- Culleton BF, Manns BJ, Zhang J, Tonelli M, Klarenbach S, Hemmelgarn BR. Impact of anemia on hospitalization and mortality in older adults. *Blood*. 2006;107(10):3841–3846.
- Penninx BW, Pahor M, Cesari M, et al. Anemia is associated with disability and decreased physical performance and muscle strength in the elderly. *J Am Geriatr Soc*. 2004;52(5):719–724.
- Salisbury AC, Alexander KP, Reid KJ, et al. Incidence, correlates, and outcomes of acute, hospital-acquired anemia in patients with acute myocardial infarction. *Circ Cardiovasc Qual Outcomes*. 2010;3(4):337–346.
- Younge JO, Nauta ST, Akkerhuis KM, Deckers JW, van Domburg RT. Effect of anemia on short- and long-term outcome in patients hospitalized for acute coronary syndromes. *Am J Cardiol*. 2012;109(4):506–510.
- Kosiborod M, Smith GL, Radford MJ, Foody JM, Krumholz HM. The prognostic importance of anemia in patients with heart failure. *Am J Med*. 2003;114(2):112–119.
- Li Z, Zhou T, Li Y, Chen P, Chen L. Anemia increases the mortality risk in patients with stroke: A meta-analysis of cohort studies. *Sci Rep*. 2016;6:26636.
- Huang WY, Weng WC, Chien YY, Wu CL, Peng TI, Chen KH. Predictive factors of outcome and stroke recurrence in patients with unilateral atherosclerosis-related internal carotid artery occlusion. *Neurol India*. 2008;56(2):173–178.
- Huang WY, Chen IC, Meng L, Weng WC, Peng TI. The influence of anemia on clinical presentation and outcome of patients with first-ever atherosclerosis-related ischemic stroke. *J Clin Neurosci*. 2009;16(5):645–649.
- Thorvaldsen P, Asplund K, Kuulasmaa K, Rajakangas AM, Schroll M. Stroke incidence, case fatality, and mortality in the WHO MONICA Project. *Stroke*. 1995;26(3):361–367.
- Muir KW, Weir CJ, Murray GD, Povey C, Lees KR. Comparison of neurological scales and scoring systems for acute stroke prognosis. *Stroke*. 1996;27(10):1817–1820.
- Nutritional anemias. Report of a WHO scientific group. *World Health Organ Tech Rep Ser*. 1968;405:5–37.
- Levey AS, Stevens LA, Schmid CH, et al; CKD-EPI (Chronic Kidney Disease Epidemiology Collaboration). A new equation to estimate glomerular filtration rate. *Ann Intern Med*. 2009;150(9):604–612.
- Ryden L, Grant PJ, Anker SD, et al. ESC Guidelines on diabetes, pre-diabetes, and cardiovascular diseases developed in collaboration with the EASD: The Task Force on diabetes, pre-diabetes, and cardiovascular diseases of the European Society of Cardiology (ESC) and developed in collaboration with the European Association for the Study of Diabetes (EASD). *Eur Heart J*. 2013;34(39):3035–3087.
- Mancia G, Fagard R, Narkiewicz K, et al. 2013 ESH/ESC guidelines for the management of arterial hypertension: The Task Force for the Management of Arterial Hypertension of the European Society of Hypertension (ESH) and of the European Society of Cardiology (ESC). *Eur Heart J*. 2013;34(28):2159–2219.
- Del Fabbro P, Luthi JC, Carrera E, Michel P, Burnier M, Burnand B. Anemia and chronic kidney disease are potential risk factors for mortality in stroke patients: A historic cohort study. *BMC Nephrol*. 2010;11:27.
- Nybo M, Kristensen SR, Mickley H, Jensen JK. The influence of anemia on stroke prognosis and its relation to N-terminal pro-brain natriuretic peptide. *Eur J Neurol*. 2007;14(5):477–482.
- Sico JJ, Concato J, Wells CK, et al. Anemia is associated with poor outcomes in patients with less severe ischemic stroke. *J Stroke Cerebrovasc Dis*. 2013;22(3):271–278.
- Hao Z, Wu B, Wang D, Lin S, Tao W, Liu M. A cohort study of patients with anemia on admission and fatality after acute ischemic stroke. *J Clin Neurosci*. 2013;20(1):37–42.
- Barlas RS, Honney K, Loke YK, et al. Impact of hemoglobin levels and anemia on mortality in acute stroke: Analysis of UK regional registry data, systematic review, and meta-analysis. *J Am Heart Assoc*. 2016;5(8):pii: e003019.
- Corona LP, Duarte YA, Lebrao ML. Prevalence of anemia and associated factors in older adults: Evidence from the SABE Study. *Rev Saude Publica*. 2014;48(5):723–731.
- Milionis H, Papavasileiou V, Eskandari A, D'Ambrogio-Remillard S, Ntaios G, Michel P. Anemia on admission predicts short- and long-term outcomes in patients with acute ischemic stroke. *Int J Stroke*. 2015;10(2):224–230.
- Stenvinkel P, Heimbürger O, Paultre F, et al. Strong association between malnutrition, inflammation and atherosclerosis in chronic renal failure. *Kidney Int*. 1999;55(5):1899–1911.
- Hojs Fabjan T, Hojs R, Tetickovic E, Pecovnik Balon B. Ischaemic stroke – impact of renal dysfunction on in-hospital mortality. *Eur J Neurol*. 2007;14(12):1351–1356.
- MacWalter RS, Wong SYS, Wong KYK. Does renal dysfunction predict mortality after acute stroke? A 7-year follow-up study. *Stroke*. 2002;33(6):130–135.
- Tsagalidis G, Akrivos T, Alevizaki M, et al. Renal dysfunction in acute stroke: An independent predictor of long-term all combined vascular events and overall mortality. *Nephrol Dial Transplant*. 2009;24(1):194–200.
- Dexter F, Hindman BJ. Effect of haemoglobin concentration on brain oxygenation in focal stroke: A mathematical modelling study. *Br J Anaesth*. 1997;79(3):346–351.
- Kim JS, Kang SY. Bleeding and subsequent anemia: A precipitant for cerebral infarction. *Eur Neurol*. 2000;43(4):201–208.
- Barles RS, McCall SJ, Bettencourt-Silva JH, et al. Impact of anemia on acute stroke outcomes depends on the type of anemia: Evidence from a UK stroke register. *J Neurol Sci*. 2017;383:26–30.

Hypertension and chronic kidney disease is highly prevalent in elderly patients with colorectal cancer undergoing primary surgery

Leszek Kozłowski^{1,A–F}, Klaudia Kozłowska^{2,B,E,F}, Jolanta Małyszko^{3,A,C–F}

¹ Department of Oncological Surgery, Cancer Center, Białystok, Poland

² 2nd Department of Nephrology, Medical University of Białystok, Poland

³ Department of Nephrology, Dialysis and Internal Medicine, Medical University of Warsaw, Poland

A – research concept and design; B – collection and/or assembly of data; C – data analysis and interpretation;

D – writing the article; E – critical revision of the article; F – final approval of the article

Advances in Clinical and Experimental Medicine, ISSN 1899–5276 (print), ISSN 2451–2680 (online)

Adv Clin Exp Med. 2019;28(10):1425–1428

Address for correspondence

Jolanta Małyszko

E-mail: jolmal@poczta.onet.pl

Funding sources

None declared

Conflict of interest

None declared

Received on July 15, 2018

Reviewed on November 2, 2018

Accepted on February 18, 2019

Published online on August 30, 2019

Abstract

Background. Colorectal cancer (CRC) is a common and lethal disease. Hypertension is the most commonly reported comorbidity among cancer patients. Data on its incidence and prevalence is very scarce.

Objectives. The aim of the study was to evaluate the prevalence of hypertension and chronic kidney disease (CKD) in a cohort of 100 consecutive patients with CRC undergoing primary surgical treatment.

Material and methods. The pilot study included 100 consecutive patients with CRC undergoing primary surgery with curative intent within 1 year in the Department of Oncological Surgery in Białystok, Poland. No neoadjuvant therapy was administered before the surgery.

Results. The prevalence of hypertension was 62% among the patients studied. Sixty-five percent of the patients were older than 65 years and hypertension was present in 78% of these elderly patients. The prevalence of CKD was 15%, while that of diabetes was 23%. All CKD patients were older than 65 years of age. The hypertensive patients were more likely to be older and anemic with higher serum fibrinogen, which reflects a general inflammatory state. Elderly hypertensive patients had significantly higher creatinine levels, lower estimated glomerular filtration rate (eGFR) levels ($p < 0.001$) and lower platelet counts.

Conclusions. It is of the utmost importance for oncology patients to have any hypertension diagnosed and treated appropriately in order to prevent complications so they may continue their therapy with the least interruption or discontinuation of treatment and to ensure the best possible outcomes.

Key words: surgery, colorectal cancer, hypertension, chronic kidney disease, elderly

Cite as

Kozłowski L, Kozłowska K, Małyszko J. Hypertension and chronic kidney disease is highly prevalent in elderly patients with colorectal cancer undergoing primary surgery. *Adv Clin Exp Med.* 2019;28(10):1425–1428. doi:10.17219/acem/104537

DOI

10.17219/acem/104537

Copyright

© 2019 by Wrocław Medical University

This is an article distributed under the terms of the Creative Commons Attribution Non-Commercial License (<http://creativecommons.org/licenses/by-nc-nd/4.0/>)

Introduction

Colorectal cancer (CRC) is a common and lethal disease, the 3rd most commonly diagnosed cancer in males and the 2nd most common in females, though the incidence varies markedly.¹ Surgery is the only curative modality for localized colon cancer. For patients who have undergone potentially curative resection of a colon cancer, the goal of postoperative (adjuvant) chemotherapy is to eradicate micrometastases, thereby reducing the likelihood of disease recurrence and increasing the chances of recovery.² Chemotherapy carries a risk of significant toxicities, including emesis, diarrhea, febrile neutropenia, and cardiotoxicity. The frequency and severity of these side effects vary according to the specific drugs used and to the mode of administration. Hypertension is the most commonly reported comorbidity in cancer patients, with a rising incidence that is in line with the aging population of the developed world.¹ In addition, it is also the most common comorbidity reported in cancer registries.¹ However, detailed data on its incidence and prevalence is very scarce. Chemotherapy is a cardiovascular risk factor, particularly when combined with radiotherapy, which is responsible for increasing the incidence of cardiovascular events.³ The aim of this study was to evaluate the prevalence of hypertension and chronic kidney disease (CKD) in a cohort of patients with CRC undergoing primary surgical treatment with curative intent.

Patients and methods

The pilot study included 100 consecutive patients with CRC undergoing primary surgery with curative intent within 1 year in the Department of Oncological Surgery in Białystok, Poland. No neoadjuvant therapy was administered before the surgery. The analyzed data came from the demographic, clinical and laboratory parameters from medical charts. Blood pressure was measured with standard protocols. Hypertension was defined as either a blood pressure of at least 140/90 mm Hg or the use of hypertension medication. Chronic kidney disease was defined according to the 2012 Kidney Disease: Improving Global Outcomes (KDIGO) guidelines,⁴ with estimated glomerular filtration rate (eGFR) estimated using the Chronic Kidney Disease Epidemiology Collaboration (CKD-EPI) formula.⁵

The study was approved by the appropriate ethics review board. The data were analyzed using STATISTICA v. 13.1 software (StatSoft Inc., Tulsa, USA). The normality of variable distribution was tested using the Shapiro–Wilk W test. Student's t-test was used in statistical analysis to compare differences between groups, with a p-value <0.05 considered statistically significant (when appropriate).

Results

The prevalence of hypertension among all of the patients studied was 62%, but among the elderly patients it was 78%. The mean age of the study population was 67 ±11 years; 65% of the patients were older than 65 years. The prevalence of diabetes was 23%, while the prevalence of CKD was 15%. All CKD patients were older than 65 years of age. The clinical characteristics of the studied patients is shown in Table 1. The hypertensive patients tended to be older and anemic with higher serum fibrinogen, which reflects a general inflammatory state. When we grouped the patients according to age (≤65 years vs >65 years) and presence of hypertension, the elderly hypertensive patients had significantly higher serum creatinine levels (79.56 ±22.1 μmol/L vs 70.72 ±21.22 μmol/L; p < 0.01), lower corresponding eGFR levels according to the CKD-EPI formula (75.5 ±15.97 mL/min/1.72 m² vs 95.72 ±18.00 mL/min/1.72 m²; p < 0.001), higher red blood cell distribution width (RDW) (14.8 ±3.45% vs 13.49 ±2.69%; p < 0.05), and lower platelet counts (248.17 ±106.21 × 10⁹/L vs 299.50 ±140.36 × 10⁹/L; p < 0.05).

Table 1. Clinical and biochemical data of colorectal cancer (CRC) patients with and without hypertension

Parameter	No hypertension (n = 54)	Hypertension (n = 46)
Age [years]	64.51 ±1.62	69.61 ±7.73*
BMI [kg/m ²]	26.98 ±5.51	28.52 ±3.48
Sodium [mmol/L]	139.25 ±2.86	139.54 ±2.72
Potassium [mmol/L]	4.44 ±0.49	4.35 ±0.55
Hematocrit [%]	36.48 ±6.23	39.27 ±5.12*
Hemoglobin [g/L]	117.8 ±27.5	130.4 ±19.1*
Erythrocyte count [×10 ¹² /L]	4.30 ±0.47	4.49 ±0.49*
MCV [fl]	91.32 ±4.91	104.11 ±10.26
MCH [pg]	29.02 ±2.91	27.28 ±4.29*
RDW [%]	11.60 ±6.96	12.18 ±1.33
Leukocyte count [10 ⁹ /L]	7.21 ±3.51	7.41 ±2.54
Platelet count [10 ⁹ /L]	267.11 ±101.88	241.38 ±118.45
Creatinine [μmol/L]	78.68 ±22.10	80.44 ±22.10
Urea [mmol/L]	6.11 ±0.34	5.59 ±1.62
eGFR by CKD-EPI [mL/min/1.72 m ²]	84.59 ±21.23	80.77 ±16.76
APTT [s]	31.78 ±4.17	30.91 ±6.03
INR	1.06 ±0.21	1.05 ±0.25
Fibrinogen [μmol/L]	9.79 ±2.15	10.76 ±2.14*
Glucose [mmol/L]	6.02 ±1.42	6.38 ±1.30
Pulse pressure [mm Hg]	47 ±12	50 ±14
Mean arterial pressure [mm Hg]	97 ±10	104 ±11

BMI – body mass index; MCV – mean corpuscular volume; MCH – mean content of hemoglobin, aptt activated partial thromboplastin time; RDW – red blood cell distribution width; eGFR – estimated glomerular filtration rate; CKD-EPI – Chronic Kidney Disease Epidemiology Collaboration formula; APTT – activated partial thromboplastin time; INR – international normalized ratio. Conversion factors to SI units are as follows: for glucose – 0.0555, for creatinine – 88.4, for hemoglobin – 10, for fibrinogen – 0.0294, and for urea – 0.357; *p < 0.05.

Discussion

In our study, in patients with CRC, the prevalence of hypertension was very high. It was even higher, reaching 78%, in patients older than 65 years. Fraeman et al.⁶ estimated incidence rates of new-onset hypertension in 25,090 adult cancer patients (16% of whom had CRC) and found that crisis-level hypertension (systolic blood pressure >180 mm Hg or diastolic blood pressure >120 mm Hg) was most commonly seen in patients treated for gastric, ovarian, lung, and CRCs. New-onset hypertension was observed during active treatment in about 1/3 of the cancer patients. However, data on the prevalence of hypertension in CRC is very limited. In addition, all of the patients with CKD were over 65 years of age.

In a cohort of patients with CRC in Oman, the prevalence of hypertension was 42% and the prevalence of diabetes was 25%.⁷ Their population was younger (56 years) than ours (mean age: 67 years). In another study on 138 patients with CRC in Malaysia, the prevalence of type 2 diabetes and hypertension was 13% and 34.8%, respectively.⁸ The prevalence of hypertension and type 2 diabetes in relatively young patients (mean age: 53 years) with CRC in Iran was 13.38% and 8.69%, respectively.⁹ It should be stressed that the vast majority of published studies report the effects of CRC treatment and the incidence of adverse events, while data on the prevalence of hypertension and other comorbidities at the time of diagnosis or surgery is lacking. An updated systematic review and comparative meta-analysis by Abdel-Rahman et al.¹⁰ included randomized phase II and phase III trials of patients with solid tumors treated with sunitinib, axitinib, cediranib, or regorafenib describing daily events of hypertension, left ventricular dysfunction, bleeding, or thrombosis. Patients treated with these 4 agents had a significantly increased risk of all-grade hypertension and bleeding.¹¹ However, the data on the prevalence of hypertension before the therapy was not presented. Abdel-Qadir et al.¹¹ evaluated 77 phase III randomized, controlled trials and reported that angiogenesis inhibitors increased the risk of hypertension, arterial thromboembolism, cardiac ischemia, and cardiac dysfunction. Falchook et al.¹² studied patients with advanced solid tumors – including CRC – which were refractory to standard therapy who were treated with a combination of bevacizumab and sorafenib. Two-thirds of the patients experienced adverse events of grade 2 or higher, most commonly hand and foot syndrome (n = 27; 24%) and hypertension (n = 24; 21%).

The prevalence of CKD was reported to be high in patients with solid tumors,¹³ but the data is also limited. A high prevalence of CKD was reported in 2 other studies as well: ~33% and 27%.^{14,15} In the Belgian Renal Insufficiency and Anticancer Medications study (BIRMA), impaired kidney function, i.e., an estimated Modification Diet in Renal Disease (eMDRD) of <90 mL/min/1.73 m² was reported in 59.5% of CRC cases.¹⁶ In a Korean retrospective

study on 8,223 cancer patients with 1 or more serum creatinine measurements available, the CKD prevalence in CRC patients was 10.2%.¹⁷ This figure is slightly lower than in our study, most likely due to the younger age of the population studied (56 ±14 years vs 67 ±11 years). Moreover, as shown in this study, CKD was associated with an increase in the overall mortality rate of cancer patients (including breast cancer) – approx. 12% – independent of other known risk factors.¹⁷ The possible associations between CKD, hypertension and malignancy were reviewed recently.^{18,19}

Attention should also be paid to the limitations of our study, which consisted of a relatively small sample pooled in just 1 center. The population prevalence of hypertension and CKD was not compared with that of the group of patients with CRC. The fairly homogeneous study group and the lack of a control group might be considered limitations. As we did not perform any follow-up, we cannot indicate any specific benefits coming from paying special attention to the presence and appropriate treatment of any particular comorbidity.

It should be pointed out that large, randomized, controlled trials in general report hypertension as a side effect, but adding the prevalence of elevated blood pressure as a comorbidity would be of great clinical relevance. New-onset or worsening systemic hypertension can be found with numerous chemotherapeutics and is particularly common with antiangiogenic drugs.³ Therefore, the evaluation and treatment of hypertension is a practical starting point for the treatment of cardiotoxicity induced mainly by angiogenic inhibitors. It is of the utmost importance for oncology patients to have any hypertension diagnosed and treated appropriately in order to prevent complications so they may continue their therapy with the least interruption and no discontinuation of treatment and to ensure the best possible outcomes, as patients with early CRC and diabetes or hypertension have a significantly greater risk of cancer recurrence and death after treatment.⁹ In addition, as the prevalence of CKD and hypertension may be further exacerbated by adjuvant therapy, an assessment of kidney function is prerequisite before the introduction of adjuvant treatment.

References

1. Siegel RL, Miller KD, Jemal A. Cancer statistics, 2017. *CA Cancer J Clin*. 2017;67(1):7–30.
2. Sargent D, Sobrero A, Grothey A, et al. Evidence for cure by adjuvant therapy in colon cancer: Observations based on individual patient data from 20,898 patients on 18 randomized trials. *J Clin Oncol*. 2009; 27(6):872–877.
3. Herrmann J, Yang EH, Iliescu CA, et al. Vascular toxicities of cancer therapies: The old and the new – an evolving avenue. *Circulation*. 2016;133(13):1272–1289.
4. KDIGO 2012 Clinical Practice Guideline for the Evaluation and Management of Chronic Kidney Disease. *Kidney Int Suppl* (2011). 2013;3(1): 1–163.
5. Levey AS, Stevens LA, Schmid CH, et al; CKD-EPI (Chronic Kidney Disease Epidemiology Collaboration). A new equation to estimate glomerular filtration rate. *Ann Intern Med*. 2009;150(9):604–612.

6. Fraeman KH, Nordstrom BL, Luo W, Landis SH, Shantakumar S. Incidence of new-onset hypertension in cancer patients: A retrospective cohort study. *Int J Hypertens*. 2013;2013:379252.
7. Kumar S, Burney IA, Zahid KF, et al. Colorectal cancer patient characteristics, treatment and survival in Oman: A single center study. *Asian Pac J Cancer Prev*. 2015;16(12):4853–4858.
8. Othman NH, Zin AA. Association of colorectal carcinoma with metabolic diseases: Experience with 138 cases from Kelantan, Malaysia. *Asian Pac J Cancer Prev*. 2008;9(4):747–751.
9. Ahmadi A, Mobasheri M, Hashemi-Nazari SS, Baradaran A, Choobini ZM. Prevalence of hypertension and type 2 diabetes mellitus in patients with colorectal cancer and their median survival time: A cohort study. *J Res Med Sci*. 2014;19(9):850–854.
10. Abdel-Rahman O, Fouad M. Risk of cardiovascular toxicities in patients with solid tumors treated with sunitinib, axitinib, cediranib or regorafenib: An updated systematic review and comparative meta-analysis. *Crit Rev Oncol Hematol*. 2014;92(3):194–207.
11. Abdel-Qadir H, Ethier JL, Lee DS, Thavendiranathan P, Amir E. Cardiovascular toxicity of angiogenesis inhibitors in treatment of malignancy: A systematic review and meta-analysis. *Cancer Treat Rev*. 2017;53:120–127.
12. Falchook GS, Wheler JJ, Naing A, et al. Dual antiangiogenic inhibition: A phase I dose escalation and expansion trial targeting VEGF-A and VEGFR in patients with advanced solid tumors. *Invest New Drugs*. 2015;33(1):215–224.
13. Launay-Vacher V. Epidemiology of chronic kidney disease in cancer patients: Lessons from the IRMA study group. *Semin Nephrol*. 2010;30(6):548–556. doi:10.1016/j.semnephrol.2010.09.003
14. Dogan E, Izmirlı M, Ceylan K, et al. Incidence of renal insufficiency in cancer patients. *Adv Ther*. 2005;22(4):357–362.
15. Launay-Vacher V, Izzedine H, Rey JB, et al. Incidence of renal insufficiency in cancer patients and evaluation of information available on the use of anticancer drugs in renally impaired patients. *Med Sci Monit*. 2004;10:CR209–212.
16. Janus N, Launay-Vacher V, Byloos E, et al. Cancer and renal insufficiency results of the BIRMA study. *Br J Cancer*. 2010;103(12):1815–1821.
17. Na SY, Sung JY, Chang JH, et al. Chronic kidney disease in cancer patients: An independent predictor of cancer-specific mortality. *Am J Nephrol*. 2011;33(2):121–130.
18. Małyszko J, Kozłowski L, Kozłowska K, Małyszko M, Małyszko J. Cancer and the kidney: Dangerous liaisons or price paid for the progress in medicine? *Oncotarget*. 2017;8(39):66601–66619.
19. Małyszko J, Małyszko M, Kozłowski L, Kozłowska K, Małyszko J. Hypertension in malignancy: An underappreciated problem. *Oncotarget*. 2018;9(29):20855–20871.

Is intestinal stasis sufficient by itself in promoting enterocolitis in a non-genetic rat model of Hirschsprung's disease?

Magdalini Mitroudi^{1,A–F}, Dimitra Psalla^{2,A,B,E}, Konstantina Kontopoulou^{3,B,E,F},
Konstantinos Theocharidis^{4,B,F}, Dimitrios Sfoungaris^{1,A,C–F}

¹ 1st Department of Pediatric Surgery, Aristotelion University of Thessaloniki, General Hospital G. Gennimatas, Greece

² Laboratory of Pathology, School of Health Sciences, Faculty of Veterinary Medicine, Aristotelion University of Thessaloniki, Greece

³ Laboratory of Microbiology, G. Gennimatas General Hospital, Thessaloniki, Greece

⁴ Department of Pathology, G. Gennimatas General Hospital, Thessaloniki, Greece

A – research concept and design; B – collection and/or assembly of data; C – data analysis and interpretation;
D – writing the article; E – critical revision of the article; F – final approval of the article

Advances in Clinical and Experimental Medicine, ISSN 1899–5276 (print), ISSN 2451–2680 (online)

Adv Clin Exp Med. 2019;28(10):1429–1436

Address for correspondence

Dimitrios Sfoungaris
E-mail: dsfounga@auth.gr

Funding sources

None declared

Conflict of interest

None declared

Acknowledgements

We would like to thank Prof. Necdet Sut of Trakya University, Turkey, and Erasmus partner, for his valuable help in the statistical analysis of our results.

* These authors contributed equally to this work.

Received on July 18, 2018

Reviewed on August 26, 2018

Accepted on May 14, 2019

Cite as

Mitroudi M, Psalla D, Kontopoulou K, Theocharidis K, Sfoungaris D. Is intestinal stasis sufficient by itself in promoting enterocolitis in a non-genetic rat model of Hirschsprung's disease? *Adv Clin Exp Med.* 2019;28(10):1429–1436. doi:10.17219/acem/109342

DOI

10.17219/acem/109342

Copyright

© 2019 by Wrocław Medical University

This is an article distributed under the terms of the Creative Commons Attribution Non-Commercial License (<http://creativecommons.org/licenses/by-nc-nd/4.0/>)

Abstract

Background. Hirschsprung's disease-associated enterocolitis (HE) is a life-threatening septic complication of Hirschsprung's disease (HD), leading to bacterial translocation (BT) and sepsis. Many factors, such as intestinal stasis, HD-related inherited immune disorders and abnormal mucosal secretion have been implicated in its pathogenesis.

Objectives. To investigate the effect of intestinal stasis as an independent factor in the pathogenesis of HE intestinal lesions and its systematic effects.

Material and methods. The rectal ganglion cells of 46 Wistar rats were chemically ablated through local benzalkonium chloride (BAC) injection, in order to create a HD model (megacolon rats) that does not carry the possible genetic burden of HD. The animals were sacrificed either on the 20th or 25th day after ablation and were examined for histopathological changes on the wall of the small intestine, presence of bacterial translocation in body organs, body biometrics, and white blood cell count (WBC) and hemoglobin concentration. The results were compared to control animals.

Results. In the megacolon rats, severe damage on the small intestine as well as BT proportional to the extent of the intestinal damage and to the time elapsed after ablation was observed. Significant effects on the WBCs, hemoglobin concentration and biometric parameters were also observed.

Conclusions. In megacolon rats, intestinal stasis can lead by itself to a full-blown HE. The HE lesions that promote BT are present even in regions distant from the aganglionic bowel and are proportional to the time elapsed under the influence of intestinal stasis. Systematic effects such as growth retardation are also produced.

Key words: sepsis, bacterial translocation, intestinal obstruction, megacolon, ganglion cell ablation

Introduction

Hirschsprung's disease (HD) is a congenital disease characterized by a lack of ganglion cells in a segment of the terminal bowel (aganglionosis), causing functional obstruction and distension of the proximal bowel (megacolon).^{1,2} In 6–26% of HD cases, Hirschsprung's enterocolitis (HE) can develop, which is accompanied by considerable morbidity.^{2,3} The pathogenesis of HE appears complex and is not completely understood.⁴ It presents with both gastrointestinal (GI) and generalized symptoms ranging from fever and diarrhea to bloodstained stools and septic shock, while in chronic cases it affects somatic growth.^{5–7}

Initially, gradual intestinal obstruction, bacterial overgrowth and bacterial translocation (BT) were proposed as causative mechanisms.⁸ However this has been repeatedly questioned, because HE can occur even after surgical correction of HD, or after decompressing colostomy.⁹ This led to the investigation of additional possible HE causative factors, such as deficiency of the immune system and compromise of local intestinal mucus production.^{10–12} These factors could be inherited through complex HD genetics.⁴

The goal of this study was to investigate whether aganglionosis-induced intestinal stasis can by itself cause HE. In order to eliminate the interference of other possible HD-related factors, we used an animal model without HD genetic burden, in which aganglionosis was created through local chemical ablation of ganglion cells. We investigated the effects of intestinal stasis by studying the degree of intestinal damage, the degree of BT and the effects on somatic growth. This information could lead to a better understanding of the pathophysiology of HE and to a more targeted and timely management of the patients.

Material and methods

Animals

A total of 62 Wistar rats aged 28 days were used. All the rats were obtained from the same breeding center. They were housed in macrolon cages, 1 rat per cage, at 20–22°C room temperature. The rats were fed with standard rat chow diet.

Five of our animals were used in a pilot study to establish the appropriate time for sacrifice, in order to study the animals at 2 different stages of disease, but without death ensuing. These rats were ablated as described below and monitored at least once a day for symptoms of decreased activity, poor feeding and abdominal distension; stool production, weight and height (nose to rump length) were also measured. We observed that at least 2 symptoms were present by the 18th day after ganglion cell ablation. Two rats, randomly selected, were sacrificed on the 20th day post-treatment and 3 on the 25th day. These animals were assigned respectively to the M20 and M25 groups of animals, according to the investigative protocol, as described below.

Experimental design

The animals were randomly assigned to 4 groups as follows: group 1 (N) (n = 8) – animals with no treatment; group 2 (S) (n = 8): sham animals, injected with saline in the submucosa of the colon; group 3 (M20) (n = 23): megacolon animals, treated for chemical ablation, as described below, sacrificed on the 20th day post-treatment; group 4 (M25) (n = 23): megacolon animals, treated for chemical ablation, as described below, sacrificed on the 25th day post-treatment. We refer to group 1 (N) and group 2 (S) collectively as “ganglionic” animals. We refer to group 3 (M20) and group 4 (M25) collectively as “megacolon” animals.

The animal protocol was approved by the State Institutional Animal Care and Use Committee and by the Ethics Committee of Animal Research, Aristotelion University of Thessaloniki.

At 28 days of age, nonfasted ganglionic littermates (groups N and S) were anesthetized by intramuscular injection of 30 mg/kg ketamine hydrochloride. Body weight and body height were measured. Blood was collected from the lateral tail vein at the start of the study and from the aorta at the time of sacrifice.

The animals of groups M20 and M25 were anesthetized, positioned supine and were injected at 8 points of the rectum circumference between 0.2 cm to 1 cm above the anal verge with 50 µL of 0.1% benzalkonium chloride (BAC) solution in deionized water. A 22-gauge needle attached to a 50-µL micro syringe was used. The injection site was marked with India ink 1:100 (vol/vol). Group S animals were subjected to the same procedure using 0.9% NaCl solution instead of BAC. There was no intervention in group N.

On the day of sacrifice, the animals were anesthetized. Their abdominal fur was shaved and the skin was cleaned and disinfected with iodine solution. The abdomen was opened through a 4 cm midline incision. Blood was collected from the abdominal aorta and the internal organs were collected under aseptic conditions for bacteriological investigation. The rats were then killed by infusing potassium chloride (KCl) in the heart.

Organ sampling for bacterial translocation assessment

For BT assessment, the mesenteric lymph nodes (MLN), spleen, liver, kidneys, and lungs were collected separately, weighed and homogenized in 9 mL sterile pre-reduced 1:4 Ringer's solution, seeded in culture media and incubated. Each type of colony was submitted to Gram staining, catalase assay and anaerobic assay.

Blood sampling

White blood cells were evaluated according to standard laboratory methods. For hematological analyses, 1 mL of blood was collected in an anticoagulant

(ethylenediaminetetraacetic acid (EDTA)) tube. A Coulter T890® device (Beckman Coulter, Brea, USA) was used for white blood cell count (WBC).

Histological preparation

The entire intestine (including the anus) was excised, washed gently with cold phosphate-buffered saline (PBS) and fixed with 10% neutral-buffered formalin at room temperature for 48–72 h (Fig. 1). Specimens 1 cm long were sampled from the terminal ileum (5 cm proximally to the ileocolic valve) and cut into segments. All specimens were immersed in alcohol and xylol, and then embedded in paraffin. Examination was performed on 4–6 µm hematoxylin and eosin (H&E)-stained sections. Four sections from each rat were examined. Light microscopic studies were reviewed in a blinded manner. Tissue damage, severity and the depth of inflammation were evaluated, according to criteria listed below.



Fig. 1. Intestine of megacolon rat showing the reduced diameter of the rectum (R) and sigmoid (S)

Histological grading system

Mucosal lesion damage was assessed and graded according to the “tissue damage degree” criteria proposed by Chiu et al.¹³ (Table 1). The severity and depth of inflammation were scored separately according to the histological classification system described by Cheng et al.¹⁴ (Table 1). The highest score obtained in each parameter in each animal was recorded. Their sum represented

Table 1. Histological findings, total damage and enterocolitis grading system

Histological findings	GRADE
Tissue damage	
Normal structure of villi	0
Development of small subepithelial space at the villous apex	1
Enlarged subepithelial space but without change in villous length and width	2
Few shortened villi and presence of cells in the lumen	3
The majority of villi are shortened and widened with crypt hyperplasia and cells in the lumen	4
Blunting of all villi with elongated crypts and increased number of cells in the lumen	5
Severity of inflammation	
No inflammation, rare neutrophil	0
Mild inflammatory infiltrates, no necrosis	1
Moderate to marked inflammatory infiltrates and mucosal necrosis	2
Transmural necrosis	3
Depth of inflammation	
None	0
Mucosa	1
Submucosa	2
Muscularispropria	3
Subserosa and serosa	4
Total enterocolitis score	
Severity of inflammation grade + depth of inflammation grade	range: 0–7
Total damage score	
Total enterocolitis score + tissue damage grade	range: 0–12

the “total enterocolitis score”.¹⁴ To take under consideration all the above parameters, we used a combined score – the “total damage score”, calculated by adding the “total enterocolitis score” and “tissue damage grade” (Table 1).

Statistical analysis

Before the beginning of the study, a sample size calculation was performed with 80% power and an error set at 0.05 (two-sided). The Kruskal–Wallis test was used for comparison of the parameters due to the non-normal distribution. Then, the Mann–Whitney U test was used for pairwise comparisons of the groups when a significant difference was obtained. The data was presented as means and standard deviation (SD), and $p < 0.05$ was considered statistically significant.

Results

All rats survived during the experimental period. The histological examination of the BAC-treated rectums confirmed the ablation of intestinal ganglia in all of these

Table 2. Comparison of histological findings, hematological findings, weight (Weight_e) and height (Height_e) between the groups at the time of sacrifice. Means \pm SD are reported. P-value <0.05 indicates groups are significantly different

Variable	Groups				p-value
	normal (n = 8), mean \pm SD	sham (n = 8), mean \pm SD	M20 (n = 23), mean \pm SD	M25 (n = 23), mean \pm SD	
Tissue damage	0 \pm 0	0 \pm 0	3.1 \pm 1.3	4.7 \pm 0.5	<0.001
Severity of inflammation	0 \pm 0	0 \pm 0	1.6 \pm 0.9	2.5 \pm 0.5	<0.001
Depth of inflammation	0 \pm 0	0 \pm 0	1.1 \pm 1.1	3.2 \pm 0.9	<0.001
Total damage score	0 \pm 0	0 \pm 0	6 \pm 3	10.4 \pm 1.7	<0.001
Height_e [cm]	27.63 \pm 1.99	27.00 \pm 2.56	22.35 \pm 1.22	22.78 \pm 0.99	<0.001
Weight_e [g]	243.00 \pm 1.77	242.88 \pm 1.88	231.48 \pm 3.14	230.78 \pm 2.02	<0.001
WBC_e [$10^3/\mu$ L]	7.15 \pm 1,628.32	7,362.50 \pm 1,281.67	11,947.82 \pm 4,775.11	13,234.34 \pm 8,554.30	<0.017
NEUe [$10^3/\mu$ L]	3,383.38 \pm 722.85	3,913.38 \pm 973.06	10,061.70 \pm 4,311.34	11,588.35 \pm 7,840.43	<0.001
Hb_e [g/dL]	12.53 \pm 1.01	12.37 \pm 1.06	10.53 \pm 1.54	11.29 \pm 1.30	0.001

SD – standard deviation; Weight_e – body weight at the time of sacrifice; Height_e – body height at the time of sacrifice; WBC – white blood cells; NEU – neutrophils; Hb – hemoglobin.

animals. Non BAC-treated animals (Normal and Sham groups) did not produce histological signs of ganglion ablation, as expected.

Biometric parameters

Between the 17th and the 20th day, the megacolon animals began eating less food and produced less fecal material. By the 25th day, all megacolon animals showed decreased activity, poor feeding, less stool production, and abdominal distension. All rats continued to gain weight and height. However, the body weight at the time of sacrifice in both M20 group (M20 Weight_e: 231.48 \pm 3.14 g) and M25 group (M25 Weight_e: 230.78 \pm 2.02 g) remained significantly lower, compared to the respective parameters in the ganglionic groups ($p < 0.001$). The body height at the time of sacrifice in the M20 group (M20 Height_e: 22.35 \pm 1.22 cm) and M25 group (M25 Height_e: 22.78 \pm 0.99 cm) remained significantly lower compared to the rats of the ganglionic groups ($p < 0.001$) (Table 2, Fig. 2,3). Differences in weight and height between the M20 and M25 groups were not statistically significant.

Histological examination of the terminal ileum

No injury or inflammation was observed in the N and S groups (Fig. 4), which showed normal mucosa and glands. However, in the M20 and M25 groups, the intestinal structure was damaged (Fig. 5,6). Epithelial ulceration and infiltration with a mixed leukocyte population were observed. Denuded villi were discovered, accompanied by expansion of the subepithelial space with moderate or massive epithelial elevation. The total damage score in the M25 group was significantly higher than in the M20 group (total damage – M20: 6 \pm 3 vs M25: 10.4 \pm 1.7) ($p < 0.001$) (Table 2).

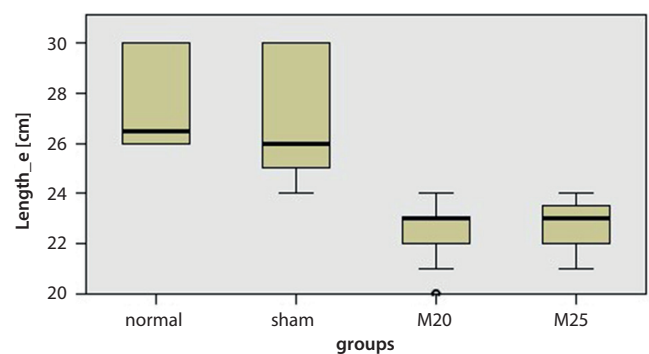


Fig. 2. Nose to rump length at sacrifice (Length_e) [cm] in N, S, M20, and M25 groups at the time of sacrifice (means \pm SD)

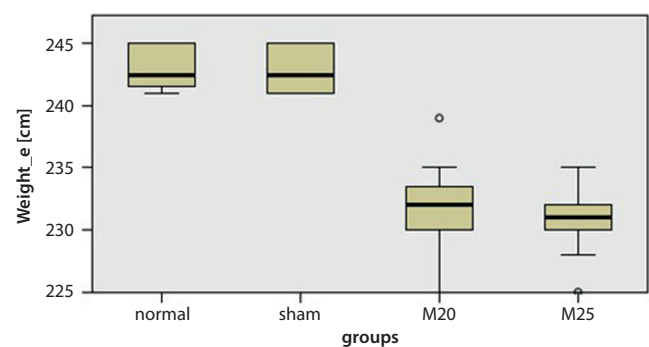


Fig. 3. Weight (Weight_e) [g] in N, S, M20, and M25 groups at the time of sacrifice (means \pm SD)

Bacterial translocation

All rats were tested for the presence of bacteria in their MLN, liver, spleen, kidneys, and lungs. No bacteria were cultured from these organs among the control and sham rats. *Escherichia coli*, *Enterococcus* spp., *Bacillus*, *Proteus mirabilis*, and *Clostridium* spp. were isolated only among the megacolon groups. *Escherichia coli* translocated at a higher incidence compared to other bacteria.

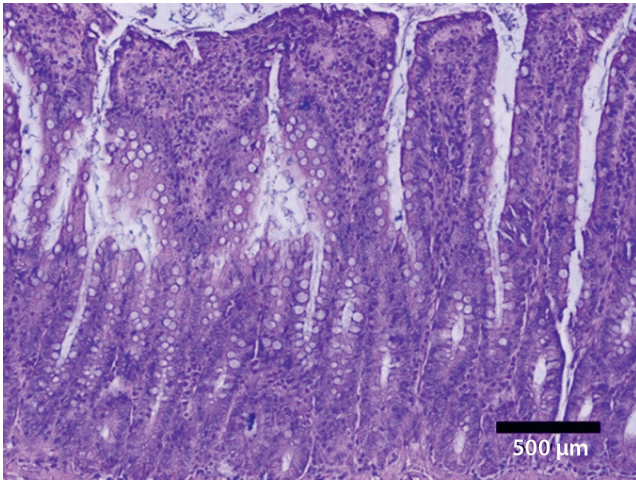


Fig. 4. Sham animal. Histological section showing intact epithelium. The number of lymphocytes and plasma cells in the lamina propria are within normal limits. H&E staining, bar: 500 μm

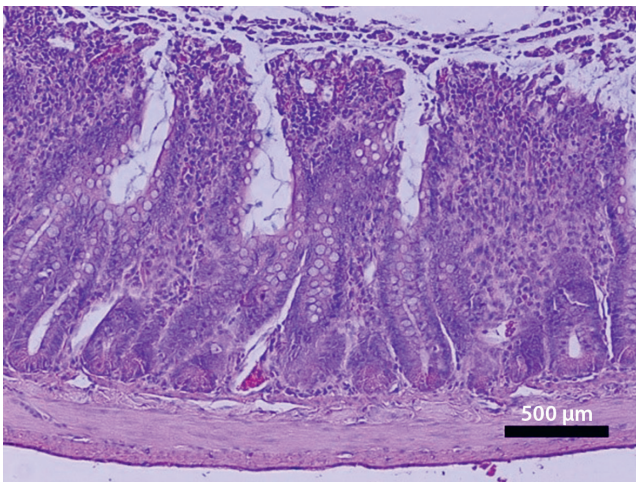


Fig. 5. Megacolon animal, M20 group. Histological section demonstrating ulceration of the epithelium and moderate infiltration by a mixed leukocyte population. H&E staining, bar: 500 μm

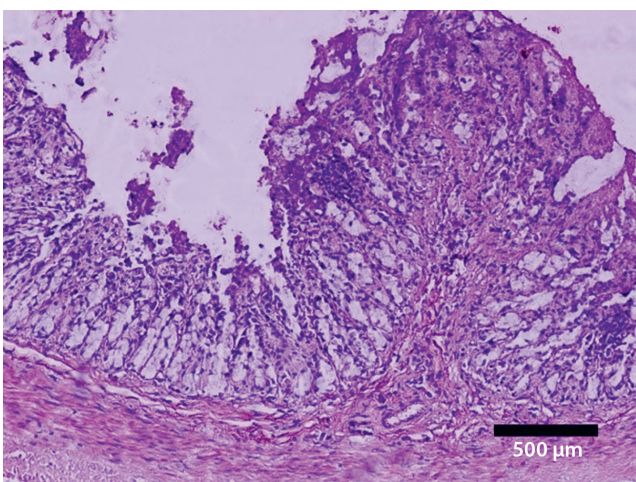


Fig. 6. Megacolon animal, M25 group. Histological section demonstrating severe destruction/necrosis of the epithelium extending to the lamina propria and infiltration by leukocytes. H&E staining, bar: 500 μm

Escherichia coli was observed in 73.9% of the rats in the M20 group and, more specifically, in 65.21% of the mesenteric lymph nodes, 34.78% of the spleens, 30.43% of the livers, 26.08% of the kidneys, and 4.34% of the lungs. All M25 rats showed viable *E. coli* bacteria in extra-intestinal sites: in 100% of the MLN, 78.26% of the spleens, 91.3% of the livers, 69.56% of the kidneys, and 60.86% of the lungs.

Hematological findings

The megacolon rats showed a significant increase in the number of WBC and neutrophils (NEU) compared to the ganglionic rats (Table 2, Fig. 7,8). Among the M20 and M25 groups, WBC count was significantly different (M20 WBC_e: 11,947.82 ± 4,775.11/μL vs M25

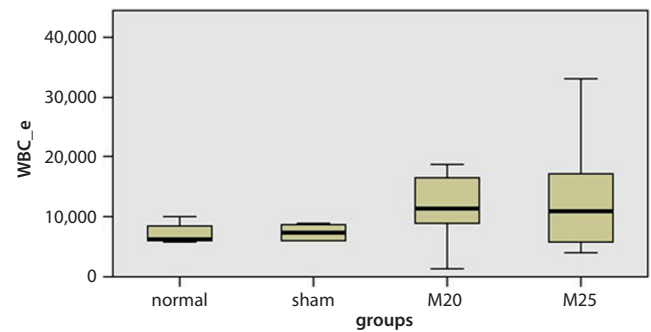


Fig. 7. White blood cells (WBC) in N, S, M20, and M25 group at the end of the experiment (means ±SD)

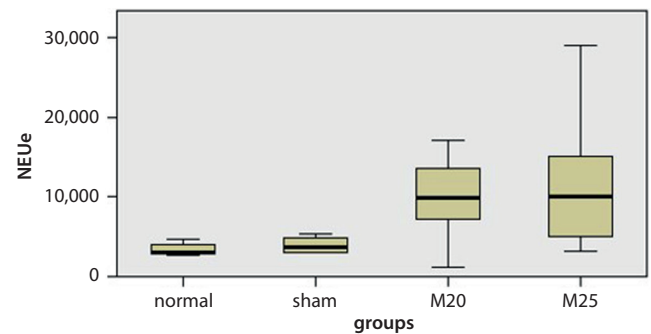


Fig. 8. Number of neutrophils (NEU) in N, S, M20, and M25 groups at the end of the experiment (means ±SD)

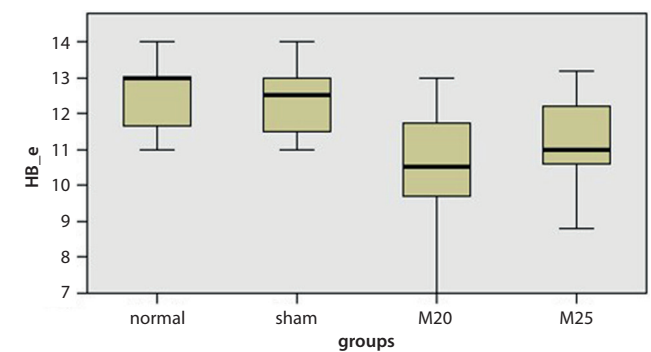


Fig. 9. Hemoglobin concentration levels (Hb) [gr/dL] in N, S, M20, and M25 groups at the end of the experiment (means ±SD)

WBC_e: 13,234.34 \pm 8,554.3/ μ L) and NEU (M20 NEU_e: 10061.70 \pm 4,311.34/ μ L vs M25 NEU_e: 11,588.35 \pm 7,840.43/ μ L).

There was a significant reduction in hemoglobin concentration between the ganglionic and the megacolon groups (normal Hb_e: 12.53 \pm 1.01 gr/dL vs M20 Hb_e: 10.53 \pm 1.54 gr/dL vs M25 Hb_e: 11.29 \pm 1.3 gr/dL) (Table 2, Fig. 9). There was no significant difference between the M20 and M25 groups ($p = 0.117$).

Discussion

Hirschsprung's enterocolitis is characterized by severe inflammation of the intestinal wall, intestinal distention and sepsis that can lead to death.¹ Many factors have been studied to explain the etiology and development of HE as well as its consequences.

Historically, the first proposed etiologic mechanism for HE was fecal stasis proximally to the aganglionic segment causing intestinal distention, which in turn increased intestinal permeability and promoted bacterial invasion and translocation. However, this mechanism does not explain neither the occurrence of HE in patients with HD without distended bowel (such as those after decompressive colostomy, or those with surgically corrected HD) nor the presence of HE lesions in the aganglionic bowel segment.^{11,15}

This paradox has led researchers to investigate the effects of many other factors of the development of HE, acting independently or in concert, such as microbiome alteration and impaired mucosal barrier function. These can be caused by variations in the components and amount of mucus, immunological deficiency, either local or systemic, with deficient white cell function, mucosal immunity defects, increased prostaglandin E1 activity, impaired motility associated with protein sensitization, and sucrase-isomaltase deficiency.^{11,12,16–20} These conditions could be the expression of the complex genetics of HD.²¹ Increased HE risk in patients with Down syndrome,^{22,23} cartilage-hair hypoplasia,²⁴ family history of HD, and female sex point to a possible genetic contribution to the etiology of HE.²⁵ The presence of major associated congenital anomalies involving either the cardiac, GI, genitourinary, or central nervous system is also correlated with a more severe course of HE.²¹

Despite the fact that an ever-growing number of HD-associated mutations have been shown to be associated with a more severe morbidity, especially in the *Ret-GDNF* and *ET-3-EDNRB* genes, no precise genetic abnormality has been shown to cause HE.^{26,27}

Several studies report that HE seems to be more common in patients with a longer aganglionic segment, but it is not clear whether this tendency is related to the underlying long-segment HD genetic predisposition.²⁸

Other risk factors not connected with genetic predisposition have also been implicated in the development of HE. Among these is delay in HD diagnosis, the type of surgical operation, and the development of postoperative

complications such as strictures and obstruction.^{9,29} These factors could act by creating reservoirs for stagnant intestinal contents that favor chronic inflammation, ulceration and impaired motility.

In order to exclude the confounding factors present in genetic HD animal models, we used a chemical model of HD instead of a genetic model and we investigated the effects of intestinal stasis on the intestinal wall, which is not adjacent to the aganglionic segment and not directly affected by the alterations in the mucosa caused by induced aganglionosis. We also examined the presence and extent of BT under the absence of HD-related genetic factors.

In order to ablate the ganglion cells and create HD conditions, benzalkonium chloride (BAC) was injected into the anorectal wall of normal rats. It is a cationic surfactant agent that adheres to the cell membrane, causing irreversible depolarization, injuring the cell membrane and producing severe cell damage and cell death.³⁰ Its use for this purpose was first described by Sato et al. in 1978.³⁰ Researchers have practiced BAC injections either directly per annum or during laparotomy.^{30–32}

We used the per annum endorectal injection model, because it causes less mortality.³² It has been observed that ganglion cell ablation occurs around the 14th day after BAC treatment, as evidenced by histology³² and clinical symptomatology.

To our knowledge, experimental studies on HE^{33–35} have only been performed on genetic HD models. Fujimoto et al., using the piebald-lethal (PL) model,^{34,35} reported significant histological evidence of enterocolitis in the ganglionic portion of the colon, accompanied by acute splenitis, but no bacterial cultures were performed.

On the contrary, Caniano et al., using the same model,¹⁰ found no evidence of enterocolitis in the colon, whereas BT was present in only 10% of mice sacrificed between 12 and 70 days of age. However, BT was present in 38% of spontaneously dying mice. In their opinion, these findings suggest that other mechanisms, in addition to local colonic inflammation, contribute to the development of HE. By studying IgG, IgM and IgA levels, they concluded that a reduction in immunologic integrity was the reason for sepsis. However, their search for BT and HE lesions was conducted only on the spleen and the colon, respectively. Although the genetic model used in the 2 abovementioned experiments was the same, the lack of predetermined criteria for enterocolitis and differences in animal care and housing conditions may have contributed to different results. Other investigators have performed detailed studies on the HE lesions and patterned classifications regarding the grade of inflammation.¹⁴

Our findings suggest that HE lesions can develop after fecal stasis, regardless of genetic or other local contributing factors. These can appear even in the small bowel, away from the obstruction site. These lesions could act as gateways for BT through the lymphatics and mucosal blood vessels towards the portal and systematic circulation.³⁶

Fecal stasis can also develop after scarring of severe intestinal lesions or adhesions following the operation for HD stasis and may trigger new HE lesions.³⁷ These possible events may explain HE occurring in patients with successful HD surgery or who carry a stoma.⁹

We investigated many extra-intestinal sites for BT and we found a strong positive correlation between total intestinal damage score and cultured bacteria on MLN, liver, spleen, pancreas, kidney, and lung tissues in our megacolon rats, suggesting a causal relation between HE lesions and sepsis. Bacterial translocation was observed in the MLN in a considerably larger number of cases than in the spleen or other organs. *Escherichia coli* translocated to a higher frequency compared to other bacteria and this could be the consequence of its abundant colonization in the bowel. During the 5-day interval between the M20 and M25 groups, there was a significant progression of the tissue damage and increase of inflammation markers, as well as increased frequency and spread of BT, even to the lungs. This coincided with a deterioration of body homeostasis, as shown by WBC counts and biometric parameters.

The increase in WBC and NEU counts observed in the megacolon groups is consistent with the presence of intestinal inflammation and BT (Table 2) (Fig. 3,4). However, the increase of WBC count between the M20 and M25 groups, while statistically significant, was not proportional to the escalation of the intestinal inflammation and BT, which may be due to the variable response of individual mice to the extreme septic burden. In some of these, overwhelming sepsis suppresses the bone marrow and reduces WBC production³⁸ while in others the immune system is still able to react more effectively. It is likely that for this reason, the WBC values obtained in the M25 group are more widespread than in other groups (Fig. 7, Table 2).

In the present study, all of the megacolon rats experienced reduced food intake and decreased excretion of feces by the 18th day after endorectal injections. This was reflected in their biometric growth indices in the M20 and M25 groups (Table 2). This is in line with the findings of other researchers, that anorexia, reduced caloric intake and increased catabolism are prominent during sepsis.³⁹

The present study suggests that the intestinal stasis itself may be the causative agent that can affect the intestine, even at a distance, causing HE and leading to bacterial translocation, systemic inflammation and sepsis. The development of HE lesions is gradual, and so is the intensity and extent of BT. Sepsis could affect the growth and development of the animal's body both through decreased food intake and increased catabolism.


Conclusions


Our study shows that HE can develop as a consequence of intestinal stasis alone.


Functional intestinal obstruction results in inflammation of the intestinal wall and BT to regional lymph nodes and distally located organs. *Escherichia coli* translocate to extra-intestinal sites at a higher frequency compared to other bacteria. The severity of the lesions of HE and the extent of BT is proportional to the time elapsed since the onset of intestinal stasis. Systematic effects, such as an increase in WBC and NEU counts, are also prominent. The decrease in hemoglobin concentration and restraint of somatic growth may result from inflammatory stress, sepsis and reduced food intake.

ORCID iDs

Magdalini Mitroudi  <https://orcid.org/0000-0002-5181-8887>

Dimitra Psalla  <https://orcid.org/0000-0002-1539-4124>

Konstantina Kontopoulou  <https://orcid.org/0000-0003-0121-8688>

Konstantinos Theocharidis  <https://orcid.org/0000-0001-7213-6925>

Dimitrios Sfountaris  <https://orcid.org/0000-0001-5567-5118>

References

- Hirschsprung H. Stuhtrageit Neugeborener infolge Dilatationen und Hypertrophie des Colons. *Jahrbuch Kinderheilkunde*. 1887;27:1.
- Pastor AC, Osman F, Teitelbaum DH, Caty MG, Langer JC. Development of a standardized definition for Hirschsprung's-associated enterocolitis: A Delphi analysis. *J Pediatr Surg*. 2009;44(1):251–256.
- Elhalaby EA, Coran AG, Blane CE, Hirsch RB, Teitelbaum DH. Enterocolitis associated with Hirschsprung's disease: A clinical-radiological characterization based on 168 patients. *J Pediatr Surg*. 1995;30(1):76–83.
- Pini Prato A, Rossi V, Avanzini S, Mattioli G, Disma N, Jasonni V. Hirschsprung's disease: What about mortality? *Pediatr Surg Int*. 2011;27(5):473–478.
- Carneiro PMR, Brereton RJ, Drake DP, Kiely EM, Spitz L, Turnock R. Enterocolitis in Hirschsprung's disease. *Pediatr Surg Int*. 1992;7(5):356–360.
- Ouladsaiad M. How to manage a late diagnosed Hirschsprung's disease. *Afr J Paediatr Surg*. 2016;13(2):82–87.
- Langer JC. Hirschsprung disease. *Curr Opin Pediatr*. 2013;25(3):368–374.
- Coran AG, Teitelbaum DH. Recent advances in the management of Hirschsprung's disease. *Am J Surg*. 2000;180(5):382–387.
- Hackam DJ, Filler RM, Pearl RH. Enterocolitis after the surgical treatment of Hirschsprung's disease: Risk factors and financial impact. *J Pediatr Surg*. 1998;33(6):830–833.
- Caniano DA, Teitelbaum DH, Qualman SJ, Shannon BT. The piebald-lethal murine strain: Investigation of the cause of early death. *J Pediatr Surg*. 1989;24(9):906–910.
- Jiao CL, Chen XY, Feng JX. Novel insights into the pathogenesis of Hirschsprung's-associated enterocolitis. *Chin Med J (Engl)*. 2016;129(12):1491.
- Murphy F, Prem P. New insights into the pathogenesis of Hirschsprung's associated enterocolitis. *Pediatr Surg Int*. 2005;21(10):773–779.
- Chiu CJ, McArdle AH, Brown R, Scott HJ, Gurd FN. Intestinal mucosal lesion in low-flow states. I. A morphological, hemodynamic, and metabolic reappraisal. *Arch Surg*. 1970;101(4):478–483.
- Cheng Z, Dhall D, Zhao L, et al. Murine model of Hirschsprung-associated enterocolitis. I. Phenotypic characterization with development of a histopathologic grading system. *J Pediatr Surg*. 2010;45(3):475–482.
- Rossi V, Avanzini S, Mosconi M, et al. Hirschsprung-associated enterocolitis. *J Gastrointest Dig Syst*. 2014;4:170.
- Gosain A, Brinkman AS. Hirschsprung's-associated enterocolitis. *Curr Opin Pediatr*. 2015;27(3):364–369.
- Wilson-Storey D, Scobie WG. Impaired gastrointestinal mucosal defense in Hirschsprung's disease: A clue to the pathogenesis of enterocolitis? *J Pediatr Surg*. 1989;24(5):462–464.
- Fujimoto T, Miyano T. Abnormal expression of the blood group antigen (BGA) in colon of Hirschsprung's disease. *Pediatr Surg Int*. 1994;9(4):242–247.

19. Wilson-Storey D, Scobie WG, Raeburn JA. Defective white blood cell function in Hirschsprung's disease: A possible predisposing factor to enterocolitis. *J R Coll Surg Edinb*. 1988;33(4):185–188.
20. Teitelbaum DH, Qualman SJ, Caniano DA. Hirschsprung's disease: Identification of risk factors for enterocolitis. *Ann Surg*. 1988;207(3):240–244.
21. Puri P, Shinkai T. Pathogenesis of Hirschsprung's disease and its variants: Recent progress. *Semin Pediatr Surg*. 2004;13(1):18–24.
22. Menezes M, Puri P. Long-term clinical outcome in patients with Hirschsprung's disease and associated Down's syndrome. *J Pediatr Surg*. 2005;40(5):810–812.
23. Morabito A, Lall A, Gull S, Mohee A, Bianchi A. The impact of Down's syndrome on the immediate and long-term outcomes of children with Hirschsprung's disease. *Pediatr Surg Int*. 2006;22(2):179–181.
24. Mäkitie O, Heikkinen M, Kaitila I, Rintala R. Hirschsprung's disease in cartilage-hair hypoplasia has poor prognosis. *J Pediatr Surg*. 2002;37(11):1585–1588.
25. Passarge E. The genetics of Hirschsprung's disease: Evidence for heterogeneous etiology and a study of sixty-three families. *N Engl J Med*. 1967;276(3):138–143.
26. Bolk S, Pelet A, Hofstra RMW, et al. A human model for multigenic inheritance: Phenotypic expression in Hirschsprung disease requires both the RET gene and a new 9q31 locus. *Proc Natl Acad Sci U S A*. 2000;97(1):268–273.
27. Parisi MA, Kapur RP. Genetics of Hirschsprung disease. *Curr Opin Pediatr*. 2000;12(6):610–617.
28. Surana R, Quinn FM, Puri P. Evaluation of risk factors in the development of enterocolitis complicating Hirschsprung's disease. *Pediatr Surg Int*. 1994;9(4):234–236.
29. Lee CC, Lien R, Chian MC, et al. Clinical impacts of delayed diagnosis of Hirschsprung's disease in newborn infants. *Pediatr Neonatol*. 2012;53(2):133–137.
30. Sato A, Yamamoto M, Imamura K, Kashiki Y, Kunieda T, Sakata K. Pathophysiology of aganglionic colon and anorectum: An experimental study on aganglionosis produced by a new method in the rat. *J Pediatr Surg*. 1978;13(4):399–435.
31. Yoneda A, Shima H, Nemeth L, Oue T, Puri P. Selective chemical ablation of the enteric plexus in mice. *Pediatr Surg Int*. 2002;18(4):234–237.
32. Qin HH, Lei N, Mendoza J, Dunn JC. Benzalkonium chloride-treated anorectums mimicked endothelin-3-deficient aganglionic anorectums on manometry. *J Pediatr Surg*. 2010;45(12):2408–2411.
33. Webster W. Aganglionic megacolon in piebald-lethal mice. *Arch Pathol*. 1974;97(2):111–117.
34. Fujimoto T. Natural history and pathophysiology of enterocolitis in the piebald lethal mouse model of Hirschsprung's disease. *J Pediatr Surg*. 1988;23(3):237–242.
35. Fujimoto T, Reen DJ, Puri P. Inflammatory response in enterocolitis in the piebald lethal mouse model of Hirschsprung's disease. *Pediatr Res*. 1988;24(2):152–155.
36. Berg RD, Garlington AW. Translocation of certain indigenous bacteria from the gastrointestinal tract to the mesenteric lymph nodes and other organs in a gnotobiotic mouse model. *Infect Immun*. 1979;23(2):403–411.
37. Awonuga AO, Belotte J, Abuanzeh S, Fletcher NM, Diamond MP, Saed GM. Advances in the pathogenesis of adhesion development: The role of oxidative stress. *Reprod Sci*. 2014;21(7):823–836.
38. Loftus TJ, Mohr AM, Moldawer LL. Dysregulated myelopoiesis and hematopoietic function following acute physiologic insult. *Curr Opin Hematol*. 2018;25(1):37–43.
39. Peters T, Peters JC. The biosynthesis of rat serum albumin. VI. Intracellular transport of albumin and rates of albumin and liver protein synthesis in vivo under various physiological conditions. *J Biol Chem*. 1972;247(12):3858–3863.